DSpace Institution

DSpace Repository http://dspace.org

Mathematics Thesis and Dissertations

2026-06

Fitted Numerical Methods for Singularly Perturbed Parabolic Diffusion-Type Problems with Boundary Layers

Amare, Worku

http://ir.bdu.edu.et/handle/123456789/17003

Downloaded from DSpace Repository, DSpace Institution's institutional repository

BAHIR DAR UNIVERSITY

COLLEGE OF SCIENCE

DEPARTMENT OF MATHEMATICS

Fitted Numerical Methods for Singularly Perturbed Parabolic Diffusion-Type Problems with Boundary Layers

By

Amare Worku Demsie

June 11, 2026

Bahir Dar, Ethiopia

BAHIR DAR UNIVERSITY

COLLEGE OF SCIENCE

DEPARTMENT OF MATHEMATICS

Fitted Numerical Methods for Singularly Perturbed Parabolic Diffusion-Type Problems with Boundary Layers

By

Amare Worku Demsie

Principal Supervisor: Awoke Andargie Tiruneh (Ph.D, Professor)

Co-Supervisor: Endalew Getnet Tsega (Ph.D, Associate Professor)

A Dissertation Submitted to the Department of Mathematics, College of Science, Bahir Dar University in Partial Fulfillment of the Requirements for the Degree of Doctor of Philosophy in Mathematics.

June 11, 2026

Bahir Dar, Ethiopia

BAHIR DAR UNIVERSITY

COLLEGE OF SCIENCE

DEPARTMENT OF MATHEMATICS

Approval of Dissertation

This is to certify that the dissertation entitled **" Fitted Numerical Methods for Singularly Perturbed Parabolic Diffusion-Type Problems with Boundary Layers"** submitted to Bahir Dar University, College of Science, Department of Mathematics for the award of degree of Doctor of Philosophy in Mathematics, is the research work done by **"Mr. Amare Worku Demsie"** under our supervision. The contents of this dissertation have not been submitted elsewhere for the award of any degree.

Awoke Andargie Tiruneh (PhD, Professor)

Principal Supervisor's Name	Signature	06/18/2026 Date

Endalew Getnet Tsega (PhD, Associate Professor)

Co-Supervisor's Name	Signature	06/18/2026 Date

BAHIR DAR UNIVERSITY

COLLEGE OF SCIENCE

DEPARTMENT OF MATHEMATICS

Approval of Dissertation

We here by certify that we have examined this dissertation entitled **”Fitted Numerical Methods for Singularly Perturbed Parabolic Diffusion-Type Problems with Boundary Layers”** by **Amare Worku Demsie**. We recommend that **Amare Worku Demsie** is approved for the degree of Doctor of Philosophy in Mathematics.

Board of Examiners

Wondosen Gebeyaw Melesse (PhD, Associate Professor)

External examiner’s name | Signature | Date 06/8/2026

Getachew Adamu Derese (PhD, Associate Professor)

Internal examiner’s name | Signature | Date 06/8/2026

Hunegnaw Dessie Assres (PhD, Associate Professor)

Chair person’s name | Signature | Date 06/8/2026

Declaration

I, Amare Worku Demsie, declare that the work contained in this dissertation, titled Fitted Numerical Methods for Singularly Perturbed Parabolic Diffusion-Type Problems with Boundary Layers, has been completed in accordance with the University's Regulations and Code of Practice for Research Degree Programs and has not been submitted for consideration for any other academic honors. The work is the candidate's own work, except where indicated by specific reference in the text, and all sources that I used or quoted have been acknowledged in full.

Amare Woru Demsie		06/18/2026
Candidate's name	Signature	Date

Contents

Acknowledgment

First and foremost, I would like to express my heartfelt gratitude to the Almighty God and His mother, St. Mary, for granting me the strength, knowledge, and opportunity to undertake and complete this research successfully.

Secondly, I sincerely thank my supervisor, Professor Awoke Andargie, for his unwavering support, guidance, and invaluable feedback throughout my Ph.D. journey. I am equally grateful to my co-supervisor, Dr. Endalew Getnet, for his insightful suggestions, constructive comments, and constant encouragement. I also extend my appreciation to Dr. Birlew Belayneh, the department heads Dr. Getachew Muhabe and Dr. Hunegnaw Dessie, and all staff members of the Department of Mathematics at Bahir Dar University for their support and fostering a positive academic environment.

Thirdly, I extend my deepest gratitude to my beloved wife, Tigist Fenta, my daughter, Meklit Amare, and my sons, Kaleab and Bamlak Amare, whose endless love, understanding, and support have been my true source of strength. I am also grateful to my mother, Beyina Molla, and my uncle, Merigieta Belay Demsie, for their constant encouragement and belief in me. Special thanks go to my fellow Ph.D. candidates and friends, whose motivation and companionship have made this journey brighter and more fulfilling.

Fourthly, I would like to acknowledge Bahir Dar University and Woldia University for their financial support and provision of essential facilities. I am especially thankful to the staff of the Department of Mathematics at Woldia University for providing a fully furnished office during my mother's illness, a kindness I will never forget. I also thank everyone who supported and encouraged me throughout this journey.

Special thanks goes to my friends, Dr. Dagnachew Mengstie, Dr. Anteneh Alemu, Dr. Meseret Muche , Dr Sisay Demeke and Dr. Yonas Eshetu, whose encouragement, shared experiences, and constructive feedback inspired me from the very beginning.

Finally, I sincerely thank La-al Hotel in Woldia City, North Wollo, for offering a supportive environment, reliable Wi-Fi, and study-friendly lodges, which greatly contributed to my productivity and well-being during my Ph.D. studies.

Acronyms

$1D$	One dimensional.
$2D$	Two dimensional.
$3D$	Three dimensional.
CDR	Convection-diffusion-reaction.
CDREs	Convection-diffusion-reaction equations.
DEs	Differential Equations.
EFOFDM	Exponentially fitted operator finite difference method.
FDM	Finite difference method.
FEM	Finite element method.
FMFDM	Fitted mesh finite difference method.
FMMs	Fitted mesh methods.
FOM	Fitted operator method.
FVM	Finite volume method.
NSFDM	Non-standard finite difference method.
PDEs	Partial differential Equations.
PPs	Perturbation problems.
RD	Reaction-diffusion.
RDEs	Reaction-diffusion equations.
SPPDDEs	Singularly perturbed parabolic differential-difference equations.
SPPPDEs	Singularly perturbed parabolic partial differential equations.
SPPs	Singularly perturbed problems.

List of Symbols

C	A generic positive constant independent of $h, \Delta t$ and ε.
$C^{(2,1)}$	Space of twice differentiable in space and one time differentiable functions.
$E^{N,M}, R^{N,M}$	ε-uniform maximum absolute error and order of convergence.
$h, \Delta t$	Step sizes in the spatial and temporal directions.
N, M	Number of spatial and temporal mesh points.
P_ε	Set of perturbation problems.
$\psi(x,t), \psi^j(x), \psi_i^j$	Continuous, semi-discrete and discrete solutions.
$\varepsilon, C_\varepsilon$	Perturbation parameters of the original and modified SPPs.
$\mathscr{D}_t, \overline{\mathscr{D}}_t$	Open and closed temporal domain.
$\mathscr{D}_x, \overline{\mathscr{D}}_x$	Open and closed spatial domain.
$\mathscr{D}_{xt}, \overline{\mathscr{D}}_{xt}$	Open and closed space-time domain.
$\overline{\mathscr{D}}_t^M, \overline{\mathscr{D}}_x^N$	Temporal and spatial meshes.
$\mathscr{L}_\varepsilon, \mathscr{L}_{C_\varepsilon}^N, \mathscr{L}_{C_\varepsilon}^{N,M}$	Continuous, semi-discrete and discrete differential operators.
$\partial \mathscr{D}_{xt}$	Boundary of the space-time domain.

List of Tables

List of Figures

List of Publications

The following manuscripts, which are parts of this dissertation, have been published and / or submitted for publication to some reputable journals:

1. A Uniformly Convergent Scheme for Singularly Perturbed Unsteady Reaction Diffusion Problems. Journal of Applied Mathematics, 2025(1), p.4603501. https://doi.org/10.1155/jama/4603501.

2. A Fitted Linear Multi-step Approach for Singularly Perturbed Parabolic-Type Reaction-Diffusion Problems Using Shishkin Meshes. International Journal of Mathematics and Mathematical Sciences, 2025(1), p.5553428. https://doi.org/10.1155/ijmm/5553428.

3. An Exponentially Fitted Upwind Scheme for Singularly Perturbed Differential Equations with Mixed Shift Parameters. Journal of Mathematics, 2025(1),p.3048746. https://doi.org/10.1155/jom/3048746.

4. An accelerated fourth-order fitted numerical approach for singularly perturbed reaction-diffusion problems of small time lag. Palestine Journal of Mathematics, 14(3), 92-110. https://pjm.ppu.edu/paper/2229-accelerated-fourth-order-fitted-numerical-approach-singularly-perturbed-reaction.

5. A Midpoint Upwind Numerical Scheme for Singularly Perturbed Differential Difference Equations. Abstract and Applied Analysis, 2026(1),p.6686763. https://doi.org/10.1155/aaa/6686763.

6. A Hybrid Computational Approach for Singularly Perturbed Parabolic Differential Equations Involving Small Negative Shift Parameters. **In press** :doi.org/10.1155/ijmm/9646984.

List of Conference Participation

1. A Higher-Order Parameter Uniformly Convergent Scheme for Singularly Perturbed Differential Difference Equations: presented in the 5^{th} African Graduate Student Conference (AGSC-V-BDU), Bahir Dar University, Ethiopia, May 12-13, 2025.

2. A Uniformly Convergent Scheme for Singularly Perturbed Unsteady Reaction–Diffusion Problems: presented in the 13^{th} National Conference on Recent Trends in Scientific Research, Science College, Bahir Dar University, Ethiopia, 20–21 June 2025.

3. ε-Uniformly Convergent Second-Order Scheme for Singularly Perturbed Differential Difference Equations: presented at, Sivas Cumhuriyet University, International Multidisciplinary Scientific Research Congress, Turkey, 04–06 July 2025.

4. A Fitted Numerical Approach for Singularly Perturbed Delay Differential Equations with Shift Parameters: presented in the 8^{th} International Mediterranean Congress on Scientific Research, Antalya, Turkey, 13–15 August 2025.

5. A Higher-order Fitted Numerical Schemes for Singularly Perturbed Delay Differential Equations of the Reaction-Diffusion Type: presented in the 3^{th} International Scientific Research and Innovation Congress , Nakhchivan-Azerbaijan, Turkey, 9–11 June 2025.

Seminar Presentation: A Fourth-order Fitted Numerical Method for Singularly Perturbed Reaction-Diffusion Problems of Small Time Lag. Held on 30 Feb 2026 at Department of Mathematics, College of Science, Bahir Dar University, Bahir Dar, Ethiopia.

Abstract

This dissertation focuses on the formulation and analysis of various fitted numerical methods for the solution of singularly perturbed parabolic diffusion-type problems characterized by boundary layers, both in the presence and absence of small temporal delays and spatial shift parameters. These types of problems arise frequently across a wide range of modeling contexts, including biological and chemical reaction processes, heat and mass transfer, control theory, neuronal variability, and population dynamics and epidemiology. Because the highest-order derivative term in the problems under consideration is multiplied by a small parameter ε, $0 < \varepsilon \ll 1$, the solutions exhibit multi-scale behavior, including boundary layers, interior layers, oscillations, and sharp gradients confined to narrow regions of the spatial domain. These features pose significant numerical challenges. Consequently, standard numerical methods such as finite difference, finite element, and finite volume methods applied on uniform meshes generally fail to produce accurate approximations unless prohibitively fine discretizations are employed. Such refinements, however, significantly increase computational cost and may also amplify round-off errors. To overcome these computational challenges, a Taylor series approximation is employed to transform the delay and advance terms, thereby reducing the original time-delay and spatial-shift problem into an asymptotically equivalent singularly perturbed problem. This reformulation places the problem within a standard singular perturbation framework while preserving its essential asymptotic structure. Based on this reformulated framework, we construct and rigorously analyze several fitted numerical methods for the classes of problems under consideration. The proposed approaches employ uniform meshes for temporal discretization and both uniform and piecewise-uniform Shishkin meshes for spatial discretization, depending on the nature of the problem. Specifically, the dissertation develops and analyzes second- and fourth-order fitted spatial discretization methods, including nonstandard finite difference schemes, fitted linear multistep methods, exponentially fitted upwind schemes, midpoint-upwind schemes, and hybridized numerical schemes, together with Crank–Nicolson and implicit Euler time-stepping strategies. The validity of the proposed methods is established through rigorous stability and parameter-uniform convergence analyses and is further supported by extensive numerical experiments. The maximum absolute errors and corresponding orders of convergence are computed and presented in tabular and graphical forms for clarity and comparison. The results demonstrate excellent agreement between theoretical predictions and numerical experiments, confirming that the proposed methods exhibit superior accuracy and convergence behavior compared with several existing approaches in the literature.

Chapter 1

General Introduction

In this chapter, we provide a comprehensive discussion of the fundamental concepts that frame the entire dissertation. It begins with an overview of the background of the study, establishing the context and rationale for the research. This is followed by a detailed review of relevant literature, highlighting previous findings and identifying gaps that the present study aims to address. The chapter also outlines the specific objectives that guide the research, as well as the significance of the study in contributing to both theoretical knowledge and practical applications. In addition, it introduces the research design and the general mathematical procedures employed throughout the dissertation. Finally, the chapter concludes with an explanation of the overall organization of the dissertation, offering readers a clear road map of the chapters that follow.

1.1 Background of the Study

Many real-life situations in science and engineering are modeled by parameter-dependent equations, including algebraic, transcendental, differential, integral, integro-differential, and differential-difference equations. The presence of non-linearity, variable coefficients, complex boundary geometries, and small perturbation parameters often prevents these models from admitting exact analytical solutions [1].

The study of the effects of a small parameter ε, $(0 < \varepsilon \ll 1)$, in various model equations such as differential and differential-difference equations is referred to as perturbation theory [2]. This theory is originated in nineteenth-century celestial mechanics, where gravitational interactions were observed to perturb planetary motions [3, 4]. Later on, it is used in the study of boundary layer phenomena in fluid and gas dynamics as presented in [5, 6]. Gradually, the development of perturbation theory is growing to singular perturbation for solving non-linear oscillations and employed as a key research areas extended to differential and delay differential equations [7, 8].

Furthermore, based on the influence of the perturbation parameter ε, perturbation problems can be categorized as regular perturbation problems (RPPs) and singular perturbation problems (SPPs). In RPPs, there is no significant effect on the behavior of the solution as the perturbation parameter approaches zero. Whereas, in the case of singular perturbation problems, the solution shows a non-uniform behavior (or rapid changes) as the perturbation parameter approaches zero [8]. Mathematically, the theory can be explained as in the following manner: Let $\psi_\varepsilon(x,t)$ be the solution of the perturbed problem (P_ε) and $\psi_0(x,t)$ be the solution of the reduced problem P_0 at $\varepsilon = 0$. If $\lim_{\varepsilon\to 0} \psi_\varepsilon(x,t) = \psi_0(x,t)$, then P_ε is a RPPs, otherwise it is a SPPs.

In terms of time-scale effects of the perturbation parameter ε, SPPs are classified as cumulative-type and layer-type problems. Cumulative-type SPPs exhibit the influence of ε only over long time intervals in oscillatory systems. Layer-type SPPs, in contrast, show rapid solution variation in narrow regions called layers, with steep gradients, while remaining smooth elsewhere [3]. These are further divided into boundary-layer and interior-layer problems depending on layer location.

1.1.1 Singularly Perturbed Parabolic Partial Differential Equations

Singularly perturbed parabolic partial differential equations are distinguished by the presence of a small parameter ε multiplying the highest-order derivative term, which fundamentally alters the nature of their solutions by introducing multiple spatial or temporal scales. As noted in [9], such equations naturally arise in a wide range of physical and biological contexts. For instance, in fluid dynamics, SPPPDEs model the behavior of flows with small viscosity, as exemplified by the Navier-Stokes equations at high Reynolds numbers, where sharp boundary layers develop. Similarly, they govern heat and mass transfer processes, capturing phenomena where diffusion acts over thin spatial regions or rapid temporal changes. In biological systems, SPPPDEs serve as the mathematical foundation for diffusive models used to represent complex spatio-temporal phenomena, including pattern formation, population dispersal, and chemical signaling, reflecting the interplay of slow and fast processes governed by the small parameter ε.

Further, SPPDDEs are a class of SPPPDEs that include at least one delay and/or advance term, capturing dependencies on the system's past or future states in addition to its present condition [10]. Delays in such systems are typically classified as either temporal lags or spatial shifts, both arising from small parameters that govern slow or localized dynamics. Temporal lags, common in biology, control systems [89], neuroscience [23], and epidemiology, result from mechanisms such as incubation periods, gestation times, feedback delays, or synaptic transmission, and often lead to multi-scale behavior or sharp transitions in time. Spatial shifts, frequently observed in reaction-diffusion systems, boundary layer flows, and internal layer problems, emerge from small diffusion coefficients, inverse Reynolds numbers, or multi-scale spatial effects, and give rise to rapid spatial variations or interface formation.

1.1.2 Locations of Boundary Layers for SPPPDEs

Boundary layers are thin regions near the boundary of the spatial domain where the solution changes rapidly [2]. The term was introduced by Ludwig Prandtl in 1904, whose pioneering work showed how even small fluid viscosities can significantly influence flow behavior [6]. Solutions of SPPPDEs typically exhibit layer behavior within narrow regions whose locations vary from problem to problem, making it difficult to design a single method applicable to all classes of SPPs. To address this challenge, one must first identify the positions or locations of boundary and interior layers by examining a class of convection–diffusion SPPPDEs subject to appropriate initial and boundary conditions as presented in [14].

$$\begin{cases} \psi_t(x,t) - \varepsilon\psi_{xx}(x,t) + a(x,t)\psi_x(x,t) + b(x,t)\psi(x,t) = f(x,t), \quad \forall (x,t) \in \mathscr{D}_{xt}, \\ \begin{cases} \psi(x,0) = \mathscr{S}_0(x), \quad \forall x \in \overline{\mathscr{D}_x}, \\ \psi(0,t) = \mathscr{S}_l(t), \quad \forall t \in \overline{\mathscr{D}_t}, \\ \psi(1,t) = \mathscr{S}_r(t), \quad \forall t \in \overline{\mathscr{D}_t}. \end{cases} \end{cases} \tag{1.1}$$

where ε is the perturbation parameter and $\mathscr{D}_{xt} = \mathscr{D}_x \times \mathscr{D}_t = (0,1) \times (0,T]$. Assuming the smoothness, boundedness, and continuity of the coefficients and source terms in problem (1.1), the locations of boundary and interior layers can be characterized as follows:

Case I: For $a(x,t) \neq 0$ and $b(x,t) \geq 0$, $\forall (x,t) \in \overline{\mathscr{D}_{xt}}$ [Convection-diffusion case]

- If $a(x,t) > 0$, a strong boundary layer forms near $x = 1$.
- If $a(x,t) < 0$, a strong boundary layer forms near $x = 0$.

Case II: $a(x,t)$ and $b(x,t)$ are smooth; $f(x,t)$ is bounded but discontinuous at $x = \alpha$.

- If $a(x,t) > 0$, a strong boundary layer forms near $x = 1$, and a weak interior layer appears to the left of $x = \alpha \in \mathscr{D}_x$.
- If $a(x,t) < 0$, a strong boundary layer forms near $x = 0$, and a weak interior layer appears to the right of $x = \alpha \in \mathscr{D}_x$.

Case III: $b(x,t)$ is smooth; $a(x,t)$ and $f(x,t)$ are bounded but discontinuous at $x = \alpha$.

- If $a(x,t) > 0$ for $x \in (0,\alpha)$ and $a(x,t) < 0$ for $x \in (\alpha,1)$, strong twin interior layers form at $x = \alpha \in \mathscr{D}_x$.
- If $a(x,t) < 0$ for $x \in (0,\alpha)$ and $a(x,t) > 0$ for $x \in (\alpha,1)$, the solution becomes unbounded.

Case IV: $a(x,t) = 0$, $\forall (x,t) \in \overline{\mathscr{D}_{xt}}$; $x = \alpha \in \mathscr{D}_{xt}$ [Reaction-diffusion case]

- If $b(x,t) > 0$, strong twin boundary layers arise near $x = 0$ and $x = 1$.
- If f is discontinuous at $x = \alpha$, boundary layers occur at $x = 0$ and $x = 1$, with an interior

layer at $x = \alpha \in \mathscr{D}_x$.

- If $b(x,t) < 0$, the solution exhibits rapid oscillations.

To support the above theoretical assumptions, we use the following numerical examples [2].

Example 1.1. Consider the convection-diffusion SPPDEs of the following forms:

- Left Boundary Layer:

$$\begin{cases} \psi_t(x,t) - \varepsilon\psi_{xx}(x,t) - \psi_x(x,t) = -e^{-x/\varepsilon}e^{-t}, \quad 0 < x < 1,\ t > 0, \\ \begin{cases} \psi(x,0) & = e^{-x/\varepsilon}, \\ \psi(0,t) & = e^{-t} \text{ and } \psi(1,t) = e^{-x/\varepsilon}e^{-t}. \end{cases} \end{cases}$$

where the exact solution is given by $\psi(x,t) = e^{-x/\varepsilon}e^{-t}$.

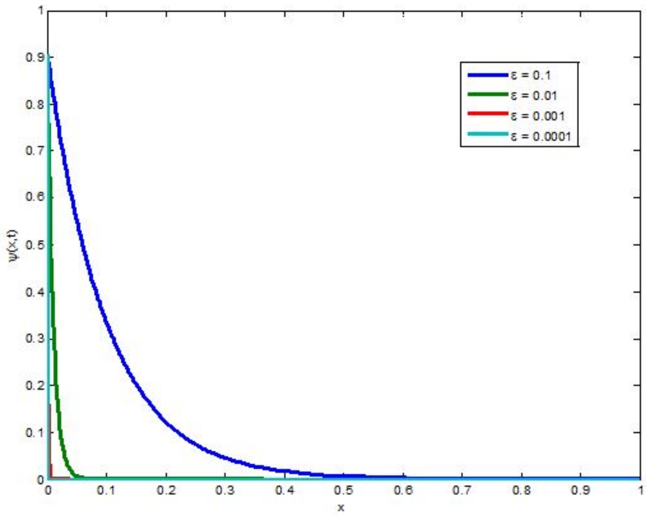

Figure 1.1: Left boundary layer

- Right Boundary Layer:

$$\begin{cases} \psi_t(x,t) - \varepsilon\psi_{xx}(x,t) + \psi_x(x,t) = -\left(1 - e^{-(1-x)/\varepsilon}\right)e^{-t}, \qquad 0 < x < 1,\ \ t > 0, \\ \psi(x,0) = 1 - e^{-(1-x)/\varepsilon}, \\ \psi(0,t) = \left(1 - e^{-1/\varepsilon}\right)e^{-t} \text{ and } \psi(1,t) = 0. \end{cases}$$

where the exact solution is given by $\psi(x,t) = \left(1 - e^{-(1-x)/\varepsilon}\right)e^{-t}$.

Example 1.2. Consider the reaction-diffusion SPPDEs of the following forms:

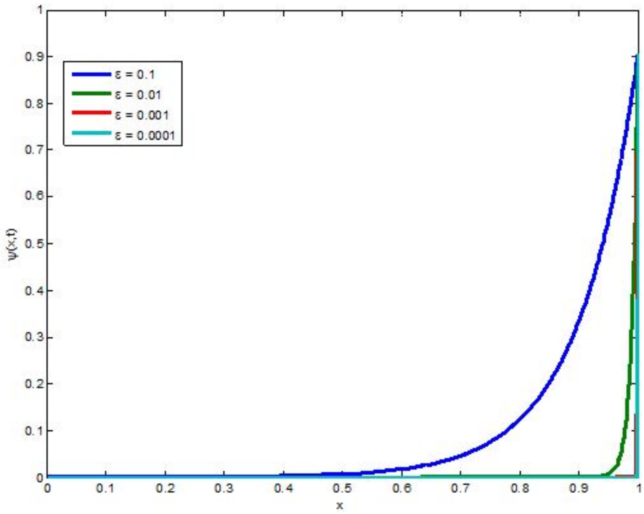

Figure 1.2: Right boundary layer

- Twin Boundary Layers:

$$\begin{cases} \psi_t - \varepsilon\psi_{xx} + \psi = -\dfrac{1}{\varepsilon}\left(e^{-x/\varepsilon} + e^{-(1-x)/\varepsilon}\right)e^{-t}, & 0 < x < 1,\ t > 0, \\ \psi(x,0) = e^{-x/\varepsilon} + e^{-(1-x)/\varepsilon}, \\ \psi(0,t) = \left(1 + e^{-1/\varepsilon}\right)e^{-t} \ \text{ and } \ \psi(1,t) = \left(1 + e^{-1/\varepsilon}\right)e^{-t}. \end{cases}$$

where the exact solution is given by $\psi(x,t) = \left(e^{-x/\varepsilon} + e^{-(1-x)/\varepsilon}\right)e^{-t}$.

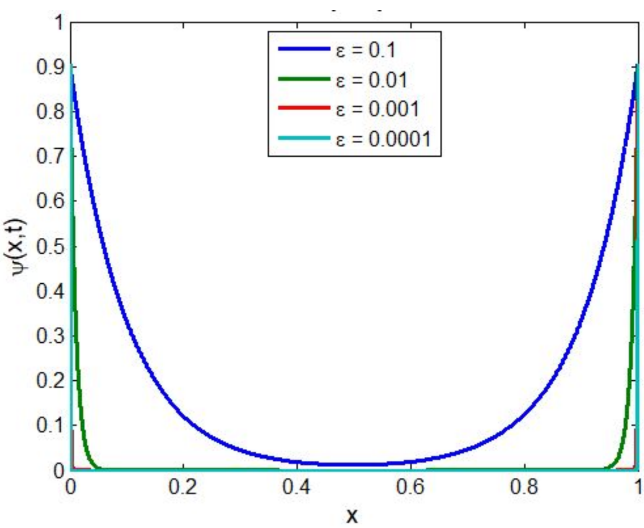

Figure 1.3: Twin boundary layer

1.1.3 Computational Meshes

To solve SPPPDEs both accurately and efficiently, numerical methods often use special computational meshes designed to capture regions where the solution changes very rapidly, such as boundary or interior layers. These meshes refine the grid in the layer regions while keeping it coarser elsewhere, allowing the numerical scheme to resolve steep gradients without excessive computational cost. This approach ensures that the solution remains accurate across the entire domain, even in regions with sharp variations.

Uniform Meshes: uniform meshes are computational grids in which all nodes are evenly spaced across the domain, making it the simplest mesh to construct and analyze [5]. While suitable for problems with smooth solutions, uniform meshes are ineffective for singularly perturbed problems with boundary or interior layers, as they cannot resolve sharp gradients without an extremely fine discretization, resulting in reduced accuracy and non-uniform convergence with respect to the perturbation parameter ε.

Shishkin Meshes: Shishkin meshes are piecewise-uniform, layer-adapted grids that resolve boundary or interior layers by using fine spacing within the layer region and coarser spacing elsewhere [11]. The domain is partitioned into subintervals, with the transition point prescribed in advance using parameters such as the perturbation size ε and the number of mesh intervals N. As noted in [2], Shishkin meshes are straightforward to construct and analyze, and when combined with suitable numerical schemes, they yield parameter-uniform convergence. Their error bounds, however, typically contain logarithmic factors of order $O(N^{-1}\ln N)$. These properties admit the following mathematical formulation, determined by the layer locations in (1.1).

Case I: If $a(x,t) < 0$ and the boundary layer is at $x = 0$, then partitioning the domain $\mathscr{D}_x = (0,1)$ into two sub-intervals as $(0,\tau)$ and $(\tau,1)$ with $\dfrac{N}{2}$ for $N \geq 2^m, m \geq 4$, where the transition point τ and step length h determined as follows:

$$
\begin{aligned}
\tau &= min\{\frac{1}{2}, C\varepsilon lnN\}, C \geq 1/\alpha \text{ and } 0 < a(x,t) \leq \alpha. \\
h_i &= \begin{cases} \frac{2\tau}{N}, & \text{for } i = 1,2,3,\ldots \frac{N}{2} \qquad \text{(fine region)}. \\ \frac{2(1-\tau)}{N}, & \text{for } i = \frac{N}{2}+1,\ldots N \qquad \text{(coarse region)}. \end{cases}
\end{aligned}
$$

Case II: If $a(x,t) > 0$ and the boundary layer is at $x = 1$ and partitioning the domain $\mathscr{D}_x = (0,1)$ into sub-intervals as $(0,\tau)$ and $(\tau,1)$ with $\dfrac{N}{2}$ for $N \geq 2^m, m \geq 4$, the transition point τ and the

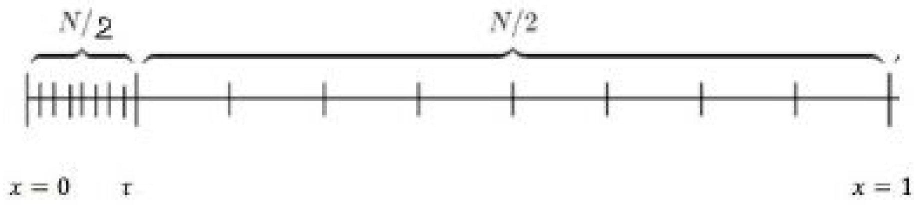

Figure 1.4: Shishkin mesh for left boundary layer with $N = 16$

step length h determined as follows:

$$\begin{aligned} \tau &= min\{\frac{1}{2}, C\varepsilon lnN\}, C \geq 1/\alpha \text{ and } a(x,t) \geq \alpha > 0. \\ h_i &= \begin{cases} \frac{2(1-\tau)}{N}, & \text{for } i = 1,2,3,\ldots \frac{N}{2} \quad \text{(coarse region).} \\ \frac{2\tau}{N}, & \text{for } i = \frac{N}{2}+1,\ldots N \quad \text{(fine region).} \end{cases} \end{aligned}$$

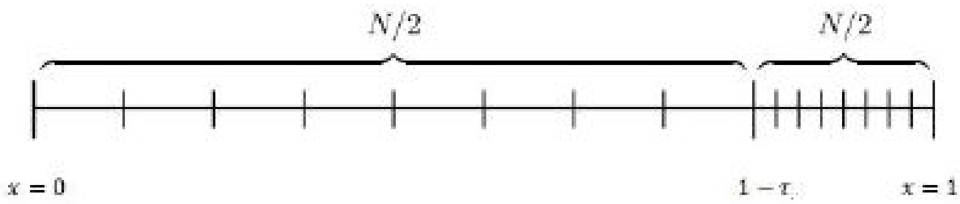

Figure 1.5: Shishkin mesh for right boundary layer with $N = 16$

Case III: If $a(x,t) = 0$, $b(x,t) > 0$, then the boundary layer is at $x = 0$ and $x = 1$. On partitioning the domain $\mathscr{D}_x = (0,1)$ into $(0,\tau)$ and $(1-\tau,1)$ with $\dfrac{N}{4}$ equal mesh elements and $(\tau, 1-\tau)$ with $\dfrac{N}{2}$ equal mesh elements such that $N \geq 2^m, m \geq 4$, where the transition point τ and the step length h determined as follows:

$$\begin{aligned} \tau &= min\{\frac{1}{4}, C\sqrt{\varepsilon}lnN\},\ C \geq 2/\beta \text{ and } b(x,t) \geq \beta > 0. \\ h_i &= \begin{cases} \frac{4\tau}{N}, & \text{for } i = 1,2,3,\ldots \frac{N}{4} \quad \text{(fine region).} \\ \frac{2(1-2\tau)}{N}, & \text{for } i = \frac{N}{4}+1,\ldots \frac{3N}{4} \quad \text{(coarse region).} \\ \frac{4\tau}{N}, & \text{for } i = \frac{3N}{4}+1,\ldots N \quad \text{(fine region).} \end{cases} \end{aligned}$$

Bakhvalov meshes: These meshes are smoothly graded, layer-adapted meshes designed to resolve very thin boundary layers more efficiently than piecewise-uniform meshes. It employs a smooth mesh-generating function that clusters points densely in the layer region and gradually transitions to coarser spacing elsewhere [2, 12]. This smooth grading provides higher accuracy and stronger parameter-uniform convergence than Shishkin meshes, particularly when the perturbation parameter ε is extremely small. However, Bakhvalov meshes are more involved to

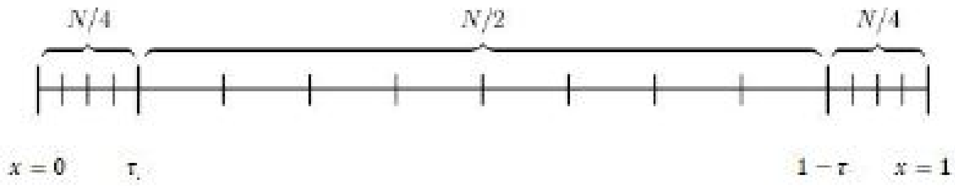

Figure 1.6: Shishkin mesh for twin boundary layers with $N = 16$

construct because they require an analytically defined stretching function.

Remark 1.1. Due to the increased complexity associated with constructing and implementing Bakhvalov meshes, this dissertation focuses solely on uniform and Shishkin meshes, which offer sufficient simplicity and effectiveness for the problems under consideration.

1.2 Some Singularly Perturbed Model Problems

Singular perturbation problems commonly occur in all branches of applied science and engineering problems. These problems are encountered in various model problems such as: parabolic convection-diffusion-reaction problems, the Navier-Stokes equations of fluid dynamics, Ground water flow and solute transport, Furnace processing metal sheet model problems and Neuronal variability model problems are few to mention.

1.2.1 Parabolic Convection-diffusion Problem

The convection-diffusion equation is a combination of the diffusion and convection equations, and describes physical phenomena where particles, energy, or other physical quantities are transferred inside a physical system due to two processes: diffusion and convection [5]. Convection-diffusion singularly perturbed problem is a mathematical model describing a process where both convection (transport by flow) and diffusion (spreading out) are important, but one term is significantly smaller than the other, denoted by a small parameter. This small parameter causes the solution to develop an abrupt changes over a very small region of the spatial domain, which complicates standard numerical solutions. The following initial-boundary value problems of heat or diffusion equation can be considered as SPPPDEs.

$$\begin{cases} \psi_t(x,t) - \gamma^2 \psi_{xx}(x,t) + \psi_x(x,t) + \psi(x,t) = f(x,t), \quad \forall (x,t) \in \mathscr{D}_{xt}, \\ \begin{cases} \psi(x,0) = \mathscr{S}_0(x), \quad 0 < x < L, \\ \psi(0,t) = \mathscr{S}_l(t), \quad 0 < t \leq T, \\ \psi(1,t) = \mathscr{S}_r(t), \quad 0 < t \leq T. \end{cases} \end{cases} \tag{1.2}$$

where $f(x,t)$ is a smooth function, L and T are the spatial and temporal interval lengths respectively and $\gamma^2 = \dfrac{K}{\eta\zeta}$ is diffusion coefficient such as mass diffusivity for particles in motion or thermal diffusivity for heat transport, K is the thermal conductivity, η is specific heat and ζ is density of the material. On setting $\gamma^2 = \varepsilon, (0 < \varepsilon \ll 1)$ the model problem is transformed in to the convection-diffusion and reaction-diffusion type SPPs. This model problem has wide range of applications in different fields of science and engineering. Fluid dynamic, Biology, Chemistry, Physics and Epidemiology are few to mention [19].

1.2.2 Navier-Stokes equation of Fluid Dynamics

The Navier-Stokes equations are a set of partial differential equations that describe the motion of viscous fluid substances [20]. These equations are derived from Newton's second law of motion (conservation of momentum) and the law of conservation of mass, modeling how forces like pressure, viscosity, and gravity influence a fluid's movement. They are used to predict the behavior of liquids and gases, such as weather patterns, ocean currents, and airflow over aircraft wings, although solving them for complex, turbulent flows is a significant mathematical challenge.

$$\begin{cases} \psi_t + \psi\psi_x + \phi\psi_y + p_x = \frac{1}{Re}(\psi_{xx} + \psi_{yy}) + f_x, \\ \phi_t + \psi\phi_x + \phi\phi_y + p_y = \frac{1}{Re}(\phi_{xx} + \phi_{yy}) + f_y, \\ \psi_x + \phi_y = 0. \end{cases} \tag{1.3}$$

where ψ and ϕ are respectively the velocity components along x and y directions and p is pressure. The parameter Re is a ratio of inertial forces to viscous forces within the fluid which is proportional to the length scale, velocity scale and inversely proportional to the kinematic viscosity of the fluid [**?**]. For sufficiently large Re ($Re \gg 1$), equation (1.3) will be a singularly perturbed equation.

1.2.3 Groundwater flow and solute transport

The transport of water and solutes through the partially saturated soil layer above the groundwater table has long been a fundamental aspect of groundwater hydrology, soil physics, and agronomy [46] . In one dimension, the theoretical basis for modeling the liquid phase water movement in unsaturated porous media can be described by Darcy's law (a mathematical principle that describes the flow of a fluid through a porous medium, such as water moving through soil or rock) of the following form:

$$\psi_t(x,t) = \mu\psi_{xx}(x,t) - v\psi_x(x,t) + \lambda\psi(x,t), \quad x > 0, t > 0. \tag{1.4}$$

where t is time, x is the horizontal distance; $\psi(x,t)$ is concentration of solute at time t and distance x; μ is the soil water diffusivity; v is the average velocity and λ is the decay coefficient. The purpose of the model is to compute the concentration of a dissolved chemical species in an aquifer at any specified time and space.

1.2.4 Furnace Processing Metal Sheet Model Equation

A large number of mathematical models appear in different areas of science and engineering such as in control theory, epidemiology, and laser optics that take into account not only the present state of a physical system but also its past history [21]. These models are described by certain classes of functional differential equations often called delay differential equations. Time delays are natural components of the dynamic processes of biology, ecology, physiology, economics and epidemiology. According to the discussions in [22], a simplified mathematical model for the control system of a furnace, which is used to process metal sheets, is represented by SPPDDEs of the following form:

$$\psi_t(x,t) - \varepsilon \psi_{xx}(x,t) = \omega(g(\psi(x,t-\delta)))\psi_x(x,t) + v\left[f(\psi(x,t-\delta) - \psi(x,t)))\right]. \tag{1.5}$$

where the temperature distribution of the metal sheet is denoted by $\psi(x,t)$. Also, the heat source and the velocity with which metal sheet is moving are denoted by f and v, respectively. Both f and ω are dependent on the term $\psi(x,t-\delta)$. The time delay of fixed length δ is induced because of the finite speed of the controlling device. This model equation is used as a base reference for the temporal delay related singularly perturbed problems.

1.2.5 Neuronal Variability Model Problem

Singularly perturbed delay differential equations model various processes in applied mathematics, for instance, in fluid mechanics, fluid dynamics, elasticity, quantum mechanics, chemical-reactor theory, reaction-diffusion processes, and other domains of fluid motion [23]. This model is the generalizations of Stein's Neuronal membrane model in the form of SPPDDEs of the form:

$$\psi_t(x,t) = \frac{\sigma^2}{2}\psi_{xx} + (\eta - \frac{x}{\theta})\psi_x + \lambda_s \psi(x+\alpha_s,t) + \omega_s \psi(x+i_s,t) + (\lambda_s + \omega_s)\psi(x,t). \tag{1.6}$$

The model is used for studying time evolution of the trajectories of the membrane potential, where the first derivative term denotes the exponential decay between two consecutive jumps caused by the input processes. The membrane potential decays exponentially to the resting level with a membrane time constant θ, η and σ are diffusion moments of the Wiener process characterizing the influence of dendritic synapses on the cell excitability. The excitatory input contributes to the membrane potential by an amplitude as with intensity λ_s, and similarly, the inhibitory input contributes by an amplitude is with intensity ω_s. Also i_s and α_s are the spatial shift parameter. Furthermore, this model serves as a base model for spatial shifts for singularly perturbed problems of the convection-diffusion and reaction-diffusion type problems [24].

1.3 Solution Methodologies for SPPPDEs

In the literature, the solution methods for SPPPDEs are typically grouped into asymptotic and fitted numerical methods. Asymptotic methods use perturbation techniques to approximate the solution structure, while fitted numerical methods modify the mesh or discretization to capture sharp boundary or interior layers.

1.3.1 Asymptotic Methods

The asymptotic method is a direct analytical technique used to obtain approximate solutions of singularly perturbed problems through an asymptotic series expansion in terms of the perturbation parameter ε [3]. In this approach, the approximate solution is constructed by determining successive terms of the expansion so that the governing differential equation, together with the prescribed initial and boundary conditions, is satisfied. Although asymptotic expansion methods provide valuable analytical insight into the behavior of singularly perturbed problems, their direct application is often restricted by several limitations.

To overcome these difficulties, a number of modified asymptotic techniques and sub-methods have been developed [4]. Nevertheless, asymptotic series expansion methods are generally applicable only to a relatively limited class of problems. In particular, these methods require prior knowledge of important solution characteristics, such as the location and width of the boundary layer. Furthermore, they are not well suited for efficiently handling higher-dimensional problems and nonlinear one-dimensional problems.

Consequently, the successful application of asymptotic methods demands substantial analytical understanding of the expected behavior of the solution. These limitations are the key motivation of the advancement of fitted numerical methods, which are designed to provide stable and accurate approximations for singularly perturbed problems without requiring detailed prior information about the boundary layer structure.

1.3.2 Fitted Numerical Methods

One of the main reasons for studying singularly perturbed problems is their solutions multi-scale futures such as formation of boundary layers, interior layers and oscillations to satisfy the given initial and boundary conditions when the perturbation parameter ε approaches zero. In these regions, solutions show steep gradients, requiring extremely fine meshes for accurate discretization. Such fine meshes increase round-off errors and computational cost, making classical methods such like FDM, FEM, and FVM inadequate. This has led to the development of fitted numerical methods, such as fitted operators and fitted meshes, which are parameter-uniformly convergent techniques [15, 16].

The fitted operator methods were introduced for solving the problem of viscous fluid past a fixed cylinder [2]. These methods have two basic sub methods called non-standard finite difference method (NSFDM) and exponentially fitted operator finite difference methods (EFOFDM). As outlined in [66], in NSFDM the discretized mesh is uniform and a positive complicated denominator function is developed for the diffusion part of the equation using the exact finite difference technique, to handle the effect of the perturbation parameter ε. This method is extendable for higher-dimensional and non-linear SPPPDEs. In the case of EFOFDMs, the discretized mesh is uniform and the exponential fitting factor is induced using the asymptotic solution behavior to control the rapid growth or decay of the solution in the boundary layer region [8, 17]. These methods are limited to linear and one-dimensional SPPPDEs.

Numerical schemes for SPPPDEs must be developed with careful attention, since boundary or interior layers can have a pronounced impact on the solution. Methods designed to address these challenges are known as fitted-mesh methods (FMMs.), in which the construction of an appropriate mesh is crucial for achieving reliable approximations of singular perturbation problems. As discussed in section (1.1.3), layer-resolving fitted meshes are commonly divided into graded meshes and Shishkin meshes [2].

1.4 Fundamental Concepts and Definitions

Definition 1.1. (**Hölder Continuity**): A function f is said to be Hölder continuous of order $\alpha \in (0,1]$ if there exists a constant $C > 0$ such that, for every pair of points x and y in its domain,

$$|f(x) - f(y)| \leq C|x-y|^{\alpha}.$$

This condition indicates that the function does not oscillate too rapidly [26].

- When $\alpha = 1$, Hölder continuity reduces to Lipschitz continuity.
- For $0 < \alpha < 1$, f may not be differentiable, but its oscillations are controlled.
- Hölder continuity is stronger than mere continuity but weaker than differentiability.

Definition 1.2. (**Hölder Compatibility**): refers to conditions imposed on the initial and boundary data at the corner points of the computational domain to ensure that the solution possesses sufficient smoothness (specifically, Hölder continuity) to exist, be unique, and have bounded derivatives [112]. Mathematically, the zeroth- and first-order compatibility conditions at the corner points $(0,0)$ and $(1,0)$ can be defined on the model equation (1.1) as follows:

$$\mathscr{S}_0(0,0) = \mathscr{S}_l(0), \mathscr{S}_0(1,0) = \mathscr{S}_r(0).$$

$$\begin{cases} \frac{\partial \mathscr{S}_l(0)}{\partial t} - \varepsilon \frac{\partial^2 \mathscr{S}_0(0,0)}{\partial x^2} + p(0)\frac{\partial \mathscr{S}_0(0,0)}{\partial x} + b(0,0)\mathscr{S}_0(0,0) = f(0,0), \\ \frac{\partial \mathscr{S}_r(0)}{\partial t} - \varepsilon \frac{\partial^2 \mathscr{S}_0(1,0)}{\partial x^2} + p(0)\frac{\partial \mathscr{S}_0(1,0)}{\partial x} + b(1,0)\mathscr{S}_0(1,0) = f(1,0). \end{cases}$$

The failure of these conditions often results in discontinuities or very rapid changes in the solution that standard numerical methods struggle to capture accurately.

Definition 1.3. (**Regularity Condition**): The regularity condition refers to a set of assumptions on the given functions (coefficients, source terms, initial, and boundary conditions) that ensure the solution of the SPPPDEs possesses a certain level of smoothness such as the Hölder space of the form $C^{\alpha,\beta}(\overline{\mathscr{D}}_{xt})$ [30]. These conditions are essential for:

- Guaranteeing existence and uniqueness of the solution.
- Enables for maximum principles and a priori bounds, for error analysis.
- Captures key solution features, such as boundary layer location and width.

If a necessary regularity condition is not met, the convergence rate of numerical methods can become very slow.

Definition 1.4. (**Infinity Norm**): Let ψ_i^j be a discrete numerical approximation to the exact solution $\psi(x_i,t^j)$ defined on a mesh $\mathscr{D}_{xt}^{N,M}$ [5]. The infinity norm of the discrete error is defined by

$$\|\psi - \psi^{N,M}\|_\infty = \max_{(x_i,t^j)\in\mathscr{D}_{xt}^{N,M}} \left|\psi(x_i,t^j) - \psi_i^j\right|.$$

This norm measures the maximum absolute error over all mesh points and is well suited for analyzing stability, discrete maximum principles, and parameter-uniform convergence of numerical schemes for SPPPDEs.

Definition 1.5. (**Spectral Radius**): Let $A \in \mathbb{C}^{n\times n}$ with eigenvalues $\lambda_1, \lambda_2, \ldots, \lambda_n$. The spectral radius of A is defined as

$$\rho(A) = \max\{|\lambda_i| : i = 1,2,\ldots,n\}.$$

It represents the maximum magnitude of eigenvalues of A [27].

Definition 1.6. (**Neumann Series**): Let $C \in \mathbb{C}^{n\times n}$ be a matrix such that $\rho(C) < 1$. Then the series $\sum_{k=0}^{\infty} C^k$ converges to $(I-C)^{-1} = \sum_{k=0}^{\infty} C^k$. This is called the Neumann series. It provides an explicit expression for the inverse of $(I-C)$ when the spectral radius of C is less than one.

Definition 1.7. (**Z-matrix**): A matrix $A = [a_{ij}] \in \mathbb{R}^{n\times n}$ is called a **Z-matrix** if

$$a_{ij} \le 0 \quad \text{for } i \ne j.$$

Definition 1.8. A matrix A is called a **nonsingular M-matrix** [28] if:

- A is a Z-matrix,
- A is invertible,
- $A^{-1} \ge 0$ (all entries of A^{-1} are nonnegative)

Definition 1.9. (**ε-Uniform Convergence**): Let (P_ε) be a family of SPPPDEs with $0 < \varepsilon \le 1$, each having a unique solution ψ_ε. Let $\psi_\varepsilon^{N,M}$ denote the numerical approximation on the mesh $\overline{\mathscr{D}}_{xt}^{N,M}$, with N and M spatial and temporal discretizations, respectively [2, 5]. The numerical solution $\psi_\varepsilon^{N,M}$ is said to *converge ε-uniformly* to ψ_ε if there exist $N_0, C > 0$, and rates $r_1, r_2 > 0$, independent of ε, such that

$$\sup_{0<\varepsilon\le 1} \|\psi_\varepsilon^{N,M} - \psi_\varepsilon\|_{\overline{\mathscr{D}}_{xt}^{N,M}} \le C\left(h^{r_1} + (\Delta t)^{r_2}\right).$$

In the case of Shishkin-type fitted meshes, which are designed to resolve boundary and interior layers, the pointwise error bound takes the form

$$\sup_{0<\varepsilon\le 1} \|\psi_\varepsilon^{N,M} - \psi_\varepsilon\|_{\overline{\mathscr{D}}_{xt}^{N,M}} \;\le\; C\Big(h^{r_1}\ln N + (\Delta t)^{r_2}\Big),$$

where the logarithmic factor $\ln N$ arises due to the non-uniform refinement near the layers, h and Δt are the spatial and temporal step sizes, r_1 and r_2 denote the orders of convergence, and $C > 0$ is independent of the perturbation parameter ε.

1.5 Literature Review

This section reviews several singularly perturbed parabolic diffusion-type problems with boundary layers, characterized by small temporal lag and spatial shift parameters. We focus on parameter-uniformly convergent numerical methods that effectively tackle the inherent challenges of these complex problems, paving the way for more reliable and accurate solutions.

1.5.1 Singularly Perturbed Reaction-Diffusion Problems

Reaction-diffusion equations describe how substance concentrations change over time and space due to diffusion (spreading) and reaction (local transformations) [29]. They can capture complex spatial patterns, such as stripes or hexagons, from initially uniform states and are widely used in chemistry, biology, physics, and fluid dynamics [31]. Here, we consider a singularly perturbed parabolic reaction-diffusion problem with appropriate initial and boundary conditions of the form:

$$\begin{cases} \mathscr{L}_\varepsilon \psi := \psi_t(x,t) - \varepsilon \psi_{xx}(x,t) + a(x,t)\psi(x,t) = f(x,t), \quad \forall (x,t) \in \mathscr{D}_{xt}, \\ \begin{cases} \psi(x,0) = \mathscr{S}_0(x), & \forall x \in \overline{\mathscr{D}}_x, \\ \psi(0,t) = \mathscr{S}_l(t), & \forall t \in \overline{\mathscr{D}}_t, \\ \psi(1,t) = \mathscr{S}_r(1,t)), & \forall t \in \overline{\mathscr{D}}_t. \end{cases} \end{cases} \tag{1.7}$$

where $\mathscr{L}_\varepsilon$ is the differential operator , $\varepsilon(0 < \varepsilon \ll 1)$, is the perturbation parameter, $\mathscr{D}_x = (0,1)$, $\mathscr{D}_t = (0,T]$ and $\mathscr{D}_{xt} = \mathscr{D}_x \times \mathscr{D}_t$. The functions $f(x,t)$ and $a(x,t)$ over $\overline{\mathscr{D}}_{xt}$, $\mathscr{S}_0(x)$ over $\overline{\mathscr{D}}_x$, $\mathscr{S}_l(t)$ and $\mathscr{S}_r(1,t))$ over $\overline{\mathscr{D}}_t$ are sufficiently smooth and satisfies the bound $a(x,t) \geq \alpha > 0$. Using the model equation in (1.7), a substantial body of literature has been developed by various researchers.

Numerical solutions of parabolic singularly perturbed reaction-diffusion problems are presented in [32]. The multi-scale solution of the considered problem is approximated by combining the backward Euler method for the time derivative on uniform mesh and central difference method for the space derivative on three different mesh types. The convergence analysis confirmed the proposed method is uniformly convergent with respect to the parameter ε.

The numerical treatment of singularly perturbed parabolic reaction-diffusion initial boundary value problems is proposed in [33]. Introducing a fitting parameter into the asymptotic solution and applying average finite difference approximation, a fitted operator finite difference method is developed. To accelerate the rate of convergence of the method, Richardson extrapolation technique is applied. Using Von-Neumann stability analysis and Lax-equivalence theorem, the proposed method is proven to be unconditionally convergent.

A fitted numerical technique for time-dependent singularly perturbed reaction-diffusion problems is employed in [34]. The continuous problem domain is discretized using the backward Euler method in the temporal direction and the non-standard finite difference method (NSFDM) in the spatial direction on uniform meshes. Stability and convergence analyses show that the proposed method achieves first-order convergence in time and second-order convergence in space.

In [35], a robust higher-order numerical method for solving singularly perturbed reaction-diffusion problems is constructed. The problem is discretized by means of the Crank-Nicolson method for the time derivative on uniform mesh and a hybrid numerical method that combined with cubic spline tension method on Shishkin meshes for the boundary layer region and central difference method for the coarse region. The convergence analysis proved that the method is second-order accurate in the coarse region and fourth-order accurate in the layer region within the spatial domain. Overall, the proposed method is uniformly convergent, with second-order accuracy in the temporal direction and higher-order accuracy in the spatial direction.

Parameter independent numerical method based on equi-distributed meshes for a class of SP parabolic-type reaction-diffusion problems with Robin boundary conditions are investigated [36]. The considered problem domain is discretized using the modified Euler method for the temporal direction on uniform meshes and a central difference method for the spatial direction via the equi-distribution of a suitably chosen monitor function. The convergence analyses and discussions have demonstrated that the proposed method exhibits parameter-uniform convergence, with second-order accuracy in space and first-order accuracy in time.

The review highlights that singularly perturbed parabolic reaction–diffusion problems have received comparatively limited attention. Moreover, many existing numerical methods exhibit reduced accuracy and low orders of convergence, which may be inadequate for resolving sharp layers. To address these limitations, we proposed a second-order fitted numerical scheme that improves both accuracy and order of convergences.

1.5.2 Singularly Perturbed RDEs with Small Time Lag

Singularly perturbed delay partial differential equations arise in various real-world contexts, such as biological and chemical reactions, and the modeling of population dynamics in epidemiology. A class of reaction-diffusion type singularly perturbed delay partial differential equations of the following form is considered:

$$\begin{cases} \psi_t(x,t) - \varepsilon\psi_{xx}(x,t) + a(x,t)\psi(x,t) + b(x,t)\psi(x,t-\delta) = f(x,t), \quad \forall (x,t) \in \mathscr{D}_{xt}, \\ \begin{cases} \psi(x,t) = \mathscr{S}_0(x,t), & \forall (x,t) \in \mu_0 = [0,1]\times[-\delta,0], \\ \psi(0,t) = \mathscr{S}_l(t), & \forall t \in \mu_l = \{(0,t) : 0 \le t \le T\}, \\ \psi(1,t) = \mathscr{S}_r(t)), & \forall t \in \mu_r = \{(1,t) : 0 \le t \le T\}. \end{cases} \end{cases} \tag{1.8}$$

where $\delta < \varepsilon$ is a small delay parameters which satisfies the relation $\delta = O(\varepsilon)$. Based on the model equation (1.8), various researchers have developed different numerical methods to obtain accurate solutions, some of which are reviewed below.

A fitted operator-based numerical method for solving unsteady singularly perturbed parabolic reaction-diffusion problems with small time lag is proposed in [37]. The problem is semi-discretized using the implicit Euler method in the temporal direction and the exponentially fitted cubic B-spline method in the spatial direction on uniform meshes. By applying the Richardson extrapolation technique in the temporal direction, the proposed method achieves second-order accurate $\varepsilon-$uniform convergence.

The authors in [38] developed a higher-order parameter-independent convergent method for solving singularly perturbed parabolic delay differential equations. The problem is discretized using a hybrid scheme on a generalized Shishkin mesh in the spatial direction and the implicit Euler scheme on a uniform mesh in the temporal direction. By applying the Richardson extrapolation technique, the resulting scheme is shown to be second-order accurate in time and fourth-order accurate, up to a logarithmic factor, in the spatial direction.

A new stable finite difference scheme for singularly perturbed reaction-diffusion time-delay problems is presented in [39]. The problem is discretized using the backward Euler scheme on a uniform mesh in the temporal direction, while a new stable finite difference scheme is developed for the spatial direction. The proposed method is shown to exhibit higher-order parameter-uniform convergence.

A fourth-order convergent method in both time and space is achieved in [40] through a non-standard fitted operator approach for large time-delay singularly perturbed reaction-diffusion problems. The problem is discretized using the Crank–Nicolson method in time and a nonstandard finite difference scheme in space on a uniform mesh. Richardson extrapolation is applied to enhance the overall accuracy of the scheme.

A class of singularly perturbed parabolic reaction-diffusion problems with time delay is studied in [41]. The original domain is decomposed into three overlapping sub-domains, consisting of two boundary layer regions and one regular region. On each sub-domain, the problem is discretized using the backward Euler scheme in time and the central difference scheme in space. The proposed method is shown to be uniformly convergent, with almost second-order accuracy in space and first-order accuracy in time.

A singularly perturbed time-delay parabolic partial differential equation is considered in [42]. A robust fitted operator finite difference method is designed for its numerical solution by replacing the classical differential operator with a fitted operator based on the Crank–Nicolson discretization. Stability analysis confirms that the proposed method is unconditionally stable and second-order convergent.

Existing studies on singularly perturbed parabolic reaction–diffusion problems with small time lag show limited attention and generally achieve low-order accuracy, which is often insufficient for resolving sharp boundary and interior layers. This reveals a clear need for higher-order, uniformly convergent schemes. To address this gap, we propose a higher-order uniformly convergent scheme that improves accuracy for such problems.

1.5.3 Singularly Perturbed Problems with Mixed Shift Parameters

Spatially delay SPPPDEs of the CDR type problems involving a small perturbation parameter multiplying the highest-order derivative term, with at least one retarded and one advanced spatial shift term. Such equations arise in various physical models, including the Navier-Stokes equations, atmospheric pollution, turbulent transport, and groundwater flow [46]. We consider a class of convection-diffusion-reaction SPPDDEs with general shift parameters in the reaction term of the form:

$$\begin{cases} \psi_t(x,t) - \mathscr{L}_\varepsilon \psi(x,t) = f(x,t), \quad \forall (x,t) \in \mathscr{D}_{xt}, \\ \begin{cases} \psi(x,t) = \mathscr{S}_0(x,t) \quad \forall (x,t) \in \mu_0 = \{(x,t) : 0 \le x \le 1,\ 0 < t \le T\}, \\ \psi(x,t) = \mathscr{S}_l(x,t) \quad \forall (x,t) \in \mu_l = \{(x,t) : -\delta \le x \le 0,\ 0 < t \le T\}, \\ \psi(x,t) = \mathscr{S}_r(x,t) \quad \forall (x,t) \in \mu_r = \{(x,t) : 1 \le x \le 1+\eta,\ 0 < t \le T\}. \end{cases} \end{cases} \tag{1.9}$$

where $\mathscr{L}_\varepsilon \psi(x,t) = \varepsilon \psi_{xx}(x,t) + a(x)\psi_x(x,t) + b(x)\psi(x-\delta,t) + c(x)\psi(x,t) + d(x)\psi(x+\eta,t)$ is the differential operator, δ and η are small delay and advance parameters with the property $\delta, \eta < \varepsilon$, respectively. Using this model equation, the following authors have contributed scholarly articles.

A fitted operator method is developed in [47] for singularly perturbed parabolic partial differential equations with spatial delay. The problem is decomposed into three piecewise sub-problems, and the delay term is approximated using Taylor series expansion to transform it into a standard singularly perturbed form. The implicit Euler method is employed for temporal discretization, while central difference schemes are used in the spatial direction. Richardson extrapolation is further applied to improve temporal accuracy, leading to a uniformly convergent method of order $O(h^2 + \Delta t^2)$.

Singularly perturbed delay differential equations are investigated in [48] by approximating the retarded terms using Taylor series expansion. The resulting time-dependent problem is discretized using a standard implicit finite difference scheme in the temporal direction through Rothe's method on a uniform mesh, while a B-spline collocation method is applied on a piecewise-uniform Shishkin mesh in the spatial direction. The proposed method is shown to achieve an order of convergence $O(M^{-1} + N^{-2}(lnN)^3)$. , where M and N are the number of mesh points used in the temporal direction and in the spatial direction, respectively.

A nonstandard finite difference technique is employed in [49] for singularly perturbed parabolic differential difference equations. The advance and delay terms are approximated using Taylor series expansion, while the resulting problem is discretized using the Crank–Nicolson method in time and a nonstandard finite difference scheme in space. The proposed method is shown to be uniformly stable and convergent with order $O(N^{-1} + \Delta t^2)$.

A higher-order hybrid finite difference technique is employed in [50] for singularly perturbed differential difference equations. The retarded terms are approximated using Taylor series expansion, and the resulting problem is discretized using the implicit Euler scheme in time and a hybrid finite difference scheme on a piecewise-uniform Shishkin mesh in space. Richardson extrapolation is applied to enhance temporal accuracy, yielding a uniformly convergent method of order $O(\Delta t^2 + N^{-2}(lnN)^2)$.

Time-dependent singularly perturbed differential-difference equations arising in neuronal dynamics are studied in [51]. The spatial shift terms are approximated using Taylor series expansion to linearize both negative and positive shifts. The temporal discretization is carried out using the Crank–Nicolson scheme on a uniform mesh, while a quadratic B-spline collocation method on an exponentially graded mesh is used in the spatial direction. The resulting method is shown to achieve uniform second-order convergence in both space and time.

A stable finite difference method is developed in [52] using the implicit Euler scheme for temporal discretization and a class of non-standard finite difference schemes with infinite series approximation for spatial derivatives. Richardson extrapolation is applied to enhance the accuracy of the scheme, yielding second-order convergence in both time and space.

First-order uniformly convergent scheme is obtained in [53] for singularly perturbed differential-difference equations using an exponential fitted operator approach. The delay and advance terms are linearized using Taylor series expansion, while the time derivative is discretized by the implicit Euler method and the spatial derivatives are approximated using an exponentially fitted finite difference operator.

Singularly perturbed parabolic differential-difference equations are studied in [54]. The spatial shift term is approximated using Taylor series expansion, while the implicit Euler method is employed for temporal discretization and a classical upwind scheme is used on Shishkin and Bakhvalov–Shishkin meshes for spatial discretization. The scheme is shown to be first-order convergent up to a logarithmic factor and optimally first-order accurate in space on both meshes.

An exponentially fitted numerical method is developed in [55] for singularly perturbed one-dimensional parabolic partial differential equations with positive and negative spatial shifts. The shift terms are first approximated using Taylor series expansion, while the time derivative is discretized using the backward Euler method and the spatial derivatives are treated using an exponentially fitted approach. The proposed method exhibits first-order convergence.

Singularly perturbed parabolic PDEs with negative shifts in the convection and reaction terms are studied in [112]. The shift terms are approximated using Taylor series expansion, and a higher-order Taylor discretization is employed in time. Galerkin FEM on a piecewise Shishkin mesh is used in space, while exponentially fitted spline-based shape functions are applied on a uniform mesh within a three-step Taylor–Galerkin framework. The method is shown to be conditionally ε-uniformly convergent, achieving third-order accuracy in time and linear accuracy in space.

This survey shows that, although considerable work has been carried out on the numerical solution of singularly perturbed parabolic differential-difference equations over the past two decades, the accurate and systematic treatment of both negative and positive shift terms remains relatively under explored. Motivated with this gap, we formulate higher-order numerical methods that effectively handle such shifts.

1.5.4 Singularly Perturbed CDREs with Shift Parameters

Singularly perturbed parabolic differential equations with spatial delay model systems whose evolution depends on both current and past spatial states. They arise in fields such as computational neuroscience, population dynamics, epidemiology, and control theory. We consider a class of such equations with small spatial shifts in the convection and reaction terms, subject to initial and boundary conditions, of the following form:

$$\begin{cases} \psi_t(x,t) - \mathscr{L}_\varepsilon \psi(x,t) = f(x,t), \quad \forall (x,t) \in \mathscr{D}_{xt}, \\ \begin{cases} \psi(0,t) = \mathscr{S}_0(x,t), \quad \forall (x,t) \in \mu_0 = \{(x,t) : 0 \le x \le 1, \;\; t = 0\}, \\ \psi(x,t) = \mathscr{S}_l(x,t), \quad \forall (x,t) \in \mu_l = \{(x,t) : -\delta \le x \le 0, \;\; 0 < t \le T\}, \\ \psi(1,t) = \mathscr{S}_r(x,t), \quad \forall (x,t) \in \mu_r = \{(x,t) : x = 1, \;\; 0 < t \le T\}. \end{cases} \end{cases} \tag{1.10}$$

where $\mathscr{L}_\varepsilon \psi(x,t) = \varepsilon \psi_{xx}(x,t) + a(x)\psi_x(x-\delta,t) + b(x)\psi(x-\delta,t)$ is a differential operator and $\delta < \varepsilon$ is a small shift parameter which satisfies the relation $\delta = O(\varepsilon)$. Using this model equation, relatively few scholars have established parameter uniformly convergent numerical methods for solving singularly perturbed delay differential equations involving small shift parameters in the convection and reaction terms.

A nonstandard finite difference scheme based on the θ-method is developed in [57] for singularly perturbed problems, using uniform meshes in both space and time. Richardson extrapolation is applied to enhance accuracy, resulting in a parameter-uniform method that achieves second-order convergence in both spatial and temporal directions.

Singularly perturbed parabolic convection–diffusion problems are studied in [106]. A domain decomposition Taylor–Galerkin finite element method is formulated for their numerical treatment. The problem is decomposed into subdomains and approximated using a Taylor–Galerkin finite element framework. The analysis shows that the proposed scheme is uniformly convergent with respect to the perturbation parameter ε.

A fitted numerical scheme is developed in [58] for singularly perturbed parabolic differential equations with delay in the zeroth and first-order derivative terms. The scheme employs the θ-

method for temporal discretization and an exponentially fitted finite difference method for spatial discretization on uniform meshes. The proposed method is shown to be parameter-uniformly convergent.

The survey indicates that the problem under consideration is under an enfat stage that it requires new and higher methods. This motivated us to formulate a higher-order hybridaid fitted numerical scheme.

Research Gap:

The overall review highlighted that existing fitted numerical methods have low accuracy and order convergence, motivating the formulation of higher-order alternatives schemes.

1.6 Research Objectives

In developing the proposed fitted numerical schemes, emphasis is placed on advancing existing methodologies by enhancing accuracy and order of convergences relative to established results in the literature, as well as on introducing alternative techniques that may facilitate further analytical and computational investigations.

1.6.1 General Objective

The general objective of this dissertation is to formulate and analyze fitted numerical methods for singularly perturbed parabolic diffusion-type problems with boundary layers.

1.6.2 Specific Objectives

The specific objectives of the dissertation are to:

- develop and analyze high-order, uniformly convergent numerical schemes for singularly perturbed parabolic reaction–diffusion problems
- construct fitted and stabilized schemes for singularly perturbed parabolic convection–diffusion problems with mixed and small shift parameters.
- design and analyze hybrid and exponentially fitted schemes for singularly perturbed parabolic problems, focusing on accuracy, stability, and convergence.

1.6.3 Significance of the Study

After the completion of the study, the findings of this dissertation will be useful to:

- Numerical analysts, by providing a higher-order fitted numerical method for solving SPPPDEs with improved accuracy and efficiency.
- Computational designers and software developers, by offering reliable numerical algorithms for scientific computing and simulation applications.
- Researchers and graduate students, by serving as a reference for further studies in singular perturbation problems and numerical analysis.

1.6.4 Scope of the Study

This dissertation is limited to fitted numerical methods for solving singularly perturbed parabolic diffusion-type four governing problems with boundary layers.

1.7 Research design and Mathematical procedures

1.7.1 Research design

This dissertation employs a computational research design to develop and analyze fitted numerical methods for the problems under study.

1.7.2 Mathematical Procedures

To accomplish the stated objectives, the following procedures are implemented.

1. Problem formulation.
2. Establish and analysis the properties of the continuous problem.
3. Develop fitted numerical methods for the considered class of problems.
4. Establish the stability and uniform convergence of the proposed methods.
5. Design and implement computational codes for the formulated methods.
6. Verify the validity of the proposed methods through numerical examples.
7. Summarize the numerical results using tables and graphical representations.

8. Draw conclusions based on theoretical predictions and numerical results.

1.8 Governing Problems

This dissertation considers four governing problems, which are categorized into two basic sub-problems. The first two belong to the class of reaction–diffusion type problems, whereas the remaining two correspond to convection–diffusion type problems.

Governing Problem-I

A class of singularly perturbed parabolic reaction–diffusion problems, subject to appropriate initial and boundary conditions [34], can be formulated as follows:

$$\begin{cases} \mathscr{L}_\varepsilon \psi := \psi_t(x,t) - \varepsilon \psi_{xx}(x,t) + a(x,t)\psi(x,t) = f(x,t), \quad \forall (x,t) \in \mathscr{D}_{xt}, \\ \begin{cases} \psi(x,0) = \mathscr{S}_0(x), & \forall x \in \overline{\mathscr{D}}_x, \\ \psi(0,t) = \mathscr{S}_l(t), & \forall t \in \overline{\mathscr{D}}_t, \\ \psi(1,t) = \mathscr{S}_r(1,t)), & \forall t \in \overline{\mathscr{D}}_t. \end{cases} \end{cases} \tag{1.11}$$

where $\mathscr{L}_\varepsilon$ is the differential operator, ε $(0 < \varepsilon \ll 1)$ is the perturbation parameter, $\mathscr{D}_x = (0,1)$, $\mathscr{D}_t = (0,T]$, and $\mathscr{D}_{xt} = \mathscr{D}_x \times \mathscr{D}_t$.

The functions $f(x,t)$ and $a(x,t)$ are sufficiently smooth in $\overline{\mathscr{D}}_{xt}$, while $\mathscr{S}_0(x)$, $\mathscr{S}_l(t)$, and $\mathscr{S}_r(t)$ are sufficiently smooth on their respective domains $\overline{\mathscr{D}}_x$ and $\overline{\mathscr{D}}_t$. Furthermore, the coefficient function $a(x,t)$ satisfies

$$a(x,t) \geq \alpha > 0, \qquad \forall (x,t) \in \overline{\mathscr{D}}_{xt}.$$

Governing Problem-II

A class of SPPDDEs arising from reaction–diffusion processes, subject to initial and interval boundary conditions [37], can be expressed as follows:

$$\begin{cases} \psi_t(x,t) - \varepsilon \psi_{xx}(x,t) + a(x,t)\psi(x,t) + b(x,t)\psi(x,t-\delta) = f(x,t), \quad \forall (x,t) \in \mathscr{D}_{xt}, \\ \begin{cases} \psi(x,t) = \mathscr{S}_0(x,t) & \mu_0 = [0,1] \times [-\delta, 0], \\ \psi(0,t) = \mathscr{S}_l(t) & \mu_l = \{(0,t) : 0 \leq t \leq T\}, \\ \psi(1,t) = \mathscr{S}_r(t)) & \mu_r = \{(1,t) : 0 \leq t \leq T\}. \end{cases} \end{cases} \tag{1.12}$$

where $\mathscr{L}_\varepsilon\psi(x,t) := \psi_t(x,t) - \varepsilon\psi_{xx}(x,t) + a(x,t)\psi(x,t) + b(x,t)\psi(x,t-\delta)$, $\varepsilon, (0 < \varepsilon \ll 1)$, is small parameter such that, $\delta < \varepsilon$ is a small delay parameters which satisfies the relation $\delta = O(\varepsilon)$.

Governing Problem-III

A class of SPPDDEs associated with convection–diffusion problems involving mixed shift parameters in the reaction term, subject to appropriate initial and interval boundary conditions [50], can be defined as follows:

$$\begin{cases} \psi_t(x,t) - \mathscr{L}_\varepsilon\psi(x,t) = f(x,t), \quad \forall (x,t) \in \mathscr{D}_{xt}, \\ \begin{cases} \psi(x,t) = \mathscr{S}_0(x,t) \quad \forall (x,t) \in \mu_0 = \{(x,t) : 0 \le x \le 1, \;\; 0 < t \le T\}, \\ \psi(x,t) = \mathscr{S}_l(x,t) \quad \forall (x,t) \in \mu_l = \{(x,t) : -\delta \le x \le 0, \;\; 0 < t \le T\}, \\ \psi(x,t) = \mathscr{S}_r(x,t) \quad \forall (x,t) \in \mu_r = \{(x,t) : 1 \le x \le 1+\eta, \;\; 0 < t \le T\}. \end{cases} \end{cases} \tag{1.13}$$

where
$\mathscr{L}_\varepsilon\psi(x,t) := \varepsilon\psi_{xx}(x,t) + a(x)\psi_x(x,t) + b(x)\psi(x-\delta,t) + c(x)\psi(x,t) + d(x)\psi(x+\eta,t)$ is the differential operator, δ and η are small delay and advance parameters with the property $\delta, \eta < \varepsilon$, respectively.

Governing Problem-IV

A class of SPPDDEs with a small shift parameter in the convection and reaction terms, subject to prescribed initial and interval boundary conditions [57], is formulated as follows:

$$\begin{cases} \mathscr{L}_\varepsilon\psi(x,t) = f(x,t), & \forall (x,t) \in \mathscr{D}_{xt} = \mathscr{D}_x \times \mathscr{D}_t = (0,1) \times (0,T], T > 0, \\ \psi(x,0) = \mathscr{S}_0(x,t), & \forall (x,t) \in \mu_0 = \left\{(x,t) : \forall x \in \overline{\mathscr{D}}_x, t = 0\right\}, \\ \psi(x,t) = \mathscr{S}_l(x,t), & \forall (x,t) \in \mu_l = \left\{(x,t) : \forall (x,t) \in [-\delta, 0] \times \overline{\mathscr{D}}_t\right\}, \\ \psi(1,t) = \mathscr{S}_r(1,t), & \forall (x,t) \in \mu_r = \left\{(x,t) : x = 1, \forall t \in \overline{\mathscr{D}}_t\right\}. \end{cases} \tag{1.14}$$

where $\mathscr{L}_\varepsilon\psi := \psi_t(x,t) - \varepsilon\psi_{xx}(x,t) + a(x,t)\psi_x(x-\delta,t) + b(x,t)\psi(x-\delta,t)$ is the differential operator, $\varepsilon \;\; (0 < \varepsilon \ll 1)$, is a perturbation parameter and $\delta < \varepsilon$ is a small shift parameter which satisfies the relation $\delta = O(\varepsilon)$.

1.9 Organization of the Dissertation

This dissertation is structured into eight chapters, each focusing on a specific aspect of the research.

Chapter (1) presents the background of the study, a comprehensive review of relevant literature, the research objectives, significance and scope of the study, the mathematical methodologies employed, governing problems, and an outline of the dissertation's structure.

Chapter (2) investigates a second-order uniformly convergent numerical scheme tailored for singularly perturbed parabolic reaction-diffusion problems as defined in governing problem (1.11).

Chapter (3) introduces a fitted linear multi-step method designed for singularly perturbed parabolic-type reaction-diffusion problems, utilizing Shishkin meshes as described in governing problem (1.11).

Chapter (4) is devoted to the development of a fourth-order parameter-uniformly convergent scheme for singularly perturbed differential-difference equations, as represented in governing problem (1.12).

Chapter (5) presents an exponentially fitted upwind scheme for singularly perturbed differential equations with mixed shift parameters, corresponding to the governing problem in (1.13).

Chapter (6) focuses on the formulation of a midpoint upwind scheme applicable to singularly perturbed differential equations characterized by small shift parameters in both convection and reaction terms, as given in governing problem (1.14).

Chapter (7) explores numerical solutions of the equations presented in governing problem (1.14), employing a hybrid finite difference scheme based on the Crank–Nicolson method over Shishkin meshes.

Chapter (8) concludes the dissertation with detailed discussions of the findings, general conclusions, and recommendations for future research directions.

Chapter 2

A Second-Order Uniformly Convergent Scheme for Singularly Perturbed Parabolic Reaction–Diffusion Problems

This chapter is devoted to the development of a fitted numerical method for solving singularly perturbed parabolic reaction–diffusion problems. Owing to the presence of a small perturbation parameter $\varepsilon, (0 < \varepsilon \ll 1)$, in the highest-order derivative, the solution exhibits boundary layers near $x = 0$ and $x = 1$, where sharp gradients occur. As a result, classical numerical methods fail to provide accurate solutions on uniform meshes. To overcome these difficulties, a second-order uniformly convergent scheme is constructed using the Crank–Nicolson method for time discretization and a non-standard finite difference approach for spatial discretization. The proposed scheme is shown to be second-order uniformly convergent in both space and time. Numerical experiments on representative model problems confirm the theoretical results and demonstrate that the proposed method outperforms several existing methods reported in the literature.

2.1 Introduction

The majority of real-life scenarios in applied science and engineering are special cases of parameter-dependent differential equations. The mathematical framework that analyzes the influence of such parameters on the behavior of solutions is known as perturbation theory. Within this framework, SPPPDEs refer to problems where the highest-order derivative is multiplied by a small parameter $\varepsilon, (0 < \varepsilon \ll 1)$. These equations have been the focus of extensive research, as documented in [5, 14, 60]. The presence of a small parameter ε in the problem under consideration, exhibits boundary and/or interior layer regions to which the solutions of the problem changes abruptly. Due to these challenges, the classical numerical methods fail to give an accurate solution in these regions unless we use very fine meshes, which produce round off errors and requires massive computational costs. This emphasises the need for parameter-independent numerical methods as discussed in [61, 62, 63]. Consequently, parameter-uniform convergent algorithms have been developed. The fitted operator approach, the fitted mesh approach and the domain decomposition approach are few to mention.

Although numerous researchers have extensively studied solution methodologies for singularly perturbed convection-diffusion problems using parameter-uniformly convergent methods, relatively few have focused on singularly perturbed reaction-diffusion problems. Notable exceptions include the works of [34, 36], who addressed problems of this type that arise in various scientific fields such as chemistry, physics, biology, and fluid dynamics. These problems typically model the spatio-temporal evolution of species, densities, or concentrations involving at least two interacting variables [31].

Due to the low accuracy and order of convergence as pointed out from the review, we inspired and developed a fitted numerical scheme for problems. The proposed method employs NSFDM in the spatial direction and the Crank–Nicolson approach in the temporal direction, both implemented on uniform meshes. Theoretical and numerical analyses reveal that the scheme achieves second-order accuracy in both space and time.

2.2 Problem formulation

Consider a class of singularly perturbed parabolic reaction–diffusion problems, as formulated in the governing problem (1.11), together with the associated initial and boundary conditions presented in [34].

$$\begin{cases} \mathscr{L}_\varepsilon \psi := \psi_t(x,t) - \varepsilon \psi_{xx}(x,t) + a(x,t)\psi(x,t) = f(x,t), \quad \forall (x,t) \in \mathscr{D}_{xt}, \\ \begin{cases} \psi(x,0) = \mathscr{S}_0(x), & \forall x \in \overline{\mathscr{D}}_x, \\ \psi(0,t) = \mathscr{S}_l(t), & \forall t \in \overline{\mathscr{D}}_t, \\ \psi(1,t) = \mathscr{S}_r(1,t)), & \forall t \in \overline{\mathscr{D}}_t. \end{cases} \end{cases} \tag{2.1}$$

where $\mathscr{L}_\varepsilon \psi(x,t)$ is the differential operator, $\varepsilon (0 < \varepsilon \ll 1)$, is the perturbation parameter, $\mathscr{D}_x = (0,1)$, $\mathscr{D}_t = (0,T]$ and $\mathscr{D}_{xt} = \mathscr{D}_x \times \mathscr{D}_t$. To ensure the existence of a unique solution, the functions $a(x,t)$ and $f(x,t)$ are assumed to be sufficiently smooth, bounded and satisfy

$$a(x,t) \geq \alpha > 0, \quad \forall (x,t) \in \overline{\mathscr{D}}_{xt}. \tag{2.2}$$

2.3 Properties of the Analytic Solution

This section focuses on the bounds of the analytic solution $\psi(x,t)$ of problem (2.1) and its derivatives using Hölder's continuity with appropriate compatibility conditions. We assumed that the data $a, f \in C^{(4,2)}(\overline{\mathscr{D}}_{xt})$, and the exact solution $\psi(x,t) \in C^{(4,2)}(\overline{\mathscr{D}}_{xt})$ are sufficiently smooth. As outlined in [63], the required compatibility conditions at the corner points $(0,0)$ and $(1,0)$ are defined as $\mathscr{S}_0(0,0) = \mathscr{S}_l(0)$, $\mathscr{S}_0(1,0) = \mathscr{S}_r(0)$ and satisfies

$$\begin{cases} \frac{\partial \mathscr{S}_l(0)}{\partial t} - \varepsilon \frac{\partial^2 \mathscr{S}_0(0)}{\partial x^2} + a(0,0)\mathscr{S}_0(0) = f(0,0), \\ \frac{\partial \mathscr{S}_r(0)}{\partial t} - \varepsilon \frac{\partial^2 \mathscr{S}_0(1)}{\partial x^2} + a(1,0)\mathscr{S}_0(1) = f(1,0). \end{cases} \tag{2.3}$$

The above conditions together with the bound in (2.2) ensure that the solution $\psi(x,t)$ of problem (2.1) exhibits twin boundary layers of width $O(\sqrt{\varepsilon})$ at x = 0 and x = 1 as $\varepsilon \to 0$.

Lemma 2.1. *(Continuous Maximum Principle): Let $\phi(x,t)$ be any sufficiently smooth function satisfying $\phi(x,t) \geq 0, \forall (x,t) \in \partial \mathscr{D}_{xt} = \overline{\mathscr{D}}_{xt} \setminus \mathscr{D}_{xt}$ and $\mathscr{L}_\varepsilon \phi(x,t) \geq 0, \forall (x,t) \in \mathscr{D}_{xt}$ [34]. Then, $\phi(x,t) \geq 0, \forall (x,t) \in \overline{\mathscr{D}}_{xt}$*

Proof. Suppose that $(x^*,y^*) \in \mathscr{D}_{xt}$ such that $\phi(x^*,y^*) = min_{(x,t)\in\overline{\mathscr{D}}_{xt}} \phi(x,t) < 0$.
From this condition it is seen that $\phi_t(x^*,y^*) = 0$, $\phi_x(x^*,y^*) = 0$ and $\phi_{xx}(x^*,y^*) \geq 0$. Having these all the differential operator $\mathscr{L}_\varepsilon$ can also be defined in the following manner.

$$\begin{aligned} \mathscr{L}_\varepsilon \phi(x^*,y^*) &= \phi_t(x^*,y^*) - \varepsilon \phi_{xx}(x^*,y^*) + a(x^*,y^*)\phi(x^*,y^*), \\ &= -\varepsilon \phi_{xx}(x^*,y^*) + a(x^*,y^*)\phi(x^*,y^*), \\ &\leq 0 \quad , \, since, \phi_{xx} \geq 0, \; \phi \leq 0 \; and \; a > 0 \; at \; (x^*,y^*). \end{aligned}$$

This implies $\mathscr{L}_\varepsilon \phi(x^*,y^*) \leq 0$, which contradicts to our assumption $\mathscr{L}_\varepsilon \psi(x,y) \geq 0$.
Hence, $\phi(x,t) \geq 0$, $\forall (x,t) \in \overline{\mathscr{D}}_{xt}$. □

Lemma 2.2. *(Uniform Stability Estimate): Let $\psi(x,t) \in C^{2,1}(\overline{\mathscr{D}}_{xt})$ be the solution of the continuous problem of equation* (2.1) *[64]. Then it satisfies the bound*

$$|\psi(x,t)| \leq \alpha^{-1}||f|| + max\{|\mathscr{S}_0(x)|, |\mathscr{S}_l(t)|, |\mathscr{S}_r(t)|\}.$$

Proof. To prove this Lemma, we defined two barrier functions $\Omega^\pm$ as follows

$$\Omega^\pm(x,t) = \alpha^{-1}||f|| + max\{|\mathscr{S}_0(x)|, |\mathscr{S}_l(t)|, |\mathscr{S}_r(t)|\} \pm \psi(x,t),$$

When $t = 0$,

$$\begin{aligned}\Omega^{\pm}(x,0) &= \alpha^{-1}||f|| + max\{|\mathscr{S}_0(x)|, |\mathscr{S}_l(0)|, |\mathscr{S}_r(0)|\} \pm \psi(x,0),\\ &= \alpha^{-1}||f|| + max\{|\mathscr{S}_0(x)|, |\mathscr{S}_l(0)|, |\mathscr{S}_r(0)|\} \pm \mathscr{S}_0(x) \geq 0.\end{aligned}$$

When $x = 0$,

$$\begin{aligned}\Omega^{\pm}(0,t) &= \alpha^{-1}||f|| + max\{|\mathscr{S}_0(0)|, |\mathscr{S}_l(t)|, |\mathscr{S}_r(t)|\} \pm \psi(0,t),\\ &= \alpha^{-1}||f|| + max\{|\mathscr{S}_0(0)|, |\mathscr{S}_l(t)|, |\mathscr{S}_r(t)|\} \pm S_l(t) \geq 0.\end{aligned}$$

When $x = 1$,

$$\begin{aligned}\Omega^{\pm}(1,t) &= \alpha^{-1}||f|| + max\{|\mathscr{S}_0(1)|, |\mathscr{S}_l(t)|, |\mathscr{S}_r(t)|\} \pm \psi(1,t),\\ &= \alpha^{-1}||f|| + max\{|\mathscr{S}_0(0)|, |\mathscr{S}_l(t)|, |\mathscr{S}_r(t)|\} \pm \mathscr{S}_r(t) \geq 0.\end{aligned}$$

Combining all these on the domain $\mathscr{D}_{xt}$ results

$$\begin{aligned}\mathscr{L}_\varepsilon\Omega^{\pm}(x,t) &= \frac{\partial\Omega^{\pm}(x,t)}{\partial t} - \varepsilon\frac{\partial^2\Omega^{\pm}(x,t)}{\partial x^2} + a(x,t)\Omega^{\pm}(x,t),\\ &= a(x,t)\alpha^{-1}||f|| + a(x,t) \times max\{|\mathscr{S}_0(x)|, |\mathscr{S}_l(t)|, |\mathscr{S}_r(t)|\}\\ &+ \alpha^{-1}||f|| \pm \mathscr{L}_\varepsilon\psi(x,t),\\ &= \alpha^{-1}||f|| + a(x,t) \times max\{|\mathscr{S}_0(x)|, |\mathscr{S}_l(t)|, |\mathscr{S}_r(t)|\} \pm f(x,t) \geq 0.\end{aligned}$$

Hence, from Lemma (2.1) it is shown that $\Omega^{\pm}(x,t) \geq 0$, $\forall (x,t) \in \overline{\mathscr{D}}_{xt}$. □

Lemma 2.3. *Let $\psi(x,t)$ be the solution of the problem (2.1). Then we have*

$$\left|\psi^{(i,j)}(x,t)\right| \leq C\left[1 + \varepsilon^{-i/2}\left(\exp(-\sqrt{\frac{\alpha}{\varepsilon}}x + \exp(-\sqrt{\frac{\alpha}{\varepsilon}}(1-x))\right)\right]$$

where $0 \leq i + 2j \leq 4$.

Proof. To prove this, we first decompose the solution of the problem (2.1) into regular and singular forms of the following manner outlined in [95]:

$$\psi(x,t) = v(x,t) + w_l(x,t) + w_r(x,t) \tag{2.4}$$

where

- $v(x,t)$ is a regular solution obtained outside the layer region.
- $w_l(x,t)$ is a singular solution obtained inside the layer region near $x = 0$.
- $w_r(x,t)$ is a singular solution obtained inside the layer region near $x = 1$.

Case I: Regular Solution and It's bounds.
The regular solution $v(x,t)$ satisfy the reduced problem (2.1) ($\varepsilon = 0$).

$$a(x,t)v(x,t) = f(x,t) \implies v(x,t) = \frac{f(x,t)}{a(x,t)}.$$

Since $a(x,t), f(x,t) \in C^{(4,2)}(\overline{\mathscr{D}}_{xt})$ and $a(x,t) \geq \alpha > 0$, $v(x,t)$ is smooth and differentiable in $C^{(4,2)}(\overline{\mathscr{D}}_{xt})$.
Now we use mathematical induction to show

$$\left|v^{i,j}(x,t)\right| \leq C, \text{ for all } i+2j \leq 4.$$

Base case:

- for $i = 0,\ j = 0$, gives $|v(x,t)| = \left|\frac{f(x,t)}{a(x,t)}\right| \leq \frac{||f||_\infty}{\alpha}$.
- for $i = 1,\ j = 0$, gives $v_x = \frac{f_x a - f a_x}{a^2} \implies |v_x| \leq C$.
- for $i = 0,\ j = 1$, gives $v_t = \frac{f_t a - f a_t}{a^2} \implies |v_t| \leq C$.

Inductive case:
Assume that for all $i+2j \leq \zeta$ ($\zeta \leq 3$), we have

$$|v^{i,j}(x,t)| \leq C.$$

We prove the case where $i+2j = \zeta+1 \leq 4$. Since $v(x,t) = \frac{f(x,t)}{a(x,t)}$, and by applying the Leibniz and chain rules, each higher-order derivative of $v^{i,j}$ can be expressed as a rational function involving derivatives of f and a, along with powers of a. Given that f and a are smooth, and a is bounded below by a positive constant $\alpha > 0$, it follows that:

$$\left|v^{i,j}(x,t)\right| \leq C, \text{ for all } i+2j \leq 4. \tag{2.5}$$

Case II: Singular Solution and it's bounds.
We now construct the singular solutions $w_l(x,t)$, $w_r(x,t)$, which satisfy

$$w_t - \varepsilon w_{xx} + a(x,t)w = 0 \tag{2.6}$$

designed to correct the mismatch of $v(x,t)$ at the boundaries $x = 0$ and $x = 1$.
The general behavior of these layer terms is:

$$\begin{cases} w_l(x,t) \approx \phi_l(t)exp\left(\mu x\right), \\ w_r(x,t) \approx \phi_r(t)exp\left(\mu(1-x)\right) \end{cases} \tag{2.7}$$

where $\mu = \sqrt{\frac{\alpha}{\varepsilon}}$ is the decay rate.
Using Eq. (2.7) into Eq. (2.6) and simplifying gives

$$\begin{cases} \partial_x^i w_l(x,t) \leq C\varepsilon^{-i/2}\exp(-\mu x) \\ \partial_x^i w_r(x,t) \leq C\varepsilon^{-i/2}\exp(-\mu(1-x)) \end{cases} \tag{2.8}$$

and time derivatives ∂_t^j are bounded assuming smooth compatibility conditions.
Hence, for all $i+2j \leq 4$, we have

$$\begin{cases} \left|w_l^{i,j}(x,t)\right| \leq C\varepsilon^{-i/2}\exp(-\sqrt{\frac{\alpha}{\varepsilon}}x) \\ \\ \left|w_r^{i,j}(x,t)\right| \leq C\varepsilon^{-i/2}\exp(-\sqrt{\frac{\alpha}{\varepsilon}}(1-x) \end{cases} \tag{2.9}$$

Finally, using (2.5) and (2.9) gives

$$\begin{aligned} \left|\psi^{i,j}(x,t)\right| &\leq \left|V^{i,j}(x,t)\right| + \left|w_l^{i,j}(x,t)\right| + \left|w_r^{i,j}(x,t)\right| \\ &\leq C + C\varepsilon^{-i/2}\exp(-\mu x) + C\varepsilon^{-i/2}\exp(-\mu(1-x)) \\ &= C\left[1+\varepsilon^{-i/2}\left(\exp(-\sqrt{\frac{\alpha}{\varepsilon}}x) + \exp(-\sqrt{\frac{\alpha}{\varepsilon}}(1-x)\right)\right] \end{aligned}$$

Hence, we conclude that

$$\left|\psi^{i,j}(x,t)\right| \leq C\left[1+\varepsilon^{-i/2}\left(\exp(-\sqrt{\frac{\alpha}{\varepsilon}}x) + \exp(-\sqrt{\frac{\alpha}{C_\varepsilon}}(1-x)\right)\right]$$

□

2.4 Formulation of the Numerical Scheme

This section deals with the semi-discretization of the problem along the temporal and spatial directions. Finally, we combined the two discretized problems together and found the fully discrete solution of the proposed problem stated in ((2.1)).

2.4.1 Temporal discretization:

Divide the time domain $[0,T]$ into equal number of M subintervals of length Δt

$$\overline{\mathscr{D}}_t^M = \left\{ t^j : t^j = j\Delta t, j = 0,1,2,3,\ldots M \text{ and } \Delta t = \frac{T}{M} \right\}. \tag{2.10}$$

Using the Crank-Nicolson method [13] on the model problem (2.1), we get the following semi-discrete formulation:

$$\begin{cases} \frac{\psi^{j+1}-\psi^j}{\Delta t} = \varepsilon(\frac{\psi_{xx}^{j+1}+\psi_{xx}^j}{2}) - \frac{((a\psi)^{j+1}+(a\psi)^j)}{2} + \frac{f^{j+1}+f^j}{2}, \\ \begin{cases} \psi(x,0) = \mathscr{S}_0(x), & \forall x \in \overline{\mathscr{D}}_x, \\ \psi(0,t^{j+1}) = \mathscr{S}_l(t^{j+1}), & 0 \leq j \leq M-1, \\ \psi(1,t^{j+1}) = \mathscr{S}_r(1,t^{j+1})), & 0 \leq j \leq M-1. \end{cases} \end{cases} \tag{2.11}$$

Rearranging the j^{th} and $(j+1)^{th}$ time level equations gives

$$\begin{cases} -\varepsilon\psi_{xx}^{j+1}(x) + (\frac{2}{\Delta t} + a^{j+1})\psi^{j+1}(x) = \varepsilon\psi_{xx}^j(x) + (\frac{2}{\Delta t} - a^j)\psi^j(x) + (f^{j+1}+f^j)(x), \\ \begin{cases} \psi(x,0) = \mathscr{S}_0(x), & \forall x \in \overline{\mathscr{D}}_x, \\ \psi(0,t^{j+1}) = \mathscr{S}_l(t^{j+1}), & 0 \leq j \leq M-1, \\ \psi(1,t^{j+1}) = \mathscr{S}_r(1,t^{j+1}) & 0 \leq j \leq M-1. \end{cases} \end{cases} \tag{2.12}$$

To check the semi-discrete maximum principle and stability estimate of the temporal direction of the proposed scheme, we first rewrite problem (2.12) at $(j+1)^{th}$ time level in-terms of spatial variables of the following form:

$$\begin{cases} \mathscr{L}^*\Gamma := -\varepsilon\Gamma''(x) + B(x)\Gamma(x) = g(x), & \forall x \in \overline{\mathscr{D}}_x, \\ \Gamma(0) = \mathscr{S}_l(t^{j+1}),\ \Gamma(1) = \mathscr{S}_r(t^{j+1}), & \forall t^{j+1} \in \overline{\mathscr{D}}_t^M. \end{cases} \tag{2.13}$$

where $\mathscr{L}^*$ is a semi-discrete operator , $\Gamma(x) = \psi^{j+1}(x)$, $B(x) = (\frac{2}{\Delta t} + a^{j+1})$ and $g(x) = \varepsilon\psi_{xx}^j(x) + (\frac{2}{\Delta t} - a^j)\psi^j(x) + (f^{j+1}+f^j)(x)$.

Lemma 2.4. *(Semi-discrete Maximum Principle): If $\Gamma^{j+1}(x) \in C^2(\overline{\mathscr{D}}_x)$ is the solution of the semi-discrete problem (2.13) such that $\Gamma^{j+1}(0) \geq 0, \Gamma^{j+1}(1) \geq 0$ on $\partial\overline{\mathscr{D}}_x$ and $\mathscr{L}_\varepsilon^*\Gamma^{j+1}(x) \geq 0,\ \forall x \in \mathscr{D}_x$, then $\Gamma^{j+1}(x) \geq 0,\ \forall x \in \overline{\mathscr{D}}_x$ [43].*

Proof. Let $x^* \in \overline{\mathscr{D}}_x$ such that $\Gamma^{j+1}(x^*) = min_{x\in\overline{\mathscr{D}}_x}\Gamma^{j+1}(x) < 0$ and since $\Gamma^{j+1}(0) \geq 0$, $\Gamma^{j+1}(1) \geq 0$ then $x^* \notin \{0,1\}$ that is $x^* \in \mathscr{D}_x$.
Moreover, since $\Gamma_x^{j+1}(x^*) = 0$ and $\Gamma_{xx}^{j+1}(x^*) \geq 0$, we get

$$\begin{aligned} \mathscr{L}_\varepsilon{}^*\Gamma^{j+1}(x^*) &= -\varepsilon\Gamma_{xx}^{j+1}(x^*) + B(x^*)\Gamma^{j+1}(x^*), \\ &\leq 0. \end{aligned}$$

This shows that $\mathscr{L}_\varepsilon{}^*\Gamma^{j+1}(x^*) \leq 0$, which contradicts to the assumption $\mathscr{L}_\varepsilon{}^*\Gamma^{j+1}(x) \geq 0$. Consequently, we conclude that the minimum of $\Gamma^{j+1}(x)$ is non-negative. □

Lemma 2.5. *(Stability Estimate): Let $\Gamma(x)$ be the solution of the semi-discrete problem (2.13) [34]. Then we have*

$$||\Gamma(x)|| \leq \beta_1^{-1}||\mathscr{L}_{\varepsilon}{}^{*}\Gamma(x)|| + ||\Gamma(x)||_{\mathscr{D}_x},\ B(x) \geq \beta_1 > 0.$$

Proof. To prove this Lemma, we defined two barrier functions $\Omega^{\pm}$ as follows

$$\Omega^{\pm}(x) = \beta_1^{-1}||g|| + max\{|\mathscr{S}_l(t)|, |\mathscr{S}_r(t)|\} \pm \Gamma(x),$$

When $x = 0$,

$$\begin{aligned} \Omega^{\pm}(0) &= \beta_1^{-1}||g|| + max\{|\mathscr{S}_l(t)|, |\mathscr{S}_r(t)|\} \pm \Gamma(0), \\ &= \beta_1^{-1}||g|| + max\{|\mathscr{S}_l(t)|, |\mathscr{S}_r(t)|\} \pm \mathscr{S}_l(t) \geq 0. \end{aligned}$$

When $x = 1$,

$$\begin{aligned} \Omega^{\pm}(1) &= \beta_1^{-1}||g|| + max\{|\mathscr{S}_l(t)|, |\mathscr{S}_r(t)|\} \pm \Gamma(1), \\ &= \beta_1^{-1}||g|| + max\{|\mathscr{S}_l(t)|, |\mathscr{S}_r(t)|\} \pm \mathscr{S}_r(t) \geq 0. \end{aligned}$$

Combining all these on the domain $\mathscr{D}_x$ results

$$\begin{aligned} \mathscr{L}^{*}{}_{\varepsilon}\Omega^{\pm}(x) &= -\varepsilon\frac{d^2\Omega^{\pm}(x)}{dx^2} + B(x)\Omega^{\pm}(x), \\ &= B(x)\beta_1^{-1}||g|| + B(x) \times max\{|\mathscr{S}_l(t)|, |\mathscr{S}_r(t)|\} \\ &+ \beta_1^{-1}||g|| \pm \mathscr{L}^{*}{}_{\varepsilon}\Gamma(x), \\ &= \beta_1^{-1}||g|| + B(x) \times max\{|\mathscr{S}_l(t)|, |\mathscr{S}_r(t)|\} \pm g(x) \geq 0. \end{aligned}$$

The application of Lemma (2.1) gives $\Omega^{\pm}(x) \geq 0,\ \forall (x) \in \overline{\mathscr{D}}_x$. Hence, $\Gamma(x)$ is bounded by a non-negative constant as required. □

The local truncation error of the semi-discrete problem (2.12) is given by $e^{j+1} \equiv \psi(x,t_j) - \psi^{j+1}$, where ψ^{j+1} is the computed solution of the proposed boundary value problem. Moreover, this error measures the contribution of each time step to the global error of the temporal semi-discretization.

Lemma 2.6. *(Local Error Estimate): [65], suppose that*

$$\left|\frac{\partial^i \psi(x,t)}{\partial t^i}\right| \leq C \quad , \forall (x,t) \in \overline{\mathscr{D}}_x \text{ and } 0 \leq i \leq 2.$$

Then the local error estimate in the temporal direction is given by

$$||e^{j+1}||_{\infty} \leq C_1(\Delta t)^3. \tag{2.14}$$

Proof. To prove this, we employ Taylor series expansion of the functions ψ^j and ψ^{j+1} about $(x,t^{j+1/2})$

$$\psi^j = \psi(x,t^{j+1/2}) - \frac{\Delta t}{2}\psi_t(x,t^{j+1/2}) + \frac{(\Delta t)^2}{8}\psi_{tt}(x,t^{j+1/2}) + O((\Delta t)^3), \tag{2.15}$$

$$\psi^{j+1} = \psi(x,t^{j+1/2}) + \frac{\Delta t}{2}\psi_t(x,t^{j+1/2}) + \frac{(\Delta t)^2}{8}\psi_{tt}(x,t^{j+1/2}) + O((\Delta t)^3), \tag{2.16}$$

Subtracting Eq.(2.15) from Eq.(2.16) gives

$$\frac{\psi^{j+1}-\psi^j}{\Delta t} = \psi_t(x,t^{j+1/2}) + O((\Delta t)^2), \tag{2.17}$$

Substituting Eq.(2.17) in Eq.(2.1) we get

$$\begin{aligned}\frac{\psi^{j+1}-\psi^j}{\Delta t} &= \varepsilon\psi_{xx}(x,t^{j+1/2}) - (a\psi)(x,t^{j+1/2}) \\ &\quad + f(x,t^{j+1/2}) + O((\Delta t)^2),\end{aligned} \tag{2.18}$$

where $f(x,t^{j+1/2}) = \frac{f(x,t^{j+1})+f(x,t^j)}{2}$ $\psi(x,t^{j+1/2}) = \frac{\psi(x,t^{j+1})+\psi(x,t^j)}{2}$ and $a(x,t^{j+1/2}) = \frac{a(x,t^{j+1})+a(x,t^j)}{2}$. The solution to the local error is given by

$$\begin{cases}\mathscr{L}^* e^{j+1} = O((\Delta t)^3), \\ e^{j+1}(0) = 0,\ e^{j+1}(1) = 0.\end{cases} \tag{2.19}$$

Thus, using the maximum principle in Lemma (2.4), the required result is satisfied.
Hence, $||e^{j+1}||_\infty \le C_1\Delta^3 t$ as required. □

Lemma 2.7. *(Global Error Estimate) :[65], based on the assumption of Lemma (2.6) the global error estimate of the semi-discretization at j^{th} time level is given by*

$$||E^j||_\infty \le C_2(\Delta t)^2. \tag{2.20}$$

Proof. Since the global error estimate of the j^{th} time level is given by

$$\begin{aligned}||E^j||_\infty &= ||\sum_{s=1}^{j} e^s||_\infty,\ \text{since, } j \le T/\Delta t, \\ &\le ||e^1||_\infty + ||e^2||_\infty + \cdots + ||e^s||_\infty, \\ &\le C_1 j\Delta^3 t,\ \text{using Lemma (2.6)}, \\ &\le C_1(T)(\Delta t)^2, \quad \text{since } j\Delta t \le T, \\ &\le C_2(\Delta t)^2,\ C_2 = C_1 T.\end{aligned} \tag{2.21}$$

where C_2 is a constant independent of the parameter ε and time step length Δt. □

Hence, the proposed scheme is second-order accurate in the temporal direction.

2.4.2 Spatial Discretization:

Let the spatial domain $[0,1]$ be divided into equal number of N subintervals each of width h. Then the domain $\overline{\mathscr{D}}_x$ is partitioned as follows:

$$\overline{\mathscr{D}}_x^N = \left\{ x_0 = 0, x_i = ih, x_N = 1,\ i = 1,2,3,\ldots N-1 \text{ and } h = \frac{1}{N} \right\}. \tag{2.22}$$

Non-Standard Finite Difference Scheme: To construct the exact finite difference approach, we considered the following constant coefficient homogeneous differential equations, corresponding to problem (2.12) with the discrete initial and boundary conditions as described in [66] and [**?**]:

$$\begin{cases} -\varepsilon\left[\frac{\psi_{i+1}^{j+1}-2\psi_i^{j+1}+\psi_{i-1}^{j+1}}{\mu_{i,j+1}^2}\right] + B_i\psi_i^{j+1} = \varepsilon\left[\frac{\psi_{i+1}^{j}-2\psi_i^{j}+\psi_{i-1}^{j}}{\mu_{i,j}^2}\right] - C_i\psi_i^j + f_i^{j+1} + f_i^j, \\ \begin{cases} \psi_0^{j+1} = \psi_N^{j+1} = 0, & j = 0,1,2,\ldots,M-1, \\ \psi_i^0 = 0, & i = 0,1,2,\ldots,N. \end{cases} \end{cases} \tag{2.23}$$

where $B_i = (\frac{2}{\Delta t} + a^{j+1}) \geq \beta_1 > 0$, $C_i = (\frac{2}{\Delta t} - a^j) \geq \beta_2 > 0$ and the denominator function $\mu_{i,j+1}^2$ to be determined from the following steps.
Consider the homogeneous part of Eq. (2.23) with constant coefficients, where the constant coefficients are the lower bounds of the coefficient functions as follows:

$$-\varepsilon\frac{d}{dx^2}\psi^{j+1} + \beta_1\psi^{j+1} = 0. \tag{2.24}$$

Based on this, the corresponding characteristic equation is given by $-\varepsilon\theta^2 + \beta_1 = 0$. So, the two linearly independent solutions of Eq.(2.24) are given by

$$\exp(\theta_1 x) \text{ and } \exp(\theta_1 x),\ \theta_1 = -\sqrt{\frac{\beta_1}{\varepsilon}} \ \text{ and } \ \theta_2 = \sqrt{\frac{\beta_1}{\varepsilon}}. \tag{2.25}$$

Hence, $\psi_i^{j+1} = c_1\exp(\theta_1 x_i) + c_2\exp(\theta_2 x_i)$ is the general solution of Eq.(2.24). Now, by taking the successive points and applying the theory of difference equations as discussed in [34] and [68], the following set of equations can be obtained:

$$\begin{vmatrix} \psi_{i-1}^{j+1} & \exp(\theta_1 x_{i-1}) & \exp(\theta_2 x_{i-1}) \\ \psi_i^{j+1} & \exp(\theta_1 x_i) & \exp(\theta_2 x_i) \\ \psi_{i+1}^{j+1} & \exp(\theta_1 x_{i+1}) & \exp(\theta_2 x_{i+1}) \end{vmatrix} = 0. \tag{2.26}$$

Rearranging Eq.(2.26), we get

$$\begin{vmatrix} \psi_{i-1}^{j+1} & \exp\left(\theta_1(x_i-h)\right) & \exp\left(\theta_2(x_i-h)\right) \\ \psi_{i}^{j+1} & \exp\left(\theta_1 x_i\right) & \exp\left(\theta_2 x_i\right) \\ \psi_{i+1}^{j+1} & \exp\left(\theta_1(x_i+h)\right) & \exp\left(\theta_2(x_i+h)\right) \end{vmatrix} = 0. \tag{2.27}$$

Factorizing the above equation results

$$exp(\theta_1 x_i + \theta_2 x_i) \begin{vmatrix} \psi_{i-1}^{j+1} & \exp\left(-\theta_1 h\right) & \exp\left(-\theta_2 h\right) \\ \psi_{i}^{j+1} & 1 & 1 \\ \psi_{i+1}^{j+1} & \exp\left(\theta_1 h\right) & \exp\left(\theta_2 h\right) \end{vmatrix} = 0. \tag{2.28}$$

Solving the determinant of Eq. (2.28) gives

$$\begin{aligned} & \exp((\theta_1+\theta_2)x_i)[(\exp(\theta_2 h)-\exp(\theta_1 h))\psi_{i-1}^{j+1} \\ - & (\exp(\theta_2-\theta_1)h-\exp(\theta_1-\theta_2)h)\psi_i^{j+1} \\ + & (\exp(-\theta_1 h)-\exp(-\theta_2 h))\psi_{i+1}^{j+1}]. \end{aligned} \tag{2.29}$$

Using the values of θ_1 and θ_2 in (2.25) into (2.29) and simplifying the terms using the double angle formula for hyperbolic functions, we get the exact finite difference scheme for (2.28) as follows:

$$\psi_{i-1}^{j+1} - 2\cosh\left(\sqrt{\frac{\beta_1}{\varepsilon}}\right)\psi_i^{j+1} + \psi_{i+1}^{j+1} = 0. \tag{2.30}$$

After some rearrangements, we get

$$-\varepsilon \frac{\psi_{i-1}^{j+1} - 2\psi_i^{j+1} + \psi_{i+1}^{j+1}}{4\left(\frac{\varepsilon}{\beta_1}\right)\left(\sinh^2\left(\frac{1}{2}h\sqrt{\frac{\beta_1}{\varepsilon}}\right)\right)} + \beta_1\psi_{i+1}^{j+1} = 0. \tag{2.31}$$

for $i = 1,2,\ldots,N-1$. As a result, the denominator function for the second order derivative approximation can be found as

$$\mu^2(\varepsilon,h) = 4\left(\frac{\varepsilon}{\beta_1}\right)\left(\sinh^2\left(\frac{1}{2}h\sqrt{\frac{\beta_1}{\varepsilon}}\right)\right). \tag{2.32}$$

For $i = 1,2,3,\ldots,N-1,\ j = 0,1,2,\ldots,M-1$, we defined the general variable coefficient form of the denominator function as follows:

$$\mu_{i,j+1}^2 = 4\left(\frac{\varepsilon}{B_i(x_i,t^{j+1})}\right)\left(\sinh^2\left(\frac{1}{2}h\sqrt{\frac{B_i(x_i,t^{j+1})}{\varepsilon}}\right)\right). \tag{2.33}$$

Similarly considering the homogeneous differential equation of Eq.(2.23) of the j^{th} time level can be written as

$$\varepsilon \frac{d}{dx^2}\psi^j - \beta_2 \psi^j = 0. \tag{2.34}$$

The linearly independent solutions of Eq.(2.34) is defined as $\exp(\theta_1 x)$ and $\exp(\theta_2 x)$, where $\theta_1 = -\sqrt{\frac{\beta_2}{\varepsilon}}$, $\theta_2 = \sqrt{\frac{\beta_2}{\varepsilon}}$ and $C(x_i,t^j) \geq \beta_2 > 0$.
Following the same procedure, the j^{th} level denominator function can be obtained as follows:

$$\mu_{i,j}^2 = 4\left(\frac{\varepsilon}{C(x_i,t^j)}\right)\left(\sinh^2\left(\frac{1}{2}h\sqrt{\frac{C(x_i,t^j)}{\varepsilon}}\right)\right). \tag{2.35}$$

Remark 2.1. Furthermore, on taking Taylor series expansions about the point (x_i,t^{j+1}) the denominator function well approximates the classical step length as shown below.

$$h^2 \approx \mu_{i,j+1}^2 = h^2\,\Phi^4 + \frac{h^4\,\Phi^6}{12} + \frac{h^6\,\Phi^8}{180} + \cdots, \text{where } \Phi = \sqrt{\frac{B(x_i,t^{j+1})}{\varepsilon}}.$$

2.4.3 The Fully Discretized Problem:

In this section, we combined the temporal and spatial semi-discretized results by substituting Eq.(2.33) and Eq.(2.35) into Eq.(2.23) as follows

$$\begin{aligned} -\varepsilon\frac{\left[\psi_{i+1}^{j+1} - 2\psi_i^{j+1} + \psi_{i-1}^{j+1}\right]}{\mu_{i,j+1}^2} + B_i\Psi_i^{j+1} &= \varepsilon\frac{\left[\psi_{i+1}^{j} - 2\psi_i^{j} + [\psi_{i-1}^{j}\right]}{\mu_{i,j}^2} \\ &- C_i\psi_i^j + H_i^j. \end{aligned} \tag{2.36}$$

Simplifying these equations we get, the following tri-diagonal systems of equations for the proposed problem in (2.1) with its initial-boundary conditions.

$$\begin{cases} \mathscr{L}_\varepsilon^{N,M} := R_i^-\,\psi_{i-1}^{j+1} + R_i^c\psi_i^{j+1} + R_i^+\,\psi_{i+1}^{j+1} = r_i^-\,\psi_{i-1}^{j} + r_i^c\,\psi_i^j + r_i^+\,\psi_{i+1}^{j} + H_i^j, \\ \begin{cases} \psi_i^0 = \mathscr{S}_0(x_i), & i = 0,1,2,\ldots,N-1, \\ \psi_0^{j+1} = \mathscr{S}_l^{j+1}(0), & j = 0,1,2,\ldots,M-1, \\ \psi_M^{j+1} = \mathscr{S}_r^{j+1}(1), & j = 0,1,2,\ldots,M-1. \end{cases} \end{cases} \tag{2.37}$$

where the coefficients of the systems are determined for $i=1,2,3,\ldots,N-1$, and $j=0,1,2,\ldots,M-1$ as follows

$$\begin{cases} R_i^- = \frac{-\varepsilon}{\mu_{i,j+1}^2}, \\ R_i^c = \left(\frac{2\varepsilon}{\mu_{i,j+1}^2} + \frac{2}{\Delta t} + a_i^{j+1}\right), \\ R_i^+ = \frac{-\varepsilon}{\mu_{i,j+1}^2}. \end{cases} \text{ and } \begin{cases} r_i^- = \frac{\varepsilon}{\mu_{i,j}^2}, \\ r_i^c = -\left(\frac{2\varepsilon}{\mu_{i,j}^2} + \frac{2}{\Delta t} + a_i^j\right), \\ r_i^+ = \frac{\varepsilon}{\mu_{i,j}^2}, \\ H_i^j = f_i^{j+1} + f_i^j. \end{cases} \tag{2.38}$$

Furthermore, since the boundary values of ψ_0^{j+1} and ψ_N^{j+1} are given from (2.1), we found the remaining values of ψ_i^{j+1},for $i=1,2,3,\ldots,N-1$ as follows.

$$\begin{pmatrix} R_0^c & R_0^+ & 0 & 0 & \ldots & 0 \\ R_1^- & R_1^c & R_1^+ & 0 & \ldots & 0 \\ 0 & R_2^- & R_2^c & R_2^+ & 0 & 0 \\ \vdots & \ddots & \ddots & \ddots & \ddots & \vdots \\ 0 & \ldots & \ldots & R_{N-2}^- & R_{N-2}^c & R_{N-2}^+ \\ 0 & \ldots & \ldots & \ldots & R_{N-1}^- & R_{N-1}^c \end{pmatrix} \begin{pmatrix} \psi_1^{j+1} \\ \psi_2^{j+1} \\ \psi_3^{j+1} \\ \vdots \\ \psi_{N-2}^{j+1} \\ \psi_{N-1}^{j+1} \end{pmatrix}$$

$$= \begin{pmatrix} r_0^c & r_0^+ & 0 & 0 & \ldots & 0 \\ r_1^- & r_1^c & r_1^+ & 0 & \ldots & 0 \\ 0 & r_2^- & r_2^c & r_2^+ & 0 & 0 \\ \vdots & \ddots & \ddots & \ddots & \ddots & \vdots \\ 0 & \ldots & \ldots & r_{N-2}^- & r_{N-2}^c & r_{N-2}^+ \\ 0 & \ldots & \ldots & \ldots & r_{N-1}^- & r_{N-1}^c \end{pmatrix} \begin{pmatrix} \psi_1^{j+1} \\ \psi_2^{j+1} \\ \psi_3^{j+1} \\ \vdots \\ \psi_{N-2}^{j+1} \\ \psi_{N-1}^{j+1} \end{pmatrix} + \begin{pmatrix} H_1^j \\ H_2^j \\ H_3^j \\ \vdots \\ H_{N-2}^j \\ H_{N-1}^j \end{pmatrix}. \tag{2.39}$$

For the sake of simplicity the matrix is rearranged to its compact form as follows

$$R\psi_i^{j+1} = rH_i^j. \tag{2.40}$$

By the definition in (1.8), the tridiagonal system in (2.40) constitutes an M-matrix. So, to obtain the solution by matrix inverse method, first we must check whether the M-matrix R is non-singular and has positive inverse or not.

Theorem 2.1. Let $R \in \mathbb{R}^{n\times n}$ be a Z-matrix. Then the following statements are equivalent [27]:

1. R is a nonsingular M-matrix.
2. R is invertible and $R^{-1} \geq 0$.

Proof. **(1) $\Rightarrow$ (2):** Since R is a nonsingular M-matrix, there exist a scalar $s > 0$ and a non-negative matrix $B \in \mathbb{R}^{n\times n}$ such that

$$R = sI - B.$$

Let $C = s^{-1}B$. Then $C \geq 0$ and, since R is nonsingular, $\rho(C) < 1$.
Hence the Neumann series applies:

$$(I-C)^{-1} = \sum_{k=0}^{\infty} C^k.$$

Therefore,

$$R^{-1} = \frac{1}{s}(I-C)^{-1} = \frac{1}{s}\sum_{k=0}^{\infty} C^k.$$

Since $C \geq 0$, we have $C^k \geq 0$ for all k, and hence

$$R^{-1} \geq 0.$$

Thus R is invertible with a non negative inverse.
(2) $\Rightarrow$ (1):
Assume R is a Z-matrix and $R^{-1} \geq 0$.
Let $x \geq 0$ and define

$$y = R^{-1}x.$$

Then $y \geq 0$, and multiplying both sides by R gives

$$Ry = x \geq 0.$$

Hence, the system preserves positivity structure.
This shows that a Z-matrix with a non-negative inverse is a nonsingular M-matrix. □

Thus R is a nonsingular M-matrix and we solve the system by matrix inverse method.
Lemma 2.8. *(Discrete Maximum Principle): Let ϕ_i^{j+1} be any mesh function defined on $\overline{\mathscr{D}}_{xt}^{N.M}$ such that $\phi_0^{j+1} \geq 0$ and $\phi_N^{j+1} \geq 0$ [2]. Then $\mathscr{L}^{N,M}\phi_i^{j+1} \geq 0,$ for $i = 1,2,3,...,N-1$ implies that $\phi_i^{j+1} \geq 0$, for $i = 0,1,2,...,N$.*

Proof. Suppose that there exists a mesh point $(i^*, j+1)$ for $i^* \in \{1,2,3,\ldots,N-1\}$ such that $\phi_{i^*}^{j+1} = min_{0\leq i\leq N}\phi_i^{j+1}$ and assume that $\phi_{i^*}^{j+1} < 0,\ \phi_{i^*+1}^{j+1} - \phi_{i^*}^{j+1} > 0,\ \phi_{i^*-1}^{j+1} - \phi_{i^*}^{j+1} > 0$ and $\mathscr{L}^{N,M}\phi_i^{j+1} \geq 0$. Since $i^* \notin \{0,N\}$ and $i^* \in \{1,2,3,\ldots,N-1\}$, we have that

$$\begin{aligned}
\mathscr{L}^{N,M}\phi_{i^*}^{j+1} &= -\varepsilon\left[\frac{\phi_{i^*+1}^{j+1} - 2\phi_{i^*}^{j+1} + \phi_{i^*-1}^{j+1}}{\mu_{i^*}^2}\right] + \beta_2\phi_{i^*}^{j+1}, \\
&= -\varepsilon\left[\frac{(\phi_{i^*+1}^{j+1} - \phi_{i^*}^{j+1}) + (\phi_{i^*-1}^{j+1} - \phi_{i^*}^{j+1})}{\mu_{i^*}^2}\right] + \beta_2\phi_{i^*}^{j+1} \leq 0.
\end{aligned}$$

This implies that $\mathscr{L}^{N,M}\phi_{i^*}^{j+1} \leq 0$, which contradicts to the assumption $\mathscr{L}^{N,M}\phi_i^{j+1} \geq 0$. Hence, $\phi_i^{j+1} \geq 0,$ for $i = 0,1,2,...,N$. □

Lemma 2.9. *(Stability Estimate): Suppose that ϕ_i^{j+1} be any mesh function at $(j+1)^{th}$ level such that $\phi_0^{j+1} = 0 = \phi_N^{j+1}$ [34]. Then*

$$\left|\phi_i^{j+1}\right| \leq \frac{1}{\beta} \max_{1\leq j\leq M-1} \left|\mathscr{L}_\varepsilon^{N,M} \phi_i^{j+1}\right|, \text{ for } 1 \leq i \leq N-1.$$

Proof. Let $\Omega = \frac{1}{\beta}\max_{1\leq i\leq N-1}\left|\mathscr{L}_\varepsilon^{N,M}\phi_i^{j+1}\right|$ and $(\Omega^{\pm})_i^{j+1}$ be the barrier functions defined by

$$(\Omega^{\pm})_i^{j+1} = \Omega \pm \phi^{j+1}.$$

Since $(\Omega^{\pm})_0^{j+1} = (\Omega^{\pm})_N^{j+1} > 0$ and for $1 \leq i \leq N-1$, we get

$$\begin{aligned}
\mathscr{L}_\varepsilon^{N,M}(\Omega^{\pm})_i^{j+1} &= -\varepsilon\left[\frac{\Omega\pm\phi_{i+1}^{j+1} - 2\left(\Omega\pm\phi_i^{j+1}\right) + \Omega\pm\phi_{i-1}^{j+1}}{\mu_i^2}\right] \\
&+ \left(\frac{1}{\Delta t} + a_i^{j+1}\right)\left(\Omega\pm\phi_i^{j+1}\right), \\
&= \left(\frac{1}{\Delta t} + a_i^{j+1}\right)\Omega \pm \mathscr{L}_\varepsilon^{N,M}\phi_i^{j+1}, \\
&= \frac{1}{\beta}\left(\frac{1}{\Delta t} + a_i^{j+1}\right)\max\left|\mathscr{L}_\varepsilon^{N,M}\phi_i^{j+1}\right| \pm \mathscr{L}_\varepsilon^{N,M}\phi_i^{j+1}.
\end{aligned}$$

Since, $\left(\frac{1}{\Delta t} + a_i^{j+1}\right) > \beta$, we have $\mathscr{L}_\varepsilon^{N,M}(\Omega^{\pm})_i^{j+1} \geq 0$.
Thus, the Lemma in (2.8) gives $(\Omega^{\pm})_i^{j+1} \geq 0, \;\; 0 \leq i \leq N$.
Hence, the stability estimate of the discrete scheme at $(j+1)^{th}$ time level is proved. □

Lemma 2.10. *[68], for a fixed number of meshes N and for $\varepsilon \to 0$, it holds that*

$$\lim_{\varepsilon\to 0}\max_{1\leq i\leq N-1}\frac{\exp\left(-\frac{\alpha x_i}{\sqrt{\varepsilon}}\right)}{\varepsilon^{i/2}} = 0 \;\; \textit{and} \;\; \lim_{\varepsilon\to 0}\max_{1\leq i\leq N-1}\frac{\exp\left(-\frac{\alpha(1-x_i)}{\sqrt{\varepsilon}}\right)}{\varepsilon^{i/2}} = 0.$$

Proof. Using the partition $[0,1] := \{0 = x_0 < x_1 < x_2 <, \ldots, x_N = 1\}$ for the interior grid points, we have

$$\max_{1\leq i\leq N-1}\frac{\exp\left(\frac{-\alpha x_i}{\varepsilon^j}\right)}{\varepsilon^j} \leq \max_{1\leq i\leq N-1}\frac{\exp\left(\frac{-\alpha x_1}{\varepsilon^j}\right)}{\varepsilon^j} = \max_{1\leq i\leq N-1}\frac{\exp\left(\frac{-\alpha h}{\varepsilon^j}\right)}{\varepsilon^j}$$

.

and

$$\max_{1\leq i\leq N-1}\frac{\exp\left(\frac{-\alpha(1-x_i)}{\varepsilon^j}\right)}{\varepsilon^j} \leq \max_{1\leq i\leq N-1}\frac{\exp\left(\frac{-\alpha(1-x_{n-1})}{\varepsilon^j}\right)}{\varepsilon^j} = \max_{1\leq i\leq N-1}\frac{\exp\left(\frac{-\alpha h}{\varepsilon^j}\right)}{\varepsilon^j}$$

.

Since $x_1 = h = x_{n-1}$, then using the L'Hospital's rule, we get

$$\begin{aligned}
\lim_{\varepsilon \to 0} \frac{\exp\left(\frac{-\alpha h}{\varepsilon^j}\right)}{\varepsilon^j} &= \lim_{p=1/\varepsilon \to \infty} \frac{p^j}{\exp(\alpha h p)}, \\
&= \lim_{p=1/\varepsilon \to \infty} \frac{j!}{(\alpha h)^j \exp(\alpha h p)}, \\
&= 0.
\end{aligned}$$

This completes the proof. □

2.5 Uniform Convergence Analysis

Theorem 2.2. Let $\psi(x,t^{j+1})$ and ψ_i^{j+1} be the solutions of (2.12) and (2.36) respectively [34]. Then the bound

$$\max_{0 \le i \le N,\ 0 \le j \le M} \left| \psi_i^{j+1} - \psi(x,t^{j+1}) \right| \le Ch^2.$$

Proof. Using the differential and difference equations, the truncation error is given by

$$\begin{aligned}
\left| \mathscr{L}_\varepsilon^{N,M}(\psi^{j+1}(x_i) - \psi_i^{j+1}) \right| &= \left| -\varepsilon \frac{d^2 \psi^{j+1}(x_i)}{dx^2} + \varepsilon \delta^2 \psi_i^{j+1} \right| \\
&= \left| -\varepsilon \frac{d^2 \psi^{j+1}(x_i)}{dx^2} + \frac{\varepsilon}{(\mu_i^{j+1})^2} \left(\psi_{i-1}^{j+1} - 2\psi_i^{j+1} + \psi_{i+1}^{j+1} \right) \right|
\end{aligned} \tag{2.41}$$

Using the Taylor series expansions of $\psi_{i-1}^{j+1}, \psi_{i+1}^{j+1}$ and $\frac{1}{\mu_i^{j+1}}$ truncated up to order five, we have

$$\begin{cases}
\psi_{i-1}^{j+1} = \Sigma_{i=0}^4 (-1)^i \frac{h^i}{i!} \frac{d^i \psi^{j+1}(\zeta_i)}{dx^i} + O\left(\frac{h^5}{5!}\right), & \zeta_i \in (x_{i-1}, x_{i+1}), \\
\psi_{i+1}^{j+1} = \Sigma_{i=0}^4 \frac{h^i}{i!} \frac{d^i \psi^{j+1}(\zeta_i)}{dx^i} + O\left(\frac{h^5}{5!}\right), & \zeta_i \in (x_{i-1}, x_{i+1}), \\
\frac{1}{(\mu_i^{j+1})^2} = \frac{(B_i^{j+1})^2}{4 sinh^2(B_i h/2)} = \frac{(B_i^{j+1})^2}{4} \left(\frac{4}{(B_i^{j+1})^2} - \frac{1}{3} + \frac{(B_i^{j+1} - ih)^2}{60} \right)
\end{cases} \tag{2.42}$$

Using the series expansions (2.42) in (2.41) gives

$$\begin{aligned}
&\left| \mathscr{L}_\varepsilon^{N,M}(\psi^{j+1}(x_i) - \psi_i^{j+1}) \right| \\
&= |-\varepsilon \frac{d^2 \psi_i^{j+1}}{dx^2} + \varepsilon \frac{d^2 \psi_i^{j+1}}{dx^2} + \left(\frac{\varepsilon}{12} \frac{d^4 \psi_i^{j+1}(\zeta_i)}{dx^4} - \frac{\varepsilon (B_i^{j+1})^2}{12} \frac{d^2 \psi_i^{j+1}}{dx^2} \right) h^2 \\
&+ \left(\frac{\varepsilon (B_i^{j+1})^4}{240} \frac{d^2 \psi_i^{j+1}}{dx^2} - \frac{\varepsilon (B_i^{j+1})^2}{144} \frac{d^4 \psi_i^{j+1}(\zeta_i)}{dx^4} \right) h^4 + \frac{\varepsilon (B_i^{j+1})^2}{2880} \frac{d^4 \psi_i^{j+1}(\zeta_i)}{dx^4} h^6|,
\end{aligned}$$

Also using the bounds of the derivatives in Lemma (2.3) and Lemma (2.10) gives

$$\left|\mathscr{L}_{\varepsilon}^{N,M}(\psi^{j+1}(x_i)-\psi_i^{j+1})\right| \le C_1h^2+C_2h^4+C_3h^6.$$

Applying the discrete maximum principle in Lemma (2.8), we get

$$\max_{0\le i\le N,\ 0\le j\le M}\left|\psi_i^{j+1}-\psi(x,t^{j+1})\right| \le Ch^2.$$

Consequently, the proposed scheme is of second-order accurate to the spatial direction. □

Theorem 2.3. For the analytic solution $\psi(x,t)$ of (2.1) and the fully discrete solution ψ_i^j of (2.37), the uniform error estimate at $(j+1)^{th}$ can be defined as

$$\max_{0\le i\le N,\ 0\le j\le M}\left|\psi_i^{j+1}-\psi(x,t^{j+1})\right| \le C\left(h^2+(\Delta t)^2\right). \tag{2.43}$$

Proof. Using the triangle inequality, we have the following facts

$$\begin{aligned}
\left|\psi(x,t^{j+1})-\psi_i^{j+1}\right| &= \left|\psi(x,t^{j+1})-\psi_i^{j+1}(x_i)+\psi_i^{j+1}(x_i)-\psi_i^{j+1}\right|,\\
&\le \left|\psi(x,t^{j+1})-\psi_i^{j+1}(x_i)\right|+\left|\psi_i^{j+1}(x_i)-\psi_i^{j+1}\right|,\\
&= Ch^2+C(\Delta t)^2t,\ \text{using Lemma (2.7) and Theorem (2.2)},\\
&= C(h^2+(\Delta t)^2).
\end{aligned}$$

The overall construction of the uniform convergence analysis proves, the proposed scheme is of second-order in both the spatial and temporal directions. □

2.6 Numerical Results and Discussions

To validate the applicability of the proposed scheme, two test problems were considered. For simulation analysis, we employed $\varepsilon-$ uniform maximum absolute error and the corresponding order of convergence are evaluated using the double mesh principle [120].

Example 2.1. Consider a singularly perturbed parabolic reaction-diffusion problems of the form in [36]

$$\begin{cases} \psi_t - \varepsilon\psi_{xx} + \frac{1+x^2}{2}\psi = t^3, & \forall(x,t) \in (0,1)\times(0,1], \\ \psi(x,0) = 0, & \forall x \in [0,1], \\ \psi(0,t) = -\frac{128}{35}\pi^{-1/2}t^{7/2} = \psi(1,t), & \forall t \in (0,1]. \end{cases}$$

Example 2.2. Consider a singularly perturbed parabolic reaction-diffusion problems of the form in [35]

$$\begin{cases} \psi_t - \varepsilon\psi_{xx} + (1+x^2+t^2e^t)\psi = e^t - 1 + sin(\pi x), \; (x,t) \in (0,1)\times(0,1], \\ \psi(x,0) = 0, x \in [0,1], \\ \psi(0,,t) = U(1,t) = 0, \; t \in (0,1]. \end{cases}$$

Let $\psi^{N,M}(x_i,t_j)$ and $\psi^{2N,2M}(x_{2i},t_{2j})$ be the numerical solutions with mesh lengths $(h,\Delta t \neq 0)$ and $(h/2,\Delta t/2 \neq 0)$ respectively, then the maximum absolute error and corresponding order of convergence can be determined as in the following forms:

- The maximum absolute error is given by

$$E_\varepsilon^{N,M} = \max_{0\le i,j\le N,M} \left|\psi^{N,M}(x_i,t_j) - \psi^{2N,2M}(x_{2i},t_{2j})\right|. \tag{2.44}$$

- The $\varepsilon-$ uniform absolute error is given by

$$E^{N,M} = \max_{\varepsilon} E_\varepsilon^{N,M}. \tag{2.45}$$

- Corresponding ε-uniform order of convergence is $R^{N,M} = log_2\left(\frac{E^{N,M}}{E^{2N,2M}}\right)$.

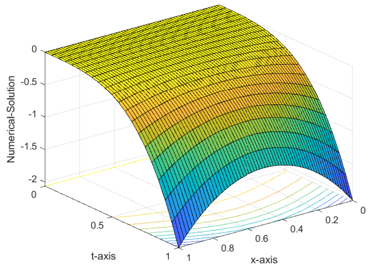

(a) $\varepsilon = 10^{-0}$

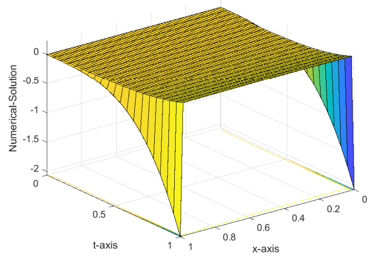

(b) $\varepsilon = 10^{-5}$

Figure 2.1: 3D solution graph of Example (2.1) with values $N = 32, M = 10$

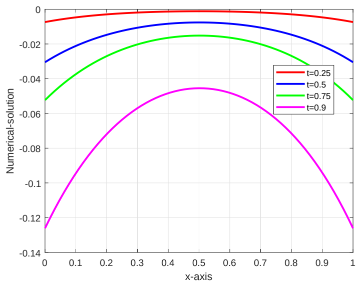

(a) $\varepsilon = 10^{-0}$

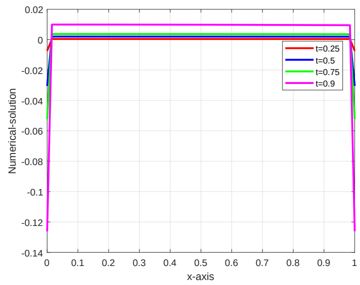

(b) $\varepsilon = 10^{-5}$

Figure 2.2: 2D solution graph of Example (2.1) with values $N = 32, M = 10$

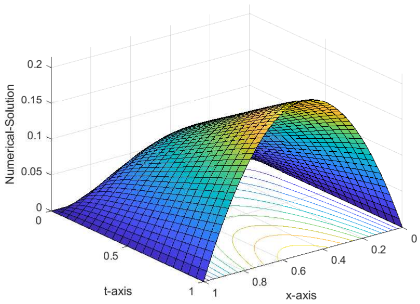

(a) $\varepsilon = 10^{-0}$

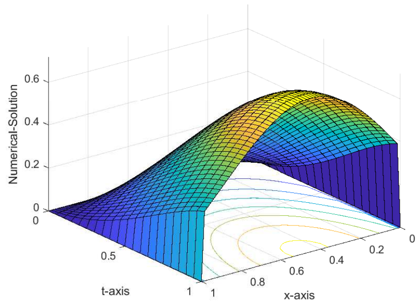

(b) $\varepsilon = 10^{-18}$

Figure 2.3: 3D solution graph of Example (2.2) with values $N = 32, M = 10$

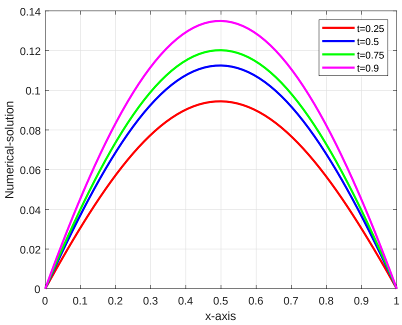

(a) $\varepsilon = 10^{-0}$

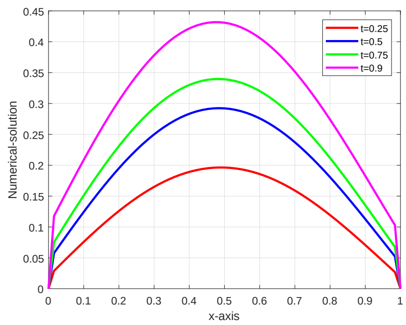

(b) $\varepsilon = 10^{-18}$

Figure 2.4: 2D solution graph of Example (2.2) with values $N = 32, M = 10$

Table 2.1: $E^{N,M}$ and $R^{N,M}$ for Example (2.1)

$\varepsilon \downarrow$	$N=64$ $M=16$	$N=128$ $M=32$	$N=256$ $M=64$	$N=512$ $M=128$
10^{-2}	5.1230e−04 1.9995	1.0214e−04 1.9987	3.1021e−05 1.9998	8.2175e−06
10^{-4}	5.2840e−04 1.9997	1.3213e−04 1.9999	3.3033e−05 2.0000	8.2584e−06
10^{-6}	5.2840e−04 1.9997	1.3213e−04 1.9999	3.3033e−05 2.0000	8.2584e−06
10^{-8}	5.2840e−04 1.9997	1.3213e−04 1.9999	3.3033e−05 2.0000	8.2584e−06
10^{-10}	5.2840e−04 1.9997	1.3213e−04 1.9999	3.3033e−05 2.0000	8.2584e−06
10^{-12}	5.2840e−04 1.9997	1.3213e−04 1.9999	3.3033e−05 2.0000	8.2584e−06
$\vdots$	$\vdots$	$\vdots$	$\vdots$	
10^{-20}	5.2840e−04 1.9997	1.3213e−04 1.9999	3.3033e−05 2.0000	8.2584e−06
$E^{N,M}$ $R^{N,M}$	5.2840e−04 1.9997	1.3213e−04 1.9999	3.3033e−05 2.0000	8.2584e−06

Table 2.2: Comparison of the $E^{N,M}$ and $R^{N,M}$ for Example (2.1)

$\varepsilon \downarrow$	$N=64$ $M=16$	$N=128$ $M=32$	$N=256$ $M=64$	$N=512$ $M=128$
Present Scheme				
$E^{N,M}$	5.2840e−04	1.3213e−04	3.3033e−05	8.2584e−06
$R^{N,M}$	1.9997	1.9999	2.0000	
Results in [36]				
$E^{N,M}$	1.2508e−02	6.1896e−03	3.0782e−03	1.5348e−03
$R^{N,M}$	1.0149	1.0078	1.0040	

To validate the applicability of our proposed scheme, we consider two model examples. We present the maximum absolute errors and the corresponding orders of convergence in Tables (2.1) and (2.3). For a fixed perturbation parameter ε, we observe that the maximum absolute errors decrease as the mesh sizes N and M are refined across a row, indicating an improvement in accuracy. Conversely, for fixed mesh sizes N and M, we find that the maximum absolute errors remain nearly uniform as ε decreases down a column, while the order of convergence approaches two. These results confirm that our scheme is second-order uniformly convergent.

Furthermore, the 3D and 2D plots in Example (2.1) (Figures (2.1) and (2.2)) and Example (2.2) (Figures (2.3) and (2.4)) show that decreasing ε leads to the formation of twin boundary layers near $x=0$ and $x=1$, in agreement with the theoretical analysis. We also compare our results

Table 2.3: $E^{N,M}$ and $R^{N,M}$for Example (2.2)

$\varepsilon \downarrow$	$N=32$ $M=10$	$N=64$ $M=40$	$N=128$ $M=60$	$N=256$ $M=640$
2^{-2}	$8.9994e-04$	$2.3001e-04$	$5.5623e-05$	$3.1221e-06$
	1.7467	1.5221	1.8821	
2^{-4}	$9.1567e-04$	$2.3912e-04$	$5.8975e-05$	$3.5678e-06$
	1.8579	1.5623	1.9956	
	⋮	⋮	⋮	⋮
2^{-16}	$9.4881e-04$	$2.3940e-04$	$5.9878e-05$	$3.7372e-06$
	1.9867	1.5826	1.9513	
2^{-18}	$9.4882e-04$	$2.3957e-04$	$5.9887e-05$	$3.7465e-06$
	1.9857	1.9986	2.0000	
2^{-20}	$9.4882e-04$	$2.3957e-04$	$5.9887e-05$	$3.7465e-06$
	1.9857	1.9986	2.0000	
2^{-22}	$9.4882e-04$	$2.3957e-04$	$5.9887e-05$	$3.7465e-06$
	1.9857	1.9986	2.0000	
2^{-24}	$9.4882e-04$	$2.3957e-04$	$5.9887e-05$	$3.7465e-06$
	1.9857	1.9986	2.0000	
$E^{N,M}$	$9.4882e-04$	$2.3957e-04$	$5.9887e-05$	$7.7465e-06$
$R^{N,M}$	1.9857	1.9986	2.0000	

Table 2.4: Comparison of the $E^{N,M}$ and $R^{N,M}$ for Example (2.2)

$\varepsilon \downarrow$	$N=32$ $M=10$	$N=64$ $M=40$	$N=128$ $M=60$	$N=256$ $M=640$
Present Scheme				
$E^{N,M}$	$9.4882e-04$	$2.3957e-04$	$5.9887e-05$	$3.7465e-06$
$R^{N,M}$	1.9857	1.9986	2.0000	
Results in [34]				
$E^{N,M}$	1.6700e − 01	4.1800e − 02	1.05e − 02	0.2600e − 02
$R^{N,M}$	1.9983	1.9931	2.0138	

with existing methods in [36] and [34], and Tables (2.2) and (2.4) demonstrate that our method achieves higher accuracy and better convergence performance in terms of both error and order of convergence.

Overall, we observe that the theoretical analysis is fully supported by the numerical experiments.

2.7 Conclusion

A fitted numerical scheme was developed and analyzed for singularly perturbed parabolic reaction–diffusion problems using the Crank–Nicolson method in time and NSFDM in space on uniform meshes. The scheme is uniformly convergent and achieves second-order convergence in both time and space. Both theoretical and numerical experiments confirm its accuracy and show that it performs better than several existing methods in the literature.

Chapter 3

A Fitted Linear Multi-Step Scheme for Singularly Perturbed Parabolic Reaction–Diffusion Problems on Shishkin Meshes

This chapter develops a fitted numerical method for singularly perturbed parabolic reaction–diffusion problems characterized by twin boundary layers near $x = 0$ and $x = 1$ due to a small diffusion parameter $\varepsilon\,(0 < \varepsilon \ll 1)$. To accurately resolve these layers, a fitted computational scheme is constructed using the implicit Euler method for temporal discretization and a linear multistep finite difference technique on Shishkin meshes for spatial discretization, together with Richardson extrapolation to enhance time accuracy. The method achieves higher-order uniform convergence in space and improved accuracy in time. Numerical experiments on standard test problems validate the theoretical results and confirm that the proposed approach is more efficient than several existing methods.

3.1 Introduction

Many model problems in science and engineering involve parameter-dependent differential equations whose small perturbation parameters significantly influence solution behavior, often preventing analytic solutions. SPPDEs, in which the highest-order derivative is multiplied by a small parameter $\varepsilon\,(0 < \varepsilon \ll 1)$, arise in various fields such as reaction–diffusion processes, fluid dynamics, elasticity, quantum mechanics, and chemical reactor theory [5, 14, 60, 61]. Their solutions typically exhibit boundary or interior layers with steep gradients or oscillations, requiring fine mesh discretization that can increase round-off errors [34]. As a result, classical numerical methods often fail to provide accurate and efficient solutions. These challenges have motivated the development of parameter-uniformly convergent methods, including fitted operator techniques, fitted meshes, and domain decomposition approaches, which are specifically designed to capture the solution behavior in layer regions effectively.

Depending on the problem, the spatial domain can be discretized using either uniform or piecewise-uniform (Shishkin) meshes. Uniform meshes, with evenly distributed points, are simple to implement and facilitate convergence analysis, as employed in [36, 106]. In contrast, Shishkin meshes cluster points in regions of rapid solution variation, such as boundary layers, effectively addressing limitations of uniform meshes. Introduced by Shishkin in 1988, these meshes have been widely used for singularly perturbed parabolic reaction–diffusion problems, with uniform discretization in time, as discussed in [19, 32, 84, 85].

Motivated by the limited accuracy and low convergence order of several existing methods for the proposed problem, this chapter aims to develop a more accurate and reliable numerical scheme. To effectively capture sharp boundary layers, a fitted approach based on Shishkin meshes is proposed, combining a fourth-order linear multistep method in space with an extrapolated second-order implicit Euler scheme in time. The resulting method achieves enhanced accuracy and improved convergence rates, while also serving as an effective alternative to existing numerical approaches.

3.2 Problem formulation

Consider a class of singularly perturbed parabolic reaction-diffusion problems, as stated in the governing problem (1.11), together with the initial and boundary conditions as presented in [117].

$$\begin{cases} \mathscr{L}_\varepsilon \psi := \psi_t(x,t) - \varepsilon \psi_{xx}(x,t) + a(x,t)\psi(x,t) = f(x,t), \quad \forall (x,t) \in \mathscr{D}_{xt}, \\ \begin{cases} \psi(x,0) = \mathscr{S}_0(x), & \forall x \in \overline{\mathscr{D}}_t, \\ \psi(0,t) = \mathscr{S}_l(t), & \forall t \in \overline{\mathscr{D}}_t, \\ \psi(1,t) = \mathscr{S}_r(1,t)), & \forall t \in \overline{\mathscr{D}}_t. \end{cases} \end{cases} \tag{3.1}$$

where $\mathscr{L}_\varepsilon \psi(x,t)$ is the differential operator, $\varepsilon (0 < \varepsilon \ll 1)$, is the perturbation parameter, $\mathscr{D}_x = (0,1)$, $\mathscr{D}_t = (0,T]$ and $\mathscr{D}_{xt} = \mathscr{D}_x \times \mathscr{D}_t$. To ensure the existence of a unique solution the functions $a(x,t)$ and $f(x,t)$ on $\overline{\mathscr{D}}_{xt}$ are assumed to be sufficiently smooth, bounded and satisfy

$$a(x,t) \geq \alpha > 0, \ \ \forall (x,t) \in \overline{\mathscr{D}}_{xt}. \tag{3.2}$$

3.3 Properties of the Analytic Solution

In this section, we present the existence of a unique solution to (3.1) which can be established with the assumption that the data are Hölder continuous and satisfy appropriate compatibility conditions at the corner points $(0,0)$ and $(1,0)$ [112]. The required compatibility conditions are

$$\mathscr{S}_0(0,0) = \mathscr{S}_l(0), \mathscr{S}_r(1,0) = \mathscr{S}_r(0). \tag{3.3}$$

and

$$\begin{cases} \frac{\partial \mathscr{S}_l(0)}{\partial t} - \varepsilon \frac{\partial^2 \mathscr{S}_0(0,0)}{\partial x^2} + a(0,0)\mathscr{S}_0(0,0) = f(0,0), \\ \frac{\partial \mathscr{S}_r(1)}{\partial t} - \varepsilon \frac{\partial^2 \mathscr{S}_r(1,0)}{\partial x^2} + a(1,0)\mathscr{S}_r(1,0) = f(1,0). \end{cases} \tag{3.4}$$

These conditions along with the bound in (3.2) ensure that the problem in (3.1) has unique solution $\psi(x,t)$ which exhibits a twin boundary layers each of width $O(\sqrt{\varepsilon})$ near $x=0$ and $x=1$.

Lemma 3.1. *(Continuous Maximum Principle).We assume that $\psi(x,t)$ is any sufficiently smooth function satisfying $\psi(x,t) \geq 0, \forall (x,t) \in \partial \mathscr{D}_{xt}$, where $\partial \mathscr{D}_{xt} = \overline{\mathscr{D}}_{xt} \setminus \mathscr{D}_{xt}$ and $\mathscr{L}_\varepsilon \psi(x,t) \geq 0, \forall (x,t) \in \mathscr{D}_{xt}$. Then $\psi(x,t) \geq 0, \forall (x,t) \in \overline{\mathscr{D}}_{xt}$, where the differential operator is defined by $\mathscr{L}_\varepsilon \psi(x,t) = \psi_t(x,t) - \varepsilon \psi_{xx} + a(x,t)\psi(x,t)$.*

Proof. The proof of this lemma is similar to the proof of Lemma (2.1) of chapter (2). □

Lemma 3.2. *(Stability Estimate). Let $\psi(x,t)$ be the solution of problem (3.1) . Then, we have*

$$|\psi(x,t)| \leq max\{|\mathscr{S}_0(x)|, |\mathscr{S}_l(t)|, \mathscr{S}_r(t)|\} + \alpha^{-1}||f||.$$

Proof. The proof of this lemma is similar to that of Lemma lema2.2 in Chapter (2). □

Lemma 3.3. *Let $\psi(x,t)$ be the solution of the problem (2.1). Then we have the bound*

$$\left|\psi^{(i,j)}(x,t)\right| \leq C\left[1 + \varepsilon^{-i/2}\left(\exp(-\sqrt{\frac{\alpha}{\varepsilon}}x + \exp(-\sqrt{\frac{\alpha}{\varepsilon}}(1-x))\right)\right], \tag{3.5}$$

where $0 \leq i + 2j \leq 4$.

Proof. The proof of this lemma is similar to that of Lemma (2.3) in Chapter (2). □

3.4 Formulation of Numerical Schemes

Following a similar approach in [34] , we discretized the problem under consideration using implicit Euler approach in the time direction on uniform meshes and the spatial direction by means of linear multi-step finite difference method on Shishkin meshes. Finally, we integrated the two discretized problems together and found the fully discrete solution of the proposed problem.

3.4.1 Temporal Semi-discretization:

Divide the time domain $[0,T]$ in to M equal number of mesh intervals with step length Δt, we get

$$\overline{\mathscr{D}}_t^M = \left\{ t^j : t^j = j\Delta t, j = 0,1,2,3,\dots M \text{ and } \Delta t = \frac{T}{M} \right\}. \tag{3.6}$$

Utilizing the procedures in [32] the temporal semi-discretization of problem (3.1) is done via the implicit-Euler approach subject to the initial and boundary conditions of the form:

$$\begin{cases} \frac{\psi^{j+1}(x)-\psi^j(x)}{\Delta t} = \varepsilon \psi_{xx}^{j+1}(x) - (b\psi)^{j+1}(x) + f^{j+1}(x), \\ \begin{cases} \psi^{j+1}(x,0) = \mathscr{S}_0(x), & \forall x \in \mathscr{D}_x, \\ \psi^{j+1}(0,t) = \mathscr{S}_l(t^{j+1}), & 0 \le j \le M-1, \\ \psi^{j+1}(1,t) = \mathscr{S}_r(1,t^{m+1}), & 0 \le j \le M-1. \end{cases} \end{cases} \tag{3.7}$$

Rearranging and simplifying (3.7), we get the $(j+1)^{th}$ time level equations as follows

$$\begin{cases} -\varepsilon \psi_{xx}^{j+1}(x) + W_3 \psi^{j+1}(x) = Z^j(x), \\ \begin{cases} \psi^{j+1}(x,0) = \mathscr{S}_0(x), & \forall x \in \mathscr{D}_x, \\ \psi^{j+1}(0,t) = \mathscr{S}_l(t^{j+1}), & 0 \le j \le M-1, \\ \psi^{j+1}(1,t) = \mathscr{S}_r(1,t^{j+1}), & 0 \le j \le M-1. \end{cases} \end{cases} \tag{3.8}$$

where $W_3(x) = (1/\Delta t + b^{j+1}(x))$ and $Z^j(x) = f^{j+1}(x) + (1/\Delta t)\psi^j(x)$. To check the discrete maximum principle and stability estimate of the temporal semi-discretization of the proposed scheme, we first rewrite equation (3.8) at $(j+1)^{th}$ time level in-terms of spatial variables as follows:

$$\begin{cases} \mathscr{L}_\varepsilon^* \Gamma := -\varepsilon \Gamma''(x) + W_3(x)\Gamma(x) = Z^j(x), & \forall x \in \overline{\mathscr{D}}_x, \\ \Gamma(0) = \mathscr{S}_l(t^{j+1}),\ \Gamma(1) = \mathscr{S}_r(1,t^{j+1}), & \forall t^{j+1} \in \overline{\mathscr{D}}_t^M. \end{cases} \tag{3.9}$$

where $\mathscr{L}_\varepsilon{}^*$ is a semi-discrete operator, $\Gamma(x) = \psi^{j+1}(x)$.

Lemma 3.4. *(Semi-discrete Maximum Principle). If $\Gamma^{j+1}(x) \in C^2(\overline{\mathscr{D}}_x)$ is the solution of the semi-discrete problem (3.9) such that $\Gamma^{j+1}(0) \geq 0, \Gamma^{j+1}(1) \geq 0$ on $\partial\overline{\mathscr{D}}_x$ and $\mathscr{L}_\varepsilon{}^*\Gamma^{j+1}(x) \geq 0,\ \forall x \in \mathscr{D}_x$, then $\Gamma^{j+1}(x) \geq 0,\ \forall x \in \overline{\mathscr{D}}_x$.*

Proof. Let $x^* \in \overline{\mathscr{D}}_x$ such that $\Gamma^{j+1}(x^*) = min_{x\in\overline{\mathscr{D}}_x}\Gamma^{j+1}(x) < 0$. Since $\Gamma^{j+1}(0) \geq 0$ and $\Gamma^{j+1}(1) \geq 0$ then $x^* \notin \{0,1\}$ that is $x^* \in \mathscr{D}_x$.
Moreover, since $\Gamma^{j+1}(x^*) = 0$ and $\Gamma^{j+1}_{xx}(x^*) \geq 0$ we have that

$$\begin{aligned} \mathscr{L}_\varepsilon{}^*\Gamma^{j+1}(x^*) &= -\varepsilon\Gamma^{j+1}_{xx}(x^*) + W_3(x^*)\Gamma^{j+1}(x^*), \\ &\leq 0. \end{aligned}$$

This shows $\mathscr{L}^*_\varepsilon\Gamma^{j+1}(x) \leq 0$. This contradicts the assumption $\mathscr{L}_\varepsilon{}^*\Gamma^{j+1}(x) \geq 0$.
Consequently, we conclude that the minimum of $\Gamma^{j+1}(x)$ is non-negative. □

Lemma 3.5. *(Stability Estimate). Let $\Gamma(x)$ be the solution of the semi-discrete problem (3.9). Then we have*

$$||\Gamma(x)|| \leq \beta_4^{-1}||\mathscr{L}_\varepsilon{}^*\Gamma(x)|| + ||\Gamma(x)||_{D_x},\ W_3(x) \geq \beta_4 > 0. \tag{3.10}$$

Proof. The proof is similar to the proof of Lemma (2.5) of chapter (2). □

As presented in [48], the local truncation error of the implicit Euler scheme for the temporal discretization is given by $e^{j+1} \equiv \psi^{j+1}(x) - \psi_i^{j+1}$, where ψ_i^{j+1} is the computed solution of (3.1). The local error estimate of each time step contributes to the global error in the temporal discretization at j^{th} time level is defined by $E^j \equiv \psi(x,t^j) - \psi^j(x)$.

Lemma 3.6. *(Local Error Estimate): The local error estimate in the temporal direction is given by*

$$||e^{j+1}||_\infty \leq C_1(\Delta t)^2. \tag{3.11}$$

Proof. Using the Taylor series expansion about (x,t^j), we have

$$\psi^{j+1} = \psi(x,t^j) + \Delta t\psi_t(x,t^j) + \frac{(\Delta t)^2}{2}\psi_{tt}(x,t^j) + O((\Delta t)^3), \tag{3.12}$$

Rearranging (3.12) gives

$$\frac{\psi^{j+1} - \psi^j}{\Delta t} = \psi_t(x,t^j) + O((\Delta t)^2). \tag{3.13}$$

Substituting (3.13) into (3.7), we get

$$\frac{\psi^{j+1}(x)-\psi^{j}(x)}{\Delta t}=\varepsilon\psi_{xx}^{j+1}(x)-(b\psi)^{j+1}(x)+f^{j+1}(x)+O((\Delta t)^2). \tag{3.14}$$

The solution to the local error is

$$\begin{cases}\mathscr{L}^{*}e^{j+1}=O((\Delta t)^2),\\ e^{j+1}(0)=0,\ e^{j+1}(1)=0.\end{cases} \tag{3.15}$$

Thus, using Lemma (3.4), the required result is satisfied and gives $||e^{j+1}||_{\infty}\leq C_1(\Delta t)^2$.

□

Lemma 3.7. *(Global Error Estimate): Under the hypothesis of Lemma* (3.6)*, the global error estimate E^{j+1} in the temporal direction is defined by*

$$||E^{j+1}||_{\infty}\leq C_2\Delta t. \tag{3.16}$$

Proof. The proof is similar to the proof of Lemma(2.7) of chapter (2). □

3.4.2 Spatial Semi-discretization:

This section discusses on the detail of the spatial domain discretization using piece-wise uniform Shishkin meshes. Since the problem domain exhibits twin boundary layers near $x=0$ and $x=1$, we follow the approach in [32] to divide the domain $\overline{\mathscr{D}}_x^N=[0,1],\ N\geq 4$ into three regions of the form $\mathscr{D}_l^N=[0,\tau],\mathscr{D}_c^N=[\tau,1-\tau]$ and $\mathscr{D}_r^N=[1-\tau,1]$ where the transition parameter

$$\tau=min\left\{\frac{1}{4},\sigma\sqrt{\varepsilon}lnN\right\},\quad \sigma\geq\frac{2}{\beta_4},\ W3(x)\geq\beta_4>0 \tag{3.17}$$

represents the width of the boundary layer, $\mathscr{D}_l^N=[0,\tau]$ and $\mathscr{D}_r^N=[1-\tau.1]$ are fine regions in which the solution varies very rapidly and $\mathscr{D}_c^N=[\tau,1-\tau]$ is the coarse region where the solution varies slowly. Moreover, the mesh is equidistant on the region $[\tau,1-\tau]$ with $N/2$ mesh elements and $N/4$ mesh elements in the fine regions $[0,\tau]$ and $[\tau,1-\tau]$. The mesh points $\overline{\mathscr{D}}_x^N=\{x_i\}_{i=0}^N$ are obtained by

$$x_i=\begin{cases}x_0=0,\\ ih_L,\ \ i=1,2,\dots,\frac{N}{4},\\ \tau+(i-\frac{N}{4})h_R,\ \ i=\frac{N}{4}+1,\dots,\frac{3N}{4},\\ 1-\tau+(i-\frac{3N}{4})h_L,\ \ i=\frac{3N}{4}+1,\dots,N-1,\\ x_N=1.\end{cases} \tag{3.18}$$

where $h_L = \frac{4\tau}{N}$ and $h_R = \frac{2(1-2\tau)}{N}$ are the step sizes of the dense and coarse regions respectively. Now consider the singularly perturbed problem in (3.8) along with its initial and boundary conditions of the following form:

$$\begin{cases} -\varepsilon \psi_{xx}^{j+1}(x) + W_3 \psi^{j+1}(x) = Z^j(x), \\ \begin{cases} \psi^{j+1}(x,0) = \mathscr{S}_0(x), & \forall x \in \mathscr{D}_x, \\ \psi^{j+1}(0,t) = \mathscr{S}_l(t^{j+1}), & 0 \le j \le M-1, \\ \psi^{j+1}(1,t) = \mathscr{S}_r(1,t^{j+1}), & 0 \le j \le M-1. \end{cases} \end{cases} \tag{3.19}$$

Now let's define three nodal values using the concept of linear multistep finite difference approximations for differential equations as outlined in [86] as follows

$$\sum_{s=0}^{2} \alpha_s U_{i-s+1}^{j+1} = \sum_{s=0}^{2} \beta_s \left(U_{xx}^{j+1}\right)_{i-s+1}, \tag{3.20}$$

where the coefficients α_s and β_s are to be determined in terms of the mesh parameter h_i. Using this equation, we define the local truncation errors as follows

$$\zeta_i^{j+1} = \alpha_0 \psi_{i-1}^{j+1} + \alpha_1 \psi_i^{j+1} + \alpha_2 \psi_{i+1}^{j+1} - \left[\beta_0 \left(\psi_{xx}^{j+1}\right)_{i-1} + \beta_1 \left(\psi_{xx}^{j+1}\right)_i + \beta_2 \left(\psi_{xx}^{j+1}\right)_{i+1}\right]. \tag{3.21}$$

Now suppose that the function $\psi^{j+1}(x_i)$ be differentiable up to sixth-order. Using the Taylor series for the terms $\psi_{i\pm1}^{j+1}$ and $\left(\psi_{xx}^{j+1}\right)_{i\pm1}$ about the point x_i as in the following manner:

$$\begin{cases} \psi_{i-1}^{j+1} = \sum_{n=0}^{6} \frac{(-1)^n}{n!} h_i^n \left(\psi_{x^n}^{j+1}\right)_i + O\left(h_i^7\right), \\ \psi_{i+1}^{j+1} = \sum_{n=0}^{6} \frac{(h_{i+1})^n}{n!} \left(\psi_{x^n}^{j+1}\right)_i + O\left(h_{i+1}^7\right), \\ \left(\psi_{xx}^{j+1}\right)_{i-1} = \sum_{n=0}^{4} \frac{(-1)^n}{n!} h_i^n \left(\psi_{x^{n+2}}^{j+1}\right)_i + O\left(h_i^7\right), \\ \left(\psi_{xx}^{j+1}\right)_{i+1} = \sum_{n=0}^{4} \frac{(h_{i+1})^n}{n!} \left(\psi_{x^{n+2}}^{j+1}\right)_i + O\left(h_{i+1}^7\right). \end{cases} \tag{3.22}$$

where $\left(\psi_{x^n}^{j+1}\right)_i$ is the n^{th} derivative of ψ_i^{j+1} at x_i and $h_i = x_i - x_{i-1}$.
Now up on using the expanded forms of (3.22) into (3.21) and simplifying it gives

$$\begin{aligned}
\zeta_i^{j+1} &= (\alpha_0+\alpha_1+\alpha_2)\,\psi_i^{j+1} + (\alpha_0 h_{i+1} - \alpha_2 h_i)\left(\psi_x^{j+1}\right)_i \\
&+ \left(\frac{\alpha_0 h_{i+1}^2}{2!} + \frac{\alpha_2 h_i^2}{2!} - (\beta_0+\beta_1+\beta_2)\right)\left(\psi_{xx}^{j+1}\right)_i \\
&+ \left(\frac{\alpha_0 h_{i+1}^3}{3!} - \frac{\alpha_2 h_i^3}{3!} - (\beta_0 h_{i+1} - \beta_2 h_i)\right)\left(\psi_{xxx}^{j+1}\right)_i \\
&+ \left(\frac{\alpha_0 h_{i+1}^4}{4!} + \frac{\alpha_2 h_i^4}{4!} - \left(\frac{\beta_0 h_{i+1}^2}{2!} + \frac{b_2 h_i^2}{2!}\right)\right)\left(\psi_{xxxx}^{j+1}\right)_i \\
&+ \left(\frac{\alpha_0 h_{i+1}^5}{5!} - \frac{\alpha_2 h_i^5}{5!} - \left(\frac{\beta_0 h_{i+1}^3}{3!} - \frac{\beta_2 h_i^3}{3!}\right)\right)\left(\psi_{xxxxx}^{j+1}\right)_i \\
&+ \left(\frac{\alpha_0 h_{i+1}^6}{6!} + \frac{\alpha_2 h_i^6}{6!} - \left(\frac{\beta_0 h_{i+1}^4}{4!} + \frac{\beta_2 h_i^4}{4!}\right)\right)\left(\psi_{xxxxxx}^{j+1}\right)_i + \dots
\end{aligned} \tag{3.23}$$

Since the finite difference approximation in (3.20) is order four and all other coefficients of (3.23) are equal to zero except the coefficient of $\left(\psi_{xxxxxx}^{j+1}\right)_i$, then we get the following set of equations.

$$\begin{cases}
\alpha_0+\alpha_1+\alpha_2 = 0, \\
\alpha_0 h_{i+1} - \alpha_2 h_i = 0, \\
\alpha_0 h_{i+1}^2 + \alpha_2 h_i^2 = 2\,(\beta_0+\beta_1+\beta_2), \\
\alpha_0 h_{i+1}^3 - \alpha_2 h_i^3 = 6\,(\beta_0 h_{i+1} - \beta_2 h_i), \\
\alpha_0 h_{i+1}^4 + \alpha_2 h_i^4 = 12\left(\beta_0 h_{i+1}^2 + \beta_2 h_i^2\right), \\
\alpha_0 h_{i+1}^5 - \alpha_2 h_i^5 = 20\left(\beta_0 h_{i+1}^3 - \beta_2 h_i^3\right), \\
\alpha_0 h_{i+1}^6 + \alpha_2 h_i^6 \neq 30\left(\beta_0 h_{i+1}^4 + \beta_2 h_i^4\right).
\end{cases} \tag{3.24}$$

To ensure that the finite difference approximation is consistent with the original differential equation, we choose $\beta_0+\beta_1+\beta_2 = 1$. This normalization guarantees that the main term ψ_i^{j+1} is correctly preserved without any scaling error. It also reduces the number of free parameters in the system, allowing the remaining coefficients to be uniquely determined so as to achieve fourth-order accuracy.

With the condition $\beta_0+\beta_1+\beta_2 = 1$, the resulting system of equations is solved using standard elimination techniques, yielding the required set of coefficients.

$$\begin{cases}
\alpha_0 = \frac{2}{h_{i+1}(h_i+h_{i+1})}, \\
\alpha_1 = \frac{-2}{h_i h_{i+1}}, \\
\alpha_2 = \frac{2}{h_i(h_i+h_{i+1})}.
\end{cases} \quad \text{and} \quad \begin{cases}
\beta_0 = \frac{h_{i+1}^2 + h_i h_{i+1} - h_i^2}{6h_{i+1}(h_i+h_{i+1})}, \\
\beta_1 = \frac{4h_i h_{i+1}(h_i+h_{i+1}) + h_i^3 + h_{i+1}^3}{6h_i h_{i+1}(h_i+h_{i+1})}, \\
\beta_2 = \frac{h_i h_{i+1} + h_i^2 - h_{i+1}^2}{6h_i(h_i+h_{i+1})}.
\end{cases} \tag{3.25}$$

expressing the second partial derivatives in (3.19) at the nodal point x_i gives

$$\begin{cases} \left(\psi_{xx}^{j+1}\right)_{i-1} = \frac{W_{3(i-1)}\psi_{i-1}^{j+1}-Z_{i-1}^{j}}{\varepsilon}, \\ \left(\psi_{xx}^{j+1}\right)_{i} = \frac{W3i\psi_{i}^{j+1}-Z_{i}^{j}}{\varepsilon}, \\ \left(\psi_{xx}^{j+1}\right)_{i+1} = \frac{W_{3(i+1)}\psi_{i+1}^{j+1}-Z_{i+1}^{j}}{\varepsilon}. \end{cases} \tag{3.26}$$

Substituting (3.25) and (3.26) into (3.21) and simplifying it, we get the fully discretized form of the proposed problem of the form:

$$\mathscr{L}_\varepsilon{}^{N,M}\psi_i^j \equiv E_i\psi_{i-1}^{j+1} + F_i\psi_i^{j+1} + G_i\psi_{i+1}^{j+1} = H_i^j, \;\; i = 1,2,3,\dots N-1. \tag{3.27}$$

where

$$\begin{cases} E_i = \frac{-2\varepsilon}{h_{i+1}(h_{i+1}+h_i)} + \frac{W_{3(i-1)}\left(h_{i+1}^2+h_ih_{i+1}-h_i^2\right)}{6h_{i+1}(h_{i+1}+h_i)}, \\ F_i = \frac{2\varepsilon}{h_ih_{i+1}} + \frac{W_{3(i)}\left(4h_ih_{i+1}(h_{i+1}+h_i)+h_i^3+h_{i+1}^3\right)}{6h_ih_{i+1}(h_{i+1}+h_i)}, \\ G_i = \frac{-2\varepsilon}{h_i(h_{i+1}+h_i)} + \frac{W_{3(i-1)}\left(h_i^2+h_ih_{i+1}-h_{i+1}^2\right)}{6h_i(h_{i+1}+h_i)}, \\ H_i^j = \left(\frac{h_{i+1}^2+h_ih_{i+1}-h_i^2}{6h_{i+1}(h_{i+1}+h_i)}\right)Z_{i-1}^j + \left(\frac{4h_ih_{i+1}(h_{i+1}+h_i)+h_i^3+h_{i+1}^3}{6h_ih_{i+1}(h_{i+1}+h_i)}\right)Z_i^j + \left(\frac{h_i^2+h_ih_{i+1}-h_{i+1}^2}{6h_i(h_{i+1}+h_i)}\right)Z_{i+1}^j, \\ W_{3(i)} = \left(\frac{1}{\Delta t} + a_i^{j+1}\right) \text{ and } Z_i^j = f_i^{j+1} + \left(\frac{1}{\Delta t}\right)\psi_i^j. \end{cases} \tag{3.28}$$

Since the resulting tridiagonal system in (3.27) is a nonsingular M-matrix by theorem (2.1) of Chapter (2), we solve it using matrix inverse method.

3.5 Uniform Convergence Analysis

Lemma 3.8. *(Discrete Maximum Principle). Assume that ϕ_i is a mesh function which satisfies $\phi_0 \geq 0$ and $\phi_N \geq 0$. Then $\mathscr{L}_\varepsilon{}^N\phi_i \geq 0, \;\; 1 \leq i \leq N-1$ implies that $\phi_i \geq 0$, for $\; 0 \leq i \leq N$.*

Proof. Let ϕ_i a mesh function such that $\phi_i^* = min_{1\leq i\leq N}\phi_i$ and assume that $\phi_i^* < 0$.
It is clear that $i \in \{0,N\}$ and therefore $(\phi_x)_i^* = 0$ and $(\phi_{xx})_i^* \geq 0$.
Using (3.22) into (3.21) and simplifying it gives

$$\begin{aligned} \mathscr{L}_\varepsilon{}^N\phi_i &= \alpha_0\phi_{i-1} + \alpha_1\phi_i + \alpha_2\phi_{i+1} - \left[\beta_0\left(\phi_{xx}\right)_{i-1} + \beta_1\left(\phi_{xx}\right)_i + \beta_2\left(\phi_{xx}\right)_{i+1}\right], \\ &= \alpha_0\phi_{i-1}^* + \alpha_1\phi_i^* + \alpha_2\phi_{i+1}^* - \left[\beta_0\left(\phi_{xx}\right)_{i-1}^* + \beta_1\left(\phi_{xx}\right)_i^* + \beta_2\left(\phi_{xx}\right)_{i+1}^*\right], \\ &< 0. \end{aligned}$$

This implies $\mathscr{L}_\varepsilon{}^N \phi_i < 0$, which contradicts to the assumption $\mathscr{L}_\varepsilon{}^N \phi_i \geq 0$. Hence, $\phi_i \geq 0$. □

Lemma 3.9. *(Uniform Stability Estimate). If ϕ_i is any mesh function such that $\phi_0 = 0 = \phi_N$, then*

$$|\phi_i| \leq \beta_4^{-1} \max_{1\leq i\leq N-1} \left|\mathscr{L}_\varepsilon{}^N \phi_i\right|, \quad 0 \leq i \leq N.$$

Proof. Let's denote $Y_i = \beta_4^{-1} \max_{1\leq i\leq N-1} \left|\mathscr{L}_\varepsilon{}^N \phi_i\right|, \quad 1 \leq i \leq N-1.$
Let us define two barrier functions $\Omega_i^{\pm} = YW_{3i} \pm \phi_i$. Following a similar approach in Lemma (2.2) and $\Omega_0^{\pm} = 0 = \Omega_N^{\pm}$, for $i = 1, 2, 3 \ldots, N-1$, we get

$$\mathscr{L}_\varepsilon{}^N \Omega_i^{\pm} = YW_{3i} + \mathscr{L}_\varepsilon{}^N \phi_i \leq 0.$$

Since $W_{3i} \geq \beta_4 > 0$, Lemma (3.8) implies that $\Omega_i^{\pm} \geq 0,\ 0 \leq i \leq N$ gives the required bound. □

Remark 3.1. Since the above bounds on the derivatives of the solution are not sharp enough for the proof of $\varepsilon-$uniform convergence, we need to derive stronger bounds. The stronger bounds are now obtained by decomposing the exact solution $\psi^{j+1}(x_i)$ in to a smooth and singular components of the following forms as described in [2, 84]:

$$\underbrace{\psi^{j+1}(x_i)}_{\text{Solution}} = \underbrace{V^{j+1}(x_i)}_{\text{Smoodh Component}} + \underbrace{W^{j+1}(x_i)}_{\text{Singular Component}} \quad \forall x \in \mathscr{D}_x.$$

Lemma 3.10. *(Error Boundedness). The error in the solution at the grid point x_i satisfies the following estimate*

$$\left|\delta_{xx}^{(4)} \psi(x_i) - \psi''(x_i)\right| \leq \begin{cases} CN^{-4}, & \forall i \in \left[\frac{N}{4}+1, \frac{3N}{4}\right], \\ C(\ln N)^4 N^{-4}, & \forall i \in \left[0, \frac{N}{4}\right] \cup \left[\frac{3N}{4}+1, N\right]. \end{cases}$$

where

$$\begin{cases} \delta_{xx}^{(4)} \psi(x_i) = \frac{-\psi_{i-2}+16\psi_{i-1}-30\psi_i+16\psi_{i+1}-\psi_{i+2}}{12h_R^2}, & h_R = \frac{2(1-2\tau)}{N}, \\ \delta_{xx}^{(4)} \psi(x_i) = \frac{-\psi_{i-2}+16\psi_{i-1}-30\psi_i+16\psi_{i+1}-\psi_{i+2}}{12h_L^2}, & h_L = \frac{4\tau}{N}. \end{cases}$$

Proof: To proof this, we first decompose the semi-discrete solution $\psi^{j+1}(x_i)$ into smooth and singular components of remark (3.1) and outlined in [84] of the following forms:

$$\psi^{j+1}(x_i) = V^{j+1}(x_i) + W^{j+1}(x_i) \tag{3.29}$$

where the smooth component $V^{j+1}(x_i)$ satisfies the non-homogeneous equation

$$\begin{cases} \mathscr{L}_\varepsilon^N V^{j+1}(x_i) = H_i^j, & i = 1,2,3,\ldots,N, \\ V^{j+1}(0) = v^{j+1}(0) \quad \text{and} \quad V^{j+1}(1) = v^{j+1}(1). \end{cases}$$

and the singular component $W^{j+1}(x_i)$ satisfies the homogeneous equation

$$\begin{cases} \mathscr{L}_\varepsilon^N W^{j+1}(x_i) = 0, & i = 1,2,3,\ldots,N, \\ W^{j+1}(0) = w^{j+1}(0), \quad \text{and} \quad W^{j+1}(1) = w^{j+1}(1). \end{cases}$$

where v^{j+1} and w^{j+1} are the exact solutions of problem (3.1) at $(j+1)^{th}$ time level. Based on this, the error in the numerical solution can be decomposed as

$$\left(\psi^{j+1} - \psi\right)(x_i) = \left(V^{j+1} - v\right)(x_i) + \left(W^{j+1} - w\right)(x_i). \tag{3.30}$$

Case I. (Error in the smooth component): The error in the smooth component satisfies the following estimate:

$$\left|\delta_{xx}^{(4)} V(x_i) - v''(x_i)\right| \le CN^{-4}, \quad \forall i \in \left[\frac{N}{4}+1, \frac{3N}{4}\right].$$

Proof. Let $x_i \in [\tau, 1-\tau]$, where τ is defined as in (3.17) and the truncation error found in (3.23), we have the bound in the smooth solution as follows:

$$\begin{aligned} \left|\mathscr{L}_\varepsilon^N \left(\delta_{xx}^{(4)} V(x_i) - v''(x_i)\right)\right| &= \left|\mathscr{L}_\varepsilon^N \left(\delta_{xx}^{(4)} V(x_i)\right) - \mathscr{L}_\varepsilon^N \left(v''(x_i)\right)\right|, \\ &\le C\left((h_i)^6 + (h_i)^4\right), C = \frac{1}{24}\{\|\beta_0\|_\infty + \|\beta_2\|_\infty\} \left\|(U_i)^{(6)}\right\|_\infty, \\ &\le C\left(h_i^4\right), \text{ since } h_i^4 = \max_{0\le i\le N}\left\{h_i^4, h_i^6\right\} \text{ and } h_i \equiv O\left(\frac{1}{N}\right), \\ &\le CN^{-4}. \end{aligned}$$

This proves the error bound in the smooth component is of fourth-order accurate to the spatial direction as presented in the theoretical session. □

Case II. (Error in the singular component): The error in the singular component satisfies the following bound:

$$\left|\delta_{xx}^{(4)} W(x_i) - w''(x_i)\right| \le C(lnN)^N N^{-4}, \quad \forall i \in \left[0, \frac{N}{4}\right] \cup \left[\frac{3N}{4}+1, N\right].$$

Proof. Considering the points $x_i \in [0,\tau] \cup [\tau, 1-\tau]$, and the truncation error defined in (3.23), the bound in the singular component can be proved as follows:

$$
\begin{aligned}
\left|\mathscr{L}_{\varepsilon}^{N}\left(\delta_{xx}^{(4)}W(x_i)-w^{''}(x_i)\right)\right| &= \left|\mathscr{L}_{\varepsilon}^{N}\left(\delta_{xx}^{(4)}V(x_i)\right)-\mathscr{L}_{\varepsilon}^{N}\left(v^{''}(x_i)\right)\right|,\\
&\leq C\left((h_i)^6+(h_i)^4\right),\ C=\frac{1}{24}\{\|\beta_0\|_\infty+\|\beta_2\|_\infty\}\left\|(U_i)^{(6)}\right\|_\infty,\\
&\leq C\left(h_i^4\right),\ \text{ since }\ h_i^4=\max_{0\leq i\leq N}\left\{h_i^4,h_i^6\right\}\ \text{ and }\ h_i\equiv O\left(\frac{\sqrt{\varepsilon}lnN}{N}\right),\\
&\leq C(lnN)^4N^{-4}.
\end{aligned}
$$

This demonstrates that the error bound in the singular component shows the scheme achieves fourth-order accuracy, with a logarithmic factor, as discussed in the theoretical analysis of Shishkin meshes. □

Using the definition provided in (3.30), in conjunction with the results established in Cases I and II, we derive the following error bounds for the spatial semi-discretization as required:

$$
\left|\delta_{xx}^{(4)}\psi(x_i)-\psi^{''}(x_i)\right|\leq C(N^{-4}+(\ln N)^4N^{-4}),\quad 0\leq i\leq N.
$$

Theorem 3.1. Let $\psi(x,t)$ and ψ_i^{j+1} be are solutions of the continuous and discrete problems in (3.1) and (3.27) at $(j+1)^{th}$ time level respectively. Then, the error estimate for the fully discrete scheme can be defined in the following form as discussed in [87]:

$$
\sup_{0\leq i\leq N,\ 0\leq j\leq M}\left|\psi(x_i,t^{j+1})-\psi_i^{j+1}\right|\leq C(N^{-4}+(\ln N)^4N^{-4}+\Delta t). \tag{3.31}
$$

Proof. Now, using Lemma (3.7) and Lemma (3.10), the uniform error estimate of the fully discrete scheme is proved as

$$
\begin{aligned}
&\sup_{0<\varepsilon\leq 1}\max_{i,j}\left\|\psi(x_i,t^{j+1})-\psi_i^{j+1}\right\|_{\mathscr{D}_x^N\times\mathscr{D}_t^M},\\
=&\sup_{0<\varepsilon\leq 1}\max_{i,j}\left\|\psi(x_i,t^{j+1})-\psi^{j+1}(x_i)+\psi^{j+1}(x_i)-\psi_i^{j+1}\right\|,\\
=&\sup_{0<\varepsilon\leq 1}\max_{i,j}\left\|\psi(x_i,t^{j+1})-\psi^{j+1}(x_i)\right\|+\sup_{0<\varepsilon\leq 1}\max_{i,j}\left\|\psi^{j+1}(x_i)-\psi_i^{j+1}\right\|,\\
\leq\ & C(N^{-4}+(\ln N)^4N^{-4}+\Delta t).
\end{aligned}
$$

Hence, the required bound can be defined as follows

$$
\sup_{0<\varepsilon\leq 1}\max_{i,j}\left\|\psi(x_i,t^{j+1})-\psi_i^{j+1}\right\|_{\mathscr{D}_x^N\times\mathscr{D}_t^M}\leq C(N^{-4}+(\ln N)^4N^{-4}+\Delta t).
$$

From the proofs, it is seen that the proposed scheme is fourth-order accurate in the spatial and first-order accurate in the temporal directions before extrapolation. □

3.6 Richardson Extrapolation Technique

As discussed in Theorem (3.1) above, it is seen that the proposed scheme has low order of accuracy in the temporal direction. This affects the overall order of convergence of the scheme. To tackle this challenge, we use the Richardson extrapolation technique in the time dircetion as described in [88].

Let $\mathscr{D}_t^{2M}$ be the mesh obtained from bisecting the time step length Δt such that $\mathscr{D}_t^M \subseteq \mathscr{D}_t^{2M}$. If $\psi^j(x_i)$ and $\overline{\psi}^j(x_i)$ be numerical solutions obtained from $\mathscr{D}_t^M$ and $\mathscr{D}_t^{2M}$ respectively, then

$$\psi(x_i,t^j) - \psi^j(x_i) = C\Delta t + R_j^M(x_i), \ \ (x_i,t^j) \in \mathscr{D}_x \times \mathscr{D}_t^M. \tag{3.32}$$

$$\psi(x_i,t^j) - \overline{\psi}^j(x_i) = C\left(\frac{\Delta t}{2}\right) + R_j^{2M}(x_i), \ \ (x,t^j) \in \mathscr{D}_x \times \mathscr{D}_t^{2M}. \tag{3.33}$$

where $\psi(x_i.t^j)$ is the exact solution of the proposed problem at j^{th} time level, $R_j^M(x)$ and $R_j^{2M}(x)$ are the remainder terms of the error with order $O(\Delta t^2)$ and C is a constant independent of the parameters ε, h and Δt. Now, subtracting the inequality (3.33) from (3.32) to obtain the extrapolation formula

$$\psi(x_i,t^j) - \psi^j(x) - 2(\psi(x_i,t^j) - \overline{\psi}^j(x)) = R_j^M(x) - R_j^{2M}(x). \tag{3.34}$$

Simplifying (3.34), gives the required numerical solution as follows

$$\psi^{ext}(x_i) = 2\overline{\psi}^j(x_i) - \psi^j(x_i). \tag{3.35}$$

Using the truncation error of the temporal discretization $\psi^j(x) = \psi(x_i,t^j) + C\Delta t + O(\Delta^2 t)$ and $\overline{\psi}^j(x_i) = \psi(x_i,t^j) + C\frac{\Delta t}{2} + O((\Delta t)^2)$ in (3.35) gives

$$\max_{0\le j\le M} \left|\psi^{ext}(x_i) - \psi^j(x_i)\right| \le C(\Delta t)^2. \tag{3.36}$$

where C is a constant independent of the parameter ε and mesh sizes N and M.

Now having all the above concepts, Theorem (3.1) is generalized as follows.

Theorem 3.2. Let ψ_i^{j+1} be the $(j+1)^{th}$ time level numerical solution of the discrete problem in (3.27) and $\psi(x_i,t^{j+1})$ be the analytical solution of problem(3.1). Then the maximum absolute error of the proposed method after Richardson extrapolation is given by

$$\sup_{0<\varepsilon<1} \max_{0\le j\le M} \left|\psi(x_i,t^{j+1}) - (\psi^{ext})_i^{j+1}\right| \le C(N^{-4} + (\ln N)^4 N^{-4} + (\Delta t)^2). \tag{3.37}$$

3.7 Numerical Results and Discussions

The effectiveness of the proposed scheme is assessed through two benchmark problems, where $\varepsilon-$uniform maximum absolute errors and convergence rates are evaluated for numerical simulation and analysis, as detailed in Chapter 2.

Example 3.1. Consider a singularly perturbed unsteady parabolic-type reaction-diffusion problem of the form in [32].

$$\begin{cases} \psi_t - \varepsilon\psi_{xx} + \frac{1+x^2}{2}\psi = e^t - 1 + sin(\pi x), \ (x,t) \in (0,1)\times(0,1], \\ \psi(x,0) = 0, x \in [0,1], \\ \psi(0,,t) = \psi(1,t) = 0, \ t \in (0,1]. \end{cases}$$

Example 3.2. Consider a singularly perturbed unsteady parabolic-type reaction-diffusion problem of the form in [34].

$$\begin{cases} \psi_t - \varepsilon\psi_{xx} + \frac{1+x^2}{2}\psi = t^3, \ (x,t) \in (0,1)\times(0,1], \\ \psi(x,0) = 0, x \in [0,1], \\ \psi(0,t) = \psi(1,t) = 0, \ t \in (0,1]. \end{cases}$$

Since the analytical solutions are unknown, we apply the doubling mesh technique to find the maximum absolute errors and the corresponding order of convergences as follows:

Before Extrapolation: Let $\psi^{N,M}(x_i,t^j)$ and $\psi^{2N,2M}(x_i,t^j)$ be the numerical solutions with mesh lengths $(h,k \neq 0)$ and $(h/2, \Delta t/2 \neq 0)$ respectively, then

- The maximum absolute error is given by

$$E_\varepsilon^{N,M} = \max_{0\le i,j\le N,M} \left|\psi^{N,M}(x_i,t^j) - \psi^{2N,2M}(x_{2i},t_{2j})\right|. \tag{3.38}$$

- The $\varepsilon-$ uniform maximum absolute error is given by

$$E^{N,M} = \max_{\varepsilon} E_\varepsilon^{N,M}. \tag{3.39}$$

- Corresponding ε-uniform order of convergence is $R^{N,M} = log_2\left(\frac{E^{N,M}}{E^{2N,2M}}\right)$.

After Extrapolation: Similarly, let $\psi^{2N,2M}(x_i,t^j)$ and $(\psi_i^j)^{ext}$ be the numerical solutions with mesh lengths $(h/2, \Delta t/2 \neq 0)$ and $(h/4, \Delta t/4 \neq 0)$ respectively, then

- The maximum absolute error is given by

$$E_{\varepsilon,ext}^{N,M} = \max_{0\le i,m\le N,M} \left|\psi^{2N,2M}(x_{2i},t_{2j}) - (\psi_i^j)^{ext}(x_i,t^j)\right|. \tag{3.40}$$

- The $\varepsilon-$ uniform maximum absolute error is given by

$$E_{ext}^{N,M} = \max_{\varepsilon} E_{\varepsilon,ext}^{N,M}. \tag{3.41}$$

- Corresponding ε-uniform order of convergence is $R_{\varepsilon,ext}^{N,M} = log_2\left(\frac{E_{ext}^{N,M}}{E_{ext}^{2N,2M}}\right)$.

Table 3.1: $E_{ext}^{N,M}$ and $R_{ext}^{N,M}$ for Example (3.1) after Richardson extrapolation

$\varepsilon \downarrow$	$N=64$ $M=40$	$N=128$ $M=160$	$N=256$ $M=640$	$N=512$ $M=2560$
2^{-6}	3.2929e − 04	8.1799e − 04	1.9994e − 04	4.6541e − 05
	2.0092	2.0325	2.1030	
2^{-8}	3.8559e − 04	9.6337e − 04	2.4072e − 04	6.0078e − 05
	2.0003	2.0012	2.0044	
2^{-10}	3.8559e − 04	9.6337e − 04	2.4072e − 04	6.0078e − 05
	2.0003	2.0012	2.0044	
2^{-12}	3.8559e − 04	9.6337e − 04	2.4072e − 04	6.0078e − 05
	2.0003	2.0012	2.0044	
2^{-14}	3.8559e − 04	9.6337e − 04	2.4072e − 04	6.0078e − 05
	2.0003	2.0012	2.0044	
2^{-16}	3.8559e − 04	9.6337e − 04	2.4072e − 04	6.0078e − 05
	2.0003	2.0012	2.0044	
2^{-18}	3.8559e − 04	9.6337e − 04	2.4072e − 04	6.0078e − 05
	2.0003	2.0012	2.0044	
$\vdots$	$\vdots$	$\vdots$	$\vdots$	$\vdots$
2^{-28}	3.8559e − 04	9.6337e − 04	2.4072e − 04	6.0078e − 05
	2.0003	2.0012	2.0044	
$E_{ext}^{N,M}$	3.8559e − 04	9.6337e − 04	2.4072e − 04	6.0078e − 05
$R_{ext}^{N,M}$	2.0003	2.0012	2.0044	
Results in [32]				
$E_{ext}^{N,M}$	0.711e − 02	0.178e − 02	0.493e − 02	0.163e − 02
$R_{ext}^{N,M}$	1.997	1.854	1.592	
Results in [34]				
$E_{ext}^{N,M}$	$1.742e-02$	$1.8201e-03$	$4.5900e-04$	$1.1502e-04$
$R_{ext}^{N,M}$	2.0395	1.9702	2.0005	

Table 3.2: $E_{ext}^{N,M}$ and $R_{ext}^{N,M}$ for Example (3.2) after Richardson extrapolation

$\varepsilon \downarrow$	$N=64$ $M=40$	$N=128$ $M=160$	$N=256$ $M=640$	$N=512$ $M=2560$
2^{-6}	$4.6129e-04$	$1.0703e-04$	$2.4800e-05$	$5.7452e-06$
	2.1076	2.1096	2.1099	
2^{-8}	$4.9970e-04$	$1.2453e-04$	$2.8997e-05$	$6.7581e-06$
	2.0046	2.1025	2.1012	
2^{-10}	$4.9970e-04$	$1.2453e-04$	$2.8997e-05$	$6.7581e-06$
	2.0046	2.1025	2.1012	
2^{-16}	$4.9970e-04$	$1.2453e-04$	$2.8997e-05$	$6.7581e-06$
	2.0046	2.1025	2.1012	
2^{-18}	$4.9970e-04$	$1.2453e-04$	$2.8997e-05$	$6.7581e-06$
	2.0046	2.1025	2.1012	
2^{-20}	$4.9970e-04$	$1.2453e-04$	$2.8997e-05$	$6.7581e-06$
	2.0046	2.1025	2.1012	
$\vdots$	$\vdots$	$\vdots$	$\vdots$	$\vdots$
2^{-30}	$4.9970e-04$	$1.2453e-04$	$2.8997e-05$	$6.7581e-06$
	2.0046	2.1025	2.1012	
$E_{ext}^{N,M}$	$4.9970e-04$	$1.2453e-04$	$2.8997e-05$	$6.7581e-06$
$R_{ext}^{N,M}$	2.0046	2.1025	2.1012	
Results in [34]				
$E_{ext}^{N,M}$	$1.742e-02$	$1.8201e-03$	$4.5900e-04$	$1.1502e-04$
$R_{ext}^{N,M}$	2.0395	1.9702	2.0005	
Results in [100]				
$E^{N,M}$	5.2840e − 04	1.3213e − 04	3.3033e − 05	8.2584e − 06
$R^{N,M}$	1.9997	1.9999	2.0000	

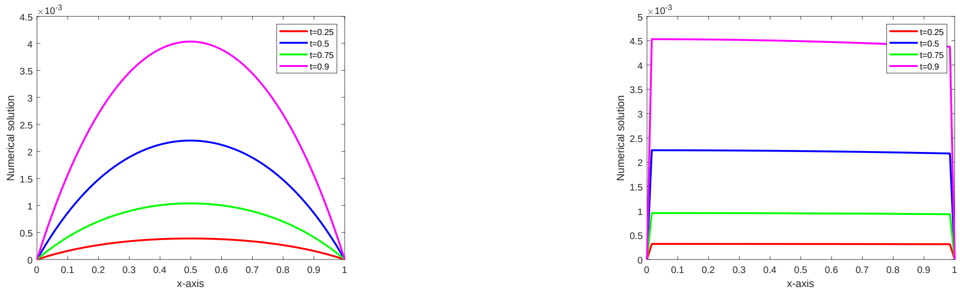

(a) $\varepsilon = 2^{-2}$ (b) $\varepsilon = 2^{-12}$

Figure 3.1: 2D solution graphs for Example (3.2) with values $N = 64, M = 40$

(a) $\varepsilon = 2^{-2}$ (b) $\varepsilon = 2^{-12}$

Figure 3.2: 3D solution graphs for Example (3.2) with values $N = 64, M = 32$

To examine the effectiveness of our proposed method, we consider two model problems. We report the maximum absolute errors along with the corresponding rates of convergence in Tables (3.1) and (3.2). For a fixed perturbation parameter ε, we observe that the errors decrease steadily as the mesh sizes N and M increase. In contrast, for fixed mesh parameters, we find that the errors remain nearly unchanged as ε decreases, which confirms the ε-uniform convergence of the scheme.

Furthermore, the 2D and 3D plots in Figures (3.1) and (3.2) clearly show the formation of twin boundary layers near $x = 0$ and $x = 1$, in agreement with the theoretical results. Finally, we compare our method with existing approaches based on both accuracy and order of convergence, and the results in Tables (3.1) and (3.2) demonstrate that our scheme outperforms the classical backward Euler and fitted operator finite difference methods in [34], as well as the backward Euler and central difference methods in [32].

3.8 Conclusion

In this chapter, we developed and analyzed a fitted numerical method for singularly perturbed parabolic reaction–diffusion problems. The proposed scheme combines the implicit Euler method for time discretization with a fourth-order fitted linear multistep method on Shishkin meshes for spatial discretization. Theoretical analysis shows that the method is parameter-uniformly convergent, achieving second-order accuracy in time and fourth-order accuracy in space after Richardson extrapolation. Numerical experiments confirm these results and demonstrate that the proposed method is more efficient than several existing approaches in the literature.

Chapter 4

An Accelerated Fourth-Order Fitted Numerical Scheme for Singularly Perturbed Parabolic Reaction–Diffusion Problems with Small Time Lag

This chapter presents a fitted numerical method for singularly perturbed delay differential equations arising in applied sciences such as biology, engineering, and population dynamics. The presence of a small perturbation parameter $\varepsilon\,(0<\varepsilon\ll 1)$ leads to sharp solution variations and boundary layer behavior. The delay term is removed using a Taylor series expansion, resulting in an asymptotically equivalent reaction–diffusion equation. A fitted numerical scheme based on the implicit Euler method in time and a finite difference approximation in space on uniform meshes is developed, with Richardson extrapolation used to improve accuracy. Theoretical analysis confirms stability and high-order convergence, while numerical results demonstrate the efficiency and superiority of the proposed method.

4.1 Introduction

Delay differential equations (DDEs) arise in modeling a wide range of real-life phenomena in engineering and science, including physiological processes [70], population dynamics [71], disease spread and control [72], diffusion in polymers [73], epidemiology [74], and hydrodynamics of liquid helium [75]. Singularly perturbed delay differential equations (SPPDDEs) are DDEs in which the highest-order derivative is multiplied by a small perturbation parameter $\varepsilon\,(0<\varepsilon\ll 1)$ and contain at least one delay term $\delta>0$. SPPDDEs commonly arise in practical applications such as biological and chemical reactions, population growth [22], and epidemiology [25] . Examples of delays include signal transmission times, driver reaction times, red blood cell production, and cell division in viral dynamics [76]. Time delays are thus natural components of dynamic processes in biology, ecology, physiology, economics, and mechanics [77].

The presence of a small perturbation parameter ε in SPPDDEs often produces boundary and/or interior layers, where the solution changes very rapidly. Due to these reasons, the standard numerical methods fail to capture these features accurately without extremely fine meshes, which increase round-off errors and computational cost [78], highlighting the need for parameter-independent schemes [63]. To address this, several parameter-uniformly convergent methods have been developed [79, 80], including fitted operator techniques, fitted meshes, and domain decomposition methods. Extensive studies have applied such schemes to parabolic SPPDDEs arising from reaction–diffusion problems [37, 81, 82].

Although existing schemes have provided valuable contributions, they often exhibit limitations in accuracy and low orders of convergence. Inspired with these limitations, we formulated and analyzed a fitted numerical method for reaction–diffusion SPPDDEs with small time lag. The proposed scheme employs Crank–Nicolson and NSFD approaches in the temporal and spatial discretization on uniform meshes, respectively.

4.2 Problem formulation

This chapter deals with a class of singularly perturbed parabolic differential–difference equations presented in the governing problem (1.12).

$$\begin{cases} \psi_t(x,t) - \varepsilon\psi_{xx}(x,t) + a(x,t)\psi(x,t) + b(x,t)\psi(x,t-\delta) = f(x,t), \quad \forall (x,t) \in \mathscr{D}_{xt}, \\ \begin{cases} \psi(x,t) = \mathscr{S}_0(x,t) & \forall (x,t) \in \mu_0 = [0,1] \times [-\delta, 0], \\ \psi(0,t) = \mathscr{S}_l(t) & \forall t \in \mu_l = \{(0,t) : 0 \leq t \leq T\}, \\ \psi(1,t) = \mathscr{S}_r(t)) & \forall t \in \mu_r = \{(1,t) : 0 \leq t \leq T\}. \end{cases} \end{cases} \tag{4.1}$$

where $\mathscr{L}_{\varepsilon,\delta}\psi(x,t) := \psi_t(x,t) - \varepsilon\psi_{xx}(x,t) + a(x,t)\psi(x,t) + b(x,t)\psi(x,t-\delta)$ is a differential operator and $\varepsilon, (0 < \varepsilon \ll 1)$, is a singular perturbation parameter such that, $\delta < \varepsilon$ is a small delay parameters which satisfies the relation $\delta = O(\varepsilon)$. To control sudden blow ups in the reaction terms, the functions $a(x,t), b(x,t)$ and $f(x,t)$ on $\overline{\mathscr{D}}_{xt}$ are assumed to be sufficiently smooth, bounded, and satisfy

$$a(x,t) + b(x,t) \geq \alpha > 0, b(x,t) \geq 0 \quad \forall (x,t) \in \overline{\mathscr{D}}_{xt}. \tag{4.2}$$

Following the approach in [24] and assuming that $\delta < \varepsilon$, we approximate the delay term via Taylor series expansion as follows:

$$\psi(x,t-\delta) = \psi(x,t) - \delta\psi_t(x,t) + O(\delta^2). \tag{4.3}$$

Utilizing (4.3) into (4.1), we get a transformed equation together with the initial and boundary conditions of the form below:

$$\begin{cases} \mathscr{L}_{C_\varepsilon}\psi := \psi_t(x,t) - C_\varepsilon(x,t)\psi_{xx}(x,t) + A(x,t)\psi(x,t) = F(x,t), & \forall (x,t) \in \mathscr{D}_{xt}, \\ \begin{cases} \psi(x,0) = \mathscr{S}_0(x) & \forall x \in \mu_b = \left\{(x,0) : x \in \overline{\mathscr{D}}_x\right\}, \\ \psi(0,t) = \mathscr{S}_l(0,t) & \forall (x,t) \in \mu_l = \left\{(x,t) : x = 0, t \in \overline{\mathscr{D}}_t\right\}, \\ \psi(1,t) = \mathscr{S}_r(1,t)) & \forall (x,t) \in \mu_r = \left\{(x,t) : x = 1, t \in \overline{\mathscr{D}}_t\right\}. \end{cases} \end{cases} \tag{4.4}$$

where $C_\varepsilon(x,t) \geq C_\varepsilon > 0$ is a modified perturbation parameter to (4.4) such that $0 \leq C_\varepsilon \ll 1$.

$$\begin{cases} Q(x,t) = 1/(1 - \delta b(x,t)) & \forall (x,t) \in \overline{\mathscr{D}}_{xt}, \\ C_\varepsilon(x,t) = \varepsilon Q(x,t) & \forall (x,t) \in \overline{\mathscr{D}}_{xt}, \\ A(x,t) = (a(x,t) + b(x,t))Q(x,t) & \forall (x,t) \in \overline{\mathscr{D}}_{xt}, \\ F(x,t) = Q(x,t)f(x,t) & \forall (x,t) \in \overline{\mathscr{D}}_{xt}. \end{cases} \tag{4.5}$$

For the existence of a unique solution, the functions $A(x,t)$ and $F(x,t)$ on $\overline{\mathscr{D}}_{xt}$ are assumed to be sufficiently smooth, bounded, and satisfy

$$A(x,t) \geq \beta > 0 \quad \forall (x,t) \in \overline{\mathscr{D}}_{xt}. \tag{4.6}$$

4.3 Properties of the Analytic Solution

The existence and uniqueness of the solution of problem (4.4) can be established by assuming the data is Hölder continuous on the domain $\overline{\mathscr{D}}_{xt}$ [83]. The required compatibility condition at the corner points $(0,0)$ and $(1,0)$ are defined as $\mathscr{S}_0(0,0) = \mathscr{S}_l(0)$, $\mathscr{S}_0(1,0) = \mathscr{S}_r(0)$ and satisfy

$$\begin{cases} \frac{\partial \mathscr{S}_l(0)}{\partial t} - C_\varepsilon \frac{\partial^2 \mathscr{S}_0(0,0)}{\partial x^2} + A(0,0)\mathscr{S}_0(0,0) = F(0,0), \\ \frac{\partial \mathscr{S}_r(0)}{\partial t} - C_\varepsilon \frac{\partial^2 \mathscr{S}_0(1,0)}{\partial x^2} + A(1,0)\mathscr{S}_0(1,0) = F(1,0). \end{cases} \tag{4.7}$$

where $\mathscr{S}_0(x,t)$, $\mathscr{S}_l(x,t)$ and $\mathscr{S}_r(x,t)$ are supposed to be sufficiently smooth functions. These conditions ensure that the problem in (4.4) has unique solution $\psi(x,t) \in C^{(4,2)}\left(\overline{\mathscr{D}}_{xt}\right)$ which exhibits boundary layers each of width $O(\sqrt{C_\varepsilon})$ at x = 0 and x = 1.

Lemma 4.1. *(Continuous Maximum Principle): Assume that $\phi(x,t)$ is any sufficiently smooth function satisfying $\phi(x,t) \geq 0, \forall (x,t) \in \partial\mathscr{D}_{xt} = \overline{\mathscr{D}}_{xt} \setminus \mathscr{D}_{xt}$ and $\mathscr{L}_{C_\varepsilon}\phi(x,t) \geq 0, \forall (x,t) \in \mathscr{D}_{xt}$ then, $\phi(x,t) \geq 0, \forall (x,t) \in \overline{\mathscr{D}}_{xt}$, where the differential operator is defined by $\mathscr{L}_{C_\varepsilon}\phi(x,t) = \phi_t(x,t) - C_\varepsilon\phi_{xx} + A(x,t)\phi(x,t)$.*

Proof. The proof is similar to the proof of Lemma (2.1) of Chapter (2). □

Lemma 4.2. *(Uniform Stability Estimate): If $\psi(x,t) \in C^{2,1}(\overline{\mathscr{D}}_{xt})$ be the solution of the continuous problem in problem (4.4) ,then it satisfies the bound*

$$|\psi(x,t)| \leq \beta^{-1}||F|| + max\{|\mathscr{S}_0(x)|, |\mathscr{S}_l(t)|, |\mathscr{S}_r(t)|\}.$$

Proof. The proof is similar to the proof of Lemma (2.2) of Chapter (2). □

Lemma 4.3. *As presented in [**?**] let $\psi(x,t)$ be the solution of the problem (4.4) at the time level j . Then we have*

$$\left|\psi^{i,j}(x,t)\right| \leq C\left[1 + C_{\varepsilon}^{-i/2}\left(\exp(-\sqrt{\frac{\beta}{C_{\varepsilon}}}x + \exp(-\sqrt{\frac{\beta}{C_{\varepsilon}}}(1-x))\right)\right]. \tag{4.8}$$

where $0 \leq i + 2j \leq 4$ and β is the lower bound of $A(x,t)$ as shown in (4.6).

Proof. The proof is similar to the proof of Lemma (2.3) of Chapter (2). □

4.4 Formulation of Numerical Schemes

This section deals with the semi-discretization of the problem along the temporal and spatial directions. Finally, we combined the two discretized problems together and found the fully discrete solution of the proposed problem defined in ((4.4)).

4.4.1 Temporal discretization:

Divide the time domain $[0,T]$ in to equal number of M mesh intervals of length j

$$\overline{\mathscr{D}}_t^M = \left\{t^j : t^j = j\Delta t, j = 0,1,2,3,\ldots M \text{ and } \Delta t = \frac{T}{M}\right\}. \tag{4.9}$$

Following the approach in [65] and using Crank Nicolson method, the problem (4.4) is discretized in following forms:

$$\begin{cases} \frac{\psi^{j+1}-\psi^j}{\Delta t} = -C_{\varepsilon}\left(\frac{\psi_{xx}^{j+1}+\psi_{xx}^j}{2}\right) - \frac{((A^{j+1}\psi)^{j+1}+(A^j\psi)^j)}{2} + \frac{f^{j+1}+f^j}{2}, \\ \begin{cases} \psi(x,0) = \mathscr{S}_0(x), & \forall x \in \mathscr{D}_x, \\ \psi(0,t_{j+1}) = \mathscr{S}_l(t^{j+1}), & 0 \leq j \leq M-1, \\ \psi(1,t_{j+1}) = \mathscr{S}_r(1,t^{j+1})), & 0 \leq j \leq M-1. \end{cases} \end{cases} \tag{4.10}$$

Again rearranging the j^{th} and $(j+1)^{th}$ time level equations gives

$$\begin{cases} -C_\varepsilon \psi_{xx}^{j+1}(x) + W_1(x)\psi^{j+1}(x) = h(x), \\ \begin{cases} \psi(x,0) = \mathscr{S}_0(x), & \forall x \in \mathscr{D}_x, \\ \psi(0,t^{j+1}) = \mathscr{S}_l(t^{j+1}), & 0 \le j \le M-1, \\ \psi(1,t^{j+1}) = \mathscr{S}_r(1,t^{j+1}), & 0 \le j \le M-1. \end{cases} \end{cases} \tag{4.11}$$

where $W_1(x) = (\frac{2}{\Delta t} + A^{j+1})$ and $h(x) = C_\varepsilon \psi_{xx}^j(x) + W_2(x)\psi^j(x) + (f^{j+1} + f^j)(x)$ and $W2(x) = (\frac{2}{\Delta t} - A^j)$. To check the semi-discrete maximum principle and stability estimate of the temporal direction of the proposed scheme, we first rewrite (4.11) at $(j+1)^{th}$ time level in-terms of spatial variables as follows:

$$\begin{cases} \mathscr{L}^*\Gamma :\equiv -C_\varepsilon \Gamma''(x) + W_1(x)\Gamma(x) = h(x), & \forall x \in \overline{\mathscr{D}}_x, \\ \Gamma(0) = \mathscr{S}_l(t^{j+1}),\ \Gamma(1) = \mathscr{S}_r(t^{j+1}), & \forall t^{j+1} \in \overline{\mathscr{D}}_t^M. \end{cases} \tag{4.12}$$

where $\mathscr{L}_\varepsilon{}^* = -C_\varepsilon \Gamma''(x) + W_1(x)\Gamma(x)$ is a semi-discrete operator , $\Gamma(x) = \psi^{j+1}(x)$.

Lemma 4.4. *(Semi-discrete Maximum Principle): If $\Gamma^{j+1}(x) \in C^2(\overline{\mathscr{D}}_x)$ is the solution of the semi-discrete problem (4.12) such that $\Gamma^{j+1}(0) \ge 0, \Gamma^{j+1}(1) \ge 0$ on $\partial\overline{\mathscr{D}}_x$ and $\mathscr{L}^*\Gamma^{j+1}(x) \ge 0,\ \forall x \in \mathscr{D}_x$, then $\Gamma^{j+1}(x) \ge 0,\ \forall x \in \overline{\mathscr{D}}_x$.*

Proof. The proof is similar to the proof of Lemma (2.4) of Chapter (2). □

Lemma 4.5. *(Stability Estimate): Let $\Gamma(x)$ be the solution of the semi-discrete problem (4.12).Then we have*

$$||\Gamma(x)|| \le \beta_3^{-1}||\mathscr{L}^*\Gamma(x)|| + ||\Gamma(x)||_{\mathscr{D}_x},\ W1(x) \ge \beta_3 > 0. \tag{4.13}$$

Proof. The proof is similar to the proof of Lemma (2.5) of Chapter (2). □

The local truncation error of the semi-discrete problem (4.11) is given by $e^{j+1} \equiv \psi(x,t_j) - \psi^{j+1}$, where ψ^{j+1} is the computed solution of the proposed boundary value problem. Moreover, this error measures the contribution of each time step to the global error of the temporal semi-discretization.

Lemma 4.6. *(Local Error Estimate): Suppose that*

$$\left|\frac{\partial^i \psi(x,t)}{\partial t^i}\right| \le C, \forall (x,t) \in \overline{\mathscr{D}}_x \text{ and } 0 \le i \le 2.$$

Then the local error estimate in the temporal direction is given by

$$||e^{j+1}||_\infty \le C_1(\Delta t)^3. \tag{4.14}$$

Proof. The proof is similar to the proof of Lemma (2.6) of Chapter (2). □

Lemma 4.7. *(Global Error Estimate): Based on the assumption of Lemma (4.6) the global error estimate of the semi-discretization at j^{th} time level is given by*

$$||E^j||_\infty \leq C_2(\Delta t)^2. \tag{4.15}$$

Proof. The proof is similar to the proof of Lemma (2.7) of Chapter (2). □

4.4.2 Spatial Domain Discretization

Let the domain $[0,1]$ be divided into N equal mesh points of width h, giving the discretization of $\overline{\mathscr{D}}_x$ as:

$$\overline{\mathscr{D}}_x^N = \left\{x_0 = 0, x_i = ih, x_N = 1,\ i = 1,2,3,\dots N-1 \text{ and } h = \frac{1}{N}\right\}. \tag{4.16}$$

Non-Standard Finite Difference Scheme: To construct the exact finite difference approach, we considered the following constant coefficient homogeneous differential equations, corresponding to problem (4.4) with the discrete initial and boundary conditions as described in [66] and [**?**]:

$$\begin{cases} -C_\varepsilon\left[\frac{\psi_{i+1}^{j+1}-2\psi_i^{j+1}+\psi_{i-1}^{j+1}}{\eta_{i,j+1}^2}\right] + W_{1i}\psi_i^{j+1} = C_\varepsilon\left[\frac{\psi_{i+1}^{j}-2\psi_i^{j}+\psi_{i-1}^{j}}{\eta_{i,j}^2}\right] - W_{2i}\psi_i^j + f_i^{j+1} + f_i^j, \\ \begin{cases} \psi_0^{j+1} = \psi_N^{j+1} = 0, & j = 0,1,2,\dots,M-1, \\ \psi_i^0 = 0, & i = 0,1,2,\dots,N. \end{cases} \end{cases} \tag{4.17}$$

The denominator functions $\eta_{i,j+1}^2$ and $\eta_{i,j}^2$ to be determined from the following steps.
Consider the homogeneous part of (4.17) with constant coefficients, where the constant coefficients are the lower bounds of the coefficient functions as follows:

$$-C_\varepsilon\frac{d}{dx^2}\psi^{j+1} + \beta_3\psi^{j+1} = 0. \tag{4.18}$$

The corresponding characteristic equation is given by $-C_\varepsilon\theta^2 + \beta_2 = 0$. So, the two linearly independent solutions of (4.18) are given by

$$\exp(\theta_1 x) \text{ and } \exp(\theta_1 x),\ \theta_1, \theta_2 = \pm\sqrt{\frac{\beta_3}{C_\varepsilon}}. \tag{4.19}$$

Hence, $\psi_i^{j+1} = c_1\exp(\theta_1 x_i) + c_2\exp(\theta_2 x_i)$ is the general solution of (4.18). Now, by taking the successive points and applying the theory of difference equations as presented in [34] and [68], the following set of equations can be obtained:

$$\begin{vmatrix} \psi_{i-1}^{j+1} & \exp\left(\theta_1 x_{i-1}\right) & \exp\left(\theta_2 x_{i-1}\right) \\ \psi_{i}^{j+1} & \exp\left(\theta_1 x_{i}\right) & \exp\left(\theta_2 x_{i}\right) \\ \psi_{i+1}^{j+1} & \exp\left(\theta_1 x_{i+1}\right) & \exp\left(\theta_2 x_{i+1}\right) \end{vmatrix} = 0. \tag{4.20}$$

Rearranging (4.20), we get

$$\begin{vmatrix} \psi_{i-1}^{j+1} & \exp\left(\theta_1 (x_i - h)\right) & \exp\left(\theta_2 (x_i - h)\right) \\ \psi_{i}^{j+1} & \exp\left(\theta_1 x_{i}\right) & \exp\left(\theta_2 x_{i}\right) \\ \psi_{i+1}^{j+1} & \exp\left(\theta_1 (x_i + h)\right) & \exp\left(\theta_2 (x_i + h)\right) \end{vmatrix} = 0. \tag{4.21}$$

Factorizing the above equation gives

$$exp(\theta_1 x_i + \theta_2 x_i) \begin{vmatrix} \psi_{i-1}^{j+1} & \exp\left(-\theta_1 h)\right) & \exp\left(-\theta_2 h\right) \\ \psi_{i}^{j+1} & 1 & 1 \\ \psi_{i+1}^{j+1} & \exp\left(\theta_1 h\right) & \exp\left(\theta_2 h\right) \end{vmatrix} = 0. \tag{4.22}$$

Solving the determinant in (4.22) gives

$$\begin{aligned} & exp((\theta_1+\theta_2)x_i)[(exp(\theta_2 h) - exp(\theta_1 h))\psi_{i-1}^{j+1} \\ - \quad & (exp(\theta_2-\theta_1)h - exp(\theta_1-\theta_2)h)\psi_{i}^{j+1} \\ + \quad & (exp(-\theta_1 h) - exp(-\theta_2 h))\psi_{i+1}^{j+1}]. \end{aligned} \tag{4.23}$$

Replacing $\theta_1 = -\sqrt{\frac{\beta_3}{C_\varepsilon}}$ and $\theta_2 = \sqrt{\frac{\beta_3}{C_\varepsilon}}$ in (4.23) and simplifying the terms using the double angle formula for hyperbolic functions, we get the exact finite difference scheme for (4.23) as follows:

$$\psi_{i-1}^{j+1} - 2\cosh\left(\sqrt{\frac{\beta_3}{C_\varepsilon}}\right)\psi_{i}^{j+1} + \psi_{i+1}^{j+1} = 0. \tag{4.24}$$

After some rearrangements, we get

$$-C_\varepsilon \frac{\psi_{i-1}^{j+1} - 2\psi_{i}^{j+1} + \psi_{i+1}^{j+1}}{4\left(\frac{C_\varepsilon}{\beta_3}\right)\left(\sinh^2\left(\frac{1}{2}h\sqrt{\frac{\beta_3}{C_\varepsilon}}\right)\right)} + \beta_3\psi_{i+1}^{j+1} = 0. \tag{4.25}$$

for $i = 1, 2, \ldots, N-1$. As a result, the denominator function for the second order derivative approximation can be found as

$$\eta^2(C_\varepsilon, h) = 4\left(\frac{C_\varepsilon}{\beta_3}\right)\left(\sinh^2\left(\frac{1}{2}h\sqrt{\frac{\beta_3}{C_\varepsilon}}\right)\right). \tag{4.26}$$

For $i=1,2,3,\ldots,N-1,\ j=0,1,2,\ldots,M-1$, we defined the general variable coefficient form of the denominator function as follows:

$$\eta_{i,j+1}^2 = 4\left(\frac{C_\varepsilon}{W_1(x_i,t^{j+1})}\right)\left(\sinh^2\left(\frac{1}{2}h\sqrt{\frac{W_1(x_i,t^{j+1})}{C_\varepsilon}}\right)\right). \tag{4.27}$$

Similarly considering the homogeneous differential equation (4.3) of the j^{th} time level can be written as

$$C_\varepsilon \frac{d}{dx^2}\psi^j - \beta_4\psi^j = 0. \tag{4.28}$$

The linearly independent solutions of (4.28) is defined as $exp(\theta_1 x)$ and $exp(\theta_2 x)$, where $\theta_1,\theta_2 = \pm\sqrt{\frac{\beta_4}{C_\varepsilon}}$ and $W_2(x_i,t^j)\geq\beta_4>0$.
Following the same procedure, the j^{th} level denominator function can be obtained as follows:

$$\eta^2(C_\varepsilon,h) = 4\left(\frac{C_\varepsilon}{\beta_4}\right)\left(\sinh^2\left(\frac{1}{2}h\sqrt{\frac{\beta_4}{C_\varepsilon}}\right)\right). \tag{4.29}$$

Similarly we can define the general variable coefficient denominator function for the j^{th} time level as follows:

$$\eta_{i,j}^2 = 4\left(\frac{C_\varepsilon}{W_2(x_i,t^j)}\right)\left(\sinh^2\left(\frac{1}{2}h\sqrt{\frac{W_2(x_i,t^j)}{C_\varepsilon}}\right)\right). \tag{4.30}$$

Remark 4.1. As we have discussed in chapter (2) of remark (2.1), here we take the approximate value of the standard mesh length with the denominator function as follows:

$$h^2 \approx \eta_{i,j+1}^2 = h^2\alpha^4 + \frac{h^4\Phi^6}{12} + \frac{h^6\Phi^8}{180} + \cdots, \text{where } \Phi = \sqrt{\frac{W_1(x_i,t^{j+1})}{C_\varepsilon}}.$$

4.4.3 The Fully Discrete Problem:

In this section we combined the temporal and spatial semi-discretized results by substituting (4.27) and (4.29) into (4.11) as follows

$$\begin{aligned} -C_\varepsilon \frac{\left[\psi_{i+1}^{j+1} - 2\psi_i^{j+1} + \psi_{i-1}^{j+1}\right]}{\eta_{i,j+1}^2} + W_{1i}^{j+1}\psi_i^{j+1} &= C_\varepsilon \frac{\left[\psi_{i+1}^j - 2\psi_i^j + [\psi_{i-1}^j\right]}{\eta_{i,j}^2} \\ &- W_{2i}^j\psi_i^j + f_i^j + f^{j+1} \end{aligned} \tag{4.31}$$

Simplifying these equations we get, the tri-diagonal system of equations of the form:

$$\begin{cases} \mathscr{L}_{C_\varepsilon}^{N,M} := R_i^- \psi_{i-1}^{j+1} + R_i^c \psi_i^{j+1} + R_i^+ \psi_{i+1}^{j+1} = G_i^j, \\ \begin{cases} \psi_i^0 = \mathscr{S}_0^0(x_i), & i = 0,1,2,\ldots,N-1, \\ \psi_0^{j+1} = \mathscr{S}_l^{j+1}(0), & j = 0,1,2,\ldots,M-1, \\ \psi_N^{j+1} = \mathscr{S}_r^{j+1}(1), & j = 0,1,2,\ldots,M-1. \end{cases} \end{cases} \tag{4.32}$$

where the coefficients of the tri-diagonal system are to be determined for $i = 1,2,3,\ldots,N-1$, and $j = 0,1,2,\ldots,M-1$ using the subsequent equations

$$\begin{cases} R_i^- = \frac{-C_\varepsilon}{\eta_{i,j+1}^2}, \\ R_i^c = \left(\frac{2C_\varepsilon}{\eta_{i,j+1}^2} + \frac{2}{\Delta t} + A_i^{j+1} \right), \\ R_i^+ = \frac{-C_\varepsilon}{\eta_{i,j+1}^2}, \\ G_i^j = C_\varepsilon \frac{\left[\psi_{i+1}^j - 2\psi_i^j + [\psi_{i-1}^j\right]}{\eta_{i,j}^2} - C_i^j \psi_i^j + f_i^j + f^{j+1}. \end{cases} \tag{4.33}$$

Since the resulting tridiagonal system in (4.32) is a nonsingular M-matrix by theorem (2.1) of Chapter (2), we solve it using matrix inverse method.

Lemma 4.8. *(Discrete Maximum Principle): Let ϕ_i^{j+1} be any mesh function defined on $\overline{\mathscr{D}}_{xt}^{N.M}$ such that $\phi_0^{j+1} \geq 0$ and $\phi_N^{j+1} \geq 0$ as outlined in [64]. Then $\mathscr{L}_{C_\varepsilon}^{N,M} \phi_i^{j+1} \geq 0$, for $i = 1,2,3,...,N-1$ implies that $\phi_i^{j+1} \geq 0$, for $i = 0,1,2,...,N$.*

Proof. The proof is similar to the proof of Lemma (2.8) of Chapter (2). □

Lemma 4.9. *(Uniform Stability Estimate): Suppose that ϕ_i^{j+1} be any mesh function at $(j+1)^{th}$ level such that $\phi_0^{j+1} = 0 = \phi_N^{j+1}$ [34]. Then*

$$\left|\phi_i^{j+1}\right| \leq \frac{1}{\beta} \max_{1 \leq j \leq M-1} \left|\mathscr{L}_{C_\varepsilon}^{N,M} \phi_i^{j+1}\right|, \textit{for } 1 \leq i \leq N-1.$$

Proof. The proof is similar to the proof of Lemma (2.9) of Chapter (2). □

4.5 Uniform Convergence Analysis

Theorem 4.1. Let $\psi(x,t^{j+1})$ and ψ_i^{j+1} be the solutions of (4.11) and (4.31) respectively. Then we have

$$\max_{0 \leq i \leq N,\ 0 \leq j \leq M} \left|\psi_i^{j+1} - \psi(x,t^{j+1})\right| \leq Ch^2.$$

Proof. For the proof of this theorem, we let C_ε and η as perturbation parameter and denominator function respectively.

$$\begin{aligned}
\left|\mathscr{L}^{N,M}(\psi^{j+1}(x_i)-\psi_i^{j+1})\right| &= \left|-C_\varepsilon\frac{d^2\psi^{j+1}(x_i)}{dx^2}+C_\varepsilon\delta^2\psi_i^{j+1}\right|,\\
&= \left|-C_\varepsilon\frac{d^2\psi^{j+1}(x_i)}{dx^2}+\frac{C_\varepsilon}{\eta_i^2}\left(\psi_{i-1}^{j+1}-2\psi_i^{j+1}+\psi_{i+1}^{j+1}\right)\right|,\\
&\leq Ch^2.
\end{aligned}$$

The detailed proof can be found in Theorem (2.2) of Chapter (2). □

Theorem 4.2. For the analytic solution $\psi(x,t)$ of (4.4) and the fully discrete solution ψ_i^j of (4.31), the uniform error estimate can be defined as

$$\max_{0\leq i\leq N,\ 0\leq j\leq M}\left|\psi_i^{j+1}-\psi(x,t^{j+1})\right|\leq C\left(h^2+(\Delta t)^2\right).$$

Proof. Using the triangle inequality, we have the following facts

$$\begin{aligned}
\left|\psi(x,t^{j+1})-\psi_i^{j+1}\right| &= \left|\psi(x,t^{j+1})-\psi_i^{j+1}(x_i)+\psi_i^{j+1}(x_i)-\psi_i^{j+1}\right|,\\
&\leq \left|\psi(x,t^{j+1})-\psi_i^{j+1}(x_i)\right|+\left|\psi_i^{j+1}(x_i)-\psi_i^{j+1}\right|,\\
&= Ch^2+C(\Delta t)^2,\ \text{using Lemma (4.7) and Theorem (4.1)},\\
&= C(h^2+(\Delta t)^2).
\end{aligned}$$

Hence, the proof yields the required uniform error estimate. □

The preceding analysis shows that the proposed scheme attains second-order uniform convergence prior to extrapolation. To further enhance the accuracy and raise the order of convergence, the Richardson extrapolation technique is employed, as described below.

4.6 Richardson Extrapolation Technique

The Richardson extrapolation technique is used to accelerate the order of the method. Using theorem (4.2) at the j^{th} time level, we have

$$\left|\psi_i^j-\overline{\psi}_i^j\right|\leq C(h^2+(\Delta t)^2). \tag{4.34}$$

where ψ_i^j and $\overline{\psi}_i^j$ are numerical solutions on the mesh intervals $D^{N,M}$ and $D^{2N,2M}$ respectively so that that C is a parameter independent constant [69].
Moreover, since $\overline{\psi}_i^j$ is obtained by doubling the mesh $D^{N,M}$ then, the mesh sizes $h\neq 0$ and

$\Delta t \neq 0$ in (4.34) becomes

$$\psi_i^j(x_i,t^j) - \overline{\psi}_i^j(x_i,t^j) \leq C(h^2 + (\Delta t)^2) + R^{N,M},\ (x_i,t^j) \in D^{N,M}. \tag{4.35}$$

Again using the mesh sizes $h/2,\ \Delta t/2 \neq 0$ (4.35) becomes

$$\psi_i^j(x_i,t^j) - \overline{\psi}_i^j(x_i,t^j) \leq C\left(\frac{h^2}{4} + \frac{(\Delta t)^2}{4}\right) + R^{2N,2M},\ (x_i,t^j) \in D^{2N,2M}. \tag{4.36}$$

where the remainders $R^{N,M}$ and $R^{2N,2M}$ are $O(h^4 + (\Delta t)^4)$. Taking the difference of (4.36) and (4.35) we get the subsequent general extrapolation formula.

$$\left(\psi_i^j\right)^{ext} = \frac{4\overline{\psi}_i^j - \psi_i^j}{3}. \tag{4.37}$$

where $\left(\psi_i^j\right)^{ext}$ is the numerical solution obtained from the Richardson extrapolation technique with truncated error of the form

$$\left|\psi_i^j - (\psi_i^j)^{ext}\right| \leq C(h^4 + (\Delta t)^4). \tag{4.38}$$

From these discussions, we generalized the following Theorem for the general purpose of the Richardson extrapolation technique.

Theorem 4.3. Let $(\psi_i^j)^{ext}$ be the numerical solution of (4.31) obtained after the application of Richardson extrapolation technique and ψ_i^j be the numerical solution of the problem in (4.4). Then, the maximum absolute error encountered is defined by

$$\left|\psi_i^j - (\psi_i^j)^{ext}\right| \leq C(h^4 + (\Delta t)^4).$$

From the overall constructions and discussions, we concluded that using Richardson extrapolation technique accelerates the proposed method to fourth order uniformly convergent scheme in both spacial and temporal directions.

4.7 Numerical Results and Discussions

The performance of the proposed scheme is examined using two model problems, with $\varepsilon-$uniform maximum absolute errors and convergence rates computed to evaluate its numerical behavior, as discussed in Chapter 2.

Example 4.1. Consider the singularly perturbed parabolic reaction diffusion problem subject to the initial-boundary conditions as presented in [37, 81, 82] .

$$\begin{cases} \psi_t - \varepsilon\psi_{xx} + \frac{1+x^2}{2}\psi + \psi(x,t-\delta) = t^3, & \forall(x,t) \in (0,1)\times(0,2], \\ \psi(x,t) = 0, & \forall(x,t) \in [0,1]\times[-\delta,0], \\ \psi(0,t) = 0, \psi(1,t) = 0, & \forall t \in (0,2]. \end{cases}$$

Example 4.2. Consider the unsteady 1D singularly perturbed parabolic reaction-diffusion problem subject to the initial-boundary conditions of the form outlined in [37].

$$\begin{cases} \psi_t - \varepsilon\psi_{xx} + (1.1+x^2)\psi + \psi(x,t-\delta) = t^3, & \forall(x,t) \in (0,1)\times(0,2], \\ \psi(x,t) = 0, & \forall(x,t) \in [0,1]\times[-\delta,0], \\ \psi(0,t) = 0, \psi(1,t) = 0, & \forall t \in (0,2]. \end{cases}$$

Since the analytical solutions are unknown, we apply the doubling mesh technique to find the maximum absolute errors and the corresponding order of convergences as follows:

Before Extrapolation: Let $\psi^{N,M}(x_i,t^j)$ and $\psi^{2N,2M}(x_i,t^j)$ be the numerical solutions with mesh lengths $(h,k\neq 0)$ and $(h/2,\Delta t/2\neq 0)$ respectively, then

- The maximum absolute error is given by

$$E_\varepsilon^{N,M} = \max_{0\leq i,j\leq N,M} \left|\psi^{N,M}(x_i,t^j) - \psi^{2N,2M}(x_{2i},t_{2j})\right|. \tag{4.39}$$

- The $\varepsilon-$ uniform maximum absolute error is given by

$$E^{N,M} = \max_{\varepsilon} E_\varepsilon^{N,M}. \tag{4.40}$$

- Corresponding ε-uniform order of convergence is $R^{N,M} = log_2\left(\frac{E^{N,M}}{E^{2N,2M}}\right)$.

After Extrapolation: Similarly, let $\psi^{2N,2M}(x_i,t^j)$ and $(\psi_i^j)^{ext}$ be the numerical solutions with mesh lengths $(h/2,\Delta t/2\neq 0)$ and $(h/4,\Delta t/4\neq 0)$ respectively, then

- The maximum absolute error is given by

$$E_{\varepsilon,ext}^{N,M} = \max_{0\le i,m\le N,M} \left|\psi^{2N,2M}(x_{2i},t_{2j}) - (\psi_i^j)^{ext}(x_i,t^j)\right|. \tag{4.41}$$

- The $\varepsilon-$ uniform maximum absolute error is given by

$$E_{ext}^{N,M} = \max_{\varepsilon} E_{\varepsilon,ext}^{N,M}. \tag{4.42}$$

- Corresponding *ext*-uniform order of convergence is $R_{ext}^{N,M} = log_2\left(\frac{E_{ext}^{N,M}}{E_{ext}^{2N,2M}}\right)$.

Table 4.1: $E^{N,M}$ and $R^{N,M}$for Example (4.1) before and after extrapolations

$\delta = 0.5*\varepsilon$ $\varepsilon \downarrow$	$N = 64$ $M = 20$	$N = 128$ $M = 40$	$N = 256$ $M = 80$	$N = 512$ $M = 160$
Before extrapolation				
2^{-20}	$1.3350e-03$	$3.3370e-04$	$8.3421e-05$	$2.0851e-05$
2^{-22}	$1.3350e-03$	$3.3370e-04$	$8.3423e-05$	$2.0840e-05$
2^{-24}	$1.3350e-03$	$3.3370e-04$	$8.3423e-05$	$2.0840e-05$
2^{-26}	$1.3350e-03$	$3.3370e-04$	$8.3423e-05$	$2.0840e-05$
2^{-28}	$1.3350e-03$	$3.3370e-04$	$8.3423e-05$	$2.0840e-05$
2^{-30}	$1.3350e-03$	$3.3370e-04$	$8.3423e-05$	$2.0840e-05$
2^{-32}	$1.3350e-03$	$3.3370e-04$	$8.3423e-05$	$2.0840e-05$
2^{-34}	$1.3350e-03$	$3.3370e-04$	$8.3423e-05$	$2.0840e-05$
2^{-36}	$1.3350e-03$	$3.3370e-04$	$8.3423e-05$	$2.0840e-05$
2^{-38}	$1.3350e-03$	$3.3370e-04$	$8.3423e-05$	$2.0840e-05$
2^{-40}	$1.3350e-03$	$3.3370e-04$	$8.3423e-05$	$2.0840e-05$
$E^{N,M}$	$1.3350e-03$	$3.3370e-04$	$8.3423e-05$	$2.0851e-05$
$R^{N,M}$	2.0002	2.0001	2.003	—
Results in [37]				
$E^{N,M}$	$4.8841e-02$	$2.6058e-02$	$1.3450e-02$	$6.9381e-03$
$R^{N,M}$	0.9064	0.9541	0.9550	—
Results in [82]				
$E_{\varepsilon}^{N,M}$	$1.7554e-001$	$2.6693e-001$	$3.1039e-001$	$3.5689e-01$
$R_{\varepsilon}^{N,M}$	-0.6047	-0.2176	-0.2014	—

Table 4.2: $E^{N,M}$ and $R^{N,M}$ for Example (4.2) before and after extrapolations

$\delta = 0.5 * \varepsilon$ $\varepsilon \downarrow$	$N = 32$ $M = 4$	$N = 64$ $M = 8$	$N = 128$ $M = 16$	$N = 256$ $M = 32$
Before Extrapolation				
10^{-7}	$3.3031e-03$	$8.2478e-04$	$2.0610e-04$	$5.1519e-05$
10^{-8}	$3.3031e-03$	$8.2478e-04$	$2.0610e-04$	$5.1519e-05$
10^{-9}	$3.3031e-03$	$8.2478e-04$	$2.0610e-04$	$5.1519e-05$
10^{-10}	$3.3031e-03$	$8.2478e-04$	$2.0610e-04$	$5.1519e-05$
10^{-12}	$3.3031e-03$	$8.2478e-04$	$2.0610e-04$	$5.1519e-05$
10^{-14}	$3.3031e-03$	$8.2478e-04$	$2.0610e-04$	$5.1519e-05$
10^{-16}	$3.3031e-03$	$8.2478e-04$	$2.0610e-04$	$5.1519e-05$
10^{-17}	$3.3031e-03$	$8.2478e-04$	$2.0610e-04$	$5.1519e-05$
10^{-18}	$3.3031e-03$	$8.2478e-04$	$2.0610e-04$	$5.1519e-05$
10^{-19}	$3.3031e-03$	$8.2478e-04$	$2.0610e-04$	$5.1519e-05$
10^{-20}	$3.3031e-03$	$8.2478e-04$	$2.0610e-04$	$5.1519e-05$
$E^{N,M}$	$3.3031e-03$	$8.2478e-04$	$2.0610e-04$	$5.1519e-05$
$R^{N,M}$	2.0026	2.0007	2.0002	—
Results in [37]				
$E^{N,M}$	6.7384e − 02	3.9822e − 02	2.1533e − 03	1.1184e − 03
$R^{N,M}$	0.7588	0.8870	0.9452	—
After Extrapolation				
10^{-7}	$6.9996e-06$	$4.0617e-07$	$2.5096e-08$	$1.5581e-09$
10^{-8}	$6.8718e-06$	$4.0581e-07$	$2.5096e-08$	$1.5581e-09$
10^{-9}	$6.8718e-06$	$4.0581e-07$	$2.5096e-08$	$1.5581e-09$
10^{-10}	$6.8718e-06$	$4.0581e-07$	$2.5096e-08$	$1.5581e-09$
10^{-12}	$6.8718e-06$	$4.0581e-07$	$2.5096e-08$	$1.5581e-09$
10^{-14}	$6.8718e-06$	$4.0581e-07$	$2.5096e-08$	$1.5581e-09$
10^{-16}	$6.8718e-06$	$4.0581e-07$	$2.5096e-08$	$1.5581e-09$
10^{-17}	$6.8718e-06$	$4.0581e-07$	$2.5096e-08$	$1.5581e-09$
10^{-18}	$6.8718e-06$	$4.0581e-07$	$2.5096e-08$	$1.5581e-09$
10^{-19}	$6.8718e-06$	$4.0581e-07$	$2.5096e-08$	$1.5581e-09$
10^{-20}	$6.8718e-06$	$4.0581e-07$	$2.5096e-08$	$1.5581e-09$
$E_{ext}^{N,M}$	$6.9996e-06$	$4.0617e-07$	$2.5096e-08$	$1.5581e-09$
$R_{ext}^{N,M}$	4.1052	4.0006	4.0096	—
Results in [37]				
$E_{ext}^{N,M}$	3.5282e − 03	9.1961e − 04	3.3499e − 04	5.9612e − 05
$R_{ext}^{N,M}$	1.9398	1.9684	1.9789	—

Table 4.3: $E^{N,M}$ and $R^{N,M}$for Example (4.2) for fixed ε, different values of δ

$\varepsilon = 0.1$				
$\delta = \beta * \varepsilon \downarrow$ N,M $\rightarrow$	$N = 32$ $M = 4$	$N = 64$ $M = 8$	$N = 128$ $M = 16$	$N = 256$ $M = 32$
Before extrapolation				
0.0500	$2.0604e-02$	$5.1506e-03$	$1.3074e-03$	$3.3796e-04$
	2.0001	1.9781	1.9517	
0.0250	$2.1044e-02$	$5.2591e-03$	$1.3342e-03$	$3.4461e-04$
	2.0005	1.9788	1.9530	
0.0125	$2.1259e-02$	$5.3122e-03$	$1.3474e-03$	$3.4786e-04$
	2.0007	1.9791	1.9536	
0.0100	$2.1454e-02$	$5.3605e-03$	$1.3594e-03$	$3.5082e-04$
	2.0008	1.9794	1.9542	
$E^{N,M}$	$2.1454e-02$	$5.3605e-03$	$1.3594e-03$	$3.5082e-04$
$R^{N,M}$	2.0008	1.9794	1.9542	—
$\varepsilon = 0.01$				
$\delta = \beta * \varepsilon \downarrow$ N,M $\rightarrow$	$N = 32$ $M = 4$	$N = 64$ $M = 8$	$N = 128$ $M = 16$	$N = 256$ $M = 32$
Before extrapolation				
0.00500	$4.7190e-02$	$1.1776e-02$	$2.9553e-03$	$7.4724e-04$
	2.0026	1.9945	1.9837	
0.00250	$4.7221e-02$	$1.1784e-02$	$2.9573e-03$	$7.4771e-04$
	2.0026	1.9945	1.9837	
0.00125	$4.7236e-02$	$1.1788e-02$	$2.9582e-03$	$7.4794e-04$
	2.0025	1.9945	1.9837	
0.00100	$4.7239e-02$	$1.1789e-02$	$2.9584e-03$	$7.4798e-04$
	2.0025	1.9945	1.9838	
$E^{N,M}$	$4.7239e-02$	$1.1789e-02$	$2.9584e-03$	$7.4798e-04$
$R^{N,M}$	1.9945	2.0025	1.9838	—

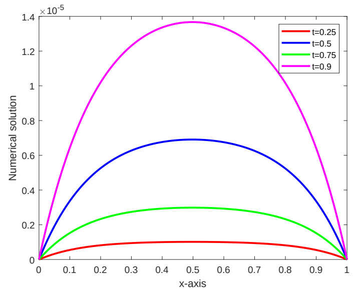

(a) $\varepsilon = 10^{-0}$

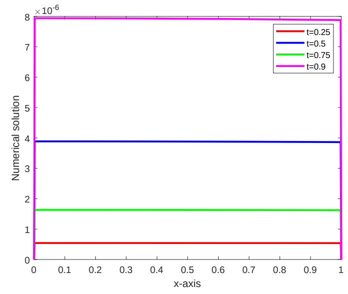

(b) $\varepsilon = 10^{-22}$

Figure 4.1: 2D solution graph for Example (4.1) with values $N = 256, M = 32$.

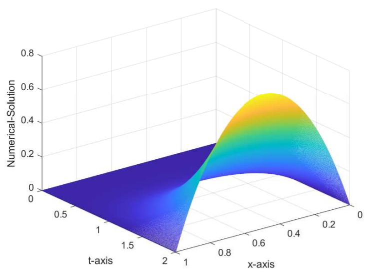

(a) $\varepsilon = 10^{-0}$

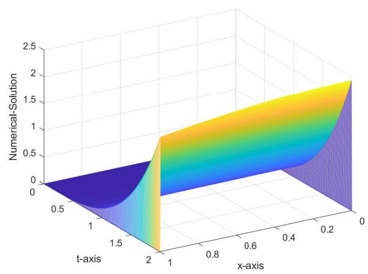

(b) $\varepsilon = 10^{-22}$

Figure 4.2: 3D solution graph for Example (4.1) with values $N = 256, M = 32$.

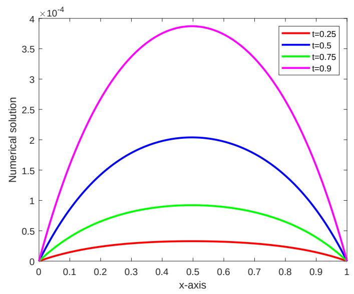

(a) $\varepsilon = 10^{-0}$

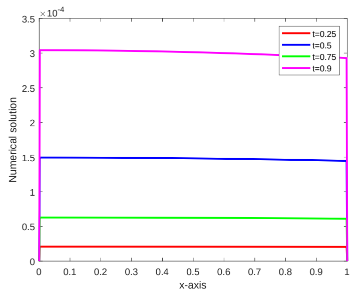

(b) $\varepsilon = 10^{-18}$

Figure 4.3: 2D solution graph for Example (4.2) with values $N = 64, M = 8$.

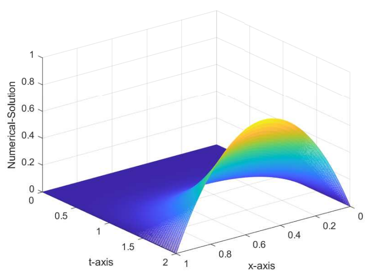

(a) $\varepsilon = 10^{-0}$

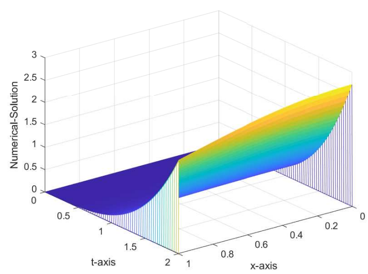

(b) $\varepsilon = 10^{-18}$

Figure 4.4: 3D solution graph for Example (4.2) with values $N = 64, M = 8$.

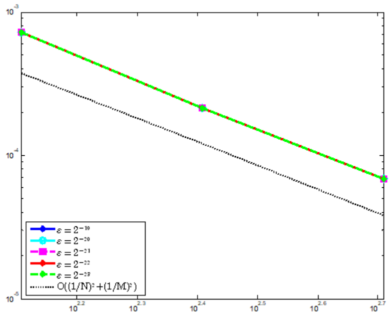

(a) Example (4.1)

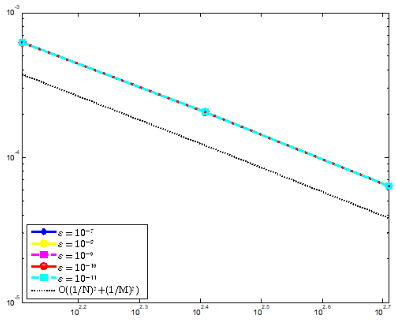

(b) Example (4.2)

Figure 4.5: Log log plots for different with values meshes $N = 64, 128, 256$ and $M = 8, 16, 32$.

To validate the effectiveness and applicability of our proposed method, we consider three model problems. We present the maximum absolute errors and the corresponding orders of convergence for Examples (4.1) and (4.2) in Tables (4.1), (4.2), and (4.3). For a fixed perturbation parameter ε, we observe that the maximum absolute errors decrease as the mesh parameters N and M increase along a row. Conversely, for fixed mesh sizes N and M, the errors remain nearly uniform across columns as ε decreases, indicating parameter-uniform behavior.

These results confirm that our scheme is uniformly convergent with fourth-order accuracy after Richardson extrapolation. Furthermore, the 2D and 3D plots in Example (4.1) (Figure (4.1)) and Example (4.2) (Figure (4.2)) clearly show that decreasing ε leads to the formation of twin boundary layers near $x = 0$ and $x = 1$, consistent with the analytical results. The log-log plots in Figure (4.5) further demonstrate the parameter-uniform convergence of the proposed scheme.

In Table (4.3), we also analyze the effect of the delay term δ. For fixed step sizes h and Δt, we observe that the maximum absolute error increases as δ decreases for $\varepsilon = 0.1$ and $\varepsilon = 0.01$. In contrast, for a fixed δ, the error decreases as the mesh is refined. This shows that smaller delay values can increase the error, suggesting that the method performs better when δ is chosen closer to ε but distinct from it. Finally, comparisons in Tables (4.1) and (4.2), based on both accuracy and order of convergence, demonstrate that our method outperforms the existing methods in [37] and [82].

4.8 Conclusion

This chapter develops a higher-order fitted numerical method for singularly perturbed parabolic reaction–diffusion problems with a small time lag. The scheme combines Crank–Nicolson time discretization with a nonstandard finite difference spatial approximation. Theoretical and numerical results confirm parameter-uniform convergence with fourth-order accuracy via Richardson extrapolation, while computational experiments demonstrate its efficiency and improved performance over existing methods.

Chapter 5

An Exponentially Fitted Upwind Scheme for Singularly Perturbed Parabolic Convection–Diffusion Problems with Mixed Shift Parameters in the Reaction Term

This chapter presents a fitted numerical method for singularly perturbed differential equations with mixed shift parameters. The presence of a small perturbation parameter $\varepsilon\,(0 < \varepsilon \ll 1)$ multiplying the highest-order derivative leads to the formation of a right boundary layer, causing classical numerical schemes on uniform meshes to lose accuracy. To address this difficulty, Taylor series expansions are employed to approximate the positive and negative shift terms, thereby transforming the original problem into an asymptotically equivalent form without shift parameters. A Crank–Nicolson scheme is applied for temporal discretization, while an exponentially fitted finite difference scheme is employed in space. The proposed method achieves uniform convergence and second-order accuracy in both time and space. Numerical experiments on three test problems validate the theoretical results and demonstrate the efficiency and superiority of the approach over existing methods.

5.1 Introduction

SPPDDEs are a class of differential equations that involve delayed or advanced arguments of the unknown function, where the highest-order derivative is multiplied by a small parameter ε, $(0 < \varepsilon \ll 1)$, leading to multi-scale behavior. Such types equations frequently arise in a variety of mathematical models, including physiological kinetics [102], evolutionary biology [90], neuronal variability [105]. Particularly, spatial delay differential equations form a subclass of SPPDDEs that incorporate at least one retarded and /or advanced argument in the spatial variable. These types of equations are employed to model a wide range of real-world phenomena, including physiological processes [70], population dynamics [71], disease spread [72], polymer diffusion [73], epidemiology [74], and liquid helium hydrodynamics [75].

The small parameter ε in the proposed problem induces right boundary layer near $x = 1$, where classical methods on uniform meshes produce oscillatory or inaccurate solutions. Extremely fine meshes may reduce errors but increase computational cost [78], highlighting the need for, fitted numerical methods [63]. To address this, various parameter-independent schemes, including fitted operator methods, fitted meshes, and domain decomposition techniques, have been developed [79, 80, 46, 63, 88]. Numerous studies have developed and analyzed parameter-uniformly convergent numerical methods for parabolic singularly perturbed differential-difference equations with small or large delays in time [40, 43, 44, 49], as well as for convection-diffusion problems with small or large spatial shifts.

In contrast, fewer studies have addressed singularly perturbed parabolic convection–diffusion equations with small or large spatial shifts. Parameter-uniformly convergent schemes have been proposed by a limited number of researchers. For example,For singularly perturbed problems, the authors in [92] employed implicit Euler and midpoint upwind schemes, and established uniform convergence of the method. A combination of the implicit Euler scheme and B-spline collocation has been developed [48]. A higher-order numerical scheme has been developed using the implicit Euler method in time and hybrid finite difference discretization on Shishkin meshes in space [50]. Furthermore, for time-dependent convection–diffusion problems with general shifts, a series of parameter-uniformly convergent numerical methods have been developed and analyzed [93, 53, 49].

Existing numerical methods for singularly perturbed problems often have limited accuracy and order of convergences. To address this, we developed a fitted numerical scheme for SPPDDEs with mixed spatial shifts, combining the Crank-Nicolson method in time with an exponentially fitted finite difference approach in space on uniform meshes.

5.2 Problem formulation

Consider a class of singularly perturbed parabolic differential–difference equations with small shift parameters, as given in the governing problem (1.13), subject to the following initial and boundary conditions [58]:

$$\begin{cases} \psi_t(x,t) + \mathscr{L}_\varepsilon \psi(x,t) = f(x,t) & \forall (x,t) \in \mathscr{D}_{xt} = \mathscr{D}_x \times \mathscr{D}_t = (0,1) \times (0,T], T > 0, \\ \psi(x,t) = \mathscr{S}_0(x,t) & \forall (x,t) \in \mu_0 = \{(x,t) : 0 \le x \le 1,\ \ 0 < t \le T\}, \\ \psi(x,t) = \mathscr{S}_l(x,t) & \forall (x,t) \in \mu_l = \{(x,t) : -\delta \le x \le 0,\ \ 0 < t \le T\}, \\ \psi(x,t) = \mathscr{S}_r(x,t) & \forall (x,t) \in \mu_r = \{(x,t) : 1 \le x \le 1+\mu,\ \ 0 < t \le T\}. \end{cases} \tag{5.1}$$

where
$\mathscr{L}_\varepsilon \psi := -\varepsilon \psi_{xx}(x,t) + a(x,t)\psi_x(x,t) + b(x,t)\psi(x-\delta,t) + c(x,t)\psi(x,t) + d(x,t)\psi(x+\eta,t)$ is the differential operator, ε is the perturbation parameter ($0 < \varepsilon \ll 1$), δ and η are small shift parameters with the property $\delta, \eta < \varepsilon$, respectively. We assumed that the data $a(x,t), b(x,t), c(x,t), d(x,t)$ and $f(x,t)$ on $\overline{\mathscr{D}}_{xt}$ are assumed to be sufficiently smooth, bounded, and independent of the perturbation parameter ε. Furthermore, the coefficients of the reaction term $c(x,t)$, the delay term $b(x,t)$ and the advance term $d(x,t)$ are assumed to satisfy the lower bound:

$$b(x,t) + c(x,t) + d(x,t) \ge \omega > 0 \quad \forall (x,t) \in \overline{\mathscr{D}}_{xt}. \tag{5.2}$$

This condition ensures the well-posedness and stability of problem (2.1) by enforcing a positive combined reaction-shift effect, thereby preventing unbounded growth, ensuring uniqueness, and enabling the derivation of a priori bounds [119]. In addition, when the value of the perturbation parameter ε approaching zero, the solution of the proposed problem exhibits left or right boundary layer in the neighbourhood of μ_l or μ_r depending on the sign $a(x) < 0$ or (> 0). But due to its physical consistency with natural flow behavior and its numerical advantages, such as stability and compatibility, the right boundary layer configuration is adopted in the proposed problem.
As presented in [92] for small shift parameters $\delta, \eta < \varepsilon$, we employ the Taylor series expansion to approximate the shift terms as follows:

$$\begin{cases} \psi(x-\delta,t) = \psi - \delta \psi_x + \frac{\delta^2}{2}\psi_{xx} + O(\delta^3), \\ \psi(x+\eta,t) = \psi + \eta \psi_x + \frac{\eta^2}{2}\psi_{xx} + O(\eta^3). \end{cases} \tag{5.3}$$

Substituting (5.3) in to (5.1), we obtained the following generalized parabolic-type singularly perturbed initial boundary value problem

$$\begin{cases} \psi_t(x,t) + \mathscr{L}_{C_\varepsilon} \psi(x,t) = f(x,t) & \forall (x,t) \in \mathscr{D}_{xt}, \\ \psi(x,t) = \mathscr{S}_0(x) & \forall (x,t) \in \mu_0 = \left\{(x,t) : x \in \overline{\mathscr{D}}_x,\ \ t = 0\right\}, \\ \psi(x,t) = \mathscr{S}_l(0,t) & \forall (x,t) \in \mu_l = \left\{(x,t) : x = 0,\ \ t \in \overline{\mathscr{D}}_t \le T\right\}, \\ \psi(x,t) = \mathscr{S}_r(1,t) & \forall (x,t) \in \mu_r = \left\{(x,t) : x = 1,\ \ t \in \overline{\mathscr{D}}_t \le T\right\}. \end{cases} \tag{5.4}$$

where
$\mathscr{L}_{C_\varepsilon}\psi := -C_\varepsilon\psi_{xx} + p(x,t)\psi_x + q(x,t)\psi, C_\varepsilon = \varepsilon - \beta_1\frac{\delta^2}{2} - \beta_2\frac{\eta^2}{2}$, $b(x,t) \geq \beta_1 > 0, d(x,t) \geq \beta_2 > 0$ with $0 < C_\varepsilon \ll 1$, $p(x,t) = a(x) - \delta b(x,t) + \eta d(x,t)$, and $q(x,t) = b(x,t) + c(x,t) + d(x,t)$. To control blow ups in the convection and reaction terms, we assumed that the coefficient functions $p(x,t)$ and $q(x,t)$ are sufficiently smooth, bounded and satisfy

$$p(x,t) \geq p^* > 0, \quad q(x,t) \geq q^* > 0, \quad (x,t) \in \overline{\mathscr{D}}_x. \tag{5.5}$$

5.3 Properties of the Analytic Solution

The existence of a unique solution of (5.4) can be established with the assumption that the data are Hölder continuous and satisfy compatibility conditions at the corner points as outlined in [32]. The required compatibility conditions are

$$\mathscr{S}_0(0,0) = \mathscr{S}_l(0) \quad \mathscr{S}_0(1,0) = \mathscr{S}_r(0). \tag{5.6}$$

and

$$\begin{cases} \frac{d\mathscr{S}_l(0)}{dt} - C_\varepsilon\frac{d^2\mathscr{S}_0(0,0)}{dx^2} + p(0,0)\frac{d\mathscr{S}_0(0,0)}{dx} + q(0,0)\mathscr{S}_0(0) = f(0,0), \\ \\ \frac{d\mathscr{S}_r(0)}{dt} - C_\varepsilon\frac{d^2\mathscr{S}_0(1,0)}{dx^2} + p(1,0)\frac{d\mathscr{S}_0(1,0)}{dx} + q(1,0)\mathscr{S}_0(1,0) = f(1,0). \end{cases} \tag{5.7}$$

These conditions ensure that the problem in (5.4) has unique solution $\psi(x,t)$ which exhibits a right boundary layer of width $O(C_\varepsilon)$ at x = 1 as presented in [94].

Now on omitting the boundary conditions at $x = 1$ and setting $\varepsilon = 0$ gives the reduced form of problem (5.4).

$$\begin{cases} \psi_t^0 + p(x)\psi_x^0 + q(x)\psi^0 = f(x,t), & \forall (x,t) \in \mathscr{D}_{xt}, \\ \psi^0(x,0) = \mathscr{S}_0(x), & \forall x \in \overline{\mathscr{D}}_x, \\ \psi^0(0,t) = 0, & \forall \in \overline{\mathscr{D}}_t. \end{cases} \tag{5.8}$$

This is a first order hyperbolic equation with initial data specified along two sides the initial points $t = 0$ and $x = 0$ of the domain $\overline{\mathscr{D}}_{xt}$ for small values of C_ε the solution $\psi(x,t)$ of (5.4) will be very close to $\psi_0(x,t)$. In order to obtain error bounds on the solution of the difference scheme it is assumed that the solution of the reduced problem (5.8) is sufficiently smooth.
For next uses, we denote the differential operator $\mathscr{L}$ as follows

$$\mathscr{L}_{C_\varepsilon}\psi(x,t) := \psi_t(x,t) - C_\varepsilon\psi_{xx}(x,t) + p(x,t)\psi_x(x,t) + q(x,t)\psi(x,t). \tag{5.9}$$

Lemma 5.1. *(Continuous Maximum Principle):Assume that $\psi(x,t)$ is any sufficiently smooth function satisfying $\psi(x,t) \geq 0, \forall (x,t) \in \partial \mathscr{D}_{xt}$ and $\mathscr{L}_{C_\varepsilon}\psi(x,t) \geq 0, \forall (x,t) \in \mathscr{D}_{xt}$ then, $\psi(x,t) \geq 0, \forall (x,t) \in \overline{\mathscr{D}}_{xt}$, where the differential operator is defined in (5.9).*

Proof. Suppose that $(x^*,t^*) \in \mathscr{D}_{xt}$ such that $\psi(x^*,t^*) = min_{(x,t)\in\overline{\mathscr{D}}_{xt}} \psi(x,t) < 0$. From this condition and elementary concepts of calculus gives $\psi_t(x^*,t^*) = 0, \;\; \psi_x(x^*,t^*) = 0$ and $\psi_{xx}(x^*,t^*) \geq 0$. Using these conditions, we defined the differential operator as follows

$$\begin{aligned}
\mathscr{L}_{C_\varepsilon}\psi(x^*,t^*) &= \psi_t(x^*,t^*) - C_\varepsilon \psi_{xx}(x^*,t^*) + p(x^*,t^*)\psi_x(x^*,t^*) + q(x^*,t^*)\psi(x^*,t^*), \\
&= -C_\varepsilon \psi_{xx}(x^*,t^*) + q(x^*,t^*)\psi(x^*,t^*), \\
&\leq 0 \quad , \; since, \psi_{xx} \geq 0, and \;\; \psi < 0 \text{ and } q > 0 \; at \; (x^*,t^*).
\end{aligned}$$

The result $\mathscr{L}_{C_\varepsilon}\psi(x^*,t^*) \leq 0$ contradicts to the assumption $\mathscr{L}_{C_\varepsilon}\psi(x,t) \geq 0$.
Therefore, it can be concluded that the minimum of $\psi(x,t)$ is non-negative. □

Lemma 5.2. *(Stability Estimate): If $\psi(x,t) \in C^{2,1}(\overline{\mathscr{D}}_{xt})$ be the solution of the continuous problem (5.4) ,then it satisfies the bound*

$$|\psi(x,t)| \leq \frac{1}{p^*}||f|| + max\{|\mathscr{S}_0(x)|, |\mathscr{S}_l(t)|, |\mathscr{S}_r(t)|\}.$$

Proof. To prove this Lemma, we defined two barrier functions $\Omega^{\pm}$ as follows

$$\Omega^{\pm}(x,t) = \frac{1}{p^*}||f|| + max\{|\mathscr{S}_0(x)|, |\mathscr{S}_l(t)|, |\mathscr{S}_r(t)|\} \pm \psi(x,t).$$

When $t = 0$, we have

$$\begin{aligned}
\Omega^{\pm}(x,0) &= \frac{1}{p^*}||f|| + max\{|\mathscr{S}_0(x)|, |\mathscr{S}_l(0)|, |\mathscr{S}_r(0)|\} \pm \psi(x,0), \\
&= \frac{1}{p^*}||f|| + max\{|\mathscr{S}_0(x)|, |\mathscr{S}_l(0)|, |\mathscr{S}_r(0)|\} \pm \mathscr{S}_0(x) \geq 0.
\end{aligned}$$

When $x = 0$, we have

$$\begin{aligned}
\Omega^{\pm}(0,t) &= \frac{1}{p^*}||f|| + max\{|\mathscr{S}_0(0)|, |\mathscr{S}_l(t)|, |\mathscr{S}_r(t)|\} \pm \psi(0,t), \\
&= \frac{1}{p^*}||f|| + max\{|\mathscr{S}_0(0)|, |\mathscr{S}_l(t)|, |\mathscr{S}_r(t)|\} \pm \mathscr{S}_l(t) \geq 0.
\end{aligned}$$

When $x = 1$, we have

$$\begin{aligned}
\Omega^{\pm}(1,t) &= \frac{1}{p^*}||f|| + max\{|\mathscr{S}_0(1)|, |\mathscr{S}_l(t)|, |\mathscr{S}_r(t)|\} \pm \psi(1,t), \\
&= \frac{1}{p^*}||f|| + max\{|\mathscr{S}_0(0)|, |\mathscr{S}_l(t)|, |\mathscr{S}_r(t)|\} \pm S_r(t) \geq 0.
\end{aligned}$$

Having all these on the domain $\mathscr{D}_{xt}$, we have

$$\begin{aligned}
\mathscr{L}_{C_\varepsilon}\Omega^{\pm}(x,t) &= \frac{\partial\Omega^{\pm}(x,t)}{\partial t} - C_\varepsilon\frac{\partial^2\Omega^{\pm}(x,t)}{\partial x^2} + p(x)\frac{\partial\Omega^{\pm}(x,t)}{\partial x} + q(x)\Omega^{\pm}(x,t),\\
&= q(x)\frac{1}{p^*}||f|| + q(x)\times max\{|\mathscr{S}_0(x)|,|\mathscr{S}_l(t)|,|\mathscr{S}_r(t)|\}\\
&+ \frac{1}{p^*}||f|| + \pm\mathscr{L}_{C_\varepsilon}\psi(x,t),\\
&= q(x)\times max\{|S_0(x)|,|S_l(t)|,|S_r(t)|\}\frac{1}{p^*}||f|| \pm f(x,t),\\
&\geq 0 \quad .
\end{aligned}$$

Using Lemma (5.1), it follows that $\Omega^{\pm}(x,t)\geq 0,\ \forall(x,t)\in\overline{\mathscr{D}}_{xt}$ which implies the required bounds. □

Lemma 5.3. *The bounds for the derivative of the solution $\psi(x,t)$ of the problem (5.4) are given by*

$$\left|\frac{\partial^{i+j}\psi(x,t)}{\partial x^i\partial t^j}\right| \leq C\left(1+{C_\varepsilon}^{-i}exp\left(\frac{p^*(1-x)}{C_\varepsilon}\right)\right) \tag{5.10}$$

where $0\leq j\leq 2$ and $0\leq i+2j\leq 4$.

The proof of this Lemma is similar to the proof of Lemma (2.3) of Chapter (2).

5.4 Formulation of Numerical Schemes

The main concern of this section is to discretize the proposed problem (5.4) in both the temporal and spatial directions. For simplicity, we first apply discretization in the temporal direction, followed by the spatial direction, using uniform meshes as outlined below:

5.4.1 Temporal Semi-discretization:

Divide the time domain $[0,T]$ in to M equal number of mesh intervals with step length Δt, we get

$$\overline{\mathscr{D}}_t^M = \left\{t_j : t^j = j\Delta t, j = 0,1,2,3,\ldots M \text{ and } \Delta t = \frac{T}{M}\right\}. \tag{5.11}$$

Following the procedures in [100], the temporal semi-discretization of problem (5.4) is done by means of the Crank-Nicolson method as follows:

$$\begin{cases} \frac{\psi^{j+1}-\psi^{j}}{\Delta t} - \frac{C_\varepsilon}{2}\left(\psi_{xx}^{j+1}+\psi_{xx}^{j}\right) + \frac{p(x)}{2}\left(\psi_{x}^{j+1}+\psi_{x}^{j}\right) + \frac{q(x)}{2}\left(\psi^{j+1}+\psi^{j}\right) \\ \qquad\qquad\qquad\qquad = \frac{1}{2}\left(f^{j+1}+f^{j}\right), \\ \begin{cases} \psi(x,0) = \mathscr{S}_0(x), & \forall x \in \mathscr{D}_x, \\ \psi(0,t^{j+1}) = \mathscr{S}_l(t^{j+1}), & 0 \le j \le M-1, \\ \psi(1,t^{j+1}) = \mathscr{S}_r(1,t^{j+1})), & 0 \le j \le M-1. \end{cases} \end{cases} \tag{5.12}$$

Simplifying and separating the $(j+1)^{th}$ and $(j)^{th}$ time levels gives

$$\begin{cases} \mathscr{L}_{C_\varepsilon} := -C_\varepsilon(\psi_{xx}^{j+1})(x) + A(x)(\psi_{x}^{j+1})(x) + B(x)\psi^{j+1}(x) = H_i^j(x), \\ \begin{cases} \psi(x,0) = \mathscr{S}_0(x), & \forall x \in \mathscr{D}_x, \\ \psi(0,t^{j+1}) = \mathscr{S}_l(t^{j+1}), & 0 \le j \le M-1, \\ \psi(1,t^{j+1}) = \mathscr{S}_r(1,t^{j+1})), & 0 \le j \le M-1. \end{cases} \end{cases} \tag{5.13}$$

where

$$\begin{cases} H_i^j(x) = C_\varepsilon(\psi_{xx}^{j})(x) - A(x)(\psi_{x}^{j})(x) + C(x)\psi^{j}(x) + (f^{j+1}+f^{j})(x), \\ A(x) = p(x), \\ B(x) = (q(x) + 2/\Delta t), \\ C(x) = (2/\Delta t - q(x))). \end{cases} \tag{5.14}$$

To check the Semi-discrete maximum principle and stability estimate of the temporal semi-discretization of the proposed scheme, we first rewrite the semi-discretized problem (5.13) at $(j+1)^{th}$ time level in-terms of spatial variables as follows

$$\begin{cases} \mathscr{L}_{C_\varepsilon}^{*} Y := -C_\varepsilon Y''(x) + A(x)Y'(x) + B(x)Y = H(x), & \forall x \in \overline{\mathscr{D}}_x, \\ Y(0) = \mathscr{S}_l(t^{j+1}),\ Y(1) = \mathscr{S}_r(t), & \forall t \in \overline{\mathscr{D}}_t^M. \end{cases} \tag{5.15}$$

where $\mathscr{L}_{C_\varepsilon}^{*}$ is a discrete operator and $Y(x) = \psi^{j+1}(x)$.

Lemma 5.4. *(Semi-discrete Maximum Principle): If $Y(x) \in C^2(\overline{\mathscr{D}}_x)$ is the solution of the semi-discrete problem (5.13) such that $Y(0) \ge 0, Y(1) \ge 0$ on $\partial\overline{\mathscr{D}}_x$ and $\mathscr{L}_{C_\varepsilon} Y(x) \ge 0,\ \forall x \in \mathscr{D}_x$, then $Y(x) \ge 0,\ \forall x \in \overline{\mathscr{D}}_x$.*

Proof. Let $x^* \in \overline{\mathscr{D}}_x$ such that $Y(x^*) = min_{x\in\overline{\mathscr{D}}_x} Y(x) < 0$ and since $Y(0) \ge 0,\ Y(1) \ge 0$ then $x^* \notin \{0,1\}$ that is $x^* \in \mathscr{D}_x$.

Moreover, since $Y"(x^*) = 0$ and $Y"(x^*) \geq 0$ we have that

$$\begin{aligned}\mathscr{L}_{C_\varepsilon} Y(x^*) &= -C_\varepsilon Y"(x^*) + A(x^*)Y'(x^*) + B(x^*)Y(x^*) \\ &\leq 0.\end{aligned}$$

This implies that $\mathscr{L}_{C_\varepsilon} Y(x^*) \leq 0$, which contradicts the assumption $\mathscr{L}_{C_\varepsilon} Y(x) \geq 0$. Hence, the minimum of $Y(x)$ is non-negative. □

The local truncation error at the $(j+1)^{th}$ time level is given by $e^{j+1} \equiv \psi(x,t^{j+1}) - \psi^{j+1}$, where ψ^{j+1} is the computed solution of the semi-discrete problem (5.13) and $\psi(x,t_{j+1})$ is the exact solution of the continuous problem (5.4). Moreover, this error measures the contribution of each time step to the global error of the temporal semi-discretization.

Lemma 5.5. *(Local Error Estimate): According to [44], we suppose that*

$$\left| \frac{\partial^j \psi(x,t)}{\partial t^j} \right| \leq C, \forall (x,t) \in \overline{\mathscr{D}}_{xt} \text{ and } 0 \leq j \leq 3$$

then the local error estimate in the temporal discretization is given by

$$||e^{j+1}||_\infty \leq C_1(\Delta t)^3, \quad j = 1,2,3,\ldots,M-1. \tag{5.16}$$

Proof. The proof of this Lemma is similar to the proof of Lemma (2.6) of Chapter (2). □

Lemma 5.6. *(Global Error Estimate): Under the hypothesis of Lemma (5.5), the global error estimate E^{j+1} in the temporal direction is defined by*

$$||E^{j+1}||_\infty \leq C_2(\Delta t)^2. \tag{5.17}$$

Proof. The proof of this Lemma is similar to the proof of Lemma (2.7) of Chapter (2). □

Lemma 5.7. *The derivative of the solution of problem (5.4) satisfies the bound*

$$\left| \frac{d^i \psi(x,t^{j+1})}{dx^i} \right| \leq C\left(1 + {C_\varepsilon}^{-i} exp\left(\frac{p^*(1-x)}{C_\varepsilon}\right)\right), \; x \in \overline{\mathscr{D}}_x, \;\; 0 \leq i \leq 4. \tag{5.18}$$

Proof. The proof of this Lemma is similar to the proof of Lemma (2.3) of Chapter (2). □

5.4.2 Spatial discretization:

A careful choice of an appropriate scheme is essential for accurate results in singularly perturbed problems, where small parameters cause abrupt changes in the solution. We use an exponentially fitted FDM with an adapted operator to preserve the diffusion term and mitigate the influence of the parameter C_ε as $C_\varepsilon \to 0$ in the boundary layer region.

For each $j = 0, 1, 2, 3, \ldots M-1$, we have the problem of the following form

$$\begin{cases} \mathscr{L}^{M}_{C_\varepsilon}\psi^{j+1}(x) := -C_\varepsilon \frac{d^2}{dx^2}\psi^{j+1}(x) + A(x)\frac{d}{dx}\psi^{j+1}(x) + B(x)\psi^{j+1}(x) = H^{j+1}(x), \\ \begin{cases} \psi^{j+1}(0) = \mathscr{S}_l(0, t^{j+1}), \\ \psi^{j+1}(1, t^{j+1}) = \mathscr{S}_r(1, t^{j+1})). \end{cases} \end{cases} \tag{5.19}$$

To solve the semi-discrete boundary value problem (5.20), we use the zeroth order asymptotic solution for right boundary layer as follows

$$\psi^{j+1}(x) = \psi_0^{j+1}(0) + \left(\mathscr{S}_r(1, t^{j+1}) - \mathscr{S}_0^{j+1}(1)\right)\exp\left(-\frac{A(1)(1-x)}{C_\varepsilon}\right) + O(C_\varepsilon). \tag{5.20}$$

where ψ_0^{j+1} is the solution of the reduced problem in (5.8) as described in [8].
Partitioning the spatial domain $\mathscr{D}_x = [0,1]$ in to N equal number of sub-intervals each of length $h = 1/N$ gives the mesh points $x_0 = 0, x_i = ih, x_N = 1$, for $i = 0, 1, 2, \ldots, N$.
Taking h very small, the discretized form of (5.20) becomes

$$\begin{cases} \psi^{j+1}(ih) = \psi_0^{j+1}(ih) + \left(\mathscr{S}_r(1, t^{j+1}) - \psi_0^{j+1}(1)\right)\exp\left(-A(1)(1/C_\varepsilon - i\rho)\right), \\ \psi_{i-1}^{j+1}(ih) = \psi_0^{j+1}(ih) + \left(\mathscr{S}_r(1, t^{j+1}) - \psi_0^{j+1}(1)\right)\exp\left(-A(1)(1/C_\varepsilon - (i-1)\rho)\right), \\ \psi_{i+1}^{j+1}(ih) = \psi_0^{j+1}(ih) + \left(\psi_r(1, t^{j+1}) - \psi_0^{j+1}(1)\right)\exp\left(-A(1)(1/C_\varepsilon - (i+1)\rho)\right). \end{cases} \tag{5.21}$$

where $\rho = h/C_\varepsilon$.
To handle the oscillations or abrupt changes to the solution of the proposed problem due to the presence of the perturbation parameter C_ε as a diffusion coefficient of the discretized problem (5.19) , we introduce an exponential fitting factor $\sigma(\rho)$ on the diffusion term and write as:-

$$-\sigma(\rho)C_\varepsilon\delta_x^2\psi^{j+1}(x) + A(x)\delta_x^0\psi^{j+1}(x) + B(x)\psi^{j+1}(x) = H^{j+1}(x). \tag{5.22}$$

Finite Difference Operators: In this section, we use the uniform mesh points $\{x_i\}_{i=0}^{N}$ with mesh length $h = x_{i+1} - x_i$ and any mesh function ψ_i to denote the following finite difference operators for multiple purposes.

$$\delta^+\psi_i^j = \frac{\psi_{i+1}^j - \psi_i^j}{h}, \quad \delta_x^-\psi_i^j = \frac{\psi_i^j - \psi_{i-1}^j}{h}, \tag{5.23}$$
$$\delta_x^0\psi_i^j = \frac{\psi_{i+1}^j - \psi_{i-1}^j}{2h} \quad \text{and} \quad \delta_x^2\psi_i^j = \frac{\psi_{i+1} - 2\psi_i + \psi_{i-1}}{h^2}.$$

Using the finite difference operators in (5.23) into (5.22) gives

$$-\sigma(\rho)C_\varepsilon\frac{\psi_{i+1}^{j+1} - 2\psi_i^{j+1} + \psi_{i-1}^{j+1}}{h^2} + A(x_i)\frac{\psi_{i+1}^{j} - \psi_{i-1}^{j+1}}{2h} + B(x_i)\psi_i^{j+1} = H(x_i, t^{j+1}). \tag{5.24}$$

Multiplying (5.24) by h, where $h \to 0$ and truncating the term $h\left(H(x_i,t^{j+1}) - q(x_i)\psi_i^{j+1}\right)$ gives

$$-\frac{\sigma(\rho)}{\rho}\left(\psi_{i+1}^{j+1} - 2\psi_i^{j+1} + \psi_{i-1}^{j+1}\right) + \frac{A(x_i)}{2}\left(\psi_{i+1}^{j} - \psi_{i-1}^{j+1}\right) = 0. \tag{5.25}$$

Using (5.22) into (5.25) and simplifying on it, we get the required fitting factor as follows

$$\sigma(\rho) = \frac{\rho A(x_i)}{2} coth\left(\frac{\rho A(x_i)}{2}\right). \tag{5.26}$$

5.4.3 The Fully Discrete Scheme

Using (5.26) into (5.25), we get the following tri-diagonal system of equations

$$\begin{cases} r_i^0\psi_{i-1} + r_i^-\psi_i + r_i^+\psi_{i+1} = H_i^j, \\ \begin{cases} r_i^0 = \frac{\sigma(\rho)C_\varepsilon}{h^2} - \frac{A_i^{j+1}}{2h}, \\ r_i^- = 2\frac{\sigma(\rho)C_\varepsilon}{h^2} + B_i^{j+1}, \\ r_i^+ = \frac{\sigma(\rho)C_\varepsilon}{h^2} + \frac{A_i^{j+1}}{2h}, \\ H_i^j = C_\varepsilon\sigma\left(\psi_{i-1}^j - 2\psi_i^j + \psi_{i+1}^j\right) - \frac{A_i^j}{2}\left(\psi_{i+1}^j - \psi_{i-1}^j\right) + C_i^j\psi_i^j + f_i^{j+1} + f_i^j. \end{cases} \end{cases} \tag{5.27}$$

since the resulting tridiagonal system in (3.27) is a nonsingular M-matrix by theorem (2.1) of Chapter (2), we solve it using matrix inverse method.

5.5 Uniform Convergence Analysis

Lemma 5.8. *(Discrete Comparison Principle): There exists a comparison function w_i^{j+1} such that $\mathscr{L}_{C_\varepsilon}^{N,M} w_i^{j+1}$, $i = 1,2,3,\ldots,N-1$ and if $\psi_0^{j+1} \le w_0^{j+1}$ and $\psi_N^{j+1} \le w_N^{j+1}$, then $\psi_i^{j+1} \le w_i^{j+1}, \forall i = 0,1,2,\ldots,N$ [107].*

Proof. Since the matrix associated with operator $\mathscr{L}_{C_\varepsilon}^{N,M}$ in (5.27) is of size $[N+1]^2$ it satisfies the property of nonsingular M-matrix as proved in Theorem (2.1) Thus, the result of this lemma guarantee the existence and uniqueness of the discrete solution. □

Lemma 5.9. *Let $w_i^{j+1} = 1 + x_i$, $i \le 0 \le N$, then there exists a positive constant C such that w_i^{j+1} such that $\mathscr{L}_{C_\varepsilon}^{N,M} w_i^{j+1} \ge C$, $1 \le i \le N-1$.*

Proof. The proof is straightforward and provides a consistent bound in C_ε for the norm of the inverse $\mathscr{L}_{C_\varepsilon}^{N,M}$.

$$\begin{aligned}\mathscr{L}_{C_\varepsilon}^{N,M} w_i^{j+1} &= -\sigma(\rho)C_\varepsilon\delta_x^2 w^{j+1}(x) + A(x)\delta_x^0 w^{j+1}(x) + B(x)w^{j+1}(x),\\ &= -\sigma(\rho)C_\varepsilon\delta_x^2(1+x_i) + A(x)\delta_x^0(1+x_i) + B(x)(1+x_i) \geq C.\end{aligned}$$

□

Lemma 5.10. *The solution ψ_i^{j+1} of the discrete scheme in (5.27) satisfies the bound* $|\psi_i^{j+1}| \leq \frac{||H||}{\beta} + Cmax\left\{|\mathscr{S}_l(0,t_i^{j+1})|, |\mathscr{S}_r(1,t_i^{j+1})|\right\},\ B(x) \geq \beta > 0.$

Proof. Considering barrier functions $(\Omega^{\pm})_i^{j+1} = \beta^{-1}||H|| + Cmax\left\{|\mathscr{S}_l(0,t_i^{j+1})|, |\mathscr{S}_r(1,t_i^{j+1})|\right\} \pm \psi_i^{j+1}$ it can be shown that $(\Omega^{\pm})_0^{j+1} \geq 0$ and $(\Omega^{\pm})_N^{j+1} \geq 0$.
Then for $1 \leq i \leq N-1$, we have

$$\begin{aligned}\mathscr{L}_{C_\varepsilon}^{N,M}\left(\Omega^{\pm}\right)_i^{j+1} &= -\sigma(\rho)C_\varepsilon\delta_x^2\left(\Omega^{\pm}\right)_i^{j+1} + A(x)\delta_x^0\left(\Omega^{\pm}\right)_i^{j+1} + B(x)\left(\Omega^{\pm}\right)_i^{j+1},\\ &= B(x)\left[\beta^{-1}||H|| + Cmax\left\{|\mathscr{S}_l(0,t_i^{j+1})|, |\mathscr{S}_r(1,t_i^{j+1})|\right\} \pm \psi_i^{j+1}\right],\\ &\geq 0.\end{aligned}$$

Using Lemma (5.8), we obtain $(\Omega^{\pm})_i^{j+1} \geq 0$, for $i = 0,1,2,\ldots,N.$ □

Lemma 5.11. *(Uniform Stability Estimate): Let ϕ_i^{j+1} be any mesh function of $(j+1)^{th}$ time level as presented in [100] such that $\phi_0^{j+1} = 0 = \phi_N^{j+1}$, then*

$$\left|\phi_i^{j+1}\right| \leq \frac{1}{\beta}\max_{1\leq j\leq N-1}\left|\mathscr{L}_{C_\varepsilon}^{N,M}\phi_i^{j+1}\right|, for\ 1 \leq i \leq N-1, where\ \ d(x) \geq \beta > 0.$$

Proof. Consider two barrier functions of the form

$$\left(\Omega^{\pm}\right)_i^{j+1} = \frac{1}{\beta}\max_{1\leq i\leq N-1}\left|\mathscr{L}_{C_\varepsilon}^{N,M}\phi_i^{j+1}\right| \pm \phi_i^{j+1}.$$

Using the result of Lemma (5.11) it is clear that $(\Omega^{\pm})_0^{j+1} \geq 0, (\Omega^{\pm})_N^{j+1} \geq 0$. Having these we want to show that $\mathscr{L}_{C_\varepsilon}^{N,M}(\Omega^{\pm})_i^{j+1} \geq 0$ for $1 \leq i \leq N-1$.

$$\begin{aligned}\mathscr{L}_{C_\varepsilon}^{N,M}\left(\Omega^{\pm}\right)_i^{j+1} &= -\sigma(\rho)C_\varepsilon\delta_x^2\left(\Omega^{\pm}\right)_i^{j+1} + A(x)\delta_x^0\left(\Omega^{\pm}\right)_i^{m+1} + B(x)\left(\Omega^{\pm}\right)_i^{j+1},\\ &= B(x_i)\left[\frac{1}{\beta}\max_{1\leq i\leq N-1}\left|\mathscr{L}_{C_\varepsilon}^{N,M}\phi_i^{j+1}\right| \pm \phi_i^{j+1}\right],\\ &\geq 0.\end{aligned}$$

There, using the discrete comparison principle gives

$$|\phi_i^{j+1}| \leq \frac{1}{\beta}\max_{1\leq i\leq N-1}\left|\mathscr{L}_{C_\varepsilon}^{N,M}\phi_i^{j+1}\right|.$$

Overall, this result guarantee the uniform stability of the discrete scheme. □

Lemma 5.12. *[58], for a fixed number of mesh numbers N and for $C_\varepsilon \to 0$, it holds that*

$$\lim_{C_\varepsilon\to 0}\max_{1\le i\le N-1}\frac{\exp\left(\frac{-\alpha x_i}{C_\varepsilon{}^j}\right)}{C_\varepsilon{}^j}=0 \;\; and \;\; \lim_{C_\varepsilon\to 0}\max_{1\le i\le N-1}\frac{\exp\left(\frac{-\alpha(1-x_i)}{C_\varepsilon{}^j}\right)}{C_\varepsilon{}^j}=0,\; j=1,2,3,\ldots \tag{5.28}$$

where and $x_i = ih,\ i = 1/N,\ 1 \le i \le N-1$.

Proof. Using the partition $[0,1] := \{0 = x_0 < x_1 < x_2 <,\ldots,x_N = 1\}$ for the interior grid points, we have

$$\max_{1\le i\le N-1}\frac{\exp\left(\frac{-\alpha x_i}{C_\varepsilon{}^j}\right)}{C_\varepsilon{}^j}\le\max_{1\le i\le N-1}\frac{\exp\left(\frac{-\alpha x_1}{C_\varepsilon{}^j}\right)}{C_\varepsilon{}^j}=\max_{1\le i\le N-1}\frac{\exp\left(\frac{-\alpha h}{C_\varepsilon{}^j}\right)}{C_\varepsilon{}^j},$$

and

$$\max_{1\le i\le N-1}\frac{\exp\left(\frac{-\alpha(1-x_i)}{C_\varepsilon{}^j}\right)}{C_\varepsilon{}^j}\le\max_{1\le i\le N-1}\frac{\exp\left(\frac{-\alpha(1-x_{i-1})}{C_\varepsilon{}^j}\right)}{C_\varepsilon{}^j}=\max_{1\le i\le N-1}\frac{\exp\left(\frac{-\alpha h}{C_\varepsilon{}^j}\right)}{C_\varepsilon{}^j}.$$

Since $x_1 = h = x_{i-1}$, then using the L'Hospital's rule we get

$$\begin{aligned}\lim_{C_\varepsilon\to 0}\frac{\exp\left(\frac{-\alpha h}{C_\varepsilon{}^j}\right)}{C_\varepsilon{}^j} &= \lim_{p=1/C_\varepsilon\to\infty}\frac{p^m}{\exp(\alpha hp)},\\ &= \lim_{p=1/C_\varepsilon\to\infty}\frac{j!}{(p^*h)^j\exp(p^*hp)},\\ &= 0.\end{aligned}$$

Combining the results obtained in the preceding steps, we see that the lemma is fully verified. Thus, the proof is complete. □

Lemma 5.13. *Let the coefficient and source functions $A(x), B(x)$ and $H(x,t^j)$ of the semi-discrete problem in (5.13) be sufficiently smooth so that $\psi^{j+1}(x) \in C^4[0,1]$ [44]. Then the discrete solution ψ_i^{j+1} of (5.27) satisfies the following error bound .*

$$||\mathscr{L}_{C_\varepsilon}^{N,M}\left(\psi^{j+1}(x)-\psi_i^{j+1}\right)||\le\frac{Ch^2}{h+C_\varepsilon}\left(1+C_\varepsilon{}^{-3}\exp\left(-\frac{\alpha(1-x_i)}{C_\varepsilon}\right)\right). \tag{5.29}$$

Proof. Using the result of Lemma (5.12) into (5.29) gives

$$||\mathscr{L}_{C_\varepsilon}^{N,M}\left(\psi^{j+1}(x)-\psi_i^{j+1}\right)||\le\frac{Ch^2}{h+C_\varepsilon}. \tag{5.30}$$

So, applying the bound in lemma (5.11), we get

$$||\psi^{j+1}(x)-\psi_i^{j+1}|| \le \frac{Ch^2}{h+C_\varepsilon}. \tag{5.31}$$

Moreover, for small value of $C_\varepsilon \ll h$ the denominator of the bound in (5.31) dominated by h and simplified as follows.

$$\sup_{0<C_\varepsilon\le 1} ||\psi^{j+1}(x)-\psi_i^{j+1}|| \le Ch. \tag{5.32}$$

These constructions proved that the spatial error is controlled by a positive constant. □

Theorem 5.1. Suppose that $\psi(x_i,t^{j+1})$ and ψ_i^{j+1} are the exact and computed solutions of (5.4) and (5.27) respectively on the discretized domain. Then for sufficiently small h the following uniform error estimate holds:

$$\sup_{0<C_\varepsilon\le 1} ||\psi^{j+1}(x)-\psi_i^{j+1}|| \le C(h+(\Delta t)^2). \tag{5.33}$$

From this we conclude that the proposed scheme is first order accurate in the spatial direction and second order accurate in the temporal direction.

5.6 Richardson Extrapolation Techniques

As stated in Theorem (5.1) above, it is seen that the proposed scheme has low accuracy and order of convergence in the spatial direction. This affects the overall order of convergence of the scheme. To tackle this challenge, we follow a similar approach as described in [88] and use the Richardson extrapolation technique in the spatial direction.

Let $\mathscr{D}_x^{2N}$ be the mesh obtained from bisecting the step length h such that $\mathscr{D}_x^N \subseteq \mathscr{D}_x^{2N}$. If ψ_i^j and $\overline{\psi}_i^j$ be numerical solutions obtained from $\mathscr{D}_x^N$ and $\mathscr{D}_x^{2N}$ respectively, then

$$\psi^j(t)-\psi_i^j(t) = Ch + R_i^N(t), \quad (x,t^j)\in \mathscr{D}_x^N \times \mathscr{D}_t. \tag{5.34}$$

$$\psi^j(t)-\overline{\psi}_i^j(t) = C\left(\frac{h}{2}\right) + R_i^{2N}(t), \quad (x,t^j)\in \mathscr{D}_x^{2N} \times \mathscr{D}_t. \tag{5.35}$$

where $\psi^j(t)$ is the exact solution of the proposed problem at j^{th} time level, $R_j^N(t)$ and $R_j^{2N}(t)$ are the remainder terms of the error with order $O(h^2)$ and C is a constant independent of the parameters ε, h and Δt. Now, using the inequalities (5.35) and (5.34) we get the error bound of the following form obtain the extrapolation formula

$$\psi^j(t) - \psi_i^j(t) - 2(\psi^j(t) - \overline{\psi}_i^j(t)) = R_j^N(t) - R_j^{2N}(t). \tag{5.36}$$

Using the truncation error of the spatial discretization $\psi^j(t) = \psi(x,t^j) + Ch + O(h^2)$ and $\overline{\psi}^j(t) = \psi(x_i,t^j) + C\frac{h}{2} + O(h^2)$ in (5.36) gives

$$\max_{0\le i\le N} \left|\psi^{ext}(t) - \psi^j(t)\right| \le Ch^2. \tag{5.37}$$

Simplifying (5.37), gives the required numerical solution as follows

$$\psi^{ext}(t) = 2\overline{\psi}^j(t) - \psi^j(t). \tag{5.38}$$

where $\psi^{ext}(t)$ is the numerical solution obtained from the extrapolation, C is a constant independent of the parameter ε and step size h and Δt.
The overall construction modifies the convergence order of the proposed scheme, as established in the theorem presented below.
Theorem 5.2. Suppose that $\psi^{j+1}(x_i)$ and ψ_i^{j+1} are the continuous and discrete solutions of (5.4) and (5.27) respectively. Then for sufficiently small h the following uniform error estimate holds:

$$\sup_{0<C_\varepsilon\le 1} ||\psi^{j+1}(x_i) - \psi_i^{j+1}|| \le C(h^2 + (\Delta t)^2). \tag{5.39}$$

This concludes that the proposed scheme is second-order accurate in both the spatial and temporal directions after the application of Richardson extrapolation.

5.7 Numerical Results and Discussions

The proposed scheme is further tested on three numerical experiments, where $\varepsilon-$uniform maximum absolute errors and convergence rates are determined to assess its accuracy and computational performance, as presented in Chapter 2.
Example 5.1. Consider the convection-diffusion SPPDDEs of the following forms:

$$\begin{cases} \psi_t - \varepsilon\psi_{xx}(x,t) + (2-x^2)\psi_x(x,t) + 2\psi(x-\delta,t) + (x-3)\psi(x,t) + \psi(x+\eta,t) \\ = 10t^2\exp^{-t}x(1-x), \qquad \forall (x,t) \in \mathscr{D}_{xt}, \\ \psi_0(x) = 0, \qquad \forall x \in \overline{\mathscr{D}_x}, \\ \psi_l(t) = 0, \qquad \forall t \in \overline{\mathscr{D}_t}, \\ \psi_r(t) = 0, \qquad \forall t \in \overline{\mathscr{D}_t}. \end{cases}$$

where $\delta = 0.6\varepsilon$ and $\eta = 0.5\varepsilon$ [92].

Example 5.2. Consider the convection-diffusion SPPDDEs of the following forms:

$$\begin{cases} \psi_t - \varepsilon\psi_{xx}(x,t) + (2-x)\psi_x(x,t) + (1+x)\psi(x-\delta,t) + (1+x^2+cos(\pi x))\psi(x,t) + 3\psi(x+\eta,t) \\ = sin(\pi x), & \forall (x,t) \in \mathscr{D}_{xt}, \\ \psi_0(x) = 0, & \forall x \in \overline{\mathscr{D}_x}, \\ \psi_l(t) = 0, & \forall t \in \overline{\mathscr{D}_t}, \\ \psi_r(t) = 0, & \forall t \in \overline{\mathscr{D}_t}. \end{cases}$$

where $\delta = 0.6\varepsilon$ and $\eta = 0.5\varepsilon$ [50].

Example 5.3. Consider the convection-diffusion SPPDDEs of the following forms:

$$\begin{cases} \psi_t - \varepsilon\psi_{xx}(x,t) + \psi_x(x,t) + (2-x^2)\psi(x-\delta,t) + (1+x^2)\psi(x,t) + \exp^x \psi(x+\eta,t) \\ = 50(x(1-x))^3, & \forall (x,t) \in \mathscr{D}_{xt}, \\ \psi_0(x) = 0, & \forall x \in \overline{\mathscr{D}_x}, \\ \psi_l(t) = 0, & \forall t \in \overline{\mathscr{D}_t}, \\ \psi_r(t) = 0, & \forall t \in \overline{\mathscr{D}_t}. \end{cases}$$

where $\delta = 0.6\sqrt{\varepsilon}$ and $\eta = 0.5\sqrt{\varepsilon}$ [93].

Since the analytical solutions are unknown, we apply the doubling mesh technique to find the maximum absolute errors and corresponding order of convergences.

Let $\psi^{N,M}(x_i,t^j)$ and $\psi^{2N,2M}(x_i,t^j)$ be the numerical solutions with mesh lengths $(h,\Delta t \neq 0)$ and $(h/2,\Delta t/2 \neq 0)$ respectively, then

- The maximum absolute error is given by

$$E_\varepsilon^{N,M} = \max_{0\le i,m\le N,M} \left|\psi^{N,M}(x_i,t^j) - \psi^{2N,2M}(x_{2i},t^{2j})\right|. \tag{5.40}$$

- The $\varepsilon-$ uniform maximum absolute error is given by

$$E^{N,M} = \max_\varepsilon E_\varepsilon^{N,M}. \tag{5.41}$$

- Corresponding ε-uniform order of convergence

$$R^{N,M} = log_2\left(\frac{E^{N,M}}{E^{2N,2M}}\right). \tag{5.42}$$

Table 5.1: $E^{N,M}$ and $R^{N,M}$ for Example (5.1) with $\delta = 0.6 * \varepsilon, \eta = 0.5 * \varepsilon$

$\varepsilon \downarrow$	$N = 64$ $M = 120$	$N = 128$ $M = 240$	$N = 256$ $M = 480$	$N = 512$ $M = 960$
Before Extrapolation.				
2^{-6}	$3.1388e-03$	$9.5444e-04$	$2.5306e-04$	$6.4253e-05$
2^{-8}	$4.1053e-03$	$1.9873e-03$	$7.8599e-04$	$2.3855e-04$
2^{-10}	$4.1031e-03$	$2.0591e-03$	$1.0305e-03$	$4.9740e-04$
2^{-12}	$4.1018e-03$	$2.0585e-03$	$1.0309e-03$	$5.1582e-04$
2^{-14}	$4.1015e-03$	$2.0583e-03$	$1.0308e-03$	$5.1578e-04$
2^{-16}	$4.1014e-03$	$2.0583e-03$	$1.0308e-03$	$5.1577e-04$
$E^{N,M}$	$4.1053e-03$	$1.9873e-03$	$1.0309e-03$	$5.1582e-04$
$R^{N,M}$	1.0467	0.9469	0.9990	—
After Extrapolation.				
2^{-6}	$1.4288e-04$	$5.1182e-05$	$1.5237e-05$	$4.2499e-06$
2^{-8}	$1.6888e-04$	$5.2882e-05$	$1.6037e-05$	$4.6499e-06$
2^{-10}	$1.6888e-04$	$5.2882e-05$	$1.6037e-05$	$4.6499e-06$
2^{-12}	$1.6888e-04$	$5.2882e-05$	$1.6037e-05$	$4.6499e-06$
2^{-14}	$1.6888e-04$	$5.2882e-05$	$1.6037e-05$	$4.6499e-06$
2^{-16}	$1.6888e-04$	$5.2882e-05$	$1.6037e-05$	$4.6499e-06$
$E^{N,M}$	$1.6888e-04$	$5.2882e-05$	$1.6037e-05$	$4.6499e-06$
$R^{N,M}$	1.6752	1.7862	1.7213	—

Table 5.2: $E^{N,M}$ and $R^{N,M}$ for Example (5.2) with $\delta = 0.6 * \varepsilon, \eta = 0.5 * \varepsilon$

$\varepsilon \downarrow$	$N = 64$ $M = 120$	$N = 128$ $M = 240$	$N = 256$ $M = 480$	$N = 512$ $M = 960$
Before Extrapolation.				
2^{-6}	$5.3432e-03$	$2.2305e-03$	$6.9293e-04$	$1.8547e-04$
2^{-8}	$5.5408e-03$	$2.8976e-03$	$1.4241e-03$	$5.7175e-04$
2^{-10}	$5.5458e-03$	$2.9021e-03$	$1.4769e-03$	$7.4790e-04$
2^{-12}	$5.5458e-03$	$2.9021e-03$	$1.4769e-03$	$7.4790e-04$
2^{-14}	$5.5458e-03$	$2.9021e-03$	$1.4769e-03$	$7.4790e-04$
2^{-16}	$5.5458e-03$	$2.9021e-03$	$1.4769e-03$	$7.4790e-04$
$E^{N,M}$	$5.5458e-03$	$2.9021e-03$	$1.4769e-03$	$7.4790e-04$
$R^{N,M}$	0.9342	0.9745	0.9808	—
After Extrapolation.				
2^{-6}	$6.2004e-05$	$1.6925e-05$	$5.0489e-06$	$1.1123e-06$
2^{-8}	$6.2022e-05$	$1.7905e-05$	$5.0708e-06$	$1.3832e-06$
2^{-10}	$6.2022e-05$	$1.7905e-05$	$5.0708e-06$	$1.3832e-06$
2^{-12}	$6.2022e-05$	$1.7905e-05$	$5.0708e-06$	$1.3832e-06$
2^{-14}	$6.2022e-05$	$1.7905e-05$	$5.0708e-06$	$1.3832e-06$
2^{-16}	$6.2022e-05$	$1.7905e-05$	$5.0708e-06$	$1.3832e-06$
$E^{N,M}$	$6.2022e-05$	$1.7905e-05$	$5.0708e-06$	$1.3832e-06$
$R^{N,M}$	1.7924	1.8201	1.8742	—

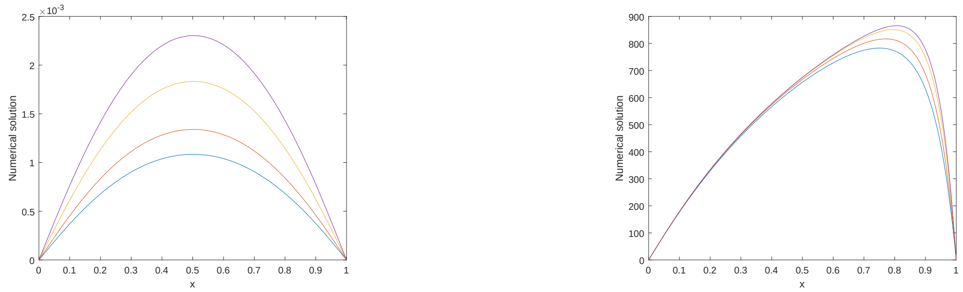

(a) $\varepsilon = 2^{-0}$ (b) $\varepsilon = 2^{-10}$

Figure 5.1: 2D Solution graphs for Example (5.2) with values $N = 128, M = 240$

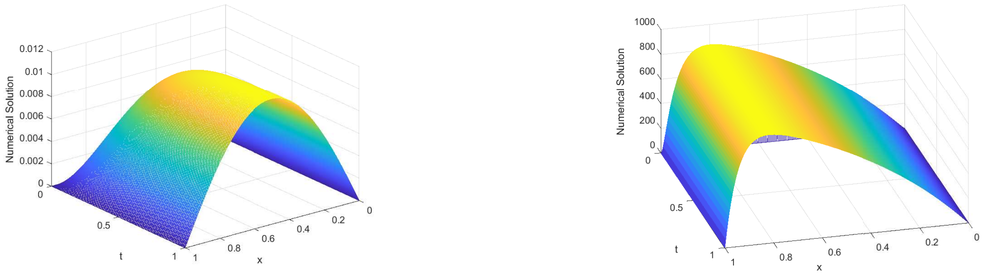

(a) $\varepsilon = 2^{-0}$ (b) $\varepsilon = 2^{-10}$

Figure 5.2: 3D Solution graphs for Example (5.2) with values $N = 128, M = 240$

Table 5.3: $E^{N,M}$ and $R^{N,M}$ for Example (5.3) with $\delta = 0.6\sqrt{\varepsilon}, \eta = 0.5\sqrt{\varepsilon}$

$\varepsilon \downarrow$	$N = 64$ $M = 8$	$N = 128$ $M = 16$	$N = 256$ $M = 32$	$N = 512$ $M = 64$	$N = 1024$ $M = 128$
2^{-6}	$3.7701e-03$	$1.9482e-03$	$1.0119e-03$	$5.2239e-04$	$2.5485e-04$
2^{-8}	$3.7721e-03$	$1.8582e-03$	$1.0195e-03$	$5.2629e-04$	$2.5625e-04$
2^{-10}	$3.7821e-03$	$1.9682e-03$	$1.0179e-03$	$5.2569e-04$	$2.7085e-04$
2^{-12}	$3.7821e-03$	$1.9682e-03$	$1.0179e-03$	$5.2569e-04$	$2.7085e-04$
2^{-14}	$3.7821e-03$	$1.9682e-03$	$1.0179e-03$	$5.2569e-04$	$2.7085e-04$
2^{-16}	$3.7821e-03$	$1.9682e-03$	$1.0179e-03$	$5.2569e-04$	$2.7085e-04$
$E^{N,M}$	$3.7821e-03$	$1.9682e-03$	$1.0179e-03$	$5.2569e-04$	$2.7085e-04$
$R^{N,M}$	0.9423	0.9512	0.9534	0.95672	—

Table 5.4: Comparison of $E^{N,M}$ and $R^{N,M}$ for Example (5.1) with different schemes.

$\varepsilon \downarrow$	$N=64$ $M=120$	$N=128$ $M=240$	$N=256$ $M=480$	$N=512$ $M=960$
Present Method				
$E^{N,M}$	$4.1053e-03$	$1.9873e-03$	$1.0309e-03$	$5.1582e-04$
$R^{N,M}$	1.0467	0.9469	0.9990	—
Upwind method in [92]				
$E^{N,M}$	$1.6716e-02$	$9.2022e-03$	$4.9863e-03$	$2.6885e-03$
$R^{N,M}$	0.8612	0.8840	0.8912	—
Midpoint Upwind in [92]				
$E^{N,M}$	$1.0729e-02$	$6.5942e-03$	$3.8199e-03$	$2.1180e-03$
$R^{N,M}$	0.7022	0.7877	0.8508	—
Cubic-B Spline in [92]				
$E^{N,M}$	$7.5020e-03$	$4.4966e-03$	$2.4450e-053$	$1.2728e-03$
$R^{N,M}$	0.7384	0.8791	0.9418	—

Table 5.5: Comparison of $E^{N,M}$ and $R^{N,M}$ for Example (5.3) with different schemes

$\varepsilon \downarrow$	$N=64$ $M=120$	$N=128$ $M=240$	$N=256$ $M=480$	$N=512$ $M=960$
Present Method				
$E^{N,M}$	$1.9682e-03$	$1.0179e-03$	$5.2569e-04$	$2.7085e-04$
$R^{N,M}$	0.9512	0.9534	0.95672	—
The method in [92]				
$E^{N,M}$	$4.4966e-03$	$2.4450e-03$	$1.2728e-053$	$6.4609e-03$
$R^{N,M}$	0.8791	0.9718	0.9715	—
The method in [50]				
$E^{N,M}$	$5.4975e-03$	$3.2062e-03$	$1.7716e-03$	$9.4594e-04$
$R^{N,M}$	0.7779	0.8558	0.9053	—
The method in [93]				
$E^{N,M}$	$4.8801e-03$	$2.4414e-03$	$1.2211e-03$	$6.1064e-04$
$R^{N,M}$	0.9492	0.9455	0.9428	—

We present the tabulated results in Tables (5.1), (5.2), and (5.3) for Examples (5.1), (5.2), and (5.3), respectively, showing the maximum absolute errors and corresponding orders of convergence. For a fixed perturbation parameter ε, we observe that the maximum absolute errors decrease consistently as the mesh points N and M increase. In contrast, for fixed values of N, M, and the shift parameters δ and η, the errors remain nearly unchanged as ε decreases, which confirms that our method is uniformly convergent.

Moreover, the 2D and 3D plots in Example (5.2) (Figures (5.1) and (5.2)) show that, for a fixed mesh, decreasing ε produces a sharp gradient near $x=1$, thereby confirming the presence of a right boundary layer in agreement with the theoretical analysis. After applying Richardson extrapolation, we observe second-order accuracy in both space and time.

Finally, we compare the performance of our method with existing approaches in [50, 92, 93] using both accuracy and order of convergence as criteria. The results in Tables (5.3) and (5.4) show that our method consistently achieves higher accuracy and better convergence rates than the competing schemes.

5.8 Conclusion

In this chapter, we developed a fitted numerical scheme for singularly perturbed differential equations with mixed shift parameters. The proposed method combines the Crank–Nicolson scheme in time with an exponentially fitted finite difference scheme in space on uniform meshes. Both theoretical analysis and numerical experiments confirm that the scheme is uniformly convergent with respect to the perturbation parameter ε and achieves second-order accuracy. In addition, the comparison results demonstrate that the method provides improved accuracy and convergence behavior compared with several existing approaches.

Chapter 6

A Fitted Midpoint Upwind Scheme for Singularly Perturbed Parabolic Problems Involving a Small Shift Parameter in the Convection and Reaction Terms

In the present chapter, we consider a class of singularly perturbed differential–difference equations with a small shift parameter in the convection and reaction terms, which frequently arise in applied mathematics and engineering. The presence of a small diffusion parameter $\varepsilon(0 < \varepsilon \ll 1)$ induces a boundary layer near the right endpoint of the spatial domain, where the solution exhibits rapid variations that challenge classical numerical methods. To overcome these difficulties, we develop and analyze a fitted numerical method. Temporal discretization is performed using the implicit Euler method, while spatial discretization employs a fitted midpoint upwind finite difference approach on uniform meshes. Stability and uniform convergence analyses confirm that the scheme achieves second-order accuracy in both time and space after applying Richardson extrapolation. Two model examples demonstrate the reliability and accuracy of the method, with numerical results validating the theoretical predictions and outperforming several existing approaches in the literature.

6.1 Introduction

Many real-world problems in science and engineering are modeled by parameter-dependent differential equations. SPDEs, in which the highest-order derivatives are multiplied by a small parameter $\varepsilon\,(0 < \varepsilon \ll 1)$, appear in areas such as control theory [89], evolutionary biology [90], and neuronal variability [23]. SPPDDEs are those SPDEs that include one or more retarded or advanced arguments in space or time, capturing memory or time-lag effects. They arise in modeling physiological processes [96], population dynamics [97] and disease spread [98].

The small diffusion parameter $\varepsilon\,(0 < \varepsilon \ll 1)$ in the proposed problem induces a boundary layer near the right endpoint, where classical numerical methods on uniform meshes, such as FDM, FEM, and FVM fail to provide accurate solutions without very fine discretization. However, fine meshes increase computational cost and round-off errors [78]. To overcome these issues, parameter-uniformly convergent schemes have been developed in [46, 47, 99], including fitted operator methods, fitted mesh techniques, and domain decomposition methods.

In addition to the aforementioned works, numerous studies have addressed solution methods for the proposed problem [50, 93, 101]. However, relatively few have developed parameter-uniformly convergent methods for singularly perturbed delay differential equations with small shift parameters in the convection and reaction terms. For instance, Kumar and Kadalbajoo [48] employed B-spline collocation on Shishkin meshes, while Woldaregay and Duressa [49, 57] proposed θ-method schemes in time combined with exponentially fitted and nonstandard finite differences in space on uniform meshes.

Motivated by the low accuracy of existing schemes and the review by Duressa et al. [59], this chapter formulates and analyzes a fitted numerical method for SPPDDEs with small shift parameters in the convection and reaction terms. .

6.2 Problem formulation

Consider a class of singularly perturbed parabolic differential-difference equations with small shift parameters in the convection and reaction terms, as specified in (1.14), subject to the associated initial and interval-boundary conditions [58].

$$\begin{cases} \mathscr{L}_\varepsilon \psi(x,t) := f(x,t), & \forall (x,t) \in \mathscr{D}_{xt} = (0,1)\times(0,T], T>0, \\ \psi(x,0) = \mathscr{S}_0(x,t), & \forall (x,t) \in \mu_0 = \left\{(x,t) : \forall x \in \overline{\mathscr{D}}_x, t=0\right\}, \\ \psi(x,t) = \mathscr{S}_l(x,t), & \forall (x,t) \in \mu_l = \left\{(x,t) : \forall (x,t) \in [-\delta,0]\times \overline{\mathscr{D}}_t\right\}, \\ \psi(1,t) = \mathscr{S}_r(1,t), & \forall (x,t) \in \mu_r = \left\{(x,t) : x=1, \forall t \in \overline{\mathscr{D}}_t\right\}. \end{cases} \tag{6.1}$$

where $\mathscr{L}_\varepsilon \psi := \psi_t(x,t) - \varepsilon \psi_{xx}(x,t) + a(x,t)\psi_x(x-\delta,t) + b(x,t)\psi(x-\delta,t)$ is the differential operator, ε $(0<\varepsilon\ll 1)$, is a perturbation parameter and $\delta<\varepsilon$ is a small shift parameter which satisfies the relation $\delta = O(\varepsilon)$. To control the sudden blowing ups in the convection and reaction terms, the functions $a(x,t), b(x,t)$ and $f(x,t)$ on $\overline{\mathscr{D}}_{xt}$ are assumed to be sufficiently smooth, bounded, and satisfy

$$a(x,t) \geq \omega > 0, b(x,t) \geq \beta > 0 \quad \forall (x) \in \overline{\mathscr{D}}_{xt}. \tag{6.2}$$

The Taylor series expansion in [65] is employed to approximate the shift terms in (6.1):

$$\begin{cases} \psi_x(x-\delta,t) = \psi_x - \delta\psi_{xx} + O(\delta^2), \\ \psi(x-\delta,t) = \psi - \delta\psi_x + \frac{\delta^2}{2}\psi_{xx} + O(\delta^3). \end{cases} \tag{6.3}$$

Using Eq.(6.3) into Eq.(6.1), we obtained the following parabolic singularly perturbed initial-boundary value problem

$$\begin{cases} \mathscr{L}_{C_\varepsilon}\psi(x,t) := \psi_t(x,t) + \mathscr{L}_{C_\varepsilon}\psi(x,t) = f(x,t) & \forall (x,t) \in \mathscr{D}_{xt}, \\ \psi(x,0) = \mathscr{S}_0(x) & \forall x \in \overline{\mathscr{D}}_x, \\ \psi(0,t) = \mathscr{S}_l(t) & \forall t \in \overline{\mathscr{D}}_t, \\ \psi(1,t) = \mathscr{S}_r(t) & \forall t \in \overline{\mathscr{D}}_t. \end{cases} \tag{6.4}$$

where $\mathscr{L}_{C_\varepsilon}\psi := -C_\varepsilon\psi_{xx} + p(x,t)\psi_x + b(x,t)\psi, 0 < C_\varepsilon(x) \leq \varepsilon - \frac{\delta^2}{2}\beta + \delta\alpha = C_\varepsilon,\ p(x,t) = a(x,t) - \delta b(x)$, and $a(x,t) \geq \alpha > 0$ and $b(x,t) \geq \delta > 0$. For small value of δ the problems (6.1) and (6.4) are asymptotically equivalent, since the difference between the two equations is $O(\delta^2)$. To ensure the existence of a unique solution, the functions $p(x,t), b(x,t)$ and $f(x,t)$ on $\overline{\mathscr{D}}_{xt}$ are assumed to be sufficiently smooth, bounded, and satisfy

$$p(x,t) \geq p^* > 0, \quad \forall x \in \overline{\mathscr{D}}_{xt}. \tag{6.5}$$

Under the condition (6.5), the solution of the problem in (6.4) develops a right boundary layer near $x = 1$ as $C_\varepsilon \to 0$.

6.3 Properties of the Analytic Solution

The existence of a unique solution of (6.4) can be established under the assumption that the problem data are Hölder continuous and satisfy the necessary compatibility conditions at the corner points, as outlined in [44]. The necessary compatibility conditions at the corner points $(0,0)$ and $(1,0)$ are defined as follows:
$\mathscr{S}_0(0,0) = \mathscr{S}_l(0)$, $\mathscr{S}_0(1,0) = \mathscr{S}_r(0)$ and satisfies

$$\begin{cases} \frac{\partial \mathscr{S}_l(0)}{\partial t} - C_\varepsilon \frac{\partial^2 \mathscr{S}_0(0,0)}{\partial x^2} + p(0)\frac{\partial \mathscr{S}_0(0,0)}{\partial x} + b(0,0)\mathscr{S}_0(0,0) = f(0,0), \\ \frac{\partial \mathscr{S}_r(1)}{\partial t} - C_\varepsilon \frac{\partial^2 \mathscr{S}_0(1,0)}{\partial x^2} + p(0)\frac{\partial \mathscr{S}_0(1,0)}{\partial x} + b(1,0)\mathscr{S}_0(1,0) = f(1,0). \end{cases} \tag{6.6}$$

where the initial and boundary functions $\mathscr{S}_0(x), \mathscr{S}_l(t)$ and $\mathscr{S}_r(t)$ are assumed to be sufficiently smooth and bounded.
Now on omitting the boundary conditions at $x = 1$ and setting $C_\varepsilon = 0$ gives the reduced form of

problem (6.4):

$$\begin{cases} \psi_t^0 + p(x)\psi_x^0 + b(x) + \psi^0 = f(x,t), & \forall (x,t) \in \mathscr{D}_{xt}, \\ \psi^0(x,0) = S_0(x), & \forall x \in \overline{\mathscr{D}}_x, \\ \psi^0(0,t) = 0, & \forall \in \overline{\mathscr{D}}_t. \end{cases} \tag{6.7}$$

This is a first order hyperbolic equation with initial data specified along two sides the initial points $t = 0$ and $x = 0$ of the domain $\overline{\mathscr{D}}_{xt}$, For small values of C_ε the solution $\psi(x,t)$ of (6.4) will be very close to $\psi^0(x,t)$. In order to obtain error bounds on the solution of the difference scheme, we assumed that the solution of the reduced problem (6.7) is sufficiently smooth.

Lemma 6.1. *(Continuous Maximum Principle): Assumed that $\psi(x,t)$ is any sufficiently smooth function satisfying $\psi(x,t) \geq 0, \forall (x,t) \in \partial\mathscr{D}_{xt}$ and $\mathscr{L}_{C_\varepsilon}\psi(x,t) \geq 0, \forall (x,t) \in \mathscr{D}_{xt}$. Then, $\psi(x,t) \geq 0, \forall (x,t) \in \overline{\mathscr{D}}_{xt}$.*

Proof. The proof of this Lemma is similar to the proof of Lemma (5.1) of Chapter (5). □

Lemma 6.2. ***(Stability Estimate)**: If $\psi(x,t) \in C^{2,1}(\overline{\mathscr{D}}_{xt})$ be the solution of the continuous problem of equation* (6.4) *,then it satisfies the bound*

$$|\psi(x,t)| \leq \frac{1}{p^*}||f|| + max\{|\mathscr{S}_0(x)|, |\mathscr{S}_l(t)|, |\mathscr{S}_r(t)|\}.$$

Proof. The proof of this Lemma is similar to the proof of Lemma (5.2) of Chapter (5). □

Lemma 6.3. *The derivatives of the solution of problem* (6.4) *satisfies the bound*

$$\left|\frac{\partial^{i+j}\psi(x,t)}{\partial x^i \partial t^j}\right| \leq C\left(1 + {C_\varepsilon}^{-i} exp\left(\frac{p^*(1-x)}{C_\varepsilon}\right)\right), \; 0 \leq j \leq 2 \; and \; 0 \leq i+j \leq 4. \tag{6.8}$$

where C is a constant independent of the perturbation parameter C_ε.

Proof. The proof of this Lemma is similar to the proof of Lemma (2.3) of Chapter (2). □

6.4 Formulation of Numerical Schemes

The main concern of this section is to discretize the proposed problem. For the sake of simplicity, we first discretized in the temporal direction and then the spatial direction using uniform meshes as follows:

6.4.1 Temporal Semi-discretization:

Dividing the time domain $[0,T]$ into M equal number of mesh intervals with step length Δt, we get

$$\overline{\mathscr{D}}_t^M = \left\{ t_j : t^j = j\Delta t,\, j = 0,1,2,3,\dots M \text{ and } \Delta t = \frac{T}{M} \right\}. \tag{6.9}$$

To discretize the temporal dimension of the problem under consideration, we follow the procedure outlined in [35] and apply the implicit Euler method to (6.4) as follows:

$$\begin{cases} \frac{\psi^{j+1}-\psi^{j}}{\Delta t} - C_\varepsilon \psi_{xx}^{j+1} + p(x,t)\psi_x^{j+1} + b(x,t)\psi^{j+1} = f^{j+1}, \\ \begin{cases} \psi(x,0) = \mathscr{S}_0(x), & \forall x \in \mathscr{D}_x, \\ \psi(0,t^{j+1}) = \mathscr{S}_l(t^{j+1}), & 0 \le j \le M-1, \\ \psi(1,t^{j+1}) = \mathscr{S}_r(1,t^{j+1})), & 0 \le j \le M-1. \end{cases} \end{cases} \tag{6.10}$$

A further simplification on (6.10) gives the $(j+1)^{th}$ time level discretized equation of the form below

$$\begin{cases} \mathscr{L}_{C_\varepsilon} := -C_\varepsilon \psi_{xx}^{j+1} + p(x,t)\psi_x^{j+1} + q(x,t)\psi^{j+1} = H_i^j, \\ \begin{cases} \psi(x,0) = \mathscr{S}_0(x), & \forall x \in \mathscr{D}_x, \\ \psi(0,t^{j+1}) = \mathscr{S}_l(t^{j+1}), & 0 \le j \le M-1, \\ \psi(1,t^{j+1}) = \mathscr{S}_r(1,t^{j+1})), & 0 \le j \le M-1. \end{cases} \end{cases} \tag{6.11}$$

where $p(x,t) = a(x,t) - \delta b(x,t), q(x) = b(x,t) + \frac{1}{\Delta t}$ and $H_i^j = f_i^{j+1} + \frac{\psi^j}{\Delta t}$.

To examine the semi-discrete maximum principle and the stability estimate of the temporal semi-discretization, we first rewrite (6.11) at the $(j+1)^{th}$ time level in terms of the initial-boundary value problem of the following form:

$$\begin{cases} \mathscr{L}_{C_\varepsilon}^* Y := -C_\varepsilon Y''(x) + p(x)Y'(x) + q(x)Y = H(x),\ \forall x \in \overline{\mathscr{D}}_x, \\ Y(0) = \mathscr{S}_l(t^{j+1}),\ Y(1) = \mathscr{S}_r(t^{j+1}),\ \forall t^{j+1} \in \overline{\mathscr{S}}_t^M. \end{cases} \tag{6.12}$$

where $\mathscr{L}_{C_\varepsilon}^*$ is a discrete operator, $Y(x) = \psi^{j+1}(x)$.

Lemma 6.4. *(Semi-discrete Maximum Principle): If $Y(x) \in C^2(\overline{\mathscr{D}}_x)$ is the solution of the semi-discrete problem of (6.11) such that $Y(0) \ge 0, Y(1) \ge 0$ on $\partial\overline{\mathscr{D}}_x = \overline{\mathscr{D}} \setminus \mathscr{D}$ and $\mathscr{L}_{C_\varepsilon}^* Y(x) \ge 0,\ \forall x \in \mathscr{D}a_x$, then $Y(x) \ge 0,\ \forall x \in \overline{\mathscr{D}}_x$.*

Proof. Let $x^* \in \overline{\mathscr{D}}_x$ such that $Y(x^*) = min_{x\in\overline{\mathscr{D}}_x} Y(x) < 0$ and since $Y(0) \ge 0,\ Y(1) \ge 0$ then

$x^* \notin \{0,1\}$ that is $x^* \in \mathscr{D}_x$. Moreover, since $Y^{'}(x^*) = 0$ and $Y^{"}(x^*) \geq 0$ we have that

$$\begin{aligned} \mathscr{L}^*_{C_\varepsilon}(x^*) &= -C_\varepsilon Y^{"}(x^*) + p(x^*)Y^{'}(x^*) + q(x^*)Y(x^*), \\ &\leq 0. \end{aligned}$$

But $\mathscr{L}^*_{C_\varepsilon} Y(x^*) \leq 0$ is a contradiction to our assumption $\mathscr{L}^*_{C_\varepsilon} Y(x) \geq 0$. □

Hence, we proved that the minimum of $\psi(x)$ is non-negative.

The local truncation error of the semi-discrete problem (6.11) at the $(j+1)^{th}$ time level is given by $e^{j+1} \equiv \psi(x, t^{j+1}) - \psi^{j+1}$, where ψ^{j+1} is the numerical solution of the proposed problem. Moreover, this error measures the contribution of each time step to the global error of the temporal semi-discretization.

Lemma 6.5. *(Local Error Estimate): The local error estimate in the temporal direction is given by*

$$||e^{j+1}||_\infty \leq C_1(\Delta t)^2. \tag{6.13}$$

Proof. The proof of this Lemma is similar to the proof of Lemma (3.6) of Chapter (3). □

Lemma 6.6. *(Global Error Estimate): Under the hypothesis of Lemma (6.5), the global error estimate E^{j+1} in the temporal direction is defined by*

$$||E^{j+1}||_\infty \leq C_2\Delta t. \tag{6.14}$$

Proof. The proof of this Lemma is similar to the proof of Lemma (2.7) of Chapter (2). □

Lemma 6.7. *The derivative of the solution of problem (6.4) satisfies the bound*

$$\left|\frac{d^i\psi(x,t^{j+1})}{dx^i}\right| \leq C\left(1 + {C_\varepsilon}^{-i} exp\left(\frac{p^*(1-x)}{C_\varepsilon}\right)\right),\ x \in \overline{\mathscr{D}}_x,\ \ 0 \leq i \leq 4. \tag{6.15}$$

where C is a constant independent of the perturbation parameter C_ε.

The proof of this Lemma is similar to the proof of Lemma (2.3) of Chapter (2).

6.4.2 Spatial discretization:

Reliable solutions in singular perturbation problems, where ε, require suitable numerical methods. We therefore use an exponentially fitted finite difference method that preserves the diffusion term through a fitted operator. In this section, the FOFDM is applied to reduce the effect of $C_\varepsilon \to 0$ in the boundary layer.

For each $j = 0, 1, 2, 3, \ldots M-1$, the interval-boundary value problem ((6.11)) gives the following discretized problem.

$$\begin{cases} \mathscr{L}_{C_\varepsilon}\psi^{j+1}(x) := -C_\varepsilon \frac{d^2}{dx^2}\psi^{j+1}(x) + p(x,t)\frac{d}{dx}\psi^{j+1}(x) + q(x,t)\psi^{j+1}(x) = H^{j+1}(x), \\ \begin{cases} \psi^{j+1}(0) = \mathscr{S}_l(0,t^{j+1}), & 0 \le j \le M-1, \\ \psi^{j+1}(1,t) = \mathscr{S}_r(1,t^{j+1})), & 0 \le j \le M-1. \end{cases} \end{cases} \tag{6.16}$$

To solve the singularly perturbed boundary value problem in (6.16), we use the O'Malley's theory of singular perturbation [8], the asymptotic solution up to the zeroth order for right boundary layer of near $x = 1$ as follows

$$\psi^{j+1}(x) = \psi_1^{j+1}(x) + \frac{p(1)}{p(x)}\left(\phi_r(1,t^{j+1}) - \psi_0^{j+1}(1)\right)\left(-\int_x^1 \left(\frac{p(x)}{C_\varepsilon} - \frac{q(x)}{p(x)}\right)dx\right) + O(C_\varepsilon). \tag{6.17}$$

Using Taylor's series expansion for $p(x)$ about $x = 1$ and restriction to their first terms, and simplifying gives

$$\psi^{j+1}(x) = \psi_1^{j+1}(x) + \left(\phi_r(1,t^{j+1}) - \psi_0^{j+1}(1)\right)\exp\left(-\frac{p(1)(1-x)}{C_\varepsilon}\right) + O(C_\varepsilon). \tag{6.18}$$

where ψ_1^{j+1} is the solution of the reduced problem of (6.7) when $C_\varepsilon = 0$ [50].
Discretizing the spatial domain $\overline{\mathscr{D}_x} = [0,1]$ into N equal number of sub-intervals each of length $h = 1/N$ and $x_0 = 0, x_i = ih, x_N = 1,$ for $i = 0,1,2,\ldots,N$ be the mesh points. Taking h very small, the discretized problem (6.18) can be defined as follows:

$$\begin{cases} \psi_i^{j+1}(ih) = \psi_1^{j+1}(ih) + \left(\phi_r(1,t^{j+1}) - \psi_0^{j+1}(1)\right)\exp\left(-p(1)(1/C_\varepsilon - i\rho)\right), \\ \psi_{i-1}^{j+1}(ih) = \psi_1^{j+1}(ih) + \left(\phi_r(1,t^{j+1}) - \psi_0^{j+1}(1)\right)\exp\left(-p(1)(1/C_\varepsilon - (i-1)\rho)\right), \\ \psi_{i+1}^{j+1}(ih) = \psi_1^{j+1}(ih) + \left(\phi_r(1,t^{j+1}) - \psi_0^{j+1}(1)\right)\exp\left(-p(1)(1/C_\varepsilon - (i+1)\rho)\right). \end{cases} \tag{6.19}$$

where $\rho = h/C_\varepsilon$.
To handle the oscillations or abrupt changes to the solution of the proposed problem due to the presence of the perturbation parameter C_ε, we introduce an exponential fitting factor $\sigma(\rho)$ on the diffusion term and write as

$$-\sigma(\rho)C_\varepsilon\delta_x^2\psi^{j+1}(x) + p(x)\delta_x^-\psi^{j+1}(x) + q(x)\psi^{j+1}(x) = H^j(x). \tag{6.20}$$

Finite Difference Operators: On uniform mesh points $\{x_i\}_{i=0}^N$ with mesh length $h = x_{i+1} - x_i$ and any mesh function ψ_i, we denote the following finite difference operators for multiple purposes.

$$\delta^{+}\psi_i^j = \frac{\psi_{i+1}^j - \psi_i^j}{h}, \quad \delta_x^{-}\psi_i^j = \frac{\psi_i^j - \psi_{i-1}^j}{h},$$
$$\delta_x^0\psi_i^j = \frac{\psi_{i+1}^j - \psi_{i-1}^j}{2h} \text{ and } \delta_x^2\psi_i^j = \frac{\psi_{i+1}^j - 2\psi_i^j + \psi_{i-1}^j}{h^2}. \tag{6.21}$$

Using the difference operators in (6.21) within (6.20), together with the midpoint upwind approach, we obtain

$$-\sigma(\rho)C_\varepsilon \frac{\psi_{i+1}^{j+1} - 2\psi_i^{j+1} + \psi_{i-1}^{j+1}}{h^2} + p_{i-1/2}\frac{\psi_i^j - \psi_{i-1}^{j+1}}{h} + q_{i-1/2}\psi_i^{j+1} = H_{i-1/2}^j, \tag{6.22}$$

where

$$\begin{cases} p_{i-1/2} = \frac{p_i + p_{i-1}}{2}, \\ q_{i-1/2} = \frac{q_i + q_{i-1}}{2}, \\ H_{i-1/2}^j = \frac{H_i + H_{i-1}^j}{2}. \end{cases}$$

Multiplying (6.22) by h, where $h \to 0$ and truncating the term $h\left(H_{i-1/2}^j - q(x_i)\psi_i^{j+1}\right)$ gives

$$-\frac{\sigma(\rho)}{\rho}\left(\psi_{i+1}^{j+1} - 2\psi_i^{j+1} + \psi_{i-1}^{j+1}\right) + p_i\left(\psi_{i+1}^j - \psi_{i-1}^{j+1}\right) = 0. \tag{6.23}$$

Using (6.19) in to (6.23) and simplifying it, we get the required fitting factor as follows

$$\sigma(\rho) = \rho p(x_i)\left(\frac{1 - \exp(-\rho p(x_i)}{\exp(\rho p(x_i) - 2 + \exp(-\rho p(x_i)}\right). \tag{6.24}$$

The finite difference method in (6.22) with the data on interval-boundary becomes

$$\begin{cases} \mathscr{L}_{C_\varepsilon}^{N,M} := -\sigma(\rho)C_\varepsilon \frac{\psi_{i+1}^{j+1} - 2\psi_i^{j+1} + \psi_{i-1}^{j+1}}{h^2} + p_{i-1/2}\frac{\psi_i^j - \psi_{i-1}^{j+1}}{h} + q_{i-1/2}\psi_i^{j+1} = H_{i-1/2}^j, \\ \begin{cases} \psi^{j+1}(0) = \phi_l(0, t^{j+1}), & 0 \le j \le M-1, \\ \psi^{j+1}(1,t) = \phi_r(1, t^{j+1})), & 0 \le j \le M-1. \end{cases} \end{cases} \tag{6.25}$$

6.4.3 The Fully Discrete Scheme

Using (6.24) into (6.22) and simplifying gives the following tri-diagonal system of equations.

$$\begin{cases} r_i^- \psi_{i-1} + r_i^0 \psi_i + r_i^+ \psi_{i+1} = H_{i-\frac{1}{2}}^j, \\ \begin{cases} r_i^- = -\frac{\sigma(\rho)C_\varepsilon}{h.^2} - \frac{p_{i-\frac{1}{2}}}{h}, \\ r_i^0 = \frac{2\sigma(\rho)C_\varepsilon}{h^2} + \frac{p_{i-\frac{1}{2}}}{h} + q_{i-\frac{1}{2}}, \\ r_i^+ = -\frac{\sigma(\rho)C_\varepsilon}{h^2}, \\ H_{i-\frac{1}{2}}^j = \frac{1}{2}\left(H_i^j + H_{i-1}^j\right). \end{cases} \end{cases} \tag{6.26}$$

Because the tridiagonal system in (6.26) is a nonsingular M-matrix by theorem (2.1) of Chapter (2), we solve it using matrix inverse method.

6.5 Uniform Convergence Analysis

As the fully discretized system matrix of (6.26) is an M-matrix, the scheme satisfies the discrete maximum principle and guarantees stable behavior.

Lemma 6.8. *(Discrete Maximum Principle): Let $z^{j+1}(x_i)$ be any mesh function satisfying $z^{j+1}(x_0) \geq 0$ and $z^{j+1}(x_N) \geq 0$. If $\mathscr{L}_{C_\varepsilon}^{N,M} z^{j+1}(x_i) \geq 0$, for $1 \leq i \leq N-1$, then $z^{j+1}(x_i) \geq 0$, for $0 \leq i \leq N$ [58].*

Proof. Let us choose the point $j \geq 1$ such that $z^{j+1}(x_i^*) = min_{x_i} z^{j+1}(x_i)$, for $1 \leq i \leq N-1$. If $z^{j+1}(x_i^*) \geq 0$, the proof is completed. But for the choice $z^{j+1}(x_i^*)$ is minimum it is seen that $z^{j+1}(x_{i+1}^*) - z^{j+1}(x_i^*) \geq 0$ and $z^{j+1}(x_i^*) - z^{j+1}(x_{i-1}^*) \leq 0$.
Using these mesh function in (6.25), we get

$$\begin{aligned} \mathscr{L}_{C_\varepsilon}^{N,M} z^{j+1}(x_i^*) &= -\sigma(\rho)C_\varepsilon \frac{(z^{j+1}(x_{i+1}^*) - z^{j+1}(x_i^*) - (z^{j+1}(x_i^* - z^{j+1}(x_{i-1}^*)))}{h^2} \\ &+ p(x_{i-1/2}^*)\frac{z(x_i^*)^{j+1} - z^{j+1}(x_{i-1}^*)}{h} + q(x_{i-1/2}^*) z^{j+1}(x_i^*), \\ &\leq 0, \text{ since } p(x_{i-1/2}^*) \geq 0 \text{ and } q(x_{i-1/2}^*) \geq 0. \end{aligned}$$

This contradicts to our assumption $\mathscr{L}_{C_\varepsilon}^{N,M} z^{j+1}(x_i) \geq 0$. This shows that $z^{j+1}(x_i^*) \geq 0$.
Hence, we concluded that the minimum of $z^{j+1}(x_i)$ is non-negative. □

Lemma 6.9. *(Uniform Stability Estimate): Let ψ_i^{j+1} be any discrete solution of (6.25) such that $\psi_0^{j+1} = 0 = \psi_N^{j+1}$, then ψ_i^{j+1} satisfies the bound*

$$|\psi(x,t)| \leq \beta^{-1} ||H_{i-1/2}^j|| + max\left\{|\mathscr{S}_l(0,t^{j+1})|, |\mathscr{S}_r(1,t^{j+1})||\right\}.$$

Proof. The proof of this lemma is similar to the proof of Lemma(2.5) of chapter (2). □

Lemma 6.10. *For a fixed mesh number N and for $C_\varepsilon \to 0$, it holds that*

$$\lim_{C_\varepsilon\to 0}\max_{1\le i\le N-1}\frac{\exp\left(\frac{-p^* x_i}{C_\varepsilon{}^j}\right)}{C_\varepsilon{}^j}=0 \;\; and \;\; \lim_{C_\varepsilon\to 0}\max_{1\le i\le N-1}\frac{\exp\left(\frac{-p^*(1-x_i)}{C_\varepsilon{}^j}\right)}{C_\varepsilon{}^j}=0. \tag{6.27}$$

where $x_i = ih$, $h = 1/N$, $1 \le i \le N-1$ and $p_{i-1/2} \ge p^* > 0$, $m = 0,1,2,\ldots M$.

Theorem 6.1. Let $\psi(x_i,t^{j+1})$ and ψ_i^{j+1} be the solutions of (6.4) and (6.26) respectively. Then the truncation error satisfies the bound

$$\left|\mathscr{L}_{C_\varepsilon}^{N,M}\left(\psi(x_i,t^{j+1})-\psi_i^{j+1}\right)\right| \le Ch\left(1+C_\varepsilon{}^{-4}\max_{1\le i\le N-1}\exp\left(\frac{p^*(1-x)}{C_\varepsilon}\right)\right). \tag{6.28}$$

Proof. Let the truncation error be given as

$$\begin{aligned}\mathscr{L}_{C_\varepsilon}^{N,M}\left(\psi(x_i,t^{j+1})-\psi_i^{j+1}\right) &= -C_\varepsilon\sigma(\rho)\left(\psi_{xx}(x_i)-\delta^+\delta^-\psi(x_i)\right)\\ &\quad +p(x_i)\left(\psi_x(x_i)-\delta^-\psi(x_i)\right)\right). \end{aligned} \tag{6.29}$$

where $C_\varepsilon\sigma(\rho) = p_i h\left(\frac{1-\exp(-\rho p(x_i)}{\exp(\rho p(x_i)-2+\exp(-\rho p(x_i)}\right)$, since $\rho = \frac{h}{C_\varepsilon}$. Taking the limit for $C_\varepsilon \to 0$, we get

$$\lim_{C_\varepsilon\to 0} C_\varepsilon\sigma(\rho) = \lim_{C_\varepsilon\to 0} p_i h\left(\frac{1-\exp(-\rho p(x_i)}{\exp(\rho p(x_i)-2+\exp(-\rho p(x_i)}\right) = Ch,$$

where C is a constant independent of the mesh length h and the parameter C_ε.
The approximation for the derivatives is defined as follows

$$\left|\psi_{xx}^{j+1}-\delta^+\delta^-\psi(x_i)\right| \le Ch^2\left|\left|\psi_{xxxx}^{j+1}(\eta)\right|\right|, \left|\psi_x^{j+1}-\delta^-\psi(x_i)\right| \le Ch\left|\left|\psi_{xx}^{j+1}(\eta)\right|\right|. \tag{6.30}$$

where $\left|\left|\psi_k^{j+1}(\eta)\right|\right| = \max_{0\le i\le N}\left|\psi_k^{j+1}(x_i)\right|$, $x_{i-1} \le \eta \le x_i$, $k = 2,4$. Using these bounds (6.29) can be reduced to the following form:

$$\left|\mathscr{L}_{C_\varepsilon}^{N,M}\left(\psi(x_i,t^{j+1})-\psi_i^{j+1}\right)\right| \le Ch^2\left|\left|\psi_{xxxx}^{j+1}(\eta)\right|\right| + Ch\left|\left|\psi_{xx}^{j+1}(\eta)\right|\right|. \tag{6.31}$$

Using the bounds in Lemma (6.7) into (6.29) gives

$$\begin{aligned}\left|\mathscr{L}_{C_\varepsilon}^{N,M}\left(\psi(x_i,t^{j+1})-\psi_i^{j+1}\right)\right| &\le Ch^2\left(1+C_\varepsilon{}^{-4}\exp\left(\frac{p^*(1-x)}{C_\varepsilon}\right)\right),\\ &+ Ch\left(1+C_\varepsilon{}^{-2}\exp\left(\frac{p^*(1-x)}{C_\varepsilon}\right)\right)\\ &\le Ch\left(1+C_\varepsilon{}^{-4}\max_{1\le i\le N-1}\exp\left(\frac{p^*(1-x)}{C_\varepsilon}\right)\right).\end{aligned}$$

since $C_\varepsilon^- 2 \leq C_\varepsilon^- 4$.
Using the results of Lemma (5.12), we establish the following generalized theorem. $\square$

Theorem 6.2. The discrete solution in (6.25) satisfies the uniform bound

$$\max_{0\leq i\leq N} \left|\psi(x_i,t^{j+1}) - \psi_i^{j+1}\right| \leq Ch. \tag{6.32}$$

From this, we conclude that the proposed midpoint upwind scheme is first-order accurate.
Theorem 6.3. Let $\psi(x_i,t^{j+1})$ and ψ_i^{j+1} be the solutions of (6.4) and (6.25) respectively. Then uniform bounds of the proposed scheme is defined by

$$\sup_{0<C_\varepsilon\ll 1}\max_{0\leq i\leq N} \left|\psi(x_i,t^{j+1}) - \psi_i^{j+1}\right| \leq C(h+\Delta t). \tag{6.33}$$

As a result, the proposed method is first-order accurate in both space and time prior to extrapolation. In the following section, we employ Richardson extrapolation to obtain higher-accuracy results.

6.6 Richardson Extrapolation Technique

In this section, we applied the Richardson extrapolation is a technique to improve both the accuracy and order of convergence of the proposed scheme with a lower computational cost. Using Theorem(6.3) at each j^{th} time level, we have the bound of the form

$$\left|\psi_i^j - \overline{\psi}_i^j\right| \leq C(h+\Delta t). \tag{6.34}$$

where ψ_i^j and $\overline{\psi}_i^j$ are numerical solutions on the meshes $\mathscr{D}_{xt}^{N,M}$ and $\mathscr{D}_{xt}^{2N,2M}$ respectively so that that C is a parameter independent constant.
Moreover, since $\overline{\psi}_i^j$ is obtained by doubling the mesh $\mathscr{D}^{N,M}$ then, the mesh sizes $h\neq 0$ and $\Delta t\neq 0$ in Eq.(6.34) becomes

$$\psi_i^j(x_i,t^j) - \overline{\psi}_i^j(x_i,t^j) \leq C(h^2+\Delta t^2) + R^{N,M},\ (x_i,t^j)\in \mathscr{D}_{xt}^{N,M}. \tag{6.35}$$

Again using the mesh sizes $h/2,\ \Delta t/2 \neq 0$ Eq.(6.35) becomes

$$\psi_i^j(x_i,t^j) - \overline{\psi}_i^j(x_i,t^j) \leq C\left(\frac{h^2}{4}+\frac{\Delta t^2}{4}\right) + R^{2N,2M},\ (x_i,t^j)\in \mathscr{D}_{xt}^{2N,2M}. \tag{6.36}$$

where the remainders $R^{N,M}$ and $R^{2N,2M}$ are $O(h^2+\Delta t^2)$. Taking the difference of Eq.(6.36) and Eq.(6.34) we get the subsequent general extrapolation formula.

$$\left(\psi_i^j\right)^{ext} = \frac{4\overline{\psi}_i^j - \psi_i^j}{3}. \tag{6.37}$$

where $\left(\psi_i^j\right)^{ext}$ is the numerical solution obtained from the Richardson extrapolation technique with truncated error of the form

$$\left|\psi_i^j - (\psi_i^j)^{ext}\right| \le C(h^2+\Delta t^2). \tag{6.38}$$

From these discussions, we generalized the following Theorem for the general purpose of the Richardson extrapolation technique.

Theorem 6.4. Let $(\psi_i^j)^{ext}$ be the numerical solution of Eq (6.25) obtained after the Richardson extrapolation technique applied and ψ_i^j be the numerical solution of the proposed model equation (6.4).Then,the maximum absolute error encountered is defined by

$$\sup_{0<C_\varepsilon\ll 1}\max_{0\le i,j\le N,M}\left|\psi_i^j - (\psi_i^j)^{ext}\right| \le C(h^2+\Delta t^2). \tag{6.39}$$

As a result of Richardson extrapolation technique, the proposed method is found to be second-order accurate in both the spatial and temporal directions.

6.7 Numerical Results and Discussions

The proposed scheme is additionally validated through two model problems, where $\varepsilon-$uniform maximum absolute errors and convergence rates are computed to examine its accuracy and numerical performance, as outlined in Chapter (2).

Example 6.1. Consider SPPDDEs of the following form presented in [57] with $\delta = 0.9*\varepsilon$:

$$\begin{cases} \psi_t(x,t) - \varepsilon\psi_{xx}(x,t) + (2-x^2)\psi_x(x-\delta,t) + (x^2+1+cos(\pi x))\psi(x-\delta,t) \\ = 10t^2(1-x)exp(-t), & \forall(x,t)\in\mathscr{D}_{xt} = (0,1)\times(0,T], T>0, \\ \mathscr{S}_0(x,t) = 0, & \forall x\in\overline{\mathscr{D}}_x \text{ and } t=0, \\ \mathscr{S}_l(x,t) = 0, & \forall(x,t)\in[-\delta,0]\times\overline{\mathscr{D}}_t, \\ \mathscr{S}_r(x,t) = 0, & x=1 \text{ and } \forall t\in\overline{\mathscr{D}}_t. \end{cases}$$

Example 6.2. Consider SPPDDEs the following forms as outlined in [106] with $\delta = 0.3 * \varepsilon$:

$$\begin{cases} \psi_t(x,t) - \varepsilon\psi_{xx}(x,t) + (2-x^2)\psi_x(x-\delta,t) + (3-x)\psi(x-\delta,t) \\ = exp(t)sin(\pi x(1-x)), \qquad \forall (x,t) \in \mathscr{D}_{xt} = (0,1)\times(0,T], T>0, \\ \mathscr{S}_0(x,t) = 0, \qquad \forall x \in \overline{\mathscr{D}}_x \text{ and } t = 0, \\ \mathscr{S}_l(x,t) = 0, \qquad \forall (x,t) \in [-\delta, 0] \times \overline{\mathscr{D}}_t, \\ \mathscr{S}_r(x,t) = 0, \qquad x = 1 \text{ and } \forall t \in \overline{\mathscr{D}}_t. \end{cases}$$

Let $\psi^{N,M}(x_i,t^j)$ and $\psi^{2N,2M}(x_{2i},t_{2j})$ be the numerical solutions before Richardson extrapolation with mesh lengths $(h, \Delta t \neq 0)$ and $(h/2, \Delta t/2 \neq 0)$ respectively, then

- The maximum absolute error is given by

$$E_{\varepsilon}^{N,M} = \max_{0\le i,j\le N,M} \left|\psi^{N,M}(x_i,t^j) - \psi^{2N,2M}(x_{2i},t_{2j})\right|. \tag{6.40}$$

- The $\varepsilon-$ uniform absolute error is given by

$$E^{N,M} = \max_{\varepsilon} E_{\varepsilon}^{N,M}. \tag{6.41}$$

- Corresponding ε-uniform order of convergence is $R^{N,M} = log_2\left(\frac{E^{N,M}}{E^{2N,2M}}\right)$.

Similarly, let $\psi^{2N,2M}(x_i,t^j)$ and $(\psi_i^j)^{ext}$ be the numerical solutions with mesh lengths $(h/2, \Delta t/2 \neq 0)$ and $(h/4, \Delta t/4 \neq 0)$ respectively, then

- The maximum absolute error is given by

$$E_{\varepsilon,ext}^{N,M} = \max_{0\le i,j\le N,M} \left|\psi^{2N,2M}(x_{2i},t_{2j}) - (\psi_i^j)^{ext}(x_i,t_j)\right|. \tag{6.42}$$

- The $\varepsilon-$ uniform maximum absolute error is given by

$$E_{ext}^{N,M} = \max_{\varepsilon} E_{\varepsilon,ext}^{N,M}. \tag{6.43}$$

- Corresponding ε, ext-uniform order of convergence is $R_{ext}^{N,M} = log_2\left(\frac{E_{ext}^{N,M}}{E^{2N,2M}}\right)$.

Table 6.1: $E^{N,M}$ and $R^{N,M}$ for Example (6.1) with $\delta = 0.9 * \varepsilon$

$\varepsilon \downarrow$	$N = 16$ $M = 16$	$N = 32$ $M = 32$	$N = 64$ $M = 64$	$N = 128$ $M = 128$
Before Extrapolation				
10^{-4}	$2.4492e-03$	$1.4391e-03$	$7.5033e-04$	$3.2436e-04$
10^{-6}	$2.4490e-03$	$1.4390e-03$	$7.5022e-04$	$3.2429e-04$
10^{-8}	$2.4490e-03$	$1.4390e-03$	$7.5022e-04$	$3.2429e-04$
10^{-10}	$2.4490e-03$	$1.4390e-03$	$7.5022e-04$	$3.2429e-04$
10^{-12}	$2.4490e-03$	$1.4390e-03$	$7.5022e-04$	$3.2429e-04$
$E^{N,M}$	$2.4492e-03$	$1.43910e-03$	$7.5033e-04$	$3.2436e-04$
$R^{N,M}$	0.7671	0.9396	1.2099	—
Results in [57]				
$E^{N,M}$	$1.4608e-02$	$8.1600e-03$	$4.3077e-03$	$2.2124e-03$
$R^{N,M}$	0.8401	0.9217	0.9613	—
After Extrapolation				
10^{-4}	$1.2102e-03$	$3.0423e-04$	$7.6105e-05$	$1.8737e-05$
10^{-6}	$1.2102e-03$	$3.0423e-04$	$7.6105e-05$	$1.8737e-05$
10^{-8}	$1.2102e-03$	$3.0423e-04$	$7.6105e-05$	$1.8737e-05$
10^{-10}	$1.2102e-03$	$3.0423e-04$	$7.6105e-05$	$1.8737e-05$
10^{-12}	$1.2102e-03$	$3.0423e-04$	$7.6105e-05$	$1.8737e-05$
$E_{ext}^{N,M}$	$1.2102e-03$	$3.0423e-04$	$7.6105e-05$	$1.8737e-05$
$R_{ext}^{N,M}$	1.9920	1.9991	2.0221	—
Results in [57]				
$E_{ext}^{N,M}$	$8.1605e-03$	$2.2125e-03$	$5.6425e-04$	$1.4182e-04$
$R_{ext}^{N,M}$	1.8830	1.9713	1.9923	—

Table 6.2: $E^{N,M}$ and $R^{N,M}$ for Example (6.1) with $\varepsilon = 10^{-4}$ and different values of δ

$\varepsilon \downarrow$	$N = 16$ $M = 16$	$N = 32$ $M = 32$	$N = 64$ $M = 64$	$N = 128$ $M = 128$
Before Extrapolation				
$\delta = 0.1 * \varepsilon$	$1.8733e-03$	$1.1436e-03$	$5.5011e-04$	$2.4793e-04$
$\delta = 0.3 * \varepsilon$	$1.8698e-03$	$1.1423e-03$	$5.4986e-04$	$2.4789e-04$
$\delta = 0.5 * \varepsilon$	$1.8673e-03$	$1.1413e-03$	$5.4967e-04$	$2.4844e-04$
$\delta = 0.7 * \varepsilon$	$1.8654e-03$	$1.1406e-03$	$5.4954e-04$	$2.4844e-04$
$\delta = 0.9 * \varepsilon$	$1.8640e-03$	$1.1400e-03$	$5.4943e-04$	$2.4841e-04$
$E^{N,M}$	$1.8733e-03$	$1.1436e-03$	$5.5011e-04$	$2.4793e-04$
$R^{N,M}$	0.7120	1.0561	1.1495	—
After Extrapolation				
$\delta = 0.1 * \varepsilon$	$1.5216e-03$	$4.4229e-04$	$1.2780e-04$	$3.6638e-05$
$\delta = 0.3 * \varepsilon$	$1.5157e-03$	$4.4058e-04$	$1.2739e-04$	$3.6496e-05$
$\delta = 0.5 * \varepsilon$	$1.5114e-03$	$4.3948e-04$	$1.2729e-04$	$3.6492e-05$
$\delta = 0.7 * \varepsilon$	$1.5082e-03$	$4.3880e-04$	$1.2718e-04$	$3.6384e-05$
$\delta = 0.9 * \varepsilon$	$1.5057e-03$	$4.2405e-04$	$1.2701e-04$	$3.6374e-05$
$E_{ext}^{N,M}$	$1.5216e-03$	$4.4229e-04$	$1.2780e-04$	$3.6638e-05$
$R_{ext}^{N,M}$	1.7825	1.7911	1.8025	—

Table 6.3: $E^{N,M}$ and $R^{N,M}$ for Example (6.2) with $\delta = 0.3 * \varepsilon$

$\varepsilon \downarrow$	$N = 32$ $M = 60$	$N = 64$ $M = 120$	$N = 128$ $M = 240$	$N = 256$ $M = 480$
Before Extrapolation				
2^{-8}	$1.8350e-03$	$9.8553e-04$	$5.5043e-04$	$2.5072e-04$
2^{-10}	$1.8738e-03$	$1.0576e-03$	$5.5729e-04$	$2.5008e-04$
2^{-12}	$1.8736e-03$	$1.0583e-03$	$5.5401e-04$	$2.7525e-04$
2^{-14}	$1.8735e-03$	$1.0582e-03$	$5.5386e-04$	$2.7537e-04$
2^{-16}	$1.8735e-03$	$1.0581e-03$	$5.5382e-04$	$2.7532e-04$
2^{-18}	$1.8735e-03$	$1.0581e-04$	$5.5381e-04$	$2.7531e-04$
2^{-20}	$1.8735e-03$	$1.0581e-03$	$5.5381e-04$	$2.7531e-04$
$E^{N,M}$	$1.8738e-03$	$1.0583e-03$	$5.5729e-04$	$2.7537e-04$
$R^{N,M}$	0.8251	0.9337	1.0275	—
Results in [106]				
$E^{N,M}$	$7.3609e-03$	$4.1402e-03$	$2.1813e-03$	$1.1057e-03$
$R^{N,M}$	0.8302	0.9245	0.9802	—
After Extrapolation				
2^{-8}	$1.2332e-03$	$3.3084e-04$	$6.0476e-05$	$1.5198e-05$
2^{-10}	$1.2312e-03$	$3.3024e-04$	$6.0446e-05$	$1.5158e-05$
2^{-12}	$1.2311e-03$	$3.3013e-04$	$6.0423e-05$	$1.5134e-05$
2^{-14}	$1.2311e-03$	$3.3013e-04$	$6.0423e-05$	$1.5134e-05$
2^{-16}	$1.2311e-03$	$3.3013e-04$	$6.0423e-05$	$1.5134e-05$
2^{-18}	$1.2311e-03$	$3.3013e-04$	$6.0423e-05$	$1.5134e-05$
2^{-20}	$1.2311e-03$	$3.3013e-04$	$6.0423e-05$	$1.5134e-05$
$E_{ext}^{N,M}$	$1.2332e-03$	$3.3084e-04$	$6.0476e-05$	$1.5198e-05$
$R_{ext}^{N,M}$	1.8982	1.9905	1.9925	—
Results in [106]				
$E_{ext}^{N,M}$	$4.1921e-03$	$3.9157e-03$	$1.0252e-03$	$2.5847e-04$
$R_{ext}^{N,M}$	1.6062	1.9334	1.9878	—

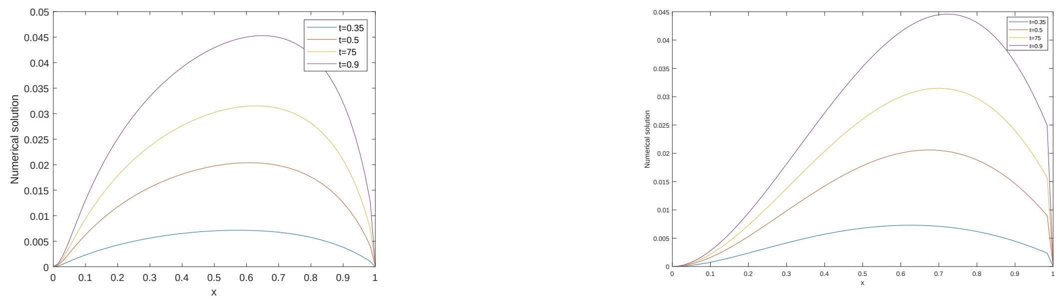

(a) $\varepsilon = 10^{-1}$ (b) $\varepsilon = 10^{-8}$

Figure 6.1: 2D Solution graphs for Example (6.1) with $\delta = 0.9\varepsilon, N = 128, M = 128$

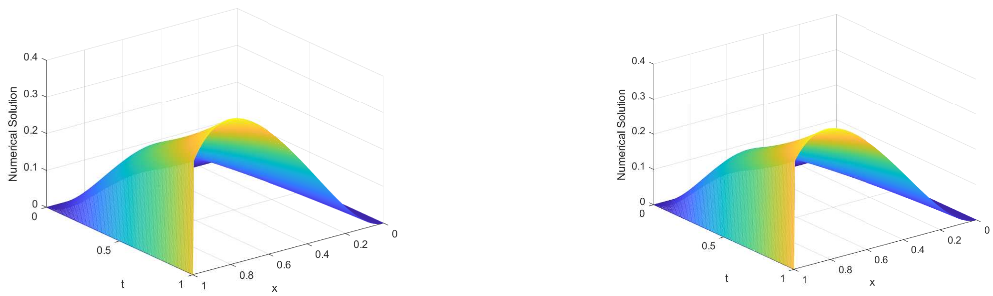

(a) $\varepsilon = 10^{-1}$ (b) $\varepsilon = 10^{-8}$

Figure 6.2: 3D Solution graphs for Example (6.2) with $\delta = 0.9\varepsilon, N = 128, M = 128$

To validate the practical effectiveness of the proposed scheme, we examine two model examples. We present the maximum absolute errors and their corresponding orders of convergence based on the results reported in Tables (6.1), (6.2), and (6.3), corresponding to Examples (6.1) and (6.2).

For a fixed perturbation parameter ε, we notice that refining the mesh by increasing the values of N and M along each row consistently enhances the accuracy and improves the observed convergence rates. On the other hand, when the mesh sizes N and M are kept fixed and the perturbation parameter ε is reduced down each column, the maximum absolute errors remain essentially unchanged, indicating parameter-uniform stability. These results confirm that the proposed scheme achieves uniform convergence with higher-order accuracy.

Furthermore, the results in Tables (6.1) and (6.2) show that applying Richardson extrapolation improves the accuracy of the scheme from first-order to second-order. In addition, Table (6.3) shows that for $\varepsilon = 10^{-4}$, increasing the magnitude of the delay parameter δ down each column reduces the boundary layer thickness and yields smaller maximum absolute errors.

The two-dimensional and three-dimensional plots in Figures (6.1) and (6.2) demonstrate that decreasing the perturbation parameter induces a sharp right boundary layer near $x = 1$. Finally, Tables (6.1) and (6.2), corresponding to Examples (6.1) and (6.2), demonstrate that the proposed method outperforms several existing approaches reported in [57, 106].

6.8 Conclusion

In this chapter, we have developed a second-order uniformly convergent numerical scheme for singularly perturbed differential difference equations. The proposed method combines the implicit Euler scheme in time with the fitted midpoint upwind finite difference scheme in space, both implemented on uniform meshes.

We have verified the reliability and robustness of the scheme through two representative model problems. We have systematically analyzed the influence of the perturbation parameter on the numerical solution using maximum absolute errors and observed orders of convergence, supported by detailed tables and graphical illustrations.

The numerical results consistently confirm the theoretical analysis, demonstrating parameter-uniform convergence and high accuracy of the proposed method. Moreover, the scheme exhibits superior performance when compared with several existing approaches reported in the literature. Overall, the presented results establish the efficiency, stability, and applicability of the proposed computational approach for solving singularly perturbed differential difference equations.

Chapter 7

A Hybrid Fitted Scheme for Singularly Perturbed Parabolic Problems with a Small Shift Parameter in the Convection and Reaction Terms

This chapter presents a fitted numerical scheme for singularly perturbed differential equations with a small negative shift in the convection and reaction terms, arising in applications such as neural networks, population dynamics, epidemiology, heat transfer with memory effects, and delayed chemical reactions. The small diffusion parameter $\varepsilon\,(0 < \varepsilon \ll 1)$ induces a right boundary layer with steep gradients, where classical methods on uniform meshes fail. To address this, a hybrid scheme is proposed, combining Crank–Nicolson in time on uniform meshes with a spatial scheme that uses midpoint upwind and central differences in coarse and layer regions on Shishkin meshes. Stability and uniform convergence analyses show the scheme is uniformly convergent with order $O\left(N^{-2}\ln^2 N + (\Delta t)^2\right)$. Numerical results confirm its superior performance compared with several existing methods.

7.1 Introduction

Many real-world problems in science and engineering can be modeled as parameter-dependent differential equations. When the highest-order derivative is multiplied by a small parameter $\varepsilon\,(0 < \varepsilon \ll 1)$, the system is classified as a SPPDE. If the equation also involves delayed or advanced arguments, it is referred to as a SPPDDEs. Such equations commonly arise in physiological kinetics [102], population dynamics, epidemiology [103], and control theory.

Due to the small parameter ε multiplying the highest-order derivative, the solution develops boundary and/or interior layers, in which classical numerical schemes lose accuracy unless very fine discretizations are used, leading to significant computational cost [78]. These challenges have motivated the development of parameter-uniform or fitted numerical methods [2, 78, 63, 36, 106, 107], including fitted mesh methods on piecewise-uniform meshes, fitted operator techniques, and domain decomposition methods on uniform meshes.

Recently, several studies have addressed the numerical solution of time-delay SPPDDEs. For example, An accelerated second-order parameter-uniformly convergent scheme for reaction–diffusion problems with small time lag was proposed in [37]. A second-order hybrid scheme for singularly perturbed convection–diffusion problems with small time lag [44]. A domain decomposition method was developed in [41] for reaction–diffusion problems with small delays. A uniformly convergent numerical collocation scheme was proposed in [108]. A nonstandard fitted operator scheme for the numerical treatment of problems with large time delays is presented in [69].

In contrast, relatively few studies have addressed SPPDDEs with small shift parameters in the convection and reaction terms. Second-order accurate solutions were achieved in [57] using a θ-method for temporal discretization together with a non-standard finite difference scheme for spatial discretization and Richardson extrapolation. A Shishkin mesh approach, together with Crank–Nicolson temporal discretization and upwind spatial discretization, is given a second-order accuracy [109]. An accelerated second-order method based on the implicit Euler scheme in time and upwind discretization on uniform meshes is introduced in [110].

Motivated by the limited accuracy and weak convergence of existing schemes, and following the observations reported in [59], a second-order fitted numerical scheme is developed for SPPPDEs with small spatial shift parameters in the convection and reaction terms. The method combines Crank-Nicolson time discretization with a hybrid spatial scheme using midpoint upwind in the outer region and central difference within the boundary layer on Shishkin meshes.

7.2 Problem formulation

Consider singularly perturbed parabolic differential–difference equations with a small shift [110] in the convection and reaction terms, as defined in governing problem (1.14).

$$\begin{cases} \psi_t - \varepsilon\psi_{xx} + a(x,t)\psi_x(x-\delta,t) + b(x,t)\psi(x-\delta,t) = f(x,t), \quad \forall (x,t) \in \mathscr{D}_{xt}, \\ \begin{cases} \psi(x,t) = \mathscr{S}_0(x,t), & \mu_0 = [0,1]\times[-\delta,0], \\ \psi(0,t) = \mathscr{S}_l(t) & \mu_l = \{(0,t) : 0 \le t \le T\}, \\ \psi(1,t) = \mathscr{S}_r(t)), & \mu_r = \{(1,t) : 0 \le t \le T\}. \end{cases} \end{cases} \tag{7.1}$$

where $\varepsilon, (0 < \varepsilon \ll 1)$, is a singular perturbation parameter and δ is a small negative shift parameter δ to satisfy the relation $\delta = O(\varepsilon)$. To control sudden blow ups in the convection and reaction terms, the functions $a(x,t), b(x,t)$ and $f(x,t)$ on $\overline{\mathscr{D}}_{xt}$are assumed to be sufficiently smooth, bounded, and satisfy

$$a(x,t) \geq A^* > 0, b(x,t) \geq B^* > 0 \quad \forall (x) \in \overline{\mathscr{D}}_{xt}. \tag{7.2}$$

Since the problem under consideration in (7.1) is not in its standard form, we employ Taylor-series approximations as follows:

$$\begin{cases} \psi_x(x-\delta,t) = \psi_x - \delta\psi_{xx} + O(\delta^2), \\ \psi(x-\delta,t) = \psi - \delta\psi_x + \frac{\delta^2}{2}\psi_{xx} + O(\delta^3). \end{cases} \tag{7.3}$$

Substituting (7.3) into (7.1) yields the standard form of the convection-diffusion-reaction problem, along with its initial and boundary conditions of the following form:

$$\begin{cases} \psi_t - C_\varepsilon \psi_{xx}(x,t) + A(x,t)\psi_x(x,t) + b(x,t)\psi(x,t) = f(x,t), \forall (x,t) \in \mathscr{D}_{xt}, \\ \begin{cases} \psi(x,0) = \mathscr{S}_0(x), & \forall x \in \overline{\mathscr{D}}_x, \\ \psi(0,t) = \mathscr{S}_l(0,t), & \forall (x,t) \in \overline{\mathscr{D}}_t, \\ \psi(1,t) = \mathscr{S}_r(1,t)), & \forall (x,t) \in \overline{\mathscr{D}}_t. \end{cases} \end{cases} \tag{7.4}$$

where $C_\varepsilon = \varepsilon - \frac{\delta^2}{2}B^* + \delta A^*$ such that $(0 < C_\varepsilon \ll 1)$, and $A(x,t) = a(x) - \delta b(x,t)$. For small values of the shift parameter δ, the problems in (7.1) and (7.4) are asymptotically equivalent, as their difference is of order $O(\delta^2)$. To ensure the existence of a unique solution of problem (7.4), we assumed that the functions $A(x,t), b(x,t)$ and $f(x,t)$ on $\overline{\mathscr{D}}_{xt}$ are sufficiently smooth, bounded and satisfy

$$A(x,t) \geq \alpha > 0, \quad \forall (x) \in \overline{\mathscr{D}}_{xt}. \tag{7.5}$$

7.3 Properties of the Analytic Solution

The existence of a unique solution of (7.4) can be established under the assumption that the problem data are Hölder continuous and satisfy the necessary compatibility conditions at the corner points, as outlined in [44]. The required compatibility condition at the corner points $(0,0)$ and $(1,0)$ are defined as $\mathscr{S}_0(0,0) = \mathscr{S}_l(0)$, $\mathscr{S}_0(1,0) = \mathscr{S}_r(0)$ to satisfy

$$\begin{cases} \frac{\partial \mathscr{S}_l(0)}{\partial t} - C_\varepsilon \frac{\partial^2 \mathscr{S}_0(0,0)}{\partial x^2} + A(0)\frac{\partial \mathscr{S}_0(0,0)}{\partial x} + b(0,0)\mathscr{S}_0(0,0) = f(0,0), \\ \frac{\partial \mathscr{S}_r(0)}{\partial t} - C_\varepsilon \frac{\partial^2 \mathscr{S}_0(1,0)}{\partial x^2} + A(0)\frac{\partial \mathscr{S}_0(1,0)}{\partial x} + b(1,0)\mathscr{S}_0(1,0) = f(1,0). \end{cases} \tag{7.6}$$

where $\mathscr{S}_0(x,t)$, $\mathscr{S}_l(x,t)$ and $\mathscr{S}_r(x,t)$ are sufficiently smooth functions. Under these conditions and the bound in (7.5), problem (7.4) admits a unique solution $\psi(x,t)$ with a right boundary layer of width $O(C_\varepsilon)$ at $x = 1$ as $C_\varepsilon \to 0$.

Lemma 7.1. *(Continuous Maximum Principle): Assume that $\psi(x,t)$ is any sufficiently smooth function satisfying $\psi(x,t) \geq 0, \forall(x,t) \in \partial\mathscr{D}_{xt}$ and $\mathscr{L}_{C_\varepsilon}\psi(x,t) \geq 0, \forall(x,t) \in \mathscr{D}_{xt}$ then, $\psi(x,t) \geq 0, \forall(x,t) \in \overline{\mathscr{D}}_{xt}$, where $\mathscr{L}_{C_\varepsilon}\psi(x,t) := \psi_t(x,t) - C_\varepsilon\psi_{xx}(x,t) + A(x,t)\psi_x(x,t) + b(x,t)\psi(x,t)$.*

Proof. For the proof of this lemma, we refer the reader to Lemma (5.1) in Chapter (5). □

Lemma 7.2. *(Stability Estimate): If $\psi(x,t) \in C^{2,1}(\overline{\mathscr{D}}_{xt})$ be the solution of the continuous problem of equation (7.4) ,then it satisfies the bound*

$$|\psi(x,t)| \leq max\{|\mathscr{S}_0(x)|, |\mathscr{S}_l(t)|, |\mathscr{S}_r(t)|\} + \alpha^{-1}||f||.$$

Proof. The proof of this Lemma is similar to the proof of Lemma (5.2) of Chapter (5). □

Lemma 7.3. *The bounds for the derivative of the solution $\psi(x,t)$ of the problem in (7.4) are given by*

$$\left|\frac{\partial^{i+j}\psi(x,t)}{\partial x^i \partial t^j}\right| \leq C(1 + C_\varepsilon^{-i} e^{\alpha(1-x)/C_\varepsilon}) \tag{7.7}$$

where $0 \leq i \leq 2$ and $0 \leq i + j \leq 4$.

Proof. For the proof of this Lemma, readers can refer in [50, 117]. □

7.4 Formulation of Numerical Schemes

This section deals with the semi-discretization of the problem along the temporal and spatial directions. Finally, we combined the two discretized problems together and found the fully discrete solution of the proposed problem defined in (7.4).

7.4.1 Temporal Semi-discretization:

Upon dividing the time domain $[0, T]$ in to M equal number of mesh intervals with step length Δt, we get

$$\overline{\mathscr{D}}_t^M = \left\{t^j : t^j = j\Delta t, j = 0, 1, 2, 3, \ldots M \text{ and } \Delta t = \frac{T}{M}\right\}. \tag{7.8}$$

Following a similar presented in [118] and employing the Crank-Nicolson scheme, the problem (7.4) is discretized in the following form:

$$\begin{cases} \frac{\psi^{j+1}-\psi^{j}}{\Delta t} - \frac{C_\varepsilon}{2}\left(\psi_{xx}^{j+1}+\psi_{xx}^{j}\right) + \frac{A(x,t)}{2}\left(\psi_{x}^{j+1}+\psi_{x}^{j}\right) + \frac{b(x,t)}{2}\left(\psi^{j+1}+\psi^{j}\right) \\ = \frac{1}{2}\left(f^{j+1}+f^{j}\right), \qquad \forall (x,t) \in \mathscr{D}_{xt}, \\ \begin{cases} \psi(x,0) = \mathscr{S}_0(x), & \forall x \in \overline{\mathscr{D}}_x, \\ \psi(0,t^{j+1}) = \mathscr{S}_l(t^{j+1}), & 0 \le j \le M-1, \\ \psi(1,t^{j+1}) = \mathscr{S}_r(1,t^{j+1})), & 0 \le j \le M-1. \end{cases} \end{cases} \tag{7.9}$$

On simplifying and separating the $(j+1)^{th}$ and $(j)^{th}$ time levels, we get

$$\begin{cases} -C_\varepsilon \psi_{xx}^{j+1}(x) + A(x,t)\psi_x^{j+1}(x) + B(x,t)\psi^{j+1}(x) = G_i^j(x), \quad \forall (x,t) \in \mathscr{D}_{xt}, \\ \begin{cases} \psi(x,0) = \mathscr{S}_0(x), & \forall x \in \overline{\mathscr{D}}_x, \\ \psi(0,t^{j+1}) = \mathscr{S}_l(t^{j+1}), & 0 \le j \le M-1, \\ \psi(1,t^{j+1}) = \mathscr{S}_r(1,t^{j+1})), & 0 \le j \le M-1. \end{cases} \end{cases} \tag{7.10}$$

where

$$\begin{cases} G_i^j(x) = C_\varepsilon(\psi^j)_{xx} - A(x,t)(\psi^j)_x - C(x)\psi^j + f_i^{j+1} + f_i^j, \\ A(x,t) = a(x,t) - \delta b(x,t), \\ B(x,t) = (b(x,t) + 2/\Delta t), \\ C(x,t) = (b(x,t) - 2/\Delta t), \ \forall (x,t) \in \overline{\mathscr{D}}_{xt}. \end{cases} \tag{7.11}$$

To check the semi-discrete maximum principle and stability estimate of the temporal direction of the proposed scheme, we first rewrite (7.10) at $(j+1)^{th}$ time level in-terms of spatial variables of the following forms:

$$\begin{cases} \mathscr{L}^*_{C_\varepsilon} Y := -C_\varepsilon Y''(x) + A(x)Y'(x) + B(x)Y = G(x), \ \forall x \in \overline{\mathscr{D}}_x \\ Y(0) = \mathscr{S}_l(t^{j+1}), \ Y(1) = \mathscr{S}_r(t^{j+1}), \ \forall t^{j+1} \in \overline{\mathscr{D}}_t^M. \end{cases} \tag{7.12}$$

where $\mathscr{L}^*{}_{C_\varepsilon}$ is a discrete operator, $Y(x) = \psi^{j+1}(x)$.

Lemma 7.4. *(Semi-discrete Maximum Principle): If $Y^{j+1}(x) \in C^2(\overline{\mathscr{D}}_x)$ is the solution of the semi-discrete problem in (7.10) such that $Y^{j+1}(0) \ge 0, Y^{j+1}(1) \ge 0$ on $\partial\overline{\mathscr{D}}_x$ and $\mathscr{L}^*_{\mathscr{C}_\varepsilon} Y^{j+1}(x) \ge 0, \ \forall x \in \mathscr{D}_x$, then $Y^{j+1}(x) \ge 0, \ \forall x \in \overline{\mathscr{D}}_x$.*

Proof. Let $x^* \in \overline{\mathscr{D}}_x$ such that $\psi^{j+1}(x^*) = min_{x\in\overline{\mathscr{D}}_x} Y^{j+1}(x) < 0$ and since $Y^{j+1}(0) \ge 0, \ Y^{j+1}(1) \ge 0$ then $x^* \notin \{0,1\}$ that is $x^* \in \mathscr{D}_x$. Moreover, since $Y_x^{j+1}(x^*) = 0$ and $Y_{xx}^{j+1}(x^*) \ge 0$, we have that

$$\mathscr{L}^*{}_{C_\varepsilon} Y^{j+1}(x^*) \quad = \quad -C_\varepsilon Y_{xx}^{j+1}(x^*) + A(x^*) Y_x^{j+1}(x^*) + B(x^*) Y^{j+1}(x^*) \leq 0.$$

But $\mathscr{L}^*{}_{C_\varepsilon} Y^{j+1}(x) \leq 0$ is a contradiction to our assumption $\mathscr{L}^*{}_{C_\varepsilon} Y^{j+1}(x) \geq 0$.
Consequently, it is proved that the minimum of $Y^{j+1}(x)$ is non-negative. □

The local truncation error of the semi-discrete problem (7.10) at the $(j+1)^{th}$ time level is given by $e^{j+1} := \psi(x, t_{j+1}) - \psi_i^{j+1}$, where ψ_i^{j+1} is the computed solution of the proposed problem. Moreover, this error measures the contribution of each time step to the global error of the temporal semi-discretization.

Lemma 7.5. *(Local Error Estimate): As outlined in [16], we suppose that*

$$\left| \frac{\partial^i \psi(x,t)}{\partial t^i} \right| \leq C, \forall (x,t) \in \overline{\mathscr{D}}_x \text{ and } 0 \leq i \leq 2$$

then the local error estimate in the temporal direction is given by

$$||e^{j+1}||_\infty \leq C_1 (\Delta t)^3, \;\; j = 1, 2, 3, \ldots, M-1. \tag{7.13}$$

Proof. The proof of this Lemma is similar to the proof of Lemma (2.6) of Chapter (2). □

Lemma 7.6. *(Global Error Estimate): Under the hypothesis of Lemma (7.5), the global error estimate of the temporal semi-discretization is defined by*

$$||E^{j+1}||_\infty \leq C_2 (\Delta t)^2. \tag{7.14}$$

Proof. The proof of this Lemma is similar to the proof of Lemma (2.7) of Chapter (2). □

Lemma 7.7. *The smooth and singular components of the solution of the problem in (4.3) satisfy the following bounds:*

$$\left| \frac{d^i \psi^{j+1}}{dx^i} \right| = \begin{cases} \left| \frac{d^i V^{j+1}}{dx^i} \right| \leq C \left(1 + C_\varepsilon^{3-i} exp\left(\frac{\alpha(1-x)}{C_\varepsilon} \right) \right), \; i = 1, 2, 3, \\ \\ \left| \frac{d^i W^{j+1}}{dx^i} \right| \leq C \left(1 + C_\varepsilon^{-i} exp\left(\frac{\alpha(1-x)}{C_\varepsilon^i} \right) \right), \; i = 1, 2, 3. \end{cases} \tag{7.15}$$

Proof. For the proof of this lemma, the reader can refer in [16]. □

7.4.2 Spatial semi-discretization:

To discretize the spatial domain $\overline{\mathscr{D}}x$, we construct a Shishkin mesh $\overline{\mathscr{D}}x^N$, adapted to the problem's boundary layer at $x = 1$. The domain is partitioned into $\overline{\mathscr{D}}_l = [0, 1-\tau]$ (a coarse region with smooth variation) and $\overline{\mathscr{D}}r = [1-\tau, 1]$ (a layer region with steep gradients), such that $\overline{\mathscr{D}}_x = \overline{\mathscr{D}}_l \cup \overline{\mathscr{D}}_r$. For $N \geq 2^Q$, $Q \geq 2$, a uniform mesh with $N/2$ intervals is placed on each subdomain, governed by the transition parameter τ as outlined in [16]:

$$\tau = min\left\{\frac{1}{2}, \tau_0 C_\varepsilon lnN\right\}, \quad \tau_0 \geq 2/\alpha. \tag{7.16}$$

The discretized domain $\overline{\mathscr{D}}_x^N = \{0 = x_0, x_1, \ldots, x_{N/2} = 1-\tau = x, \ldots, x_N = 1\}$ is defined by

$$x_i = \begin{cases} \frac{2(1-\tau)}{N} i & 0 \leq i \leq \frac{N}{2}, \\ (1-\tau) + \frac{2\tau}{N}(i - \frac{N}{2}) & \frac{N}{2}+1 \leq i \leq N. \end{cases} \tag{7.17}$$

Moreover, the mesh width $h_i = x_i - x_{i-1}, i = 1,2,3,\ldots,N$ in the spatial direction is given by

$$h_i = \begin{cases} H := \frac{2(1-\tau)}{N} & 0 \leq i \leq \frac{N}{2}, \\ h := \frac{2\tau}{N} & \frac{N}{2}+1 \leq i \leq N. \end{cases} \tag{7.18}$$

where H and h are the mesh widths in the coarse region $[0, 1-\tau]$ and the fine region $[1-\tau, 1]$ respectively. Then it is clear to see that $N^{-1} \leq H \leq 2N^{-1}$, $h = \tau_0 C_\varepsilon lnN$ and the uniform mesh can be obtained by choosing $\tau = \frac{1}{2}$.

Finite Difference Schemes: This section defines the finite difference operators for any given mesh function $\psi(x_i, t^j) = \psi_i^j$, forward, backward and central difference operators $\delta_x^+, \delta_x^-, \delta_x^0$ and δ_x^2 in space as follows

$$\begin{cases} \delta_x^+ \psi_i^j = \frac{\psi_{i+1}^j - \psi_i^j}{h_{i+1}}, \delta_x^- \psi_i^j = \frac{\psi_i^j - \psi_{i-1}^j}{h_i}, & h_i = x_i - x_{i-1}, \\ \delta_x^0 \psi_i^j = \frac{\psi_{i+1}^j - \psi_{i-1}^j}{\hat{h}_i} \text{ and } \delta_x^2 \psi_i^j = \frac{\delta_x^+ \psi_i^j - \delta_x^- \psi_i^j}{\hat{h}_i}, & \hat{h}_i = \frac{h_{i+1}+h_i}{2}. \end{cases} \tag{7.19}$$

7.4.3 The Fully Discretization Schemes

Using the hybrid finite difference scheme, which is a proper combination of the Midpoint Upwind scheme in the coarse region $[0, 1-\tau]$ and the classical central difference scheme in the layer region $[1-\tau, 1]$, we discretize the semi-discrete problem (7.10) following a similar approach presented in [21] as follows:

$$\begin{cases} \mathscr{L}_{hyb} \psi_i^{j+1} := \mathscr{L}_{mu} \psi_i^{j+1} + \mathscr{L}_{cen} \psi_i^{j+1}, & 1 \leq i \leq N-1, \\ \psi_i^0 = \mathscr{S}_0(x_i), & \text{for } 1 \leq i \leq N-1, \\ \psi_0^{j+1} = \mathscr{S}_l(t^{j+1}), \text{ and } \psi_N^{j+1} = \mathscr{S}_r(t^{j+1}), & \text{for } 1 \leq j \leq M-1. \end{cases} \tag{7.20}$$

where

$$\begin{cases} \mathscr{L}_{mu}^{C_\varepsilon}\psi_i^{j+1} := -C_\varepsilon(\delta_x^2\psi_i^{j+1}) + A_{i-\frac{1}{2}}(\delta_x^-\psi_i^{j+1}) + B_{i-\frac{1}{2}}\psi_i^{j+1} = C_\varepsilon(\delta_x^2\psi_i^j) \\ -A_{i-\frac{1}{2}}(\delta_x^-\psi_i^j) - C_{i-\frac{1}{2}}\psi_i^j + f_{i-\frac{1}{2}}^{j+1} + f_{i-\frac{1}{2}}^j, \quad for\ 1 \le i \le \frac{N}{2}, \\ \mathscr{L}_{cen}^{C_\varepsilon}\psi_i^{j+1} := -C_\varepsilon(\delta_x^2\psi_i^{j+1}) + A_i(\delta_x^0\psi_i^{j+1}) + B_i\psi_i^{j+1} = C_\varepsilon(\delta_x^2\psi_i^j) \\ -A_i(\delta_x^-\psi_i^j) - C_i\psi_i^j + f_i^{j+1} + f_i^j, \quad for\ \frac{N}{2}+1 \le i \le N-1. \end{cases} \tag{7.21}$$

Furthermore, we can determine the values of the coefficients as follows

$$\begin{cases} A_{i-\frac{1}{2}} = \frac{A_i + A_{i-1}}{2}, B_{i-\frac{1}{2}} = \frac{B_i + B_{i-1}}{2}, C_{i-\frac{1}{2}} = \frac{C_i + C_{i-1}}{2}, \\ f_{i-\frac{1}{2}}^{j+1} = \frac{1}{2}\left(f_i^{j+1} + f_{i-1}^{j+1}\right) \text{ and } f_{i-\frac{1}{2}}^j = \frac{1}{2}\left(f_i^j + f_{i-1}^j\right). \end{cases} \tag{7.22}$$

Using (7.19) into (7.21) and after some simplifications, we get

$$\begin{cases} \mathscr{L}_{mu}^{C_\varepsilon}\psi_i^{j+1} := R_i^-\psi_{i-1}^{j+1} + R_i^0\psi_i^{j+1} + R_i^+\psi_{i+1}^{j+1} = G_i^j, \quad 1 \le i \le \frac{N}{2}. \\ \text{where} \begin{cases} R_i^- = \left(\frac{-2C_\varepsilon}{(h_{i+1}+h_i)h_i} - \frac{A_{i-1/2}^{j+1}}{h_i} + \frac{B_{i-1/2}^{j+1}}{2}\right) \\ R_i^0 = \left(\frac{2C_\varepsilon}{(h_{i+1}+h_i)h_{i+1}} + \frac{2C_\varepsilon}{(h_{i+1}+h_i)h_i} + \frac{A_{i-1/2}^{j+1}}{h_i} + \frac{(B_{i-1/2}^{j+1}}{2}\right) \\ R_i^+ = \left(\frac{-2C_\varepsilon}{(h_{i+1}+h_i)h_{i+1}}\right) \\ G_i^j = r_i^-\psi_{i-1}^j + r_i^0\psi_i^j + r_i^+\psi^j + \frac{\left[f_i^j + f_{i-1}^j + f_i^{j+1} + f_{i-1}^{j+1}\right]}{2} \\ r_i^- = \left(\frac{2C_\varepsilon}{(h_{i+1}+h_i)h_i} + \frac{A_{i-1/2}^j}{h_i} + \frac{C_{i-1/2}^j}{2}\right) \\ r_i^0 = \left(\frac{-2C_\varepsilon}{(h_{i+1}+h_i)h_{i+1}} + \frac{-2C_\varepsilon}{(h_{i+1}+h_i)h_i} - \frac{A_{i-1/2}^j}{h_i} + \frac{C_{i-1/2}^j}{2}\right) \\ r_i^+ = \left(\frac{2C_\varepsilon}{(h_{i+1}+h_i)h_{i+1}}\right) \end{cases}. \end{cases} \tag{7.23}$$

$$\begin{cases} \mathscr{L}_{cen}^{C_\varepsilon}\psi_i^{j+1} := S_i^-\psi_{i-1}^{j+1} + S_i^0\psi_i^{j+1} + S_i^+\psi_{i+1}^{j+1} = H_i^j, \quad \frac{N}{2}+1 \le i \le N-1. \\ \text{where} \begin{cases} S_i^- = \left(\frac{-2C_\varepsilon}{(h_{i+1}+h_i)h_i} - \frac{A_i^{j+1}}{\hat{h}_i}\right) \\ S_i^0 = \left(\frac{2C_\varepsilon}{(h_{i+1}+h_i)h_{i+1}} + \frac{2C_\varepsilon}{(h_{i+1}+h_i)h_i} + B_i^{j+1}\right) \\ S_i^+ = \left(\frac{-2C_\varepsilon}{\hat{h}_i h_{i+1}} + \frac{A_i}{h_i}\right) \\ H_i^j = s_i^-\psi_{i-1}^j + s_i^0\psi_i^j + s_i^+\psi_{i+1}^j + f_i^{j+1} + f_i^j \\ s_i^- = \left(\frac{2C_\varepsilon}{(h_{i+1}+h_i)h_i} + \frac{A_i^j}{(h_{i+1}+h_i)}\right) \\ s_i^0 = \left(-\frac{2C_\varepsilon}{(h_{i+1}+h_i)h_{i+1}} - \frac{2C_\varepsilon}{(h_{i+1}+h_i)h_i} + C_i^j\right) \\ s_i^+ = \left(\frac{2C_\varepsilon}{\hat{h}_i h_{i+1}} - \frac{A_i^j}{h_i}\right) \end{cases}. \end{cases} \tag{7.24}$$

Because of the tri-diagonal system in (6.26), the fully discretized system (7.23)–(7.24) also satisfies a nonsingular M-matrix by theorem (2.1) of Chapter (2), we solve it using matrix inverse method.

7.5 Uniform Convergence Analysis

The convergence analysis of this section is basically based on the discretized problem in (7.4). To show the stability and $\varepsilon-$ uniform convergence of the proposed scheme, we follow the decomposition approach of numerical solutions as regular and singular components as referred in [50, 111].

Lemma 7.8. *Assume that Assume that*

$$\tau_0||A||_\infty < \frac{N}{lnN} \text{ and } \alpha N \geq \left(||B||_\infty + 2\triangle t^{-1}\right)$$

Then, we have

$$\begin{cases} R_i^- < 0,\ R_i^+ < 0, & for\ \ 1 \leq i \leq N-1, \\ |R_1^0| - |R_1^+| \geq 0,\ |R_1^0| - |R_1^-| - |R_1^+| \geq 0, & for\ \ 1 \leq i \leq N/2, \\ |R_{N-1}^0| - |R_{N-1}^-| > 0,\ |R_1^0| - |R_1^-| - |R_1^+| > 0 & for\ \ N/2 < i < N-1. \end{cases} \tag{7.25}$$

Proof. To prove this lemma, we use the location of the meshes. as follows:
Case I (The Coarse Mesh Region): For every $(j+1)^{th}$ time level in (7.23), we consider the case $1 \leq i \leq N/2$. It is seen that $R_i^+ < 0$ throughout the specified region and we check for $R_i^- < 0$ from the constructions below:

$$R_i^- = \frac{-2C_\varepsilon}{(h_{i+1}+h_i)h_i} - \frac{A_{i-1/2}}{h_i}.$$

Based on the assumption in (7.18), the step size in the coarse region is defined to be $h_i = H$. So, the above equation gives

$$\begin{aligned} R_i^- &\leq \frac{-2C_\varepsilon}{2H^2} - \frac{A_{i-1/2}}{H}, \\ &\leq -C_\varepsilon N^2 - \frac{N}{2}(A_i + A_{i-1}). \end{aligned}$$

Since $A(x_i), A(x_{i-1}) \geq \alpha > 0$, we conclude that $R_i^- < 0$ for $1 \leq i \leq N/2$ as required. From these discussions, we further deduce the following results: $|R_1^0| - |R_1^+| \geq 0$ and $|R_i^0| - |R^-| - |R^+| \geq 0$ for $1 \leq i \leq N/2$.
Case II (The Fine Mesh Region): For every $(j+1)^{th}$ time level in (7.24), we consider the case $N/2 < i \leq N-1$. It is seen that $S_i^+ < 0$ throughout the specified region. To check where S_i^- is

positive or negative, we prove as follows:

$$\begin{aligned}
S_i^- &= \frac{-2C_\varepsilon}{\hat{h}_i h_{i+1}} - \frac{A_i}{h_i}, \\
&\leq \frac{-2C_\varepsilon}{\hat{h}_i h_{i+1}} - \frac{||A||_\infty}{\hat{h}_i}, \\
&\leq -\frac{1}{\hat{h}_i}\left(\frac{2C_\varepsilon}{h_{i+1}} + ||A||_\infty\right) < 0.
\end{aligned}$$

Now, using the condition $\tau_0||A||_\infty < \frac{N}{lnN}$, we deduce that

$$\begin{aligned}
|S_i^-| + |S_i^+| &= \left(\frac{-2C_\varepsilon}{\hat{h}_i h_i} - \frac{A_i}{h_i} + \frac{-2C_\varepsilon}{\hat{h}_i h_{i+1}} + \frac{A_i}{h_i}\right), \\
&\leq \frac{-2}{\hat{h}_i}\left(\frac{C_\varepsilon}{h_i} + \frac{C_\varepsilon}{h_{i+1}}\right) < |S_i^0|.
\end{aligned}$$

Also it can be defined at $N-1$, $|S_{N-1}^-| + |S_{N-1}^+| = |S_{N-1}^0|$. The overall constructions suggested that the tri-diagonal system associated with (7.23) and (7.24) at each temporal level is an M-matrix. Hence, the operator defined in (7.20) satisfies the following discrete maximum principle on $\mathscr{D}_{xt}^{N,M}$. □

Lemma 7.9. *(Descrite Maximum Principle). If ψ_i^{j+1} be any mesh function defined on $\overline{\mathscr{D}}_x^{N,M}$ such that $\psi_0^{j+1} \geq 0, \psi_N^{j+1} \geq 0$ and $\mathscr{L}_{hyb}\psi_i^{j+1} \geq 0,\ i = 1,2,3,\ldots,N-1$, then $\psi_i^{j+1} \geq 0,\ \ i = 1,2,3,\ldots,N$.*

Proof. Suppose, for the sake of contradiction, that there exists an interior mesh point $(i^*, j+1)$ with $i^* \in \{1,2,\ldots,N-1\}$ such that

$$\psi_{i^*}^{j+1} = \min_{0\leq i\leq N} \psi_i^{j+1} \quad \text{and} \quad \psi_{i^*}^{j+1} < 0.$$

In particular, $i^* \notin \{0,N\}$, and thus $(i^*, j+1)$ is an interior minimum. Elementary calculus then implies

$$(\psi_{i^*}^{j+1})_x = 0, \qquad (\psi_{i^*}^{j+1})_{xx} \geq 0.$$

Since the hybrid operator $\mathscr{L}_{hyb}^{N,M}$ is defined as a combination of the midpoint–upwind and the central-difference operators, we examine each scheme in the region where it is active.

The Outer Region. For $1 \leq i^* \leq N/2$, the midpoint-upwind discretization gives

$$\mathscr{L}_{mu}^{N,M}\psi_{i^*}^{j+1} = -C_\varepsilon\left(\delta_x^2\psi_{i^*}^{j+1}\right) + A_{i^*-\frac{1}{2}}\left(\delta_x^-\psi_{i^*}^{j+1}\right) + B_{i^*-\frac{1}{2}}\psi_{i^*}^{j+1}.$$

At the discrete minimum, $\delta_x^2\psi_{i^*}^{j+1} \geq 0$ and $\delta_x^-\psi_{i^*}^{j+1} = 0$, while $\psi_{i^*}^{j+1} < 0$ forces the reaction term to be strictly negative. Hence,

$$\mathscr{L}_{mu}^{N,M}\psi_{i^*}^{j+1} < 0.$$

The Layer Region. For $N/2 < i^* \leq N-1$, the central-difference operator yields

$$\mathscr{L}_{cen}^{N,M}\psi_{i^*}^{j+1} = -C_\varepsilon\left(\delta_x^2\psi_{i^*}^{j+1}\right) + A_{i^*}\left(\delta_x^0\psi_{i^*}^{j+1}\right) + B_{i^*}\psi_{i^*}^{j+1}.$$

Again, $\delta_x^2\psi_{i^*}^{j+1} \geq 0$ and $\delta_x^0\psi_{i^*}^{j+1} = 0$ at the discrete minimum, and because $\psi_{i^*}^{j+1} < 0$, the reaction term is strictly negative. Thus,

$$\mathscr{L}_{cen}^{N,M}\psi_{i^*}^{j+1} < 0.$$

The Entire Region. By definition of the hybrid scheme,

$$\mathscr{L}_{hyb}^{N,M}\psi_{i^*}^{j+1} = \mathscr{L}_{mu}^{N,M}\psi_{i^*}^{j+1} + \mathscr{L}_{cen}^{N,M}\psi_{i^*}^{j+1}, \qquad 1 < i^* \leq N-1.$$

Since each term on the right-hand side is strictly negative where it applies, we conclude that

$$\mathscr{L}_{hyb}^{N,M}\psi_{i^*}^{j+1} < 0.$$

This contradicts the assumed non-negativity condition

$$\mathscr{L}_{hyb}^{N,M}\psi_{i}^{j+1} \geq 0, \qquad i = 1,2,\ldots,N-1.$$

Therefore the assumption $\psi_{i^*}^{j+1} < 0$ is impossible, and we conclude that

$$\psi_{i}^{j+1} \geq 0, \qquad i = 1,2,\ldots,N.$$

□

Lemma 7.10. *(Uniform Stability Estimate). Let ψ_i^{j+1} be the solution of the discrete problem (7.20). Then*

$$\left|\psi_i^{j+1}\right| \leq C\max_{\partial\mathscr{D}^{N,M}}\left|\psi(x_i,t^j)\right| + \alpha^{-1}\left\|\mathscr{L}_{hyb}^{N,M}\psi_i^{j+1}\right\|, \; (x_i,t^j) \in \mathscr{D}_{xt}^{N,M}. \tag{7.26}$$

Proof. Let $\Omega^{\pm}(x_i,t^{j+1})$ be two barrier functions defined as follows:

$$\Omega^{\pm}(x_i,t^{j+1}) = C\max_{\partial\mathscr{D}^{N,M}}\left|\psi(x_i,t^j)\right| + \frac{1}{p^*}\left\|\mathscr{L}_{hyb}^{N,M}\psi_i^{j+1}\right\| \pm \psi_i^{j+1}. \tag{7.27}$$

Using Lemma (7.2) and Lemma (7.9), it can be arrived at the required bound. □

Theorem 7.1. Let $\psi(x_i,t^{j+1})$ and ψ_i^{j+1} be the continuous and discrete solutions of the problems

(7.4) and (7.20), respectively; then the proposed scheme satisfies the following error estimate in the spatial direction:

$$\left|\psi(x_i,t^{j+1})-\psi_i^{j+1}\right| \leq \begin{cases} CN^{-2}, & 0\leq i\leq N/2, \\ C\left(N^{-2}ln^2N\right), & N/2<i<N. \end{cases} \tag{7.28}$$

Proof. First divide the domain into outer and layer regions of the following forms:

The Outer Region $(0\leq i\leq N/2)$: Based on the above lemma, the local truncation error in the outer region can be defined by the midpoint upwind scheme as follows:

$$\begin{aligned}
\zeta_i^{j+1} &= \left|\mathscr{L}^{N,M}_{C_\varepsilon,\text{hyb}}\left(\psi(x_i,t^{j+1})-\psi_i^{j+1}\right)\right|, \\
&\leq \mathscr{L}^{N,M}_{C_\varepsilon}\psi(x_{i-1/2},t^{j+1})-\mathscr{L}^{N,M}_{C_\varepsilon,\text{mu}}\psi(x_i,t^{j+1}), \\
&\leq C\left[N^{-1}(C_\varepsilon+N^{-1})+\left|(C_\varepsilon(\psi_{xx}^{j+1}-\delta_x^2\psi_i^{j+1}))\right|+\left|A_{i-1/2}\left(\frac{\partial}{\partial x}-\delta_x^-\right)\psi_i^{j+1}\right|\right], \\
&\leq C\left[N^{-1}(C_\varepsilon+N^{-1})\left(C_\varepsilon+h_{i+1}\left(h_i+h_{i+1}\right)\right)||\psi_{xxx}||_\infty+h_{i+1}^2\left(||\psi_{xx}||_\infty+||\psi_x||_\infty\right)\right], \\
&\leq C\left(N^{-1}(C_\varepsilon+N^{-1})\right), \\
&\leq CN^{-2}, \quad \text{since } C_\varepsilon\leq CN^{-1} \text{ in the considered region.}
\end{aligned}$$

The Layer Region $(N/2<i<N)$: In a similar approach applied in the outer region, the local truncation error determined as follows:

$$\begin{aligned}
\zeta_i^{j+1} &= \left|\mathscr{L}^{N,M}_{C_\varepsilon,\text{hyb}}\left(\psi(x_i,t^{j+1})-\psi_i^{j+1}\right)\right|, \\
&\leq \mathscr{L}^{N,M}_{C_\varepsilon}\psi(x_{i-1/2},t^{j+1})-\mathscr{L}^{N,M}_{C_\varepsilon,\text{cen}}\psi(x_i,t^{j+1}), \\
&\leq C\left(N^{-2}ln^2N\right)+\left|C_\varepsilon\left(\frac{\partial^2}{\partial x^2}-\delta_x^2\right)\psi(x_i,t^{j+1})\right|+\left|A_i\left(\frac{\partial}{\partial x}-\delta_x^0\right)\psi(x_i,t^{j+1})\right|, \\
&\leq C\left[\left(N^{-2}ln^2N\right)+C_\varepsilon h_i^2||\psi_{xxxx}||_\infty+h_i^2||\psi_{xxx}||_\infty\right], \quad \text{using Taylor series expansion,} \\
&\leq C\left(N^{-2}ln^2N\right), \quad \text{using the estimates for derivatives in Lemma (7.7)}
\end{aligned}$$

□

Using these estimates, together with the global error bound established in Lemma (7.6), we may generalize the overall bounds of the proposed scheme. Consequently, the total truncation error associated with the hybrid scheme can be expressed as follows:

Theorem 7.2. Let $\psi(x_i,t^{j+1})$ and ψ_i^{j+1} be the continuous and discrete solutions of the problems (7.4) and (7.20), respectively; then the proposed scheme satisfies the following bound:

$$\sup_{0<C_\varepsilon\ll 1}\max_{0\leq i\leq N, 0\leq j\leq M}\left|\psi(x_i,t^{j+1})-\psi_i^{j+1}\right| \leq \begin{cases} C\left(N^{-2}+(\Delta t)^2\right), & 0\leq i\leq N/2, \\ C\left(N^{-2}ln^2N+(\Delta t)^2\right), & N/2<i<N. \end{cases}$$

Proof. Combining lemma (7.6) and theorem (7.1) gives the required result. □

7.6 Numerical Results and Discussions

The proposed scheme is finally assessed using two benchmark problems, with εuniform maximum absolute errors and convergence rates computed to evaluate its accuracy and computational efficiency, as presented in Chapter 2.

Example 7.1. Consider SPPDDEs of the following form presented in [57, 109, 110] with $\delta = 0.3 * \varepsilon$:

$$\begin{cases} \psi_t(x,t) - \varepsilon\psi_{xx}(x,t) + (2-x^2)\psi_x(x-\delta,t) + (x^2+1+cos(\pi x))\psi(x-\delta,t) \\ = 10t^2(1-x)exp(-t), & \forall (x,t) \in \mathscr{D}_{xt} = (0,1)\times(0,T], T>0, \\ \mathscr{S}_0(x,t) = 0, & \forall x \in \overline{\mathscr{D}}_x \text{ and } t=0, \\ \mathscr{S}_l(x,t) = 0, & \forall (x,t) \in [-\delta,0]\times\overline{\mathscr{D}}_t, \\ \mathscr{S}_r(x,t) = 0, & x=1 \text{ and } \forall t \in \overline{\mathscr{D}}_t. \end{cases}$$

Example 7.2. Consider SPPDDEs of the following form presented in [57, 109, 110] with $\delta = 0.3 * \varepsilon$:

$$\begin{cases} \psi_t(x,t) - \varepsilon\psi_{xx}(x,t) + (2-x^2)\psi_x(x-\delta,t) + (3-x)\psi(x-\delta,t) \\ = exp(t)sin(\pi x(1-x)), & \forall (x,t) \in \mathscr{D}_{xt} = (0,1)\times(0,T], T>0, \\ \mathscr{S}_0(x,t) = 0, & \forall x \in \overline{\mathscr{D}}_x \text{ and } t=0, \\ \mathscr{S}_l(x,t) = 0, & \forall (x,t) \in [-\delta,0]\times\overline{\mathscr{D}}_t, \\ \mathscr{S}_r(x,t) = 0, & x=1 \text{ and } \forall t \in \overline{\mathscr{D}}_t. \end{cases}$$

Let $\psi^{N,M}(x_i,t^j)$ and $\psi^{2N,2M}(x_i,t^j)$ be the numerical solutions with mesh lengths $(h, \Delta t \neq 0)$ and $(h/2, \Delta t/2 \neq 0)$ respectively, then

- The maximum absolute error is given by

$$E_\varepsilon^{N,M} = \max_{0\le i,j\le N,M} \left|\psi^{N,M}(x_i,t^j) - \psi^{2N,2M}(x_i,t^j)\right|. \tag{7.29}$$

- The $\varepsilon-$ uniform maximum absolute error is given by

$$E^{N,M} = \max_{\varepsilon} E_\varepsilon^{N,M}. \tag{7.30}$$

- Corresponding ε-uniform order of convergence

$$R^{N,M} = log_2\left(\frac{E^{N,M}}{E^{2N,2M}}\right). \tag{7.31}$$

Table 7.1: $E^{N,M}$ and $R^{N,M}$ for Example (7.1) with $\delta = 0.3 * \varepsilon$

$\varepsilon \downarrow$	$N = 16$ $M = 16$	$N = 32$ $M = 32$	$N = 64$ $M = 64$	$N = 128$ $M = 128$	$N = 256$ $M = 256$
2^{-4}	$1.0129e-02$	$2.8877e-03$	$8.8280e-04$	$2.2361e-04$	$5.7853e-05$
2^{-6}	$1.0170e-02$	$2.9075e-03$	$8.9157e-04$	$2.2568e-04$	$5.9523e-05$
2^{-8}	$1.0171e-02$	$2.9077e-03$	$8.9166e-04$	$2.3452e-04$	$6.1353e-05$
2^{-10}	$1.0171e-02$	$2.9077e-03$	$8.9166e-04$	$2.3452e-04$	$6.1353e-05$
2^{-12}	$1.0171e-02$	$2.9077e-03$	$8.9166e-04$	$2.3452e-04$	$6.1353e-05$
2^{-14}	$1.0171e-02$	$2.9077e-03$	$8.9166e-04$	$2.3452e-04$	$6.1353e-05$
2^{-16}	$1.0171e-02$	$2.9077e-03$	$8.9166e-04$	$2.3452e-04$	$6.1353e-05$
2^{-18}	$1.0171e-02$	$2.9077e-03$	$8.9166e-04$	$2.3452e-04$	$6.1353e-05$
2^{-20}	$1.0171e-02$	$2.9077e-03$	$8.9166e-04$	$2.3452e-04$	$6.1353e-05$
$E^{N,M}$	$1.0171e-02$	$2.9077e-03$	$8.9166e-04$	$2.3452e-04$	$6.1353e-05$
$R^{N,M}$	1.8065	1.8205	1.9129	1.9345	—

Table 7.2: $E^{N,M}$ and $R^{N,M}$ for Example (7.2) with $\delta = 0.3 * \varepsilon$

$\varepsilon \downarrow$	$N = 16$ $M = 16$	$N = 32$ $M = 32$	$N = 64$ $M = 64$	$N = 128$ $M = 128$	$N = 256$ $M = 256$
2^{-4}	$7.8347e-03$	$2.1527e-03$	$6.3971e-04$	$1.7256e-04$	$4.3256e-05$
2^{-6}	$7.8436e-03$	$2.1537e-03$	$6.3900e-04$	$1.7176e-04$	$4.5291e-05$
2^{-8}	$7.8437e-03$	$2.1537e-03$	$6.3899e-04$	$1.7175e-04$	$4.5291e-05$
2^{-10}	$7.8437e-03$	$2.1537e-03$	$6.3899e-04$	$1.7175e-04$	$4.5291e-05$
2^{-12}	$7.8437e-03$	$2.1537e-03$	$6.3899e-04$	$1.7175e-04$	$4.5291e-05$
2^{-14}	$7.8437e-03$	$2.1537e-03$	$6.3899e-04$	$1.7175e-04$	$4.5291e-05$
2^{-16}	$7.8437e-03$	$2.1537e-03$	$6.3899e-04$	$1.7175e-04$	$4.5291e-05$
2^{-18}	$7.8437e-03$	$2.1537e-03$	$6.3899e-04$	$1.7175e-04$	$4.5291e-05$
2^{-20}	$7.8437e-03$	$2.1537e-03$	$6.3899e-04$	$1.7175e-04$	$4.5291e-05$
$E^{N,M}$	$7.8437e-03$	$2.1537e-03$	$6.3899e-04$	$1.7175e-04$	$4.5291e-05$
$R^{N,M}$	1.8647	1.7529	1.8954	1.93231	—

(a) $\varepsilon = 10^{-1}$ (b) $\varepsilon = 10^{-8}$

Figure 7.1: 2D solution graph for Example (7.2) when $N = 256, M = 256$

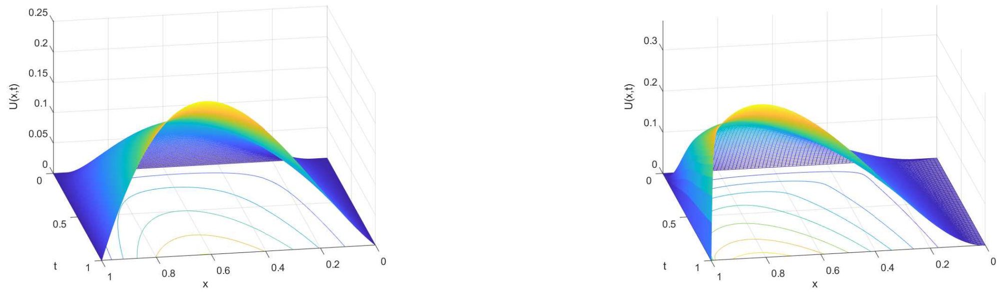

(a) $\varepsilon = 10^{-1}$ (b) $\varepsilon = 10^{-6}$

Figure 7.2: 3D solution graph for Example (7.2) when $N = 256, M = 256$

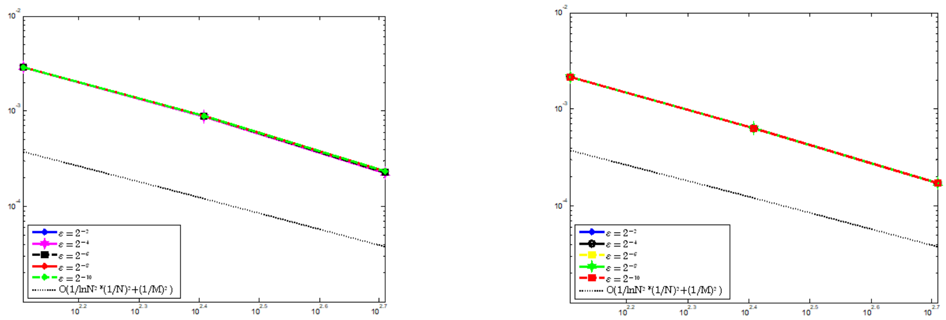

(a) Example (6.1) (b) Example (6.2)

Figure 7.3: Log log plots for different with values meshes $N = 64, 128, 256$ and $M = 8, 16, 32$.

To assess the applicability and effectiveness of the proposed scheme, we consider two model examples. Tables (7.1) and (7.2), corresponding to Examples (7.1) and (7.2), report the maximum absolute errors and the associated orders of convergence. For a fixed perturbation parameter ε, reducing the step sizes h and Δt across each row consistently decreases the maximum absolute errors, demonstrating that the numerical accuracy improves under mesh refinement. Moreover, the computed orders of convergence closely match the theoretical predictions, confirming the expected convergence behavior of the scheme.

For fixed values of h and Δt, decreasing the perturbation parameter ε down each column produces nearly unchanged maximum absolute errors. This behavior indicates that the accuracy of the scheme is essentially independent of the perturbation parameter and confirms its parameter-

Table 7.3: Comparison of $E^{N,M}$ and $R^{N,M}$ for Example (7.1) with $\delta = 0.3 * \varepsilon$

$\varepsilon \downarrow$	$N=16$ $M=16$	$N=32$ $M=32$	$N=64$ $M=64$	$N=128$ $M=128$
Present scheme				
$E^{N,M}$	$1.0171e-02$	$2.9077e-03$	$8.9166e-04$	$2.3452e-04$
$R^{N,M}$	1.8065	1.8205	1.9129	—
Results in [57]				
$E^{N,M}$	$1.3567e-02$	$7.7535e-03$	$4.1434e-03$	$2.5115e-03$
$R^{N,M}$	0.8072	0.9040	0.7223	—
Results in [109]				
$E^{N,M}$	$1.4608e-02$	$8.1600e-03$	$4.3077e-03$	$2.2124e-03$
$R^{N,M}$	0.8401	0.9217	0.9613	—

Table 7.4: Comparison of $E^{N,M}$ and $R^{N,M}$ for Example (7.2) with $\delta = 0.3 * \varepsilon$

$\varepsilon \downarrow$	$N=16$ $M=16$	$N=32$ $M=32$	$N=64$ $M=64$	$N=128$ $M=128$
Present scheme				
$E^{N,M}$	$7.8437e-03$	$2.1537e-03$	$6.3899e-04$	$1.7175e-04$
$R^{N,M}$	1.8647	1.7529	1.8954	—
Results in [57]				
$E^{N,M}$	$1.2759e-02$	$6.2559e-03$	$3.5761e-03$	$2.1620e-03$
$R^{N,M}$	0.7260	1.0282	0.8068	—
Results in [109]				
$E^{N,M}$	$1.9445e-02$	$1.0633e-02$	$6.0314e-03$	$3.2579e-03$
$R^{N,M}$	0.8709	0.8180	0.8886	—
Results in [110]				
$E^{N,M}$	$9.2814e-03$	$6.5095e-03$	$3.8028e-03$	$2.0170e-03$
$R^{N,M}$	0.5118	0.7755	0.9149	—

uniform convergence.

The two-dimensional and three-dimensional solution profiles presented in Figures (7.1) and (7.2) further illustrate the influence of the perturbation parameter. As ε decreases, the solution develops a pronounced right boundary layer near $x = 1$, which agrees with the analytical characterization of the problem. Despite the presence of this sharp layer, the proposed method accurately captures the solution behavior without loss of stability or accuracy.

Additional evidence of uniform convergence is provided by the log–log plots in Figure (7.3). The nearly parallel error and mesh-size curves, together with their comparable slopes, indicate that the numerical errors decrease at the predicted rate as the mesh is refined. These observations verify the robustness of the scheme across a wide range of perturbation parameters.

Overall, the numerical experiments strongly support the theoretical analysis. The observed error behavior, convergence rates, and layer-resolution capabilities are all consistent with the established theoretical results. Furthermore, the comparative results reported in Tables (7.3) and (7.4) demonstrate that the proposed method achieves higher accuracy and competitive convergence rates when compared with existing methods in the literature, including those presented in [57], [109], and [110]. These findings highlight the efficiency, reliability, and practical superiority of the proposed numerical scheme.

7.7 Conclusion

In this chapter, we develop and analyze a hybridized parameter-uniformly convergent scheme for solving singularly perturbed convection-diffusion problems that include a small negative shift parameter in both the convection and reaction terms. The proposed method employs the Crank-Nicolson scheme for temporal discretization on uniform meshes and a hybridized finite difference approach for spatial discretization on Shishkin meshes. The stability and convergence analysis establishes that the resulting scheme achieves uniform convergence of order $O\left(N^{-2}ln^2N+(\Delta t)^2\right)$. The overall numerical results and discussions reveal that the better performance of the present scheme compared with several existing methods in the literature.

Chapter 8

General Discussions, Conclusions and Future Works

This chapter offers a comprehensive discussion and consolidated summary of the key contributions achieved in this dissertation. In addition, it identifies several promising avenues for future research, indicating how the findings of the present study may be broadened or advanced in subsequent work.

8.1 General Discussions and Conclusions

This dissertation contributes to the development and analysis of fitted numerical schemes for solving singularly perturbed parabolic diffusion type problems. The principal findings of this work can be summarized as follows.

In chapter two, we examined a class of reaction–diffusion–type SPPPDEs. The problem was discretized using a Crank–Nicolson scheme in time and a nonstandard finite difference method on uniform spatial meshes. Stability and convergence analyses established that the resulting scheme achieves second-order accuracy in both time and space.

In chapter three, we studied reaction–diffusion–type SPPPDEs discretized with an implicit Euler scheme in time and a fitted linear multistep method on piecewise Shishkin meshes in space. The scheme was shown to be uniformly convergent, first-order in time and fourth-order in space, and was further enhanced to second-order in time through Richardson extrapolation.

In chapter four, we studied reaction–diffusion–type SPPDDEs with a small time lag, discretized using a Crank–Nicolson scheme in time and a nonstandard spatial discretization. The method was shown to be second-order accurate, and Richardson extrapolation further improved it to fourth-order in both time and space.

In chapter five, we examined convection–diffusion–reaction SPPDDEs with a small spatial mixed shift, discretized using an implicit Euler scheme in time and an exponentially fitted upwind method in space on uniform meshes. Uniform convergence and stability analyses demonstrated that the scheme attains second-order accuracy after Richardson extrapolation.

In chapter six, we considered convection–diffusion–reaction type SPPDDEs with small spatial shifts in the convection and reaction terms, discretized using an implicit Euler scheme in time and a midpoint upwind finite difference method in space. Stability and uniform convergence analyses confirmed that the scheme achieves second-order accuracy after Richardson extrapolation.

In chapter seven, we considered convection–diffusion–reaction type SPPDDEs with small spatial shifts in the convection and reaction terms, discretized using a hybridized scheme combining the Crank–Nicolson method in time and a second-order hybrid spatial discretization, midpoint upwind in coarse regions and central differences in layer regions on Shishkin meshes. Stability and uniform convergence analyses showed that the scheme is second-order accurate.

Overall, extensive numerical experiments were carried out to evaluate the performance and applicability of the proposed schemes. The computed results, including maximum absolute errors and observed orders of convergence, validate the theoretical analysis and demonstrate close agreement with practical outcomes. The schemes are higher-order, stable, and accurate, and they outperform several existing methods reported in the literature. These results underscore that the proposed schemes provide an efficient framework for solving SPPPDEs and SPPDDEs of reaction–diffusion and convection–diffusion type model problems in applied science and engineering.

8.2 Future works of the study

Due to certain constraints, this study is limited to linear reaction–diffusion and convection–diffusion SPPPDEs and SPPDDEs with small temporal lags and spatial shifts. However, many real-world phenomena are governed by nonlinear and two-dimensional singularly perturbed parabolic PDEs. As a direction for future work, the formulated numerical schemes should be extended and applied to such nonlinear, interior turning point and 2D problems to broaden their applicability and practical relevance.

Non-Linear Singularly Perturbed Parabolic PDEs: [The Methods in Chapter 3 and 4].

$$\begin{cases} \mathscr{L}_\varepsilon \psi(x,t) = f(x,t,\psi(x,t)), & \forall (x,t) \in \mathscr{D}_{xt}, \\ \psi(x,t) = \mathscr{S}_0(x), & \forall (x,t) \in \mu_0 = \left\{(x,t) : x \in \overline{\mathscr{D}}_x,\ t = 0\right\}, \\ \psi(x,t) = \mathscr{S}_l(0,t), & \forall (x,t) \in \mu_l = \left\{(x,t) : x = 0,\ t \in \overline{\mathscr{D}}_t \le T\right\}, \\ \psi(x,t) = \mathscr{S}_r(1,t), & \forall (x,t) \in \mu_r = \left\{(x,t) : x = 1,\ t \in \overline{\mathscr{D}}_t \le T\right\}. \end{cases}$$

where $\mathscr{L}_\varepsilon \psi(x,t) := \psi_t(x,t) - \varepsilon \psi_{xx}(x,t) + p(x,t)\psi_x(x,t) + q(x,t)\psi(x,t)$.

Interior Turning Point Problem of SPPPDEs: [The methods in chapter 5 an 6].

$$\begin{cases} \psi_t - \varepsilon \psi_{xx} + b(x,t)\,\psi_x + c(x,t)\,\psi(x,t) = f(x,t), & \forall (x,t) \in \mathscr{D}_{xt}, \\ \psi(x,0) = \mathscr{S}_0(x), & \forall x \in \overline{\mathscr{D}}_x, \\ \psi(0,t) = \mathscr{S}_l(0,t), & \forall t \in [0,T], \\ \psi(1,t) = \mathscr{S}_r(1,t), & \forall t \in [0,T], \end{cases}$$

where $\quad b(x,t) = 0, \quad x \in \mathscr{D}_x, \quad c(x,t), f(x,t)$ are given smooth functions.

2D Singularly Perturbed Parabolic PDEs: [The methods in Chapter 2, 3 and 7].

$$\begin{cases} \psi_t + \mathscr{L}_\varepsilon \psi(x,y,t) = f(x,y,t), & \forall (x,y,t) \in \mathscr{D}_{xyt} = \mathscr{D}_{xy} \times \mathscr{D}_t, \\ \psi(x,y,0) = \psi_0(x,y), & \forall (x,y) \in \partial \mathscr{D}_{xy}, \\ \psi(0,y,t) = \psi_x(y,t) = \psi(1,y,t), & \forall (y,t) \in \mathscr{D}_y \times \mathscr{D}_t, \\ \psi(x,0,t) = \psi_y(x,t) = \psi(x,1,t), & \forall (x,t) \in \mathscr{D}_x \times \mathscr{D}_t \end{cases} .$$

where $\mathscr{L}_\varepsilon \psi(x,y,t) := -\varepsilon\,(\psi_{yy} + \psi_{yy}) + a(x,y,t)\psi_x + b(x,y,t)\psi_y + c(x,y,t)\psi$.

Bibliography

[1] Miyaoka, Tiago Yuzo, João Frederico da Costa Azevedo Meyer, and J. M. R. Souza. ”A general boundary condition with linear flux for advection-diffusion models.” TEMA (São Carlos) 18, no. 2 (2017): 253-272.

[2] Miller, John JH, Eugene O’riordan, and Grigorii I. Shishkin. Fitted numerical methods for singular perturbation problems: error estimates in the maximum norm for linear problems in one and two dimensions. World scientific, 1996.

[3] Bender, Carl M., and Steven A. Orszag. Advanced mathematical methods for scientists and engineers: Asymptotic methods and perturbation theory. Vol. 1. New York: Springer, 1999.

[4] Holmes, Mark H. Introduction to perturbation methods. Springer Science and Business Media, 2012.

[5] Roos, Hans-Görg. ”Robust numerical methods for singularly perturbed differential equations: a survey covering 2008–2012.” International Scholarly Research Notices 2012, no. 1 (2012): 379547.

[6] Prandtl, Ludwig. ”Über Flüssigkeitsbewegung bei Kleiner Reibung.” In *Verhandlungen des III. Internationalen Mathematiker-Kongresses*, 484–491. Leipzig: B. G. Teubner, 1905.

[7] Friedrichs, Kurt O., and Wolfgang R. Wasow. ”Singular perturbations of non-linear oscillations.” (1946): 367-381.

[8] O’Malley, Robert E. ”Historical Developments in Singular Perturbations.” New York: Springer, 1974.

[9] Rai, Pratima, and Kapil K. Sharma. ”Singularly Perturbed Parabolic Differential Equations with Turning Point and Retarded Arguments.” IAENG International Journal of Applied Mathematics 45, no. 4 (2015).

[10] Baker, Christopher TH, and Fathalla A. Rihan. ”Sensitivity analysis of parameters in modelling with delay-differential equations.” Manchester Centre for Computational Mathematics, 1999.

[11] Kopteva, Natalia, and Eugene O’Riordan. ”Shishkin meshes in the numerical solution of singularly perturbed differential equations.” (2010).

[12] Bakhvalov, Nikolai Sergeevich. ”On the optimization of the methods for solving boundary value problems in the presence of a boundary layer.” Zhurnal Vychislitel’noi Matematiki i

Matematicheskoi Fiziki 9, no. 4 (1969): 841-859.

[13] Crank, John, and Phyllis Nicolson. ”A practical method for numerical evaluation of solutions of partial differential equations of the heat-conduction type.” In Mathematical proceedings of the Cambridge philosophical society, vol. 43, no. 1, pp. 50-67. Cambridge University Press, 1947. 10

[14] Sigamani, Valarmathi, J. J. Miller, Ramanujam Narasimhan, Paramasivam Mathiazhagan, and Franklin Victor. Differential Equations and Numerical Analysis. Springer: New Delhi, India, 2015.

[15] Erdoğan, Fahri, Mehmet Gökhan Sakar, and O. Saldır. ”Fitted Difference Schemes for Delay Convection–Diffusion Problems with Small Parameter.”

[16] Kadalbajoo, Mohan K., and Ashish Awasthi. ”The midpoint upwind finite difference scheme for time-dependent singularly perturbed convection-diffusion equations on non-uniform mesh.” International Journal for Computational Methods in Engineering Science and Mechanics 12, no. 3 (2011): 150-159.

[17] Oliveira, F. Aragao. ”A bout fitted finite difference operators and fitted meshes for solving singularly perturbed linear problems in one dimension, Praxis XXI, Mat/458/49 and CMUC–Centro de Mat.” Da Univ. de Coimbra (1998).

[18] Farrell, Paul, Alan Hegarty, John M. Miller, Eugene O'Riordan, and Grigory I. Shishkin. Robust computational techniques for boundary layers. Chapman and hall/CRC, 2000.

[19] Clavero, C., J. C. Jorge, and F. Lisbona. ”A uniformly convergent scheme on a nonuniform mesh for convection–diffusion parabolic problems.” Journal of Computational and Applied Mathematics 154, no. 2 (2003): 415-429.

[20] Craig, A. ”Navier–Stokes Equations (Theory and Numerical Analysis), 3rd ed., by Roger Temam, including an appendix by F. Thomasset.” Review of *Navier–Stokes Equations: Theory and Numerical Analysis*, by Roger Temam. 1987, 1226–1226.

[21] Das, Abhishek, and Srinivasan Natesan. ”Uniformly convergent hybrid numerical scheme for singularly perturbed delay parabolic convection–diffusion problems on Shishkin mesh.” Applied Mathematics and Computation 271 (2015): 168-186.

[22] Wang, P. Keng Chieh. ”Asymptotic stability of a time-delayed diffusion system.” (1963): 500-504.

[23] Musila, Miroslav, and Petr Lánský. ”Generalized Stein's model for anatomically complex neurons.” BioSystems 25, no. 3 (1991): 179-191.

[24] Bansal, Komal, and Kapil K. Sharma. ”Parameter-robust numerical scheme for time-dependent singularly perturbed reaction–diffusion problem with large delay.” Numerical

Functional Analysis and Optimization 39, no. 2 (2018): 127-154.

[25] Cooke, K., P. Van den Driessche, and Xingfu Zou. ”Interaction of maturation delay and nonlinear birth in population and epidemic models.” Journal of Mathematical biology 39, no. 4 (1999): 332-352.

[26] Adams, R.A. and Fournier, J.J., 2003. ”Sobolev spaces.” (Vol. 140). Elsevier. 21

[27] Meyer, Carl D. ”Matrix analysis and applied linear algebra.” Society for Industrial and Applied Mathematics, 2023.

[28] Berman, Abraham, and Robert J. Plemmons. ”Nonnegative matrices in the mathematical sciences.” Society for Industrial and Applied Mathematics, 1994.

[29] Nefedov, Nikolai Nikolaevich. ”Development of methods of asymptotic analysis of transition layers in reaction–diffusion–advection equations: Theory and applications.” Computational Mathematics and Mathematical Physics 61, no. 12 (2021): 2068-2087.

[30] Evans, Lawrence C. ”Partial differential equations.” Vol. 19. American mathematical society, 2022.

[31] Ji, Yanyan Claire, and Flavio H. Fenton. ”Numerical solutions of reaction-diffusion equations: Application to neural and cardiac models.” American Journal of Physics 84, no. 8 (2016): 626-638.

[32] Clavero, Carmelo, and Jose L. Gracia. ”On the uniform convergence of a finite difference scheme for time dependent singularly perturbed reaction-diffusion problems.” Applied mathematics and computation 216, no. 5 (2010): 1478-1488.

[33] Bullo, Tesfaye Aga, Gemechis File Duressa, and Guy Degla. ”Accelerated fitted operator finite difference method for singularly perturbed parabolic reaction-diffusion problems.” Computational Methods for Differential Equations 9, no. 3 (2021): 886-898.

[34] Munyakazi, Justin B., and Kailash C. Patidar. ”A fitted numerical method for singularly perturbed parabolic reaction-diffusion problems.” Computational and applied mathematics 32, no. 3 (2013): 509-519.

[35] Duressa, Gemechis File, Fasika Wondimu Gelu, and Guta Demisu Kebede. ”A robust higher-order fitted mesh numerical method for solving singularly perturbed parabolic reaction-diffusion problems.” Results in Applied Mathematics 20 (2023): 100405.

[36] Kumar, Sunil, and Higinio Ramos. ”Parameter-uniform approximation on equidistributed meshes for singularly perturbed parabolic reaction-diffusion problems with Robin boundary conditions.” Applied Mathematics and Computation 392 (2021): 125677.

[37] Negero, Naol Tufa. ”A robust fitted numerical scheme for singularly perturbed parabolic reaction–diffusion problems with a general time delay.” Results in Physics 51 (2023):

106724.

[38] Kumar, Sunil, and Mukesh Kumar. ”High order parameter-uniform discretization for singularly perturbed parabolic partial differential equations with time delay.” Computers and Mathematics with Applications 68, no. 10 (2014): 1355-1367.

[39] Podila, Pramod Chakravarthy, and Kamalesh Kumar. ”A new stable finite difference scheme and its convergence for time-delayed singularly perturbed parabolic PDEs: PC Podila, K. Kumar.” Computational and Applied Mathematics 39, no. 3 (2020): 140.

[40] Tiruneh, Awoke Andargie, Getachew Adamu Derese, and Dagnachew Mengstie Tefera. ”A Nonstandard Fitted Operator Method for Singularly Perturbed Parabolic Reaction-Diffusion Problems with a Large Time Delay.” International Journal of Mathematics and Mathematical Sciences 2022, no. 1 (2022): 5625049.

[41] Singh, Joginder, Sunil Kumar, and Mukesh Kumar. ”A domain decomposition method for solving singularly perturbed parabolic reaction-diffusion problems with time delay.” Numerical Methods for Partial Differential Equations 34, no. 5 (2018): 1849-1866.

[42] Bashier, E. B. M., and K. C. Patidar. ”A second-order fitted operator finite difference method for a singularly perturbed delay parabolic partial differential equation.” Journal of Difference Equations and Applications 17, no. 05 (2011): 779-794.

[43] Tefera, Dagnachew Mengstie, Awoke Andargie Tiruneh, and Getachew Adamu Derese. ”Fitted operator on the crank-nicolson scheme for solving a small time delayed convection-diffusion equations.” Journal of applied mathematics and informatics 40, no. 3_4 (2022): 491-505.

[44] Ayele, Mulunesh Amsalu, Awoke Andargie Tiruneh, and Getachew Adamu Derese. ”Hybrid Fitted Numerical Scheme for Singularly Perturbed Convection-Diffusion Problem with a Small Time Lag.” In Abstract and Applied Analysis, vol. 2023, no. 1, p. 4382780. Hindawi, 2023.

[45] Negero, Naol Tufa, and Gemechis File Duressa. ”A method of line with improved accuracy for singularly perturbed parabolic convection–diffusion problems with large temporal lag.” Results in Applied Mathematics 11 (2021): 100174.

[46] Kadalbajoo, Mohan K., and Vikas Gupta. ”A brief survey on numerical methods for solving singularly perturbed problems.” Applied mathematics and computation 217, no. 8 (2010): 3641-3716.

[47] Tefera, Dagnachew Mengstie, Awoke Andargie Tiruneh, and Getachew Adamu Derese. ”Numerical treatment on parabolic singularly perturbed differential difference equation via fitted operator scheme.” In Abstract and Applied Analysis, vol. 2021, no. 1, p. 1661661. Hindawi, 2021.

[48] Kumar, Devendra, and Mohan K. Kadalbajoo. ”A parameter-uniform numerical method for time-dependent singularly perturbed differential-difference equations.” Applied Mathematical Modelling 35, no. 6 (2011): 2805-2819.

[49] Woldaregay, Mesfin Mekuria, and Gemechis File Duressa. ”Uniformly convergent numerical scheme for singularly perturbed parabolic pdes with shift parameters.” Mathematical Problems in Engineering 2021, no. 1 (2021): 6637661.

[50] Gupta, Gupta, Vikas, Mukesh Kumar, and Sunil Kumar. ”Higher order numerical approximation for time dependent singularly perturbed differential-difference convection-diffusion equations.” Numerical Methods for Partial Differential Equations 34, no. 1 (2018): 357-380..

[51] Shivhare, Meenakshi, Pramod Chakravarthy Podila, Higinio Ramos, and Jesús Vigo-Aguiar. “Quadratic B-Spline Collocation Method for Time-Dependent Singularly Perturbed Differential-Difference Equation Arising in the Modeling of Neuronal Activity.” *Numerical Methods for Partial Differential Equations* 39, no. 3 (2023): 1805–1826.

[52] Kumar, Kamalesh, P. Pramod Chakravarthy, Higinio Ramos, and Jesús Vigo-Aguiar. ”A stable finite difference scheme and error estimates for parabolic singularly perturbed PDEs with shift parameters.” Journal of Computational and Applied Mathematics 405 (2022): 113050.

[53] Woldaregay, Mesfin Mekuria, and Gemechis File Duressa. “Uniformly Convergent Numerical Scheme for Singularly Perturbed Parabolic Delay Differential Equations.” In *ITM Web of Conferences*, vol. 34, 02011. Les Ulis, France: EDP Sciences, 2020.

[54] Sahu, Subal Ranjan, and Jugal Mohapatra. ”Numerical study of time delay singularly perturbed parabolic differential equations involving both small positive and negative space shifts.” Journal of Applied Analysis 28, no. 1 (2022): 121-134.

[55] Prathap, T., and R. Nageshwar Rao. ”Uniformly convergent finite difference methods for singularly perturbed parabolic partial differential equations with mixed shifts.” Journal of Applied Mathematics and Computing 69, no. 2 (2023): 1679-1704.

[56] Kumar, Sunil, and BV Rathish Kumar. ”A domain decomposition Taylor Galerkin finite element approximation of a parabolic singularly perturbed differential equation.” Applied Mathematics and Computation 293 (2017): 508-522.

[57] Woldaregay, Mesfin Mekuria, and Gemechis File Duressa. ”Accurate numerical scheme for singularly perturbed parabolic delay differential equation.” BMC Research Notes 14, no. 1 (2021): 358.

[58] Woldaregay, Mesfin Mekuria, and Gemechis File Duressa. ”Robust mid-point upwind scheme for singularly perturbed delay differential equations.” Computational and Applied Mathematics 40, no. 5 (2021): 178.

[59] Duressa, G. F., I. T. Daba, and C. T. Deressa. A systematic review on the solution methodology of singularly perturbed differential difference equations. Mathematics, 11 (5), 1108. 2023.

[60] Stynes, Martin, and David Stynes. Convection-diffusion problems. Vol. 196. American Mathematical Soc., 2018.

[61] Miller, John JH, Eugene O'riordan, and Grigorii I. Shishkin. Fitted numerical methods for singular perturbation problems: error estimates in the maximum norm for linear problems in one and two dimensions. World scientific, 1996.

[62] Rao, S. Chandra Sekhara, Sunil Kumar, and Joginder Singh. "A discrete Schwarz waveform relaxation method of higher order for singularly perturbed parabolic reaction–diffusion problems." Journal of Mathematical Chemistry 58, no. 3 (2020): 574-594.

[63] Kumar, Sunil, Aakansha, Joginder Singh, and Higinio Ramos. "Parameter-uniform convergence analysis of a domain decomposition method for singularly perturbed parabolic problems with Robin boundary conditions." Journal of Applied Mathematics and Computing 69, no. 2 (2023): 2239-2261.

[64] Mekonnen, T.B. and Duressa, G.F., 2020. Computational method for singularly perturbed two-parameter parabolic convection-diffusion problems. Cogent Mathematics and Statistics, 7(1), p.1829277

[65] Amsalu Ayele, M., Andargie Tiruneh, A. and Adamu Derese, G., 2023. Fitted scheme for singularly perturbed time delay reaction-diffusion problems. Iranian Journal of Numerical Analysis and Optimization, 13(2), pp.262-284.

[66] Mickens, Ronald E. "Nonstandard finite difference schemes for differential equations." Journal of Difference Equations and Applications 8, no. 9 (2002): 823-847.

[67] Mekonnen, Tariku Birabasa, and Gemechis File Duressa. "Uniformly Convergent Numerical Method for Two-Parametric Singularly Perturbed Parabolic Convection-Diffusion Problems." *Journal of Applied and Computational Mechanics* 7, no. 2 (2021): 535–545.

[68] Woldaregay, Mesfin Mekuria, and Gemechis File Duressa. "Boundary Layer Resolving Exact Difference Scheme for Solving Singularly Perturbed Convection-Diffusion-Reaction Equation." Mathematical Problems in Engineering 2022, no. 1 (2022): 2043323.

[69] Andargie Tiruneh, Awoke, Getachew Adamu Derese, and Mulunesh Amsalu Ayele. "Singularly perturbed reaction diffusion problem with large spatial delay via non-standard fitted operator method." Research in Mathematics 10, no. 1 (2023): 2171698.

[70] Bellen, Alfredo, and Marino Zennaro. Numerical methods for delay differential equations. OUP Oxford, 2003.

[71] Cooke, K., P. Van den Driessche, and Xingfu Zou. ”Interaction of maturation delay and nonlinear birth in population and epidemic models.” Journal of Mathematical biology 39, no. 4 (1999): 332-352.

[72] Wu, Jianhong. ”Theory and applications of partial functional differential equations.” Vol. 119. Springer Science and Business Media, 2012.

[73] Liu, Quan, Xuefeng Wang, and Daniel De Kee. ”Mass transport through swelling membranes.” International Journal of Engineering Science 43, no. 19-20 (2005): 1464-1470.

[74] Wang, Xing Tao. ”Numerical solution of delay systems containing inverse time by hybrid functions.” Applied mathematics and computation 173, no. 1 (2006): 535-546.

[75] Joseph, Daniel D., and Luigi Preziosi. ”Heat waves.” Reviews of modern physics 61, no. 1 (1989): 41.

[76] Woldaregay, Mesfin Mekuria, Worku Tilahun Aniley, and Gemechis File Duressa. ”Novel Numerical Scheme for Singularly Perturbed Time Delay Convection-Diffusion Equation.” Advances in Mathematical Physics 2021, no. 1 (2021): 6641236.

[77] Goodwin, David A., Claude F. Meares, Leslie H. DeRiemer, Carol I. Diamanti, Richard L. Goode, John E. Baumert Jr, David J. Sartoris, Robert L. Lantieri, and H. Daniel Fawcett. ”Clinical studies with In-111 BLEDTA, a tumor-imaging conjugate of bleomycin with a bifunctional chelating agent.” Journal of nuclear medicine 22, no. 9 (1981): 787-792.

[78] Kumar, Devendra. ”A parameter-uniform scheme for the parabolic singularly perturbed problem with a delay in time.” Numerical Methods for Partial Differential Equations 37, no. 1 (2021): 626-642..

[79] Buranay, Suzan Cival, Nouman Arshad, and Ahmed Hersi Matan. ”Hexagonal grid computation of the derivatives of the solution to the heat equation by using fourth-order accurate two-stage implicit methods.” Fractal and Fractional 5, no. 4 (2021): 203.

[80] Iragi, Bakulikira C., and Justin B. Munyakazi. ”A uniformly convergent numerical method for a singularly perturbed Volterra integro-differential equation.” International Journal of Computer Mathematics 97, no. 4 (2020): 759-771.

[81] Megiso, Ermias Argago, Mesfin Mekuria Woldaregay, and Tekle Gemechu Dinka. ”Fitted tension spline method for singularly perturbed time delay reaction diffusion problems.” Mathematical Problems in Engineering 2022, no. 1 (2022): 8669718.

[82] Rao, R. Nageshwar, and P. Pramod Chakravarthy. ”A fitted Numerov method for singularly perturbed parabolic partial differential equation with a small negative shift arising in control theory.” Numerical Mathematics: Theory, Methods and Applications 7, no. 1 (2014): 23-40.

[83] Bansal, Komal, and Kapil K. Sharma. ”Parameter-robust numerical scheme for time-

dependent singularly perturbed reaction–diffusion problem with large delay." Numerical Functional Analysis and Optimization 39, no. 2 (2018): 127-154.

[84] Kadalbajoo, Mohan K., and Ashish Awasthi. "Crank–nicolson finite difference method based on a midpoint upwind scheme on a non-uniform mesh for time-dependent singularly perturbed convection–diffusion equations." International Journal of Computer Mathematics 85, no. 5 (2008): 771-790.

[85] Gracia, Jose Luis, and Eugene O'Riordan. "Singularly perturbed reaction–diffusion problems with discontinuities in the initial and/or the boundary data." Journal of Computational and Applied Mathematics 370 (2020): 112638.

[86] Udo, M. O., G. A. Olayi, and R. A. Ademiluyi. "Linear multistep method for solution of second order initial value problems of ordinary differential equations: a truncation error approach." Global Journal of Mathematical Sciences 6, no. 2 (2007): 119-126.

[87] Raja, V., and A. Tamilselvan. "Difference Scheme on a Non-Uniform Mesh for Singularly Perturbed Reaction-Diffusion Equations with Integral Boundary Condition." *Numerical Analysis and Applicable Mathematics* 1, no. 1 (2020).

[88] Ayele, Mulunesh Amsalu, Awoke Andargie Tiruneh, and Getachew Adamu Derese. "Uniformly convergent scheme for singularly perturbed space delay parabolic differential equation with discontinuous convection coefficient and source term." Journal of Mathematics 2022, no. 1 (2022): 1874741.

[89] Glizer, V. Y. "Asymptotic Analysis and Solution of a Finite-Horizon H^∞ Control Problem for Singularly Perturbed Linear Systems with Small State Delay." *Journal of Optimization Theory and Applications* 117, no. 2 (2003): 295–325.

[90] Buedo-Fernández, Sebastián, and Eduardo Liz. "On the stability properties of a delay differential neoclassical model of economic growth." Electronic Journal of Qualitative Theory of Differential Equations 2018, no. 43 (2018): 1-14.

[91] Balachandran, Balakumar, Tamás Kalmár-Nagy, and David E. Gilsinn. Delay differential equations. Berlin: Springer, 2009.

[92] Ramesh, V. P., and Mohan K. Kadalbajoo. "Upwind and midpoint upwind difference methods for time-dependent differential difference equations with layer behavior." Applied Mathematics and Computation 202, no. 2 (2008): 453-471.

[93] Woldaregay, MESFIN M., and GEMECHIS F. Duressa. "Parameter uniform numerical method for singularly perturbed parabolic differential difference equations." Journal of the Nigerian Mathematical Society 38, no. 2 (2019): 223-245.

[94] Friedman, Avner. Partial differential equations of parabolic type. Courier Dover Publica-

tions, 2008.

[95] Kellogg, R. Bruce, and Alice Tsan. ”Analysis of some difference approximations for a singular perturbation problem without turning points.” Mathematics of computation 32, no. 144 (1978): 1025-1039.

[96] Bellen, Alfredo, and Marino Zennaro. Numerical methods for delay differential equations. OUP Oxford, 2003.

[97] Aziz, Imran, and Rohul Amin. ”Numerical solution of a class of delay differential and delay partial differential equations via Haar wavelet.” Applied Mathematical Modelling 40, no. 23-24 (2016): 10286-10299.

[98] Wu, Jianhong. Theory and applications of partial functional differential equations. Vol. 119. Springer Science and Business Media, 2012.

[99] Amiraliyev, G. M., and Hakki Duru. ”A note on a parameterized singular perturbation problem.” Journal of computational and applied mathematics 182, no. 1 (2005): 233-242.

[100] Demsie, Amare Worku, Awoke Andargie Tiruneh, and Endalew Getnet Tsega. ”A Uniformly Convergent Scheme for Singularly Perturbed Unsteady Reaction–Diffusion Problems.” Journal of Applied Mathematics 2025, no. 1 (2025): 4603501.

[101] Ejere, Ababi Hailu, and Gemechis File Duressa. ”An exponentially fitted non-polynomial spline approach for singularly perturbed parabolic reaction-diffusion equation with large negative shift.” Research in Mathematics 12, no. 1 (2025): 2518815.

[102] Baker, C. T., G. A. Bocharov, and F. A. Rihan. ”A report on the use of delay differential equations in numerical modelling in the biosciences. Manchester Centre for Computational Mathematics Numerical Analysis Report 343.” (1999): 1360-1725.

[103] Kuang, Yang, ed. Delay differential equations: with applications in population dynamics. Vol. 191. Academic press, 1993.

[104] Glizer, V. Y. ”Asymptotic analysis and solution of a finite-horizon H^∞ control problem for singularly perturbed linear systems with small state delay.” *Journal of Optimization Theory and Applications* 117, no. 2 (2003): 295–325.

[105] Stein, Richard B. ”Some models of neuronal variability.” Biophysical journal 7, no. 1 (1967): 37-68.

[106] Kumar, Sunil, and BV Rathish Kumar. ”A domain decomposition Taylor Galerkin finite element approximation of a parabolic singularly perturbed differential equation.” Applied Mathematics and Computation 293 (2017): 508-522.

[107] Demsie, Amare Worku, Awoke Andargie Tiruneh, and Endalew Getnet Tsega. ”A Fitted Linear Multistep Approach for Singularly Perturbed Parabolic-Type Reaction-Diffusion

Problems Using Shishkin Meshes.” International Journal of Mathematics and Mathematical Sciences 2025, no. 1 (2025): 5553428.

[108] Gelu, Fasika Wondimu, and Gemechis File Duressa. ”A uniformly convergent collocation method for singularly perturbed delay parabolic reaction-diffusion problem.” In Abstract and applied analysis, vol. 2021, no. 1, p. 8835595. Hindawi, 2021.

[109] Woldaregay, Mesfin Mekuria, and Gemechis File Duressa. ”Almost second-order uniformly convergent numerical method for singularly perturbed convection–diffusion–reaction equations with delay.” Applicable Analysis 102, no. 2 (2023): 651-671.

[110] Huka, D. B., W. G. Melesse, and F. W. Gelu. ”Numerical solution of singularly perturbed parabolic differential difference equations.” Bulletin of the Karaganda University. Mathematics Series 119, no. 3 (2025): 107-124.

[111] Govindarao, Lolugu, Jugal Mohapatra, and Abhishek Das. ”A fourth-order numerical scheme for singularly perturbed delay parabolic problem arising in population dynamics.” Journal of Applied Mathematics and Computing 63, no. 1 (2020): 171-195.

[112] Bansal, Komal, and Kapil K. Sharma. ”Parameter uniform numerical scheme for time dependent singularly perturbed convection-diffusion-reaction problems with general shift arguments.” Numerical Algorithms 75, no. 1 (2017): 113-145.

[113] Clavero, Carmelo, and Jose L. Gracia. ”On the uniform convergence of a finite difference scheme for time dependent singularly perturbed reaction-diffusion problems.” Applied mathematics and computation 216, no. 5 (2010): 1478-1488.

[114] Shishkin, Grigory I., and Lidia P. Shishkina. Difference methods for singular perturbation problems. Chapman and Hall/CRC, 2008.

[115] Roos, H-G. ”Sufficient conditions for uniform convergence on layer-adapted grids.” Computing 63, no. 1 (1999): 27-45.

[116] Woldaregay, Mesfin Mekuria, and Gemechis File Duressa. ”Uniformly convergent numerical scheme for singularly perturbed parabolic pdes with shift parameters.” Mathematical Problems in Engineering 2021, no. 1 (2021): 6637661.

[117] Clavero, C., J. L. Gracia, and J. C. Jorge. ”High-order numerical methods for one-dimensional parabolic singularly perturbed problems with regular layers.” *Numerical Methods for Partial Differential Equations: An International Journal* 21, no. 1 (2005): 149–169.

[118] Demsie, A. W., A. A. Tiruneh, and E. G. Tsega. ”An Accelerated Fourth-Order Fitted Numerical Approach for Singularly Perturbed Reaction-Diffusion Problems of Small Time Lag.” Palestine Journal of Mathematics 14, no. 3 (2025).

[119] Ejere, Ababi Hailu, and Tesfaye Tolu Feyissa. ”A novel fitted mesh scheme involving

Caputo–Fabrizio approach for singularly perturbed fractional-order differential equations with large negative shift.” Chaos, Solitons and Fractals: X 15 (2025): 100128.

[120] Johnson, Claes. ”Uniform Numerical Methods for Problems with Initial and Boundary Layers (EP Doolan, JJH Miller and WHA Schilders).” (1983): 597.